STRESS ANALYSIS IN CURVED COMPOSITES

DUE TO THERMAL LOADING

by

JARED CORNELIUS POLK

Presented to the Faculty of the Graduate School of

The University of Texas at Arlington in Partial Fulfillment

of the Requirements

for the Degree

MASTERS OF SCIENCE IN AEROSPACE ENGINEERING

The University of Texas at Arlington

December 2012

ACKNOWLEDGEMENTS

First and foremost, I would like to sincerely thank GOD ALMIGHTY for blessing me to be able to attend graduate school at the University of Texas at Arlington. Without HIS define inspiration and HIS HOLY SPIRIT, I would not have been able to accomplish this task. I would also like to acknowledge Dr. Wen Chan, my graduate thesis adviser, for the knowledge imparted to me from his Composites I, Composites II, and Mechanics of Material courses that were pivotal to my understanding of the mechanics of isotropic materials and mechanics of composite materials. Last but not least, I would like to thank two other committee members Dr. Bo Wang and Dr. Seichii Nomura. Dr. Bo Wang's finite element class was a constant reference for me as I embarked on this very ambitious endeavor. Dr. Seichii Nomura was my first college of engineering graduate professor at the University of Texas at Arlington. With his help and teaching, I was able to achieve an A in Continuum Mechanics during a very personally difficult time.

November 26, 2012

ABSTRACT

STRESS ANALYSIS IN CURVED COMPOSITES

DUE TO THERMAL LOADING

Jared Cornelius Polk, M.S.

The University of Texas at Arlington, 2012

Supervising Professor: Wen Chan

Many structures in aircraft, cars, trucks, ships, machines, tools, bridges, and buildings, consist of curved sections. These sections vary from straight line segments that have curvature at either one or both ends, segments with compound curvatures, segments with two mutually perpendicular curvatures or Gaussian curvatures, and segments with a simple curvature. With the advancements made in multi-purpose composites over the past 60 years, composites slowly but steadily have been appearing in these various vehicles, compound structures, and buildings. These composite sections provide added benefits over isotropic, polymeric, and ceramic materials by generally having a higher specific strength, higher specific stiffnesses, longer fatigue life, lower density, possibilities in reduction of life cycle and/or acquisition cost, and greater adaptability to intended function of structure via material composition and geometry.

To be able to design and manufacture a safe composite laminate or structure, it is imperative that the stress distributions, their causes, and effects are thoroughly understood in order to successfully accomplish mission objectives and manufacture a safe and reliable composite. The objective of the thesis work is to expand upon the knowledge of simply curved composite structures by exploring and ascertaining all pertinent parameters, phenomenon, and trends in stress variations in curved laminates due to thermal

loading. The simply curved composites consist of composites with one radius of curvature throughout the span of the specimen about only one axis.

Analytical beam theory, classical lamination theory, and finite element analysis were used to ascertain stress variations in a flat, isotropic beam. An analytical method was developed to ascertain the stress variations in an isotropic, simply curved beam under thermal loading that is under both free-free and fixed-fixed constraint conditions. This is the first such solution to Author's best knowledge of such a problem. It was ascertained and proven that the general, non-modified (original) version of classical lamination theory cannot be used for an analytical solution for a simply curved beam or any other structure that would require rotations of laminates out their planes in space. Finite element analysis was used to ascertain stress variations in a simply curved beam. It was verified that these solutions reduce to the flat beam solutions as the radius of curvature of the beams tends to infinity. MATLAB was used to conduct the classical lamination theory numerical analysis. A MATLAB program was written to conduct the finite element analysis for the flat and curved beams, isotropic and composite. It does not require incompatibility techniques used in mechanics of isotropic materials for indeterminate structures that are equivalent to fixed-beam problems. Finally, it has the ability to enable the user to define and create unique elements not accessible in commercial software, and modify finite element procedures to take advantage of new paradigms.

TABLE OF CONTENTS

LIST OF ILLUSTRATIONS

LIST OF TABLES

CHAPTER 1

INTRODUCTION

The purpose of this chapter is to provide a brief history on composites, their unique properties and benefits, the importance of simply curved composites, and previous work done on simply curved composites. The objectives and approach of this thesis will be discussed and outlined, respectively.

1.1 History

Composites structures have been used for millennium all across the globe. From the Incans, Mayans, Aztecs, Zulus, Egyptians, Sudanese, Kenyans, Libyans, Indians, Thais, and Chinese, composites structures have played a pivotal role in these ancient societies. These composite structures were predominantly, if not all, masonry in nature. Nevertheless, these ancient people thoroughly understood the concepts of stress transfer, reinforcement, and reinforcement support. Many of the historical structures found in Egypt (including the pyramids: of which Sudan has by far the most in the world, albeit smaller in size than those in Egypt), temples in India and Thailand, etcetera owe much of the strength and design not to just solid stone structures but composite structures as well. To be able to build the many unique and magnificent structures that existed in antiquity, it is clear not only from inspection but from common sense that a thorough understanding of mechanics of material, architecture, and advanced mathematics had to be known thousands of years before the likes of Isaac Newton, Stephen P. Timoshenko, Leonhard Euler, etcetera were even born! It is clear that one cannot not just build the modern day equivalent of the Al Khalifa Tower or the Taipei Towers in antiquity with far less tools than exist today and have those structures routinely last thousands of years with no upkeep without understanding the latter principles. There is no way to simply guess and luck to completion such engineering marvels that rival and exceed many engineered structures that exist even to this very day. Engineering is engineering; it is just as difficult if not more in antiquity as it is now. In fact, in the Holy Bible (Exodus Chapter 1: Verses 8-21) [1], the ancient Egyptians decided to punish their ancient Hebrew workers by forcing them to produce superior masonry product without a filler (straw) that had a dual use as a fibrous reinforcement. The

ancient Egyptians understood not only the filler role that the straw provided but also the reinforcement role in the mud/brick matrix as well- Holy Bible (Exodus Chapter 5: Verses 1-23) [1]. The ancient Egyptians (not being a nation of academic light weights), required that the quota be maintained even without the straw filler/reinforcement. From inspection, the quota was not only quantitative but qualitative as well. They too must have understood the logic of testing the strength of a sample of material before a batch was put into construction.

It is clear the ancient Egyptians understood the significance of a filler and reinforcement in the quantity and quality (strength parameters) of a product. Today, the reinforcement in concrete is primarily steel bars. However, other materials have been used as well. There are a number of new concrete compositions that consists of a multitude of various particulate reinforcements that have significantly increased the compressive strength of concrete. These examples are poster child examples of the two main types of reinforcements used in composites, continuous reinforcement and particulate reinforcement.

1.2 Definitions

The primary role of the reinforcement phase of a composite is to bear loads applied to a given structure. Reinforcements can consist of short or long fibers and are uniform and non-uniform in distribution. The fibers are generally very small in diameter, millimeters to nanometers. However, some unique exceptions to this "rule" include steel bars used as reinforcement in concrete. These reinforcements can be layered parallel to each other or can be woven over and under each other. Reinforcements can also consist of particulates of various sizes and shapes.

The primary role of the medium that the reinforcement phase exist in (the matrix phase) is to protect the reinforcement phase from the environmental elements, physical damage from external contact, and transfer loads via stress transfer to the reinforcement phase. The matrix phase can consist of any number of compositions. Some are very pliable, others are reasonable rigid but elastic, and others are brittle. In contemporary composite construction, a third phase is used to improve the efficiency of the

stress transfer to the reinforcement phase and to help protect and strengthen the reinforcement phase. This phase is called the interfacial phase- see Figure 1.

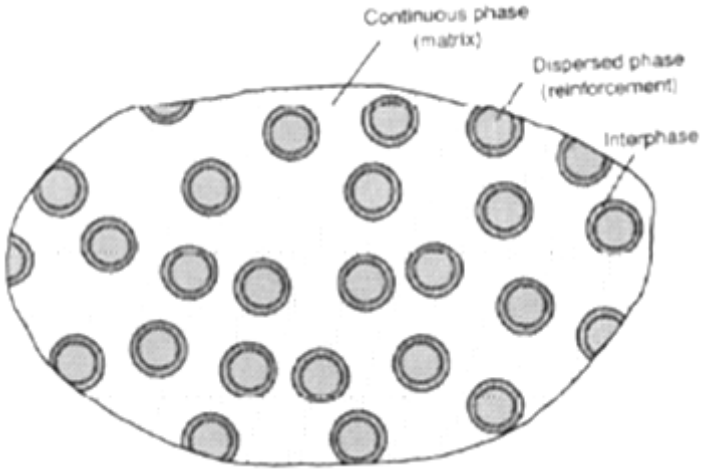

Figure 1. Representative view of the three phases of a composite [2].

The type of reinforcement and matrix used for a given composite has a significant influence on the properties of that composite. Simply changing the reinforcement while maintaining the same matrix or changing the matrix while maintaining the same reinforcement can significantly alter the properties of a composite. This variance in properties of composite is not a curse but an asset that is tamed and used to the benefit of many engineers. This is what gives composite their unique capabilities, niche, and their unique advantages over monolithic material.

> These advantages include high strength, high stiffness, long fatigue life, low density, and adaptability to the intended function of the structures. Additional improvements are realized in corrosion resistance, wear resistance, appearance, temperature-dependent behavior, environment stability, thermal insulation and conductivity, and acoustic insulation. The basis for the superior structural performance of composite materials lies in the high specific strength (strength to density ratio) and high specific stiffness (modulus to density ratio) and in the anisotropic and heterogeneous character of the material. The latter provides composite with many degrees of freedom for optimum configuration of the material system, Daniel and Ishai [2].

1.3 Curved Laminate

Structures come in all shape, sizes, weights, and compositions in order to fulfill a given function or functions. One of the key factors in determining a structure's role (outside material properties) is its shape. In many applications, simply curved structures or simply curved parts are critical to the application of a given machine, system, or structure. These curved shapes range from clamps, stiffeners, and stringers, connector assemblies for rotor shaft to gear cases, panels, beams, plates, etcetera. As with all parts or structures, proper design is critical to mission success. In order to properly design any part or structure, it is imperative to understand the way that part or structure responds to various loading conditions and environmental conditions, for a given set of boundary conditions. Understanding the displacements, strains & stresses, their variations and magnitudes, throughout that part or structures is imperative to a successful design and understanding the complete picture of the mechanical behavior.

To facilitate this understanding, many engineers, some scientist, and fewer mathematicians have tackled various aspects of a very complicated field, mechanics of composite bodies. Even with this intellectual assault, there is still very little that is known absolutely about the mechanical behavior of a composite body without the proper and appropriate usage of time consuming finite element analysis (FEA) and expensive (and often destructive) testing. Necessarily, testing is a key part of design, development, and production that is indispensable. However, FEA is not indispensable, is computationally intensive, is time consuming, and sometimes costly. This thesis will focus on stress analysis of simply curved laminates (structures/parts with only one unique radius of curvature) with continuous fibers under uniform thermal loading.

It was previously mentioned on how little the composites community knows absolutely about the mechanical behavior of a composite body without the proper and appropriate usage of time consuming finite element analysis (FEA) and expensive (and often destructive) testing. To complicate matters, even less works had been done and less understanding had concerning curved laminates. This is even more so

for curved laminates under thermal loading. According to Li and Zhao [3], "Relatively little is available for analytical displacement formulation of curved beam." Furthermore, according to Li and Zhao [3]:

> Ribeiro & Monoach [4] utilized p-version hierarchical finite elements to analyze thermoelastic geometrically nonlinear vibrations of isotropic straight and curved beams. Various analytical and numerical methods concerning temperature variation have been developed for other structural style. The constitutive equation and the numerical procedure proposed by Padovani et. Al. [5] have been used in a masonry arch subjected to a uniform temperature distribution.

As can be seen from this snapshot given by Li and Zhao [3] and the previously mentioned, there is very little if any work on curved composite beams under thermal loading that has resulted in an analytical formulation for displacements, strains, and/or stresses. The masonry arch analysis fails significantly to account for short or long fiber composites. The analysis becomes even more complicated for thermal loading problems that are statically indeterminate.

Work has been done on cylindrical shell composites. Yet, very little can be applied to the case of simply curved laminates which are by definition open sections. From mechanics of (isotropic) materials, it evident that displacement, strain, and stress distributions in open section and close section geometries vary appreciably. This variation varies appreciably if the geometric sections have rectilinear sides or curved sides. These variations are an order of magnitude more complex for anisotropic materials such as composite structures and parts. Therefore, applying results for close circular section for composite laminates to open circular section is by far more erroneous than doing the same thing for isotropic structures/parts.

Nguyen [6] studied a simply curved beam under a bending load on each end of the longitudinal span of the beam. The formulation relied on a geometric relationship between the tangential elongations of the curved beam with respect the mid-plane of the beam and the tangential elongations of the curved beam with respect to the center of curvature of the beam- see Appendix A. The resulting relationship is the tangential strain. This tangential strain relationship for a curved beam was shown to reduce to the longitudinal strain relationship for a flat beam as the radius of curvature tends to infinity. This relationship

was extended to describe the variations of strains in the other mutually orthogonal directions. However, this relationship cannot be used for the variation of the radial strain for the simply curved beam, the variation of the shear strain in the simply curved beam, or the variation of the strain in the axial direction of the simply curved beam. Therefore, only one valid strain relationship was obtained.

Furthermore Nguyen [6], attempted to use the functional multiple {R/(R+z)} that goes to one as the radius of curvature (R) tends to infinity for the summation of the stiffness of multiple lamina through the thickness (z) of the laminate to obtain the laminate stiffness matrix and subsequently the laminate compliance matrix. Even though the tangential strain relationship shows that the tangential strain varies through the thickness of the laminate, that does not mean the stiffness or the thickness of the lamina varies through the thickness of the laminate. The stiffness for elastic material would have to be constant. It is nothing more than a relationship between how much force projected on an area will create a unit strain for a given material. For a lamina, that stiffness matrix would be the same for all locations in the lamina since it is linearly elastic and quasi-homogeneous. Also, the lamina thicknesses are constant for every cross-section. Therefore, the laminate stiffness matrix and compliance matrix would be erroneous. The in- and out-of-plane loads would likewise be incorrect if the laminate stiffness matrix was used and the in- and out-of-plane deformations would be incorrect if the laminate compliance matrix was used. Therefore, even this attempt has fallen short to finding an analytical solution to a curved beam. The bending moment problem is at least an order of magnitude easier than the thermal loading problem.

Even though a term may reduce from the apparent curved beam solution to the apparent flat beam solution doesn't mean that term is correct. This is a necessary condition for the reduction from the curved beam form to the flat beam form. That is, at the bare minimum the term for the solution form should reduced from the curved beam form to the flat beam form as the radius of curvature tends to infinity. However, since it fulfills the necessary conditions doesn't guarantee that it will fulfill the sufficient conditions as well. Due to the extreme difficulty of this problem, the sufficient conditions can only be ascertained to have been met concurrently with the necessary conditions or with other factoids of a given method only after experimentations have been conducted to verify a given model, solution, and method.

Chapter 2

FINITE ELEMENT MODEL

The purpose of this chapter is to describe the finite element models used to ascertain pertinent data needed to develop an analytical relationship between stresses and thermal loadings for curved laminates that are fixed or cantilevered. From this, the MATLAB finite element code will be validated as program that is capable of accurately modeling a simply curved laminate under thermal loading.

2.1 Development of Finite Element Model

2.1.1 Assumptions

All models have assumptions built into them. These assumptions have tremendous significance on the accuracy of the models, the conditions the model can be used, and the significance of the results from the model. The assumptions used in this model are as follow:

(a) Each node of every element is connected to and stays connected to its immediate neighbors regardless of strain or stress magnitude & direction. This means the model stays connected at the nodes at all times.

(b) Any deformation is treated as a linearly elastic deformation. There are no plastic deformations, any form of yielding, or strain hardening.

(c) The models are under uniform temperature. There are no temperature gradients. There is no heat transfer. There are no internal sources of heat. The model is slowly and reversibly loaded thermally; that is, there are no stress concentrations or thermal shocks due to the rate of thermal loading.

(d) There are no body forces acting on the models.

(e) There are no residual stresses in the model due to any previous conditions. That is, before thermal loading, the model is free of any stress or strain history.

(f) All models are quasi-homogeneous or homogeneous (for monolithic materials).

(g) Model is potentially under non-plane strain and non-plane stress conditions.

2.1.2 Model Creation

MATLAB was used to develop a three-dimensional (3D) model and conduct the finite element analysis (FEA). A main file calls a number of functions that carry out specific tasks at different times throughout the span of the analysis. Initial data is entered into the main file, and then the analysis program runs at the user's command. The initial data consists of material properties of the laminate, thermal conditions, stacking sequence of laminate, model element configuration, model geometry configuration, and the boundary conditions- see Table 1.

Table 1. Table of data input for creation of model.

	Input
Material Properties	
	E1
	E2
	E3
	G23
	G13
	G12
	v23
	v13

Table 1. – *Continued*

	v12
Thermal Conditions and Properties	
	T_final
	T_intial
	alpha_1
	alpha_2
	alpha_3
Model Element Configuration	
	Number of Elements In Theta Direction
	Number of Elements In Radial Direction
	Number of Elements In Z Direction
Model Geometry Configuration	
	Plies
	Radius of Curvature
	Angle Spanned
	Ply Top and Bottom Surface (Z-Height)
	Stacking Sequence

Table 1. – *Continued*

Boundary Condition (Binary Boolean) 1 = apply 0 = don't apply	
	Right Face
	Left Face
	Front Face
	Rear Face
	Top Face
	Bottom Face

From this initial data, all other pertinent laminate properties are calculated including the stiffnesses and Poisson's ratios. This data is for three dimensional, orthotropic laminates- Table 2.

Table 2. Three dimensional stiffness components and Poisson's ratios.

	Calculated
Material Constants and Parameters	
	v21
	v31
	v32
	C11
	C22
	C33
	C12

Table 2. – *Continued*

	C23
	C13
	C21
	C32
	C31
	C44
	C55
	C66

Once the latter data in Table 1 is entered into the program and the data in Table 2 is calculated, the program builds a virtual model of the laminate as defined by the said data. The next steps are to calculate a numeric data form that enables the geometry to be discretized in a particular pattern & order and to generate symbolic versions of data forms that will be used repetitively. The type of element used for the latter is a tri-linear, isoparametric, 8-node, 24-degree of freedom element- see Figure 2. The local coordinate system is (r,s,t) where r-direction is in the length direction of the element, s-direction is in the width direction of the element, and the t-direction is in the thickness direction of the element. The domain for the element in the r-, s-, and t-directions is [-1, 1]. Each node has three degrees of freedom that are translational and in the r-, s-, and t-directions.

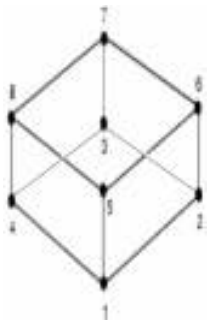

Figure 2. Tri-linear, isoparametric, 8-node, 24-degree of freedom element [6].

- Element Connectivity: The element connectivity function connects each element to its neighbors via their mutual nodes. Once this connection is formed, the elements and their nodes cannot be disconnected regardless of the forces or moments applied. This results in a model that does not break or tear. Since there are no provisions for plastic deformation, the elements elastically *stretch, twist, and bend* to infinity if the loads permit. Obviously, failure will occur long before this limit is reached.
- Symbolic Stiffness Matrix: The symbolic stiffness matrix function generates a symbolic version of the element stiffness matrix.
- Symbolic B (FEA) Matrix: The symbolic operator matrix function generates a symbolic version of the operator (partial derivative operator) matrix that operates on the displacements. The shape (interpolation) functions are exact at each corresponding node. The shape functions are:

$$N_1 = \frac{1}{8}(1-r)(1-s)(1-t) \tag{1}$$

$$N_2 = \frac{1}{8}(1+r)(1-s)(1-t) \tag{2}$$

$$N_3 = \frac{1}{8}(1+r)(1+s)(1-t) \tag{3}$$

$$N_4 = \frac{1}{8}(1-r)(1+s)(1-t) \tag{4}$$

$$N_5 = \frac{1}{8}(1-r)(1-s)(1+t) \tag{5}$$

$$N_6 = \frac{1}{8}(1+r)(1-s)(1+t) \tag{6}$$

$$N_7 = \frac{1}{8}(1+r)(1+s)(1+t) \tag{7}$$

$$N_8 = \frac{1}{8}(1-r)(1+s)(1+t) \tag{8}$$

$$[B] = \begin{bmatrix} \frac{\partial N_i}{\partial r} & 0 & 0 \\ 0 & \frac{\partial N_i}{\partial s} & 0 \\ 0 & 0 & \frac{\partial N_i}{\partial t} \\ 0 & \frac{\partial N_i}{\partial t} & \frac{\partial N_i}{\partial s} \\ \frac{\partial N_i}{\partial t} & 0 & \frac{\partial N_i}{\partial r} \\ \frac{\partial N_i}{\partial s} & \frac{\partial N_i}{\partial r} & 0 \end{bmatrix} \text{ where i = 1, 2, 3, 4, 5, 6, 7, 8} \tag{9}$$

- Symbolic Thermal Load Matrix: The symbolic thermal load matrix function generates a symbolic (variable) version of the thermal load matrix that calculates the loads on each node, at each given direction, due to temperature changes in the given element.

The unique numerical value of the stiffness matrices and thermal load matrices for each element (depending on its orientation and spatial location in the laminate) is calculated one element at time.

- C Matrix: The C matrix is a [6x6] matrix of the stiffnesses C_{ij} listed in Table 2. This matrix becomes the FEA [D] matrix.

$$[C] = [D] = \begin{bmatrix} C_{11} & C_{12} & C_{13} & 0 & 0 & 0 \\ C_{21} & C_{22} & C_{23} & 0 & 0 & 0 \\ C_{31} & C_{32} & C_{33} & 0 & 0 & 0 \\ 0 & 0 & 0 & 2C_{44} & 0 & 0 \\ 0 & 0 & 0 & 0 & 2C_{55} & 0 \\ 0 & 0 & 0 & 0 & 0 & 2C_{66} \end{bmatrix} \tag{10}$$

- Jacobian Matrix: The determinate of the Jacobian matrix for a given element is calculated.

- Element Stiffness Matrix: The numerical version of the general/symbolic stiffness matrix is calculated for the given element. Gaussian quadrature integration is not used. The primary purpose of Gaussian quadrature integration is for a numerically quick way of approximating the volume integral at specific points in the element. The whole purpose of the symbolic matrix is for rapid full integration. There are no approximating integral techniques used. The indefinite integral defined under Symbolic Stiffness Matrix is used. The indefinite integral of the symbolic stiffness matrix does not change from element to element. The form of the integral is the same for all elements. Once the indefinite integral is obtained under Symbolic Stiffness Matrix, it is just a simple exercise in evaluating the stiffness matrix at $(r,s,t) \in [-1, 1]$. Only the exact integration is used.

$$[k] = \iiint_V [B^T][D][B]dv \tag{11}$$

- Thermal Strain Matrix: A numerical thermal strain matrix is generated for the given element for thermal strains in three dimensions.
- Thermal Load Matrix: The numerical version of the general/symbolic thermal load matrix is calculated for the given element in a similar fashion and for identical reason as that done for the element stiffness matrices.

$$[f_T] = \iiint_V [B^T][D]\{\alpha T\}dv \tag{12}$$

The upshot of this part of the program is the element stiffness matrix and the thermal load matrix for each element is calculated.

The next phase of the program assembles the global stiffness matrix based on the model geometry configuration and the model element configuration. The *map* for this assembly is the element connectivity matrix. Afterwards, the external faces of the model and the nodes on those faces are collected in matrices to be utilized once the boundary conditions are applied. The boundary conditions selected in the initial data

phase for each node to be restricted in translation in a given combination of the three orthogonal directions (X, Y, Z). This restriction is set to a displacement of 0. The boundary conditions are *applied* when the rows and columns of the global stiffness matrix associated with the restricted degree of freedom are partitioned. The resulting global stiffness matrix has the same size as the original global stiffness matrix. Instead of deleting columns and rows that are associated with restricted degrees of freedom, those rows and columns are replaced with all zeros. The diagonal terms of the modified global stiffness matrix that were replaced with zeros are changed to the numerical value 1. This last step facilitates the process of solving the linear equation shown in Equation (13).

$$\{F\} = [K_{REDUCED}]\{d\} \tag{13}$$

The resulting matrix is now the reduced global stiffness matrix.

A function takes each element's thermal load matrix and assembles them into one matrix according to the mapping given in the element connectivity matrix. This new thermal load matrix becomes the {F} single column matrix/array. MATLAB executes a particular linear solver routine that is commensurate with the optimum speed & accuracy of the solution to Equation (13) for a [K] matrix with a given structure (sparseness, banded nature, etcetera). The resulting {d} single column matrix/array is the jewel of the FEA, the displacement array.

From the displacement array, the displacement function, the strains, and the stresses in each element can be calculated- see Equation (14), Equation (15), Equation (16), respectively.

$$\{\psi\} = [N]\{d\} \tag{14}$$

$$\{\varepsilon\} = [B][N]\{d\} \tag{15}$$

$$\{\sigma\} = [D]\{\varepsilon\} \tag{16}$$

2.1.3 Meshing Generation

The according to Chan, Lawrence, et. al. [7], composites modeled with mapped, regular, rectangular volume mesh provide the most accurate results. These results are not significantly more accurate than a freely, irregular, non-rectangular volume mesh. According Logan [8], models with element aspect ratios closest to 1 generally provide more accurate solutions than an equivalent model with elements having larger aspect ratios. Most models show that the smaller the aspect ratio of the elements, the faster the solutions generally converge. Due to these facts and the cubic (that is, aspect ratio = 1) nature of the tri-linear, isoparametric element used, an aspect ratio of 1 is used for all the elements. Each element corresponds to a cubic section in the mesh. That is the mesh is made up of a series or regular, mapped cubes, whose edges coincide with the edges of the elements and whose volume is equivalent to the volume of the elements. Each cubic cell in the mesh represents a finite element- see Figure 3.

Figure 3. Representative model of a simply curved composite laminate with regular cubic mesh with each cubic mesh consisting of a finite element [6].

2.2 Model Validation

2.2.1 Analytical Solution For Isotropic Flat Model

The problem that will be solved is the statically indeterminant fixed structure- see Figure 4. The structure is fixed at both ends A and B. A uniform thermal load due to $\Delta T = 100$ ºF. The structure is homogenous and made of 6061-T6 aluminum. Material properties for 6061-T6 aluminum are listed in

.

Table 3. Material properties of 6061-T6 aluminum.

Material	Property	Value
6061-T6 Aluminum alloys		
	E_1	1.00E+07
	E_2	1.00E+07
	E_3	1.00E+07
	G_23	3.80E+06
	G_13	3.80E+06
	G_12	3.80E+06
	v_23	0.33
	v_13	0.33
	v_12	0.33
	alpha_1	1.31E-05
	alpha_2	1.31E-05
	alpha_3	1.31E-05

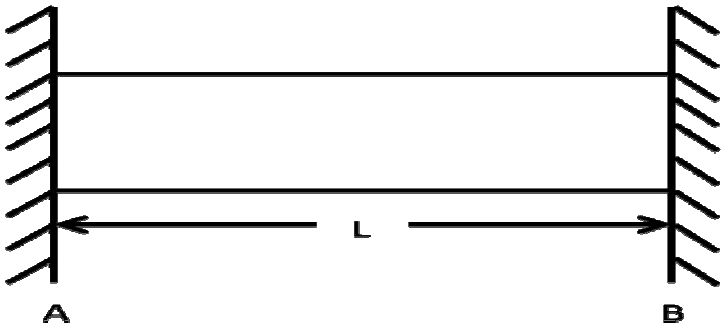

Figure 4. Typical statically indeterminant (fixed) beam problem.

For the fixed beam problem, the beam is not able to expand in the longitudinal direction. At the fixed ends, there are no expansions in either the thickness direction or the transverse direction. However, as progression occurs from the fixed ends towards the mid-length point along the longitudinal axis, the beam does have restricted variances of expansion in the thickness and transverse directions. The *freeness* of the expansions in the thickness and transverse directions do not vary linearly from zero at the fixed ends to some given maximum amount at the mid-span of the beam along its longitudinal axis.

From inspection, it can be seen that the maximum stresses will be along the longitudinal axis. The maximum stresses in the thickness (z-direction) direction and transverse (x-direction) direction will be at the fixed ends and will tend to a minimum value towards the mid-span of the beam along the longitudinal axis. Solving the statically indeterminate problem is more challenging. The material properties along with compatibility relationships are needed to ascertain the stresses. This is generally done be summing the deformations due to thermal loading & reaction forces and equating this with the compatibility relationship. Force-displacement, temperature-displacement, and constitutive relationships such as Equation (17), Equation (18), and Equation (19), respectively, are then utilized to find the unknown forces. From these forces and strains, the stresses can be ascertained.

$$\varepsilon = \frac{\delta}{L} = \frac{P}{EA} \tag{17}$$

$$\varepsilon_T = \frac{\delta_T}{L} = \alpha(\Delta T) \tag{18}$$

$$\begin{Bmatrix} \sigma_x \\ \sigma_y \\ \sigma_z \end{Bmatrix} = \frac{E}{(1+\upsilon)(1-2\upsilon)} \begin{bmatrix} (1-\upsilon) & \upsilon & \upsilon \\ \upsilon & (1-\upsilon) & \upsilon \\ \upsilon & \upsilon & (1-\upsilon) \end{bmatrix} \begin{Bmatrix} \varepsilon_x \\ \varepsilon_y \\ \varepsilon_z \end{Bmatrix} \tag{19}$$

where ε = strain, δ = elongation, L = length of beam, P = longitudinal axis load, E = Young's modulus, A = cross sectional area perpendicular to the longitudinal axis, σ = stress, δ_T = thermal elongation, ε_T = thermal strain, α = coefficient of linear thermal expansion, T = temperature, σ_T = thermal stress, and υ = Poisson's ratio

Figure 5 shows the solution for solving the statically indeterminant problem using temperature-displacement relations, force-displacement relations, and compatibility relations.

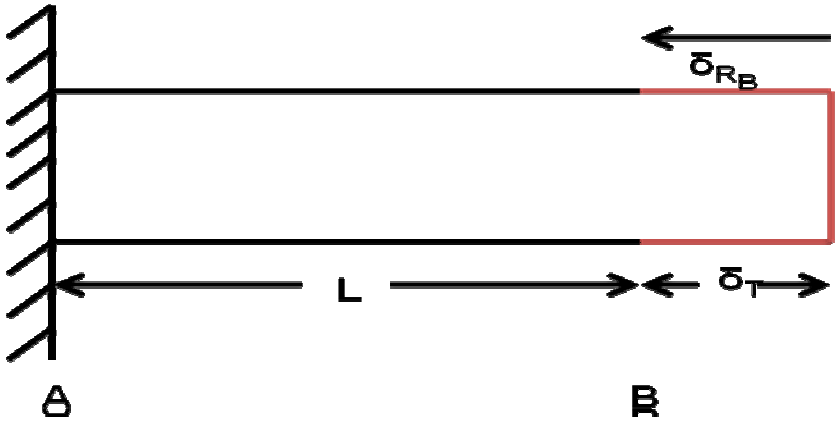

Figure 5. Typical statically indeterminant (fixed) beam problem with fixed end remove showing displacement potentials.

The equation of equilibrium in the longitudinal direction shows that the reaction from the wall at end A and B are equal in magnitude and compressive.

$$\sum_{longitudinal} Forces = 0 = R_A - R_B \Rightarrow R_A = R_B \tag{20}$$

From the compatibility condition $\delta_{AB} = \delta_{R_B} + \delta_T = 0$, the thermal elongation δ_T is equal in magnitude and opposite in direction to the mechanical elongation δ_{R_B}.

$$\delta_T = \alpha(\Delta T)L \tag{21}$$

$$\delta_{R_B} = -\alpha(\Delta T)L \tag{22}$$

Using Equation (17), Equation (18), the compatibility condition, and Poisson' ratio effect on the transverse and thickness strains due to the longitudinal strain, and Equation (19) , the stresses in the fixed-structure are ascertain as:

$$\begin{Bmatrix}\sigma_x\\ \sigma_y\\ \sigma_z\end{Bmatrix} = \frac{1.00x10^7\ \frac{lb.}{in.^2}}{(1+0.33)(1-2\cdot 0.33)}\begin{bmatrix}(1-0.33) & 0.33 & 0.33\\ 0.33 & (1-0.33) & 0.33\\ 0.33 & 0.33 & (1-0.33)\end{bmatrix}\begin{Bmatrix}-\left(1.31x10^{-5}\ \frac{in.}{in.\cdot^{\circ}F}\right)100^{\circ}F\\ 0.33\left(1.31x10^{-5}\ \frac{in.}{in.\cdot^{\circ}F}\right)100^{\circ}F\\ 0.33\left(1.31x10^{-5}\ \frac{in.}{in.\cdot^{\circ}F}\right)100^{\circ}F\end{Bmatrix}$$

$$\begin{Bmatrix}\sigma_x\\ \sigma_y\\ \sigma_z\end{Bmatrix} = \begin{Bmatrix}-13100\\ 0\\ 0\end{Bmatrix}\frac{lb.}{in.^2}$$

2.2.2 Classical Lamination Theory (CLT) Solution For Isotropic Flat Model

Classical lamination theory is the fundamental mechanics environment for ascertaining overall behavior of composite laminates. It predicts the overall behavior of composite laminate (or isotropic laminates) when used within the following assumptions [2]:

(a) Each layer (lamina) of the laminate is quasi-homogeneous and orthotropic.

(b) The laminate is thin with its lateral dimensions much larger than its thickness and is loaded in its plane only, that is, the laminate and its layers (except for their edges) are in a state of plane stress ($\sigma_z = \tau_{xz} = \tau_{yz} = 0$).

(c) All displacements are small compared with the thickness of the laminate (|u|, |v|, |w| << h).

(d) Displacements are continuous throughout the laminate.

(e) In-plane displacements vary linearly through the thickness of the laminate, that is, u and v displacements in the x- and y-directions are linear functions of z.

(f) Straight lines normal to the middle surface remain straight and normal to that surface after deformation. This implies that transverse shear strains γ_{xz} and γ_{yz} are zero.

(g) Strain-displacement and stress-strain relations are linear.

(h) Normal distances from the middle surface remain constant, that is, the transverse normal strain ε_z is zero. This implies that the transverse displacement w is independent of the thickness coordinate z.

As shown in the assumptions above, CLT is a plane stress theory. All mechanics exist is in a family of parallel planes. By convention, these planes are all parallel to the XY-plane. All deformations, stiffness, strains, stresses, etcetera will be define only in this family of planes. With CLT, a two-dimensional material stiffness matrix is developed by assuming plane stress conditions, $\sigma_z = 0$. The resulting stiffness matrix is defined as the reduced-stiffness matrix. The stress-strain relationship in a ply is given as follows (Figure 6):

$$Q_{11} = \frac{E_1}{1 - \nu_{12}\nu_{21}} \tag{23}$$

$$Q_{22} = \frac{E_2}{1 - \nu_{12}\nu_{21}} \tag{24}$$

$$Q_{12} = \frac{\nu_{12}E_2}{1 - \nu_{12}\nu_{21}} = \frac{\nu_{21}E_1}{1 - \nu_{12}\nu_{21}} \tag{25}$$

$$Q_{66} = G_{12} \tag{26}$$

$$\begin{bmatrix} \sigma_1 \\ \sigma_2 \\ \tau_6 \end{bmatrix} = \begin{bmatrix} Q_{11} & Q_{12} & 0 \\ Q_{21} & Q_{22} & 0 \\ 0 & 0 & Q_{66} \end{bmatrix} \begin{bmatrix} \varepsilon_1 \\ \varepsilon_2 \\ \gamma_6 \end{bmatrix} \tag{27}$$

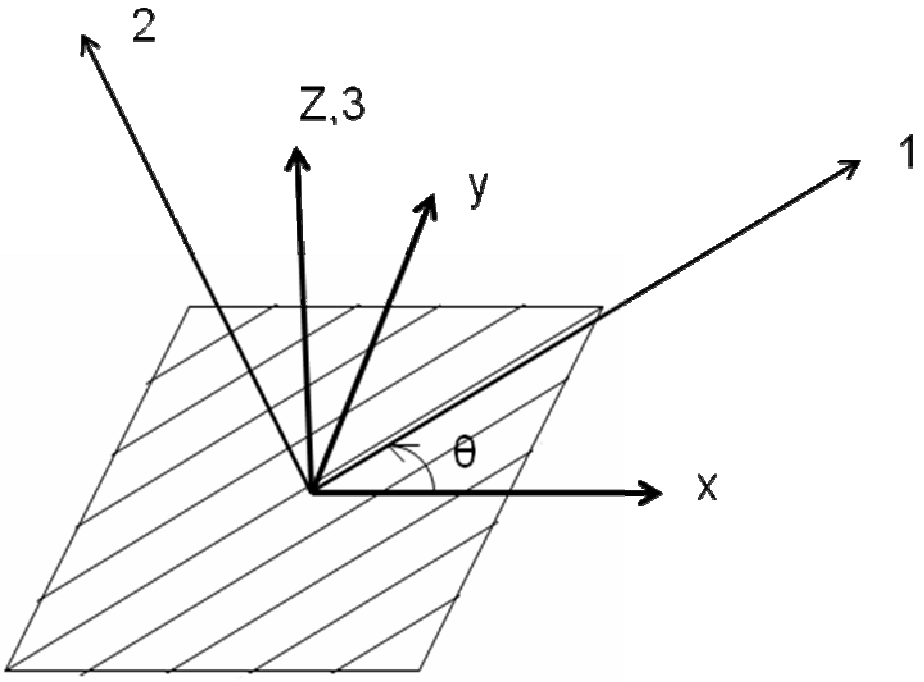

Figure 6. Representative ply with material (1,2,3) coordinate system and laminate (x,y,z) coordinate system.

Since each ply (lamina) has its own coordinate system, to define the behavior of the laminate using n-different coordinates system for an n-layered laminate would be unyielding. Therefore, a common coordinate system is defined at the center of the laminate in the mid-plane. This common coordinate system is conventionally known as the laminate coordinate system. In order to get each lamina in terms of

the laminate coordinate system, the parameters of the lamina in the material coordinate system are transformed through rotations to the laminate coordinate system:

$$[T_\sigma(\theta)] = \begin{bmatrix} m^2 & n^2 & 2mn \\ n^2 & m^2 & -2mn \\ -mn & mn & (m^2 - n^2) \end{bmatrix} \tag{28}$$

$$[T_\varepsilon(\theta)] = \begin{bmatrix} m^2 & n^2 & mn \\ n^2 & m^2 & -mn \\ 2mn & -2mn & (m^2 - n^2) \end{bmatrix} \tag{29}$$

$$[\overline{Q}_{x-y}] = [T_\sigma(-\theta)][Q_{1-2}][T_\varepsilon(\theta)] \tag{30}$$

where $m = \cos(\theta)$ and $n = \sin(\theta)$

The stress-strain relationship in a lamina is now definable in terms of the laminate coordinate system:

$$\begin{bmatrix} \sigma_x \\ \sigma_y \\ \tau_s \end{bmatrix} = \begin{bmatrix} Q_{xx} & Q_{xy} & Q_{xs} \\ Q_{yx} & Q_{yy} & Q_{ys} \\ Q_{sx} & Q_{sy} & Q_{ss} \end{bmatrix} \begin{bmatrix} \varepsilon_x^o \\ \varepsilon_y^o \\ \gamma_s^o \end{bmatrix} + z \begin{bmatrix} Q_{xx} & Q_{xy} & Q_{xs} \\ Q_{yx} & Q_{yy} & Q_{ys} \\ Q_{sx} & Q_{sy} & Q_{ss} \end{bmatrix} \begin{bmatrix} \kappa_x \\ \kappa_y \\ \kappa_s \end{bmatrix} \tag{31}$$

As stated in the assumptions for CLT, strains vary linearly through the thickness of the laminate. However, since the stiffness are different because each ply is potential unique from others due fiber orientation and ply material properties, the stress are not continuous through the thickness of the laminate- see Figure 7.

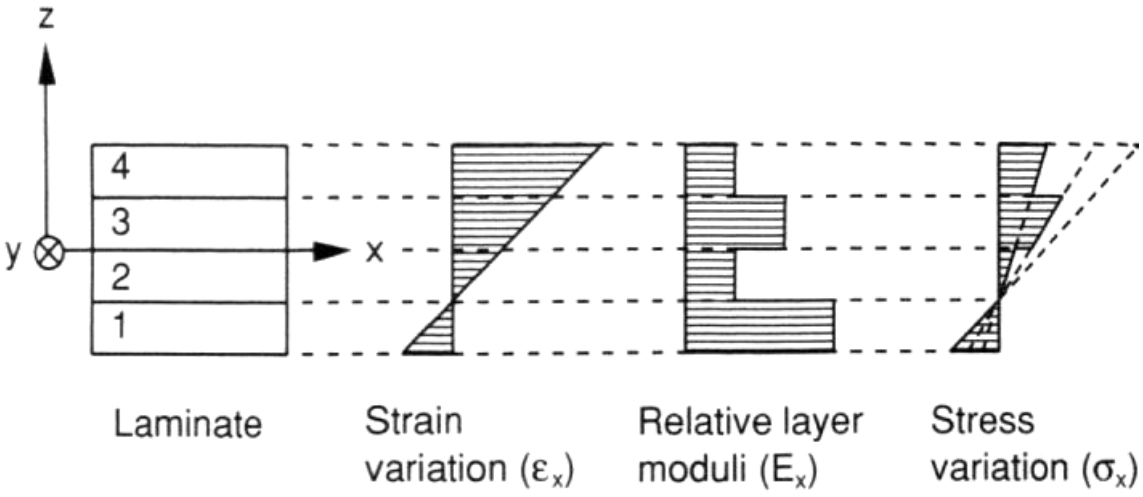

Figure 7. Illustration of linear strain variation and discontinuous stress variation in multidirectional laminate [2].

The stress strain relationship for each lamina is now differentiated from other lamina by the index k. This index represents the number of the layer as shown in Figure 7 and as shown below:

$$\begin{bmatrix}\sigma_x\\ \sigma_y\\ \tau_s\end{bmatrix} = \begin{bmatrix}Q_{xx} & Q_{xy} & Q_{xs}\\ Q_{yx} & Q_{yy} & Q_{ys}\\ Q_{sx} & Q_{sy} & Q_{ss}\end{bmatrix}_k \begin{bmatrix}\varepsilon_x^o\\ \varepsilon_y^o\\ \gamma_s^o\end{bmatrix} + z\begin{bmatrix}Q_{xx} & Q_{xy} & Q_{xs}\\ Q_{yx} & Q_{yy} & Q_{ys}\\ Q_{sx} & Q_{sy} & Q_{ss}\end{bmatrix}_k \begin{bmatrix}\kappa_x\\ \kappa_y\\ \kappa_s\end{bmatrix} \tag{32}$$

The force and moment resultants are obtained from the laminate constitutive relationship. This relationship is defined by obtaining a stiffness matrix that encapsulates all the directional stiffnesses and coupling thereof. This stiffness matrix is obtained by summing the ply stiffnesses in the laminate coordinate system through the thickness with respect to the thickness variations of each ply.

$$[A] = \sum_{K=1}^{N} \left[\overline{Q}_{x-y}\right]_k \left(z_k - z_{k-1}\right) \tag{33}$$

$$[B] = \frac{1}{2}\sum_{K=1}^{N} \left[\overline{Q}_{x-y}\right]_k \left(z_k^2 - z_{k-1}^2\right) \tag{34}$$

$$[D] = \frac{1}{3}\sum_{K=1}^{N}\left[\overline{Q}_{x-y}\right]_k \left(z_k^3 - z_{k-1}^3\right) \tag{35}$$

Since each lamina stiffness matrix is a 3x3 matrix, the [A], [B], and [D] are 3x3 matrices. These matrices are grouped together according to the order in which they are related to the in-plane and out-of-plane deformations (the mid-plane strains and curvatures). The resulting laminate stiffness matrix is given as follows:

$$ABD = \begin{bmatrix} [A] & [B] \\ [B] & [D] \end{bmatrix} = \begin{bmatrix} A & B \\ B & D \end{bmatrix} \tag{36}$$

Taking the inverse of the ABD matrix gives the laminate compliance matrix:

$$abd = \begin{bmatrix} [a] & [b] \\ [b^T] & [d] \end{bmatrix} = \begin{bmatrix} a & b \\ b^T & d \end{bmatrix} \tag{37}$$

The abd matrix is the compliance matrix of the laminate; the superscript T on the [b] matrix at abd(2,1) stands for transpose. From the ABD and abd matrices, the constitutive relationship of the laminate is defined with the in-plane and out-of-plane deformations.

$$\begin{bmatrix} N \\ M \end{bmatrix} = \begin{bmatrix} A & B \\ B & D \end{bmatrix} \cdot \begin{bmatrix} \varepsilon^o \\ \kappa \end{bmatrix} \tag{38}$$

$$\begin{bmatrix} \varepsilon^o \\ \kappa \end{bmatrix} = \begin{bmatrix} a & b \\ b^T & d \end{bmatrix} \cdot \begin{bmatrix} N \\ M \end{bmatrix} \tag{39}$$

The numerical routine for CLT was developed and run in MATLAB. By definition, in order to use CLT at least two plies must exist in the laminate. By using only two plies, none of the assumptions listed above are violated. Thus a two ply laminate is a valid laminate in which overall laminate behavior for thin laminates can be ascertained. There are only a few limiting situations, which will not appear here, where using two plies would not be sufficient for the purposes of this analysis. Two ply laminates will be

used for this analysis. There is no reason to add more plies for a thin laminate case. Furthermore, using only two plies isolates interlaminar effects on the stresses in the laminate. Having more than two plies couples at least one more ply into the overall effect of the interlaminar effects on stresses in the laminate. These cases are isotropic so any errors from the model being too thin are negated.

For the isotropic case, 6061-T6 Aluminum was used- see

. The $[0]_2$ stacking sequence was run using CLT on a two ply thick laminate. Each ply had a thickness of 0.005 inches. The thermal loading condition is $\Delta T = 100\ ^oF$. Since the MATLAB FEA code is the ultimate upshot of the verification process and FEA requires sufficient constraints in order for rigid body motion not to occur when loaded, the fixed-fixed (fixed-beam) case was analyzed using CLT. This enables a comparison with the FEA code which can be sufficiently constrained for a non-singular reduced global stiffness matrix. The cantilever problem is not evaluated using CLT because the fixed-beam problem provides a more rigorous challenge for validation.

The loading array must have an induced mechanical force N_x. This induced mechanical force is found by setting the mid-plane strain in the X-direction equal to zero (the beam is fixed in the X-direction and is not allowed to elongate or contract). The first row (equation) of the abd matrix is solved for the unknown N_x in terms of the compliances and the in- and out-of-plane deformations. The expression for N_x is:

$$N_X = -N_X^T - \frac{a_{12}}{a_{11}} N_Y^T \tag{40}$$

Note: All loads are the total loads due to $\Delta T = 100\ ^oF$. Units are standard English units

Table 4. Material properties for all 6061-T6 Aluminum cases from Table 3.

E1	1.00E+07
E2	1.00E+07
G	3.77E+06
v	0.33
alpha1	1.31E-05
alpha2	1.31E-05

abd					
1E-5	-3E-06	0	0	0	0
-3E-06	1E-5	0	0	0	0
0	0	2.7E-05	0	0	0
0	0	0	1.2	-3.96E-1	0
0	0	0	-3.96E-1	1.2	0
0	0	0	0	0	3.18302

Table 5. Total in-plane and out-of-plane loadings on the laminate.

Loadings		
N_x	64.5224	lb
Ny	195.522	lb
Ns	0	lb
Mx	0	lb*in
My	0	lb*in
Ms	0	lb*in

Table 6. In-plane and out-of-plane curvatures of the laminate.

	Mid-Plane Strains & Curvatures	
ε_x^o	0	in/in
ε_y^o	0.00174	in/in
γ_s^o	0	in/in
κ_x	0	1/in
κ_y	0	1/in
κ_s	0	1/in

Table 7. XY-plane stresses for laminate.

	Stresses		Units
	Layer 1	**Layer 2**	lb/in^2
σ_x	-13100	-13100	
σ_y	8.5E-13	8.5E-13	
τ_s	0	0	

2.2.3 Finite Element Method (FEM) Solution For Isotropic Flat Model

The MATLAB program was used to conduct the finite element analysis (FEA) for the isotropic flat beam. 5,120 elements were used with a laminate made out of 6061-T6 Aluminum with material properties given in Table 3. Each ply had a thickness of 0.005 inches, and an equivalent number of plies were used for the finite element (FE) model as was used in the CLT model. The element stresses (r,s,t) = (0,0,0) were collected along the mid-width of the beam for layers 1 and 2. In order to reduce shear stresses

in the beam due to geometry and negate the effect of Saint Venant's principal on the stresses, the beam's YZ-plane cross-section was chosen to be square; the beam was also chosen to be extremely long with respect to the depth and the width of the beam. The normalized ratio of beam's geometry was that the length to width ratio and the length to depth ratio were both 640 to 1. This puts the solution set of this problem into the assumptions used for beam theory and classical lamination theory. Without the exaggerated length to depth ratio of 640 to 1, the FE model can potential violate the plane stress assumption. The stress results for σ_x, σ_y, and τ_{xy}.

The figures have "spikes" at the fixed ends and at the mid-span of the beam. The "spikes" at the fixed end are due to edge effect and induced three dimensional stresses. The "spike" at the mid span is due to the shear strain not being constant at this point. It is well known that isoparametric elements notoriously develop spurious shear modes and "spikes" if the order of the interpolation function is not one order higher than the order variation of a given type of strain, in particular shear strain. Beams are also known to have shear strain that vary through thickness quadratically (order 2). Since the tri-linear isoparametric element used in the MATLAB FE program is of order 1, it would need to be 2 orders higher (or a tri-cubic isoparametric element) to sufficiently handle that shear mode. The consequential coupling of other strain modes via element connectivity causes a noticeable *bump* in the longitudinal stress plots as well.

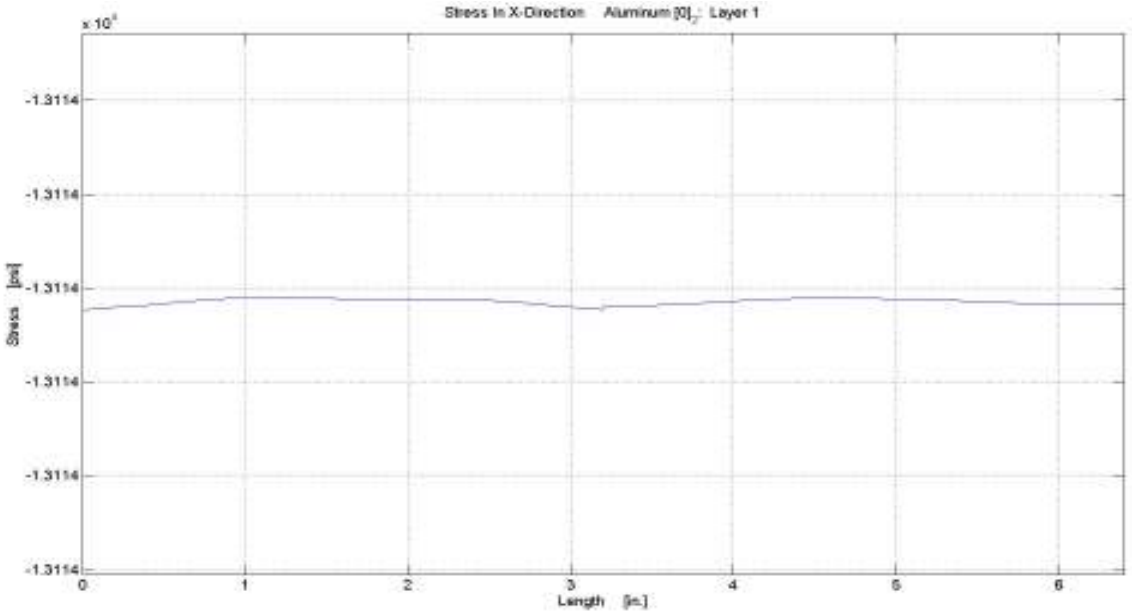

Figure 8. Stresses in the X-direction for isotropic flat beam, layer 1.

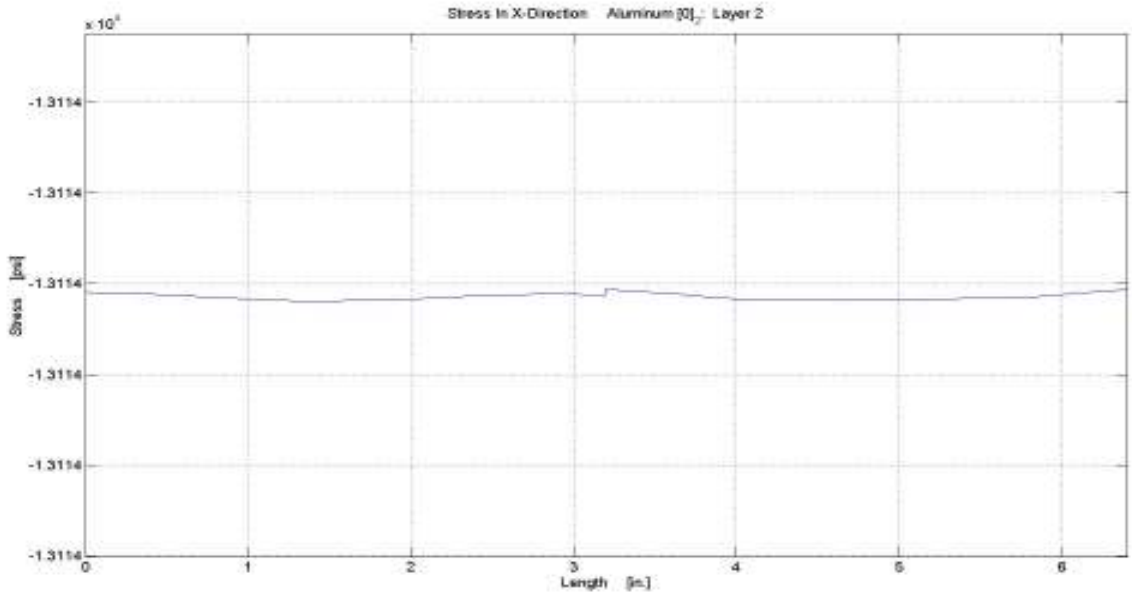

Figure 9. Stresses in the X-direction for isotropic flat beam, layer 2.

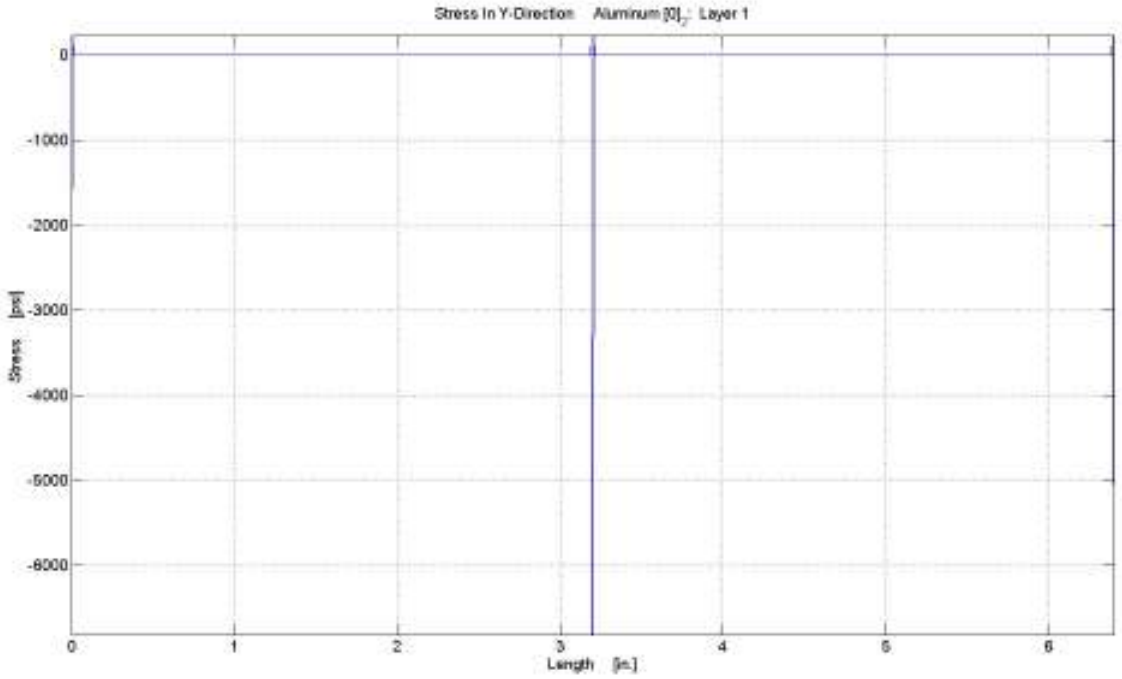

Figure 10. Stresses in the Y-direction for isotropic flat beam, layer 1.

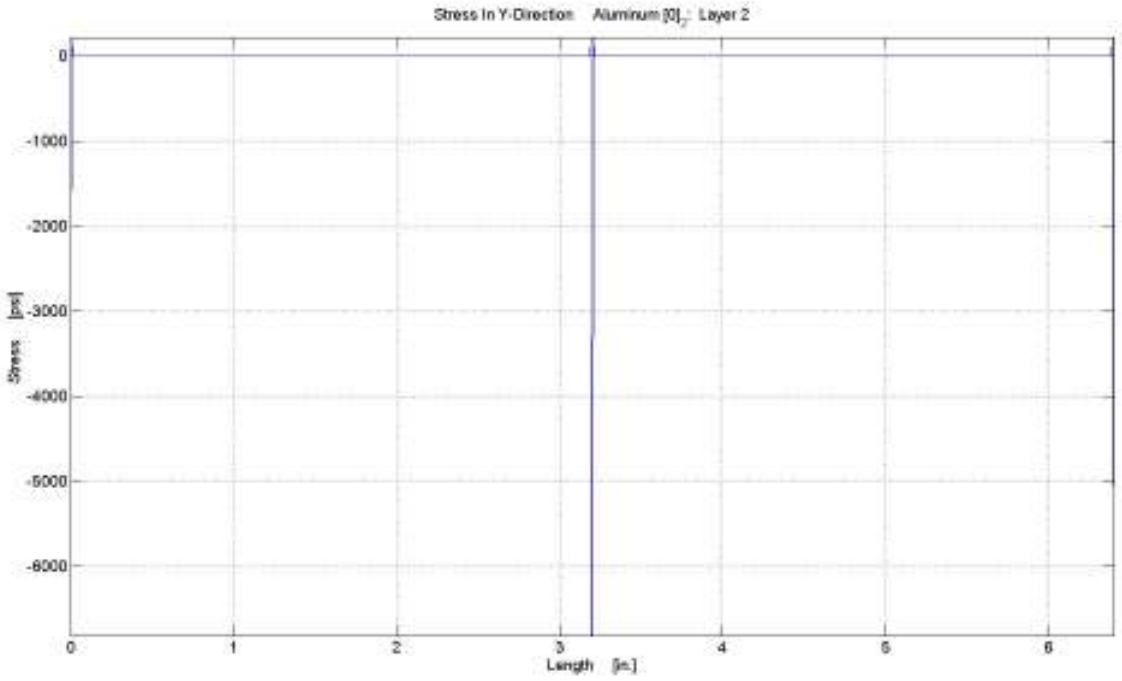

Figure 11. Stresses in the Y-direction for isotropic flat beam, layer 2.

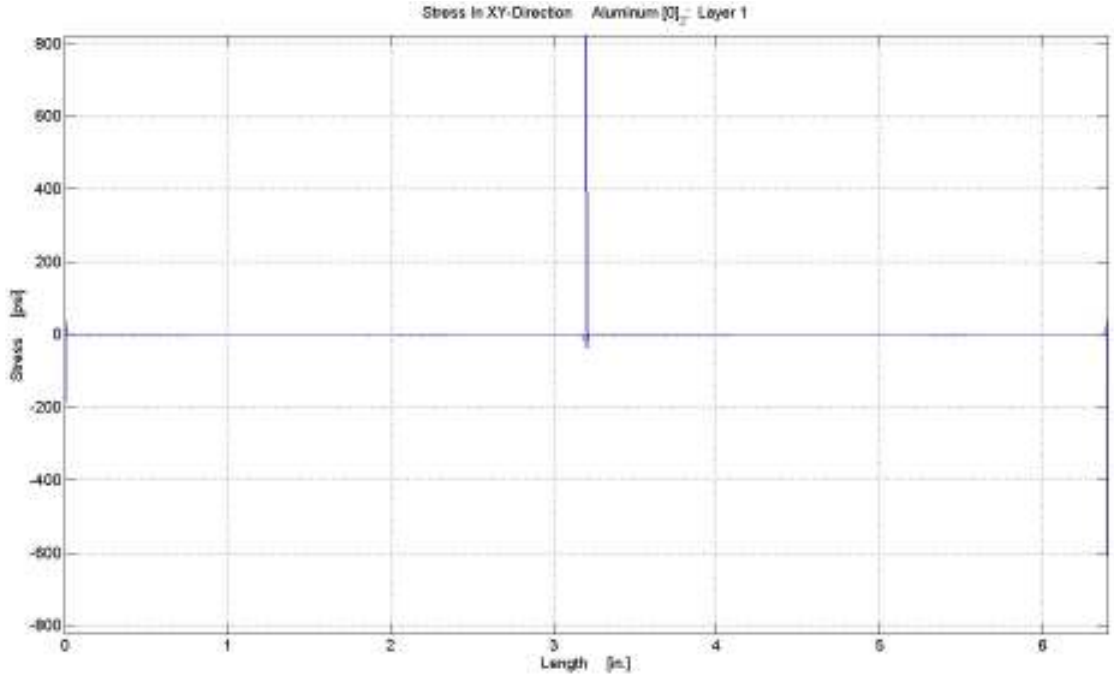

Figure 12. Stresses in the XY-direction for isotropic flat beam, layer 1.

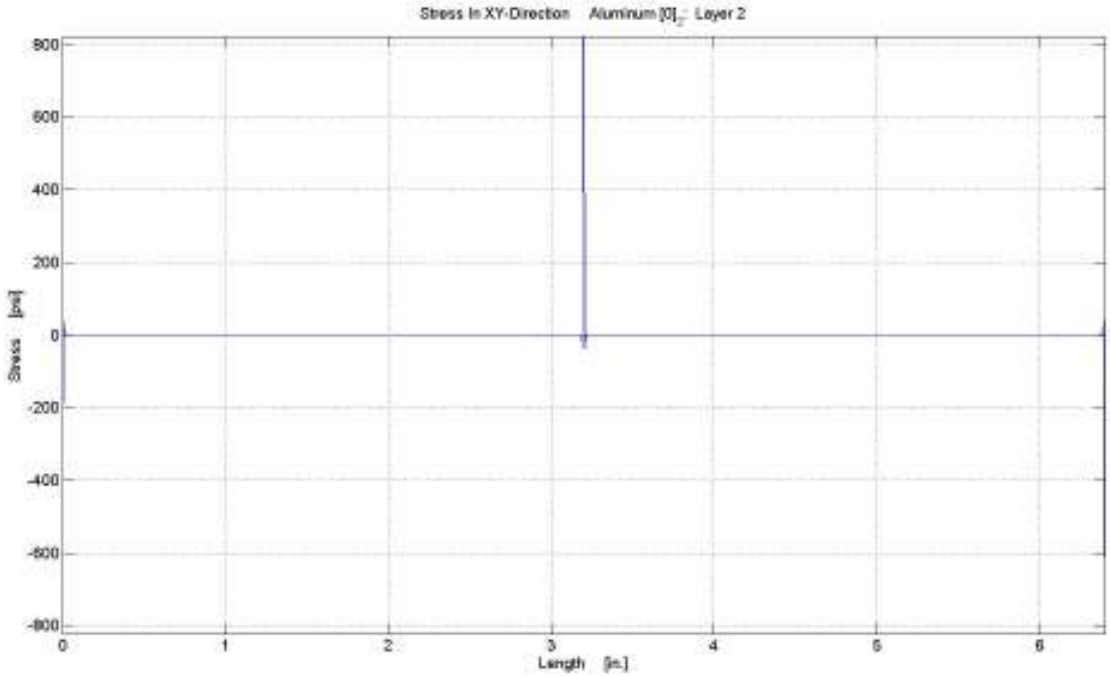

Figure 13. Stresses in the XY-direction for isotropic flat beam, layer 2.

2.2.4 Validation Of Finite Element Analysis Program For Flat Isotropic Model

The analytic beam theory solution, the classical lamination theory solution, and the MATLAB FEA program solution showed excellent agreement in the mutually calculated stresses. That is, the analytic beam theory solution does not have the shear stress τ_{xy} results but does have the σ_z. The classical lamination theory solution and the MATLAB FEA program solution do not have the σ_z result but does have the τ_{xy}. Therefore, the comparison is between the stresses that mutually coexist with respect to the three methods.

Table 8. Stress result comparison for layer 1 of flat isotropic beam. Units: lb/in^2

	Analytic Beam Theory	Classical Lamination Theory	MATLAB Finite Element
σ_x	-13100	-13100	-13114
σ_y	0	8.5E-13	-20.62 (median: 7.267e-12)
τ_{xy}	0	0	2.19e-12

Table 9. Stress result comparison for layer 2 of flat isotropic beam. Units: lb/in^2

	Analytic Beam Theory	Classical Lamination Theory	MATLAB Finite Element
σ_x	-13100	-13100	-13114
σ_y	0	8.50E-13	-20.62 (median: 5.457e-12)
τ_{xy}	0	0	2.19e-12

It can be seen from Table 8 and Table 9 that the MATLAB FEA program has been validated as being capable of providing accurate and precise (see median results of the transverse stresses) stress solution for flat isotropic beams.

2.2.5 Analytical Solution For Isotropic Curved Model

An analytical solution for the isotropic, simply curved (arc) beam under thermal loading does not exist to the best of the Author's knowledge. Many different types of curved beam solutions have been

developed for various loading conditions. The most prominent cases are those with bending moments in the plane of the curved beam at both ends of the beam. Fewer cases involve other simplistic schemes such as normal stresses to the cross-section of the beam due to hoop (circumferential) tension. These cases also include the bending moment (in the plane of the arc at both ends equal to zero) or shear stresses due to radial shear force. Other developments utilize the Airy stress potentials.

Most of these solutions have some type of inherent error in the stress results depending on how compact the cross-sections are, the ratio of the radius of curvature to the depth of the beam, the magnitude of the radius of curvature of the beam, the shape of the cross-section, the thickness of the webs relative to the flanges of the cross-sections, or some simple or complex combination thereof, etcetera. Other derivations leave out key factors such as neglecting the contribution of radial normal stress to the circumferential strain. Deformations due to normal forces and transverse shears have also been neglected in some formulations to facilitate easier stress solutions in curved beams. Others assume straight beam formulations for bending stress and shear stresses while neglecting the complex interactions that occur with curved beams which lead to minimum errors of four percent to five percent in stress results. The Airy stress formulation for the case of bending moments in the plane of the arc at both ends with equal magnitudes can lead to eight percent to nine percent error in stress results. Even more, some of the more demanding derivations require numerical methods for more accurate results (with minimum error) for terms of the stress result expressions or correction factors to account for curvature or cross-sections. Both are a sign that the methods do not yield accurate results due to inherent formulation and must be corrected after the fact or need additional effort to just ascertained minimum error in terms that compose of the stress result expressions. Even energy based methods for ascertaining stresses in curved beams are relatively (not absolutely) accurate if the curved beam is close to straight beam, that is the curved beam has a fairly large radius of curvature. Energy based methods for ascertaining stresses in curved beams that have fairly small radii of curvature require coupling terms to improve the accuracy. This is an implicit statement in the inherent inaccuracy of the solution. Even the more complex formulations require loadings to be geometrically simple; that is, all radial loads must be applied at the centroid.

What is meant by geometrically simple loadings is that the loading (for instance, bending moment) can be readily related to the geometry of the curved beam through various flexure and curvature formulations. It is natural for polar coordinate systems and can readily accommodate Cartesian coordinate systems. However, having one or more longitudinal loads (note: not an axial load that is perpendicular to a given cross-section) at an arbitrary location of the beam cannot be readily related to the beam using flexure or curvature formulations. These relationships are used to facilitate solutions (explicitly or implicitly) to beam problems where rectilinear beams are under bending moments in the plane of the beam or curved beams are under bending moments in the plane of the beam. Without geometrically simple loadings, ascertaining stress, strain, or displacement solutions for curved beams is extremely difficult if not even intractable.

These conditions are more demanding for thick beams. Even when a statically equivalent loading is applied to compensate for the off-axis loading, the primary loading must only be a bending moment at the ends of the beam in the plane of the arch. For thick beams, ignoring deformations due to axial tensions or compressions is not acceptable. Correction factors must be used again to compensate for inaccuracy inherent even in these more complex formulations because they can only be developed for geometrically simple loadings. Furthermore, the effect of radial stresses near concentrated loads is not accounted for. These stresses have appreciable effect on the maximum stresses and local deformations.

Some of the assumptions or neglected terms do not result in appreciable errors (greater than five percent) in the stress results. When solving a typical rectilinear beam problem, all these complications are generally not present for even the most complex combine loading situations. The greatest effort is usually in the time taken to solve the problem for stresses, not the effort required to solve the problem for stresses. This is just cursory survey of how difficult these problems become once curvature is added to the beams. They all have a similar theme, "Beware of the accuracy of your results"! Yet, the discussion in the previous two paragraphs concerning bending moment and axial force loading pales in comparison to the difficulty of the thermal loading problem. This problem for simply curved beams is deceptively difficult for statically determinant situations and seemingly intractably difficult for statically indeterminant

situations. This difficulty in coming up with an accurate formulation that is approximate (much more for a formulation that is exact) is the main reason that there is not a readily available close-form solution (exact solution) for the simply curved (arc) beam under thermal loading that is either statically determinant (free expansion in this case) or statically indeterminant (fixed in this case at the longitudinal ends of the arc-beam). As a result, most of these types of problems are solved using some form of numerical methods. The most predominant method by far is the finite element method (FEM).

Some have attempted to tackle this problem with varying levels of success. Since this thesis is on curved beams under thermal loading and not on curved beams under various axial and/or transverse loads with or without various bending moments, the Author will explicitly state these particular formulations by name, the assumptions, the pitfalls, and the resulting expressions.

Li and Zhao [3] studied a statically indeterminant beam used to model a bridge. They used the principal of thermal expansion and the theory of virtual work. Their goal was to ascertain the in-plane displacement of the beam (bridge) due to thermal loads. As can be seen from Figure 14, the thermal load create by a $\Delta T \neq 0$.

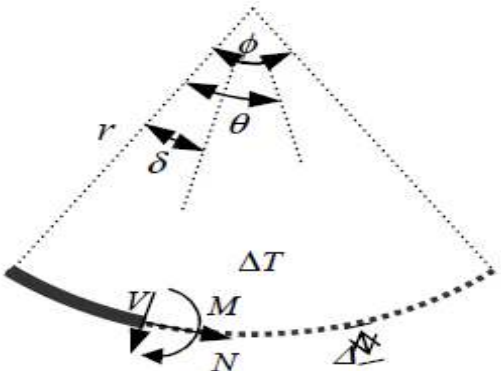

Figure 14. Li and Zhao curved beam under thermal loading.

An element of length ds was cut out from the curved beam. This element's elongation will rotate $\varepsilon_t ds$ where $\varepsilon_t = \alpha(\Delta T)$. The element will rotate through an angle $\eta_t ds$, where η_t is the curvature of the

rotation. The angle spanned by the element of length ds is δ, where $\theta < \delta < \phi$. The cut in the beam occurs at the right end of θ. They calculated the total work done by a thermal load of $\Delta T \neq 0$ by calculating the work from the axial force perpendicular to the cross-section of the element through its extension of $\varepsilon_t ds$ to the left of the cut and to the right of the cut. This was combined with the work from the moments in the plane of the curved beam through its rotation of $\eta_t ds$ to the left of the cut and to the right of the cut. The expression for the total work from the left end of the cut due to axial force and in-plane moment and from the right end of the cut is given by Equation (41):

$$\Delta_T = \int_0^{\theta} N_{1L}\varepsilon_t ds + \int_{\theta}^{\phi} N_{1R}\varepsilon_t ds + \int_0^{\theta} M_{1L}\eta_t ds + \int_{\theta}^{\phi} M_{1R}\eta_t ds \tag{41}$$

where N_{1L} = axial force to the left of the cut, N_{1R} = axial force to the right of the cut, M_{1L} = moment to the left of the cut, and M_{1R} = moment to the right of the cut.

The solution for a number of boundary conditions was calculated using this analytical approach and compared with an equivalent FEM model- see Figure 15, Figure 16, and Figure 17.

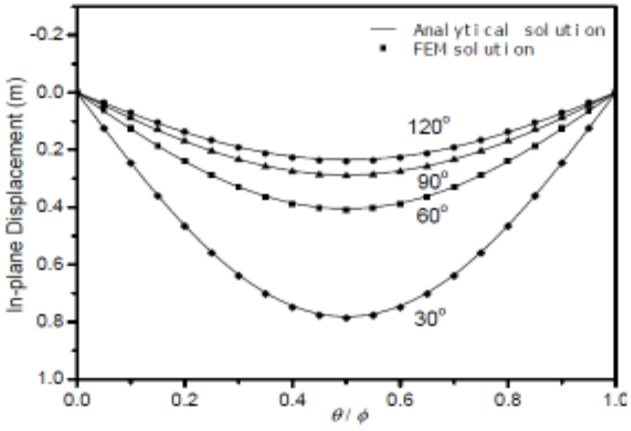

Figure 15. Curved beam with pinned-pinned ends.

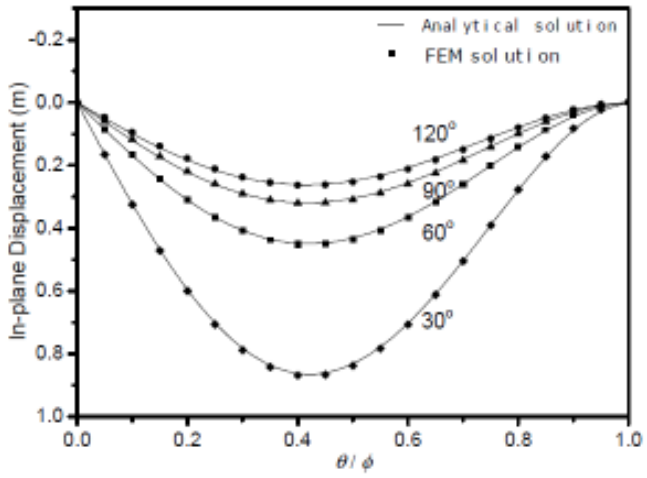

Figure 16. Curved beam with pinned end on left side and clamped in on right side.

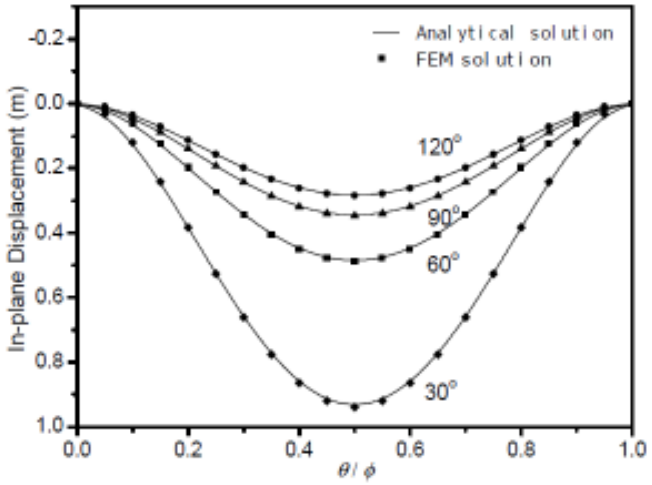

Figure 17. Curved beam with clamped-clamped ends.

The first thing that stands out about Li and Zhao results is the remarkable coincident in analytical results with FEM results. FEM results are trivially known to be a close approximation to the real (exact) solution if modeled properly. For the analytical results to match exactly with the FEM results leads to one of two conclusions:

(1) The analytical solution coincides with a remarkably accurate finite element (FE) model. The FE model is able to very accurately represent the problem.

(2) There are sufficient errors in either the FE model and/or the analytical solution for such a convergence to occur without consequences of uniquely and severely flawed data and analysis. If there are errors, this would imply that the analytical solution is not exact. The lack of exactness or precision in the results would be eerily similar to a completely different method (FE model)- an unusual coincidence.

The Author has no way of examining the FE code and model used to verify the analytical solution given by Li and Zhao. Nevertheless, the goal of their work was to calculate the in-plane displacement in the direction of the shear force V. Yet their analytical solution only takes into account axial forces perpendicular to the cross-sections of the beam and the moments in the plane of the beam. No shear forces are accounted for. Furthermore, the model does not account for the fact that the axial force at each differential segment of the arc of the beam will be different in magnitude and direction relative to its neighbors as this is not a straight beam but a curved beam. The same goes for the in-plane moment. Such can be assumed for a straight beam. However, for a curved beam, even though the cross-sections of the beam remain perpendicular to the centroidal axis of a given differential segment, it is not plane to the other differential segments to it respective left or right. This must be accounted for and is not in Li's and Zhao's analysis. With these glaring omissions and the eerily coincidental nature of the FE results and the analytical solution leads the Author to conclude that these results are not as good as Li and Zhao claimed and their plots are suspect. Li and Zhao claimed that their displacement converge to the straight beam problem displacements as the radius of curvature tends to infinity, a must. This is a necessary condition, but it is not a sufficient condition.

Hetnarski, Noda, and Tanigawa [9] also tackled stresses in a curved beam due to thermal loading. This curved beam is not a simply curved beam whose span can be defined as an arc. It is more of a straight beam that has been curved. In other words, it is not an arc beam with simple curvature that is symmetric

about its mid-span but a beam that is curved. Li and Zhao used a minimum potential energy based method to develop their analytical model. Hetnarski, Noda, and Tanigawa used the same assumptions of the theory of straight beams and basic geometric relationship between line segments with respect to a given radius of curvature of a beam with curvature before thermal loading and a new radius of curvature after thermal loading- see Appendix B. They also use basic thermal strain and constitutive relationships. Equation (42), Equation (43), Equation (44), and Equation (45) is the result for the tangential stresses:

$$\sigma_{\theta\theta} = -\alpha E(\Delta T) + \frac{1}{A}\left\{ N + \frac{M}{R}\left[1 + \frac{y}{\kappa(R+y)} \right] \right\} + \frac{E}{R+y}\int_0^y \alpha(\Delta T)dy \tag{42}$$

$$N = \int_A \alpha E(\Delta T)dA - \int_A \frac{E}{R+y}\left[\int_0^y \alpha(\Delta T)dy \right]dA \tag{43}$$

$$M = \int_A \alpha E(\Delta T)ydA - \int_A \frac{Ey}{R+y}\left[\int_0^y \alpha(\Delta T)dy \right]dA \tag{44}$$

$$\kappa = -\frac{1}{A}\int_A \frac{y}{R+y}dA \tag{45}$$

where y = distance above the center line, α = coefficient of linear thermal expansion, ΔT = change in temperature, A = cross sectional area, R = initial radius of curvature before thermal loading

However, this method is not sufficient for the purposes of this thesis. First, this method only allows the definition of tangential stresses. There is no definition for the radial stresses. In a beam with curvature under thermal loading, the material in the beam is not free to fully expand and will develop stresses. This is not accounted for in the model. Furthermore, the beam does not experience expansion in the radial direction. Only the tangential location of the outside face of the curved beam is altered by the thermal loading. In essence, the beam modeled is a beam with curvature whose thickness dimensions does not change. Only the curvature of the beam changes along with the angle of the cross-sectional areas, while a straight line segments perpendicular to the centerline remain straight and perpendicular to the center line. This is best used for smart materials whose dimensional changes under thermal loading are

small or negligible but the curvature changes aren't. For these reasons, this model is not sufficient to use nor its paradigms useful in model simply curved beams under thermal loading.

As previously stated, there are no readily available analytical solutions for a simply curved beam that is statically determinant (and much less statically indeterminant) under thermal loading- concerning stresses. Therefore, the Author developed a completely unique analytical solution for a simply curved beam that is statically determinant and statically indeterminant.

To solve the statically determinant problem, the Author developed the free-free case for the simply curved beam. That is, the statically determinant problem is a free expansion problem. To develop the solution to this problem, the beam is partitioned into infinitesimal segments along the length. Two cases are solved independently. The first case is the expansion through the thickness direction. The second case is the expansion through the longitudinal direction.

For the first case, the segments are virtually separated to show how they elongate through the thickness direction- see Figure 18. At the top and bottom surfaces of the beam, it is trivially known that the free surfaces of the beam will expand without any restriction- see Figure 19. However, the internal boundaries between two segments will not be allowed to expand freely. Yet, since both sections A and B (see Figure 20) expand the same amount, there are no mechanical forces caused by the boundary of sections A or B to enforce equal displacement at their mutual boundary. As the differential segments' length tend to zero, the two segments can be defined as super infinitesimally small single segment whose length is sufficiently large to define an interface but small enough to no longer be considered two separate segments or even one union segment- see Figure 20.

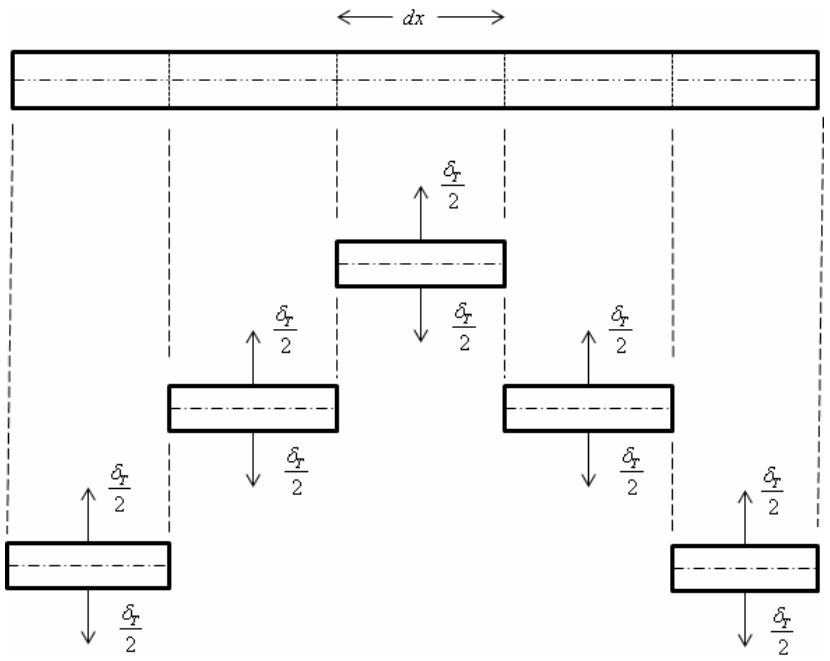

Figure 18. Representative flat beam model separated into differential segments with expansion in the thickness direction.

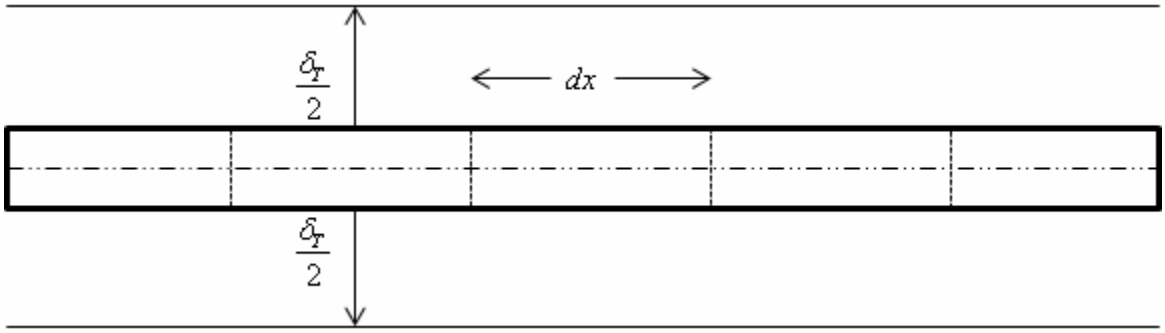

Figure 19. Representative flat beam model separated into differential segments with expansion in the thickness direction. The overall elongation in the thickness direction for differential sections is shown.

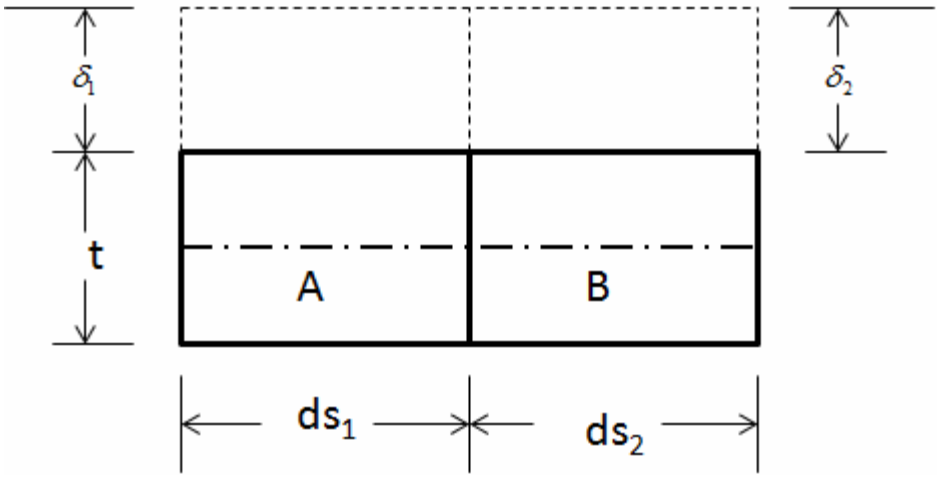

Figure 20. Two differential segments are shown only with the expansion from the top half of the surface.

For the second case, the segments are virtually separated to show how they elongate through the longitudinal direction- see Figure 21. At the left and right ends of the beam, it is trivially known that the free ends of the beam will expand without any restriction- see Figure 22. However, the internal boundaries between two segments will not be allowed to expand freely. Yet, since both sections A and B (see Figure 23) expand the same amount but in different directions at their mutual boundary, their mutual expansions cancel each other out. As a result, no mechanical loads are generated at the interface of the boundary of sections A and B. No mechanical loads are generated at the left and right ends of sections A and B- see Figure 21, Figure 22, and Figure 23. As the differential segments' length tend to zero, the two segments can be defined as super infinitesimally small single segment whose length is sufficiently large to define an interface but small enough to no longer be considered two separate segments or even one union segment- see Figure 23. It can be seen that for straight beams, elongation under a thermal loading occurs only at the ends of the beam. There are no elongations from the internal sections of the beam because each infinitesimal segment's elongation cancels out its neighbors' elongation.

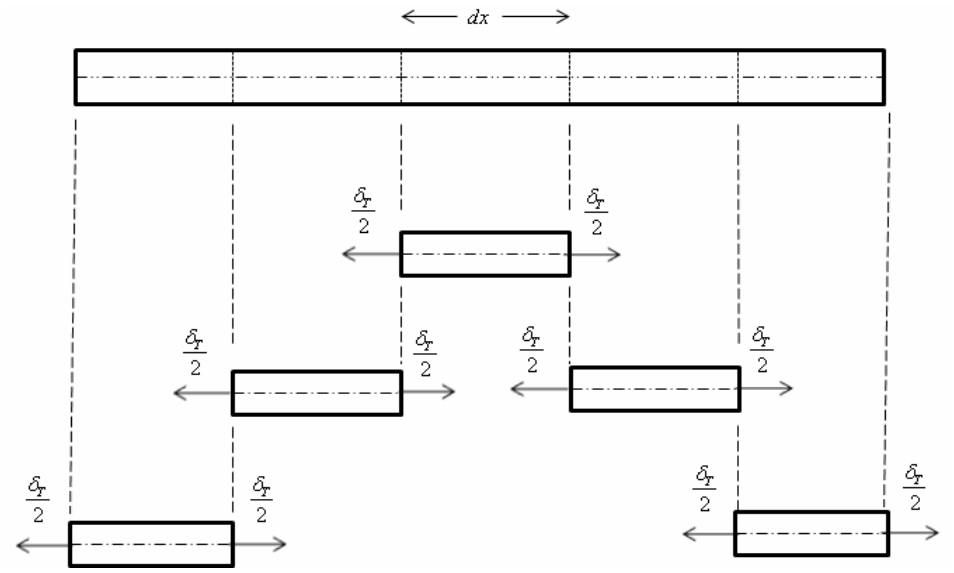

Figure 21. Representative flat beam model separated into differential segments with expansion in the longitudinal direction.

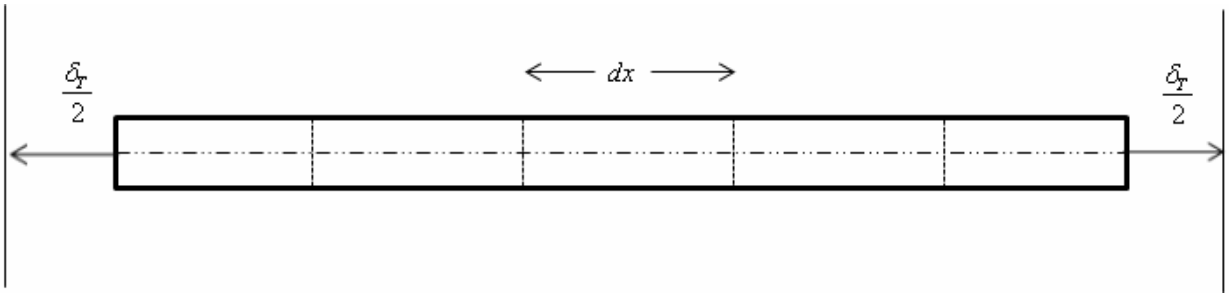

Figure 22. Representative flat beam model separated into differential segments with expansion in the thickness direction. The overall elongation in the longitudinal direction for differential sections is shown.

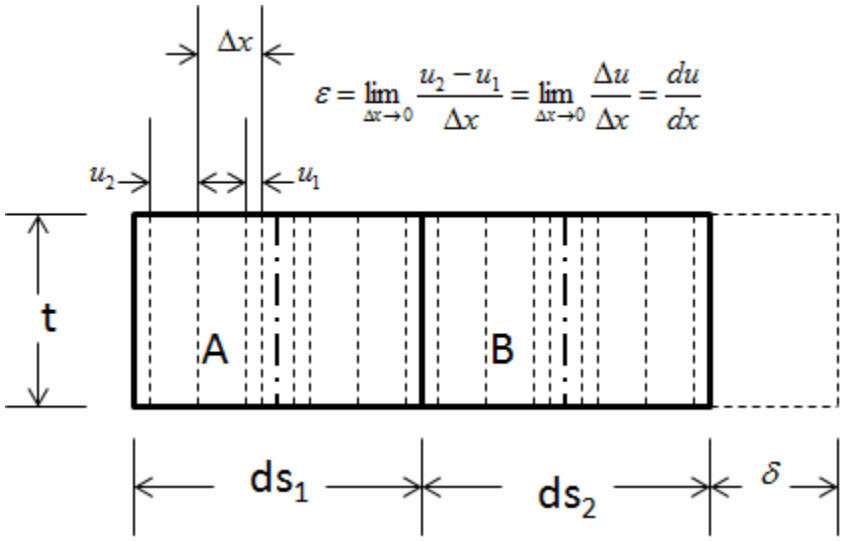

Figure 23. Two differential segments are shown only with the expansion from the right half segment B and the internal deformations.

The straight beam was expanded to the curved beam case. A free body diagram equivalent for each segment was developed to relate the coefficients of linear thermal expansion in the local longitudinal and thickness directions to that in the global Cartesian coordinate system. These coefficients of linear thermal expansion in the global Cartesian coordinate system become effective coefficients of linear thermal expansion for those two segments as the limit of the length of each segment tends to zero. This is not an actual coefficient of linear thermal expansion but an equivalent coefficient of linear thermal expansion. Two consecutive infinitesimal elements were taken from the right hand side from Figure 24 and Figure 25. By definition any curve, whether a path, trajectory, shape, etcetera, is composed of elementary straight line segments. This is by the definition of a line segment, the straight line between two points. That is every curved shape consists of a series of extremely small infinitesimal straight line segments. Any curved segment, no matter how small, can be resolved into even smaller straight line segments. Therefore, by the fundamental definitions of geometry Figure 24 and Figure 25 as straight line segments accurately represents extremely infinitesimal segments of a curve such that the curved segments are now straight line segments. As the segments become even smaller, the straight lines segments collapse to the minimum length straight line segments such that the boundaries between two segments becomes an interface region.

A series of these interfacial regions that are equidistance from some reference point (the center of curvature) form the simply curved beam.

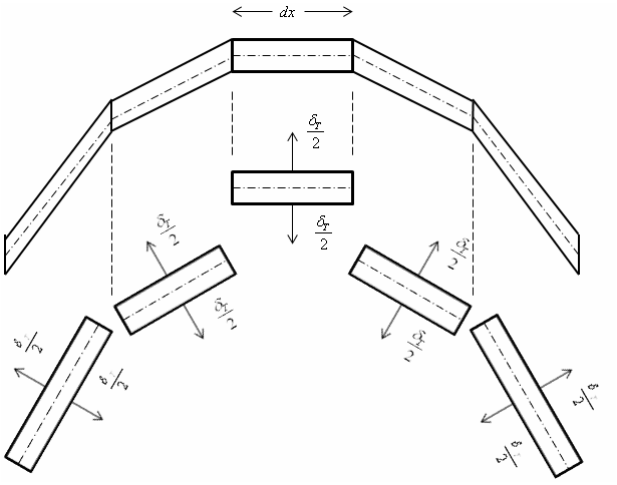

Figure 24. Representative curved beam model separated into differential segments with expansion in the thickness direction.

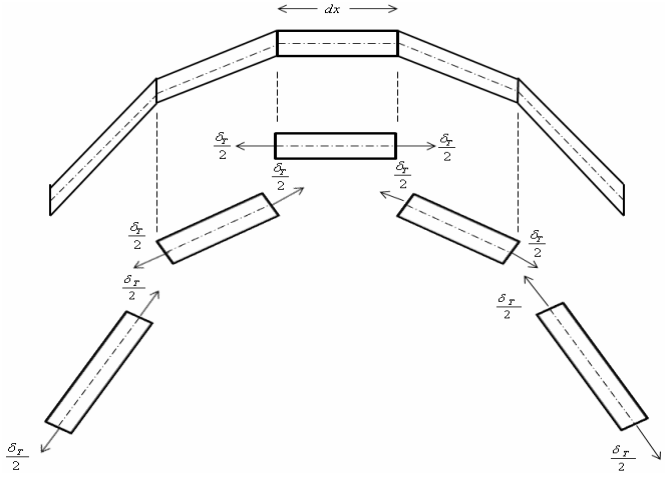

Figure 25. Representative curved beam model separated into differential segments with expansion in the longitudinal direction.

A free body diagram equivalent for each segment is that which relates the coefficients of linear thermal expansion in the local longitudinal and thickness directions to that in the global Cartesian coordinate system is shown in Figure 26.

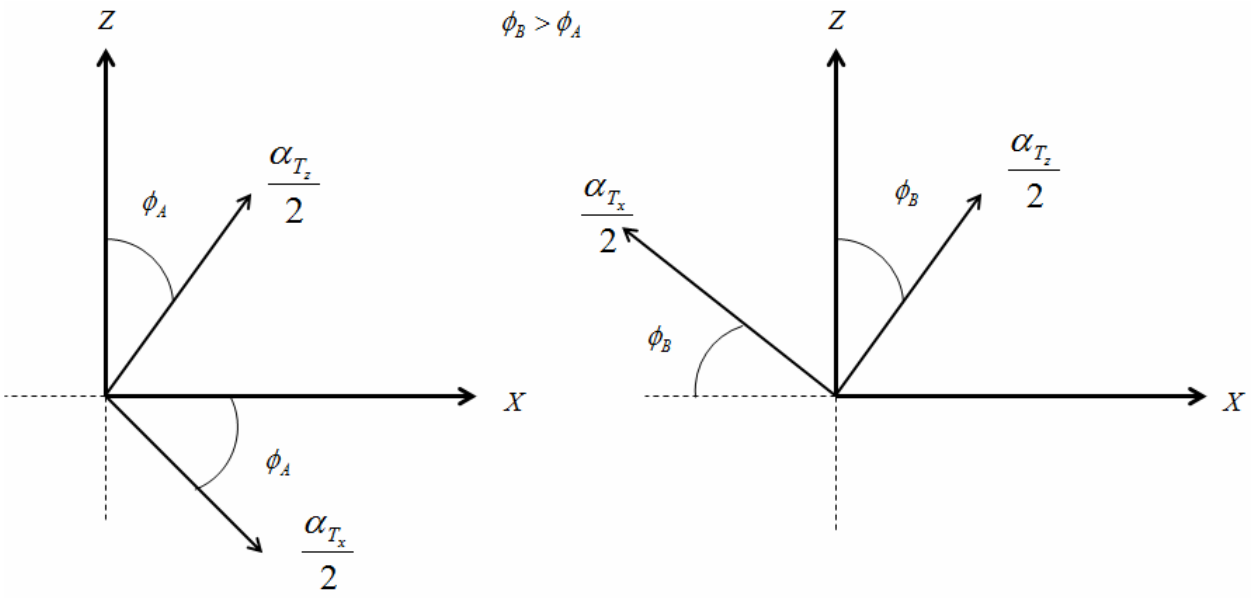

Figure 26. Free body diagram equivalent for two consecutive elements that relates the coefficients of linear thermal expansion. Upper half of segments A and B.

The angles ϕ_B and ϕ_A are the angles of segments B and A, respectively, with respect to the global Cartesian coordinate system (X, Z). On the right side of the arc, it is apparent that segment B is always at a larger angle than segment A. This diagram is for the upper half of both segments A and B. As the segments length tends to zero, the segments become extremely small, and are approximated as interfaces. The coefficients of linear thermal expansion from each segment coalesce into an effective coefficient of linear thermal expansion.

The effective coefficient of linear thermal expansion in the X-direction is given by the following expression:

$$\frac{\alpha_{T_X}}{2}\cos(\phi_A)-\frac{\alpha_{T_X}}{2}\cos(\phi_B)+\frac{\alpha_{T_Z}}{2}\sin(\phi_A)+\frac{\alpha_{T_Z}}{2}\sin(\phi_B)$$

The effective coefficient of linear thermal expansion in the Z-direction is given by the following expression:

$$-\frac{\alpha_{T_X}}{2}\sin(\phi_A)+\frac{\alpha_{T_X}}{2}\sin(\phi_B)+\frac{\alpha_{T_Z}}{2}\cos(\phi_A)+\frac{\alpha_{T_Z}}{2}\cos(\phi_B)$$

Grouping terms and expressing the above expression in the form of two equations gives:

$$\overline{\alpha}_{T_X}=\frac{1}{2}\left\{\frac{\alpha_{T_X}}{2}\left[\cos(\phi_A)-\cos(\phi_B)\right]+\frac{\alpha_{T_Z}}{2}\left[\sin(\phi_A)+\sin(\phi_B)\right]\right\} \tag{46}$$

$$\overline{\alpha}_{T_Z}=\frac{1}{2}\left\{\frac{\alpha_{T_X}}{2}\left[\sin(\phi_B)-\sin(\phi_A)\right]+\frac{\alpha_{T_Z}}{2}\left[\cos(\phi_A)+\cos(\phi_B)\right]\right\} \tag{47}$$

Note: the additional one-half term in the above equations is for the effective coefficient of linear thermal expansion because the expansion from segments A and B are being summed. Hence, the average is the expression divided by two.

In matrix form:

$$\begin{Bmatrix}\overline{\alpha}_{T_X}\\ \overline{\alpha}_{T_Z}\end{Bmatrix}_{UPPER}=\frac{1}{4}\begin{bmatrix}\cos(\phi_A)-\cos(\phi_B) & \sin(\phi_A)+\sin(\phi_B)\\ \sin(\phi_B)-\sin(\phi_A) & \cos(\phi_A)+\cos(\phi_B)\end{bmatrix}\begin{Bmatrix}\alpha_{T_X}\\ \alpha_{T_Z}\end{Bmatrix} \tag{48}$$

A free body diagram equivalent for each segment is that which relates the coefficients of linear thermal expansion in the local longitudinal and thickness directions to that in the global Cartesian coordinate system for the first case is shown in Figure 27.

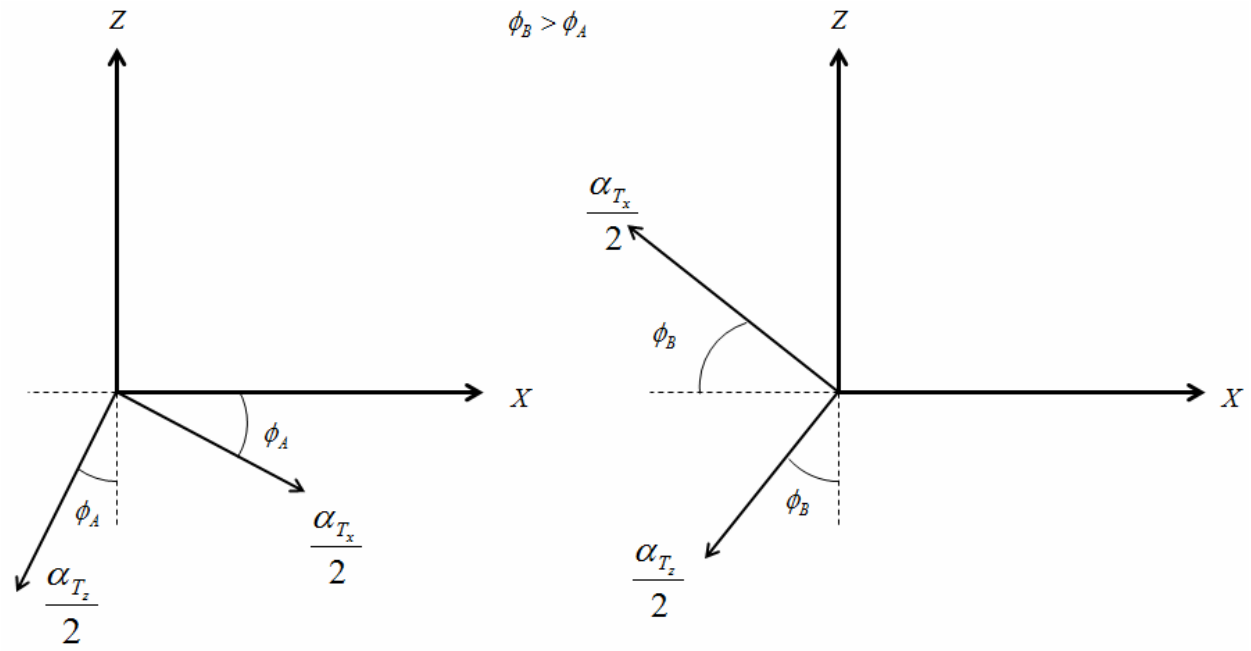

Figure 27. Free body diagram equivalent for two consecutive elements that relates the coefficients of linear thermal expansion. Lower half of segments A and B.

The angles ϕ_B and ϕ_A are the angles of segments B and A, respectively, with respect to the global Cartesian coordinate system (X, Z). On the right side of the arc, it is apparent that segment B is always at a larger angle than segment A. This diagram is for the lower half of both segments A and B. As the segments length tends to zero, the segments become extremely small, and are approximated as interfaces. The coefficients of linear thermal expansion from each segment coalesce into an effective coefficient of linear thermal expansion.

The effective coefficient of linear thermal expansion in the X-direction is given by the following expression:

$$\frac{\alpha_{T_X}}{2}\cos(\phi_A) - \frac{\alpha_{T_X}}{2}\cos(\phi_B) - \frac{\alpha_{T_Z}}{2}\sin(\phi_A) - \frac{\alpha_{T_Z}}{2}\sin(\phi_B)$$

The effective coefficient of linear thermal expansion in the Z-direction is given by the following expression:

$$-\frac{\alpha_{T_X}}{2}\sin(\phi_A)+\frac{\alpha_{T_X}}{2}\sin(\phi_B)-\frac{\alpha_{T_Z}}{2}\cos(\phi_A)-\frac{\alpha_{T_Z}}{2}\cos(\phi_B)$$

Grouping terms and expressing the above expression in the form of two equations gives:

$$\overline{\alpha}_{T_X}=\frac{1}{2}\left\{\frac{\alpha_{T_X}}{2}\left[\cos(\phi_A)-\cos(\phi_B)\right]+\frac{\alpha_{T_Z}}{2}\left[-\sin(\phi_A)-\sin(\phi_B)\right]\right\} \tag{49}$$

$$\overline{\alpha}_{T_Z}=\frac{1}{2}\left\{\frac{\alpha_{T_X}}{2}\left[\sin(\phi_B)-\sin(\phi_A)\right]+\frac{\alpha_{T_Z}}{2}\left[-\cos(\phi_A)-\cos(\phi_B)\right]\right\} \tag{50}$$

Note: the additional one-half term in the above equations is for the effective coefficient of linear thermal expansion because the expansion from segments A and B are being summed. Hence, the average is the expression divided by two.

In matrix form:

$$\begin{Bmatrix}\overline{\alpha}_{T_X}\\ \overline{\alpha}_{T_Z}\end{Bmatrix}_{LOWER}=\frac{1}{4}\begin{bmatrix}\cos(\phi_A)-\cos(\phi_B) & -\sin(\phi_A)-\sin(\phi_B)\\ \sin(\phi_B)-\sin(\phi_A) & -\cos(\phi_A)-\cos(\phi_B)\end{bmatrix}\begin{Bmatrix}\alpha_{T_X}\\ \alpha_{T_Z}\end{Bmatrix} \tag{51}$$

The next step is to ascertain how these effective coefficients of linear thermal expansion and elongations vary with a beam that is simply curved. MATLAB is used again for the numerical calculation of the effective coefficients of linear thermal expansion and elongations with a beam that is simply curved. For this situation the simply curved beam sweeps an angle of 180 degrees, 90 degrees on either side of the midsection of the beam. The test material was 6061-T6 Aluminum- see

, Figure 28,

Figure 29, Figure 30, and Figure 31.

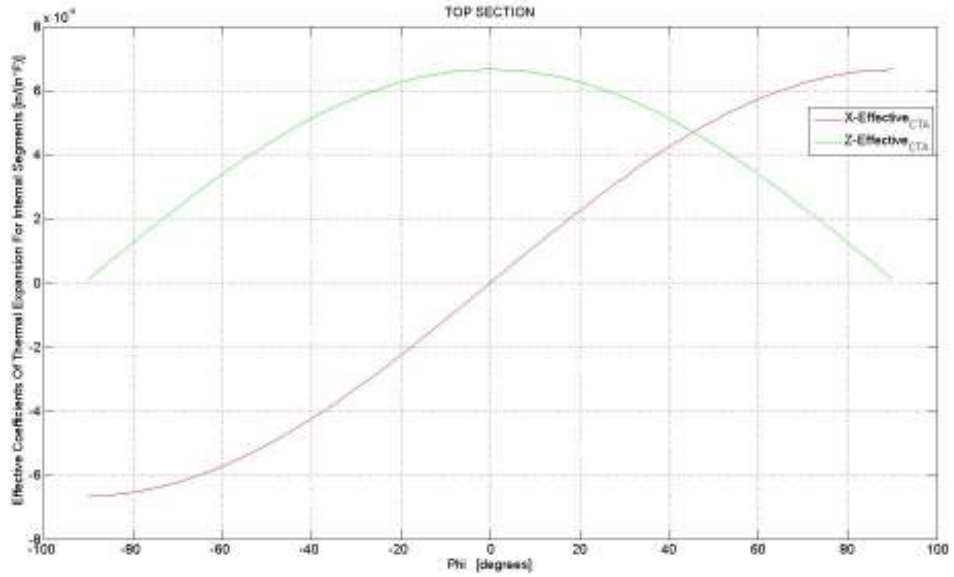

Figure 28. Effective coefficient of linear thermal expansion for internal segments for the top section of consecutive segments.

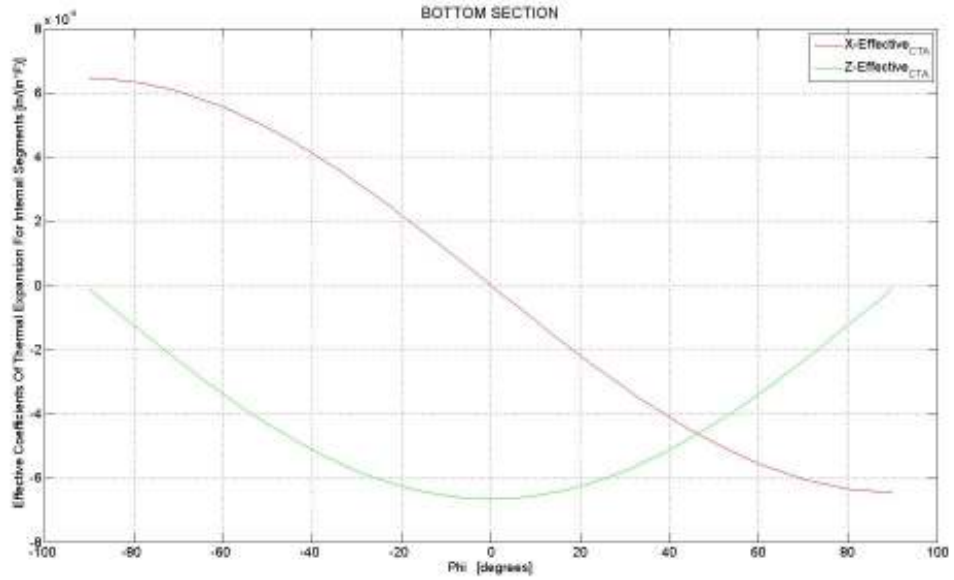

Figure 29. Effective coefficient of linear thermal expansion for internal segments for the bottom section of consecutive segments.

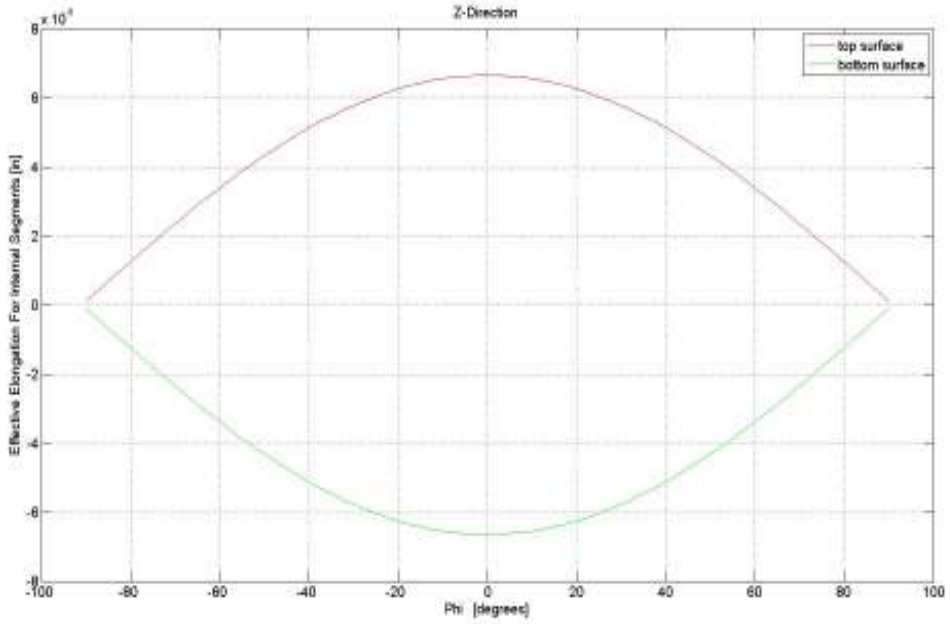

Figure 30. Effective elongation for internal segments for the bottom and top surfaces using a unit change in temperature and a unit reference dimension. Z-Direction.

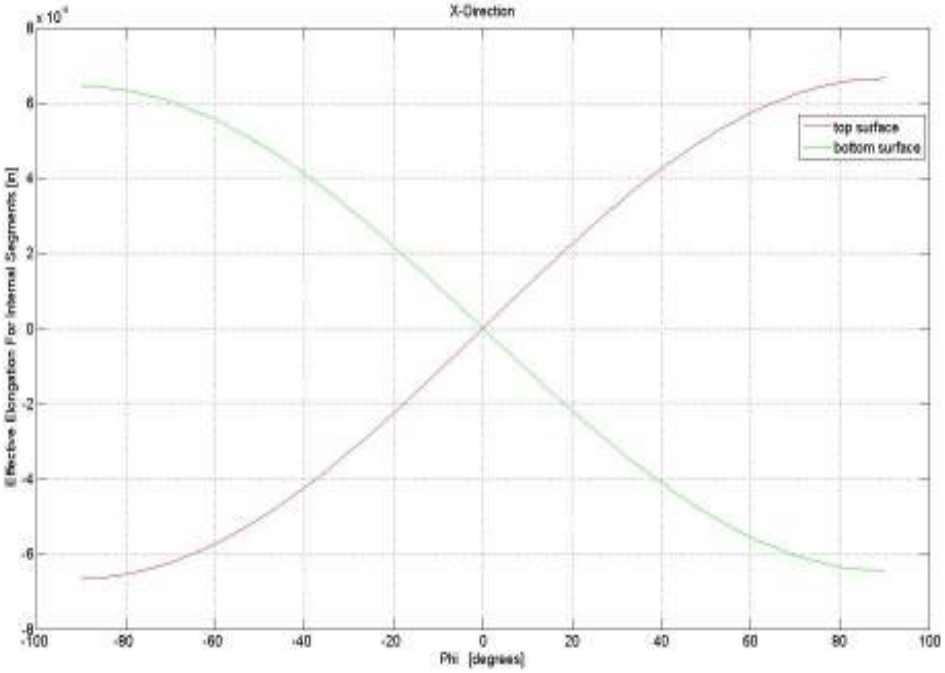

Figure 31. Effective elongation for internal segments for the bottom and top surfaces using a unit change in temperature and a unit reference dimension. X-Direction.

From Figure 28 and

Figure 29, take the starting point as the midsection of the simply curved beam. Progressing in the positive phi direction, the effective coefficient of linear thermal expansion in the Z-direction for every segment A is higher in absolute magnitude than the subsequent segment B. Flipping this relationship across the 0 degree (midsection) of the simply curved beam shows the same trend. That is, there is an effective non-uniform variation in the coefficient of linear thermal expansion the Z-direction for the simply curved beam. Even though the heating in the beam is uniform, it has a non-uniform heating like effect. Taking the starting points as the midsection of the simply curved beam again shows interesting results for the effective coefficient of linear thermal expansion in the X-direction too. Progressing in the positive phi direction, the effective coefficient of linear thermal expansion in the X-direction for every segment A is lower in absolute magnitude than the subsequent segment B. Flipping this relationship across the 0 degree (midsection) of the simply curved beam shows the same trend. That is, there is an effective non-uniform variation in the coefficient of linear thermal expansion in the X-direction for the simply curved beam.

Timoshenko [10] states that expansions and contraction under these types of conditions (in this case a pseudo non-uniform heating effect) does not allow the expansion or contraction to proceed freely in a continuous body. This results in the generation of stresses. Looking at Figure 28,

Figure 29, Figure 30, Figure 31 in the manner as previously discussed, shows that the simply curved, free-free beam will generate stress under thermal loading. For a flat, free-free beam under thermal loading, there would be no stresses.

The next step is to derive an expression for the stresses in the global Cartesian coordinate system (X, Z). The first case will be that of effective expansion through thickness direction. As shown by Figure 28,

Figure 29, Figure 30, segment A will have a higher effective expansion than segment B- see Figure 32 and Figure 33. Now, we began to take the infinitesimal segments A and B as ds_1 and ds_2 tend to

zero such that the combined lengths of both segments form an effective interface but still have an extremely small, infinitesimal length. With this configuration, the common nodes shared by segments A and B aren't compatible. That is, the common node has been separated as can be seen by the difference in height of the dashed lines. For this to happen in a real structure or part, the interface between segments A and B would have to break and tear in shear under an infinitesimally small thermal loading. Therefore, this incompatibility problem must be solved using temperature-displacement relationships, force-displacement relationships, compatibility equations, and equilibrium equation- see Equation (52), Equation (53), Equation (54), Equation (55), Equation (56), and Equation (57).

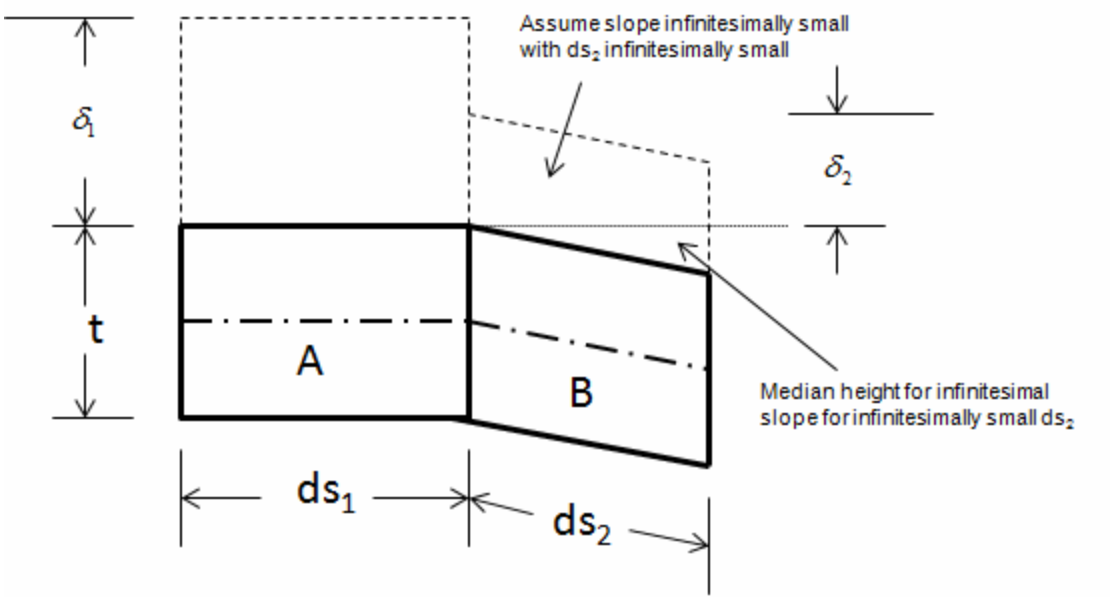

Figure 32. Representative model of two consecutive segment experiencing differential expansion due to variance in effective coefficient of linear thermal expansion in the Z-direction.

Temperature-displacement:

$$\delta_1 = \alpha_A(\Delta T)t \tag{52}$$

$$\delta_2 = \alpha_B(\Delta T)t \tag{53}$$

Force-displacement:

$$\delta_3 = \frac{P_A t}{E_A A_A} \tag{54}$$

$$\delta_4 = \frac{P_B t}{E_B A_B} \tag{55}$$

Compatibility equation:

$$\begin{aligned} \delta &= \delta_1 - \delta_3 = \delta_2 + \delta_4 \\ \alpha_A(\Delta T)t - \frac{P_A t}{E_A A_A} &= \alpha_B(\Delta T)t + \frac{P_B t}{E_B A_B} \end{aligned} \tag{56}$$

Equation of equilibrium:

$$P_A - P_B = 0 \rightarrow P_A = P_B = P \tag{57}$$

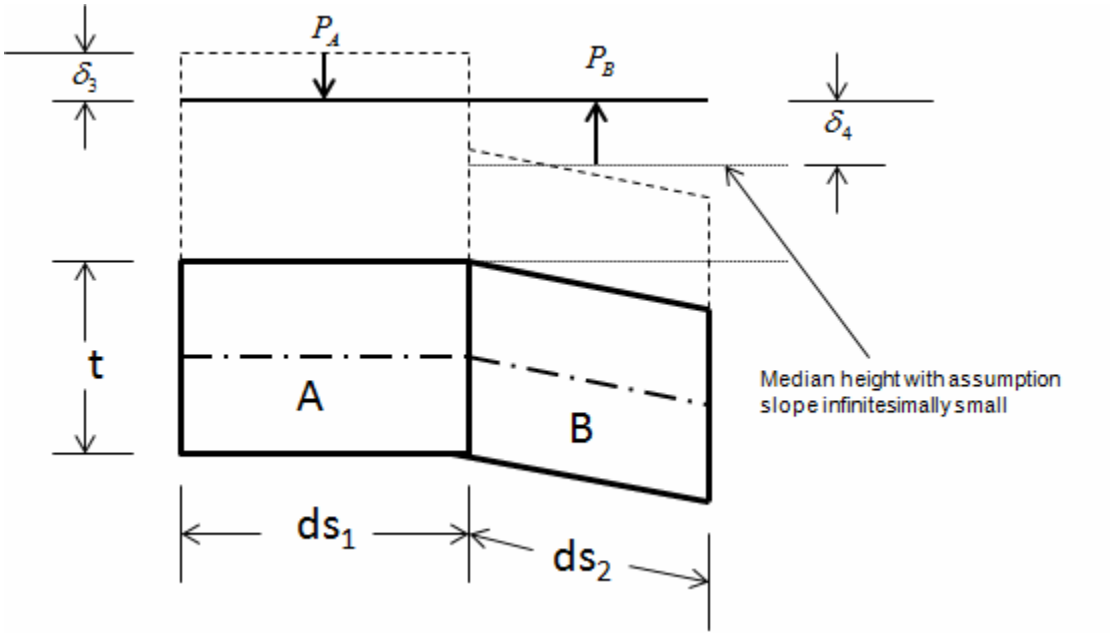

Figure 33. Representative model of two consecutive segment experiencing mechanical loads in order to enforce compatibility.

Taking Equation (56), the thickness of the beam can be cancelled out of the compatibility equation since it is common in all terms on both sides of the equality. Using Equation (56), the mechanical loads induced to enforce compatibility in the geometry of the beam at the interface of segments A and B (P_A and P_B) can be replaced by an equivalent load P. Since the beam is homogeneous and isotropic, the Young's modulus E_B and E_A for segments B and A respectively, can be replace by an equivalent Young's modulus E. The areas A_B and A_A that the mechanical loads P act on for both segments A and B are equal and can be replaced by an equivalent area A. After the latter changes, Equation (56) reduces to:

$$\alpha_A(\Delta T) - \frac{P}{EA} = \alpha_B(\Delta T) + \frac{P}{EA} \tag{58}$$

Rearranging terms…

$$\alpha_A(\Delta T) - \frac{\sigma}{E} = \alpha_B(\Delta T) + \frac{\sigma}{E} \tag{59}$$

Solving for the stress σ …

$$\sigma_Z = \frac{1}{2} E(\alpha_A - \alpha_B)(\Delta T) \tag{60}$$

The α_A and α_B in Equation (60) are the effective coefficients of linear thermal expansion in the Z-direction for segments A and B, respectively. These coefficients are defined by Equation (48) and Equation (51).

The second case will be that of effective expansion through the longitudinal direction. As shown by Figure 28,

Figure 29, and Figure 31, segment A will have a lower effective expansion than segment B- see Figure 34. Now, we began to take the infinitesimal segments A and B as ds_1 and ds_2 tend to zero such that the combined lengths of both segments form an effective interface but still have an extremely small,

infinitesimal length. The structural shape of the beam at the very small level is equivalent to that shown in Figure 32 and Figure 33. However, graphical or pictorial representations are chosen based not how much they are to scale or visually show the actual interest but how they best portray the given information. With this in mind, the curved beam section is shown as two straight line segments that are parallel to each other. The effective difference in elongation for each segment is represented not by geometry but by a color shaded region. The red section of segment B is a particular way of showing the magnitude of the expansion of that segment. The orange section of segment A is another particular way of showing the magnitude of the expansion of that segment. Since the interest is on the internal interactions at interfaces of two segments at a time, elongations on the far left side of segment A and far right side of segment B are omitted.

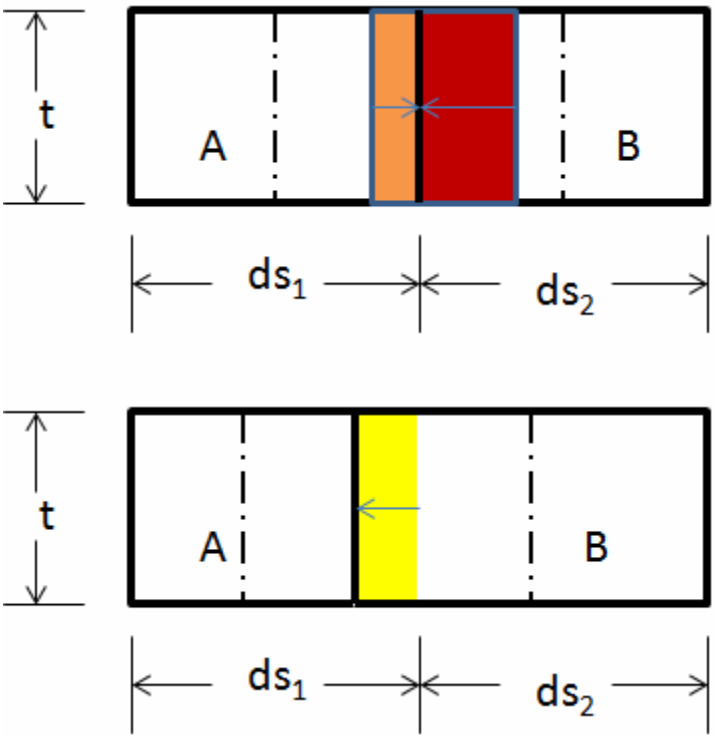

Figure 34. Representative model of two consecutive segment experiencing differential expansion due to variance in effective coefficient of linear thermal expansion in the Z-direction.

As previously mentioned, segment B has a higher expansion magnitude as that of segment A. Therefore, the right side of segment A tends to be compressed and the left side of segment B tends to be elongated. That is the interface boundary between segment A and B tends to move in the left direction on the right side of the curved beam. On the left side of the curved beam, it would tend to move in the right direction. The movement to the left is shown by the yellow shaded region.

As the arc of the beam is spanned, there is internal strain in the beam in the X-direction. Figure 21 and Figure 22 show that there will be no internal strain in the X-direction in a straight beam under thermal loading. However, Figure 25 and Figure 34 show that there will be internal strain in the X-direction in a curved beam under thermal loading. This *residual* strain due to thermal loading cannot be relieved due to the geometry of the beam. Due to the nature of the effective coefficients of linear thermal expansion, even though the beam is under uniform thermal loading, the effective coefficients of linear thermal expansion *create* a pseudo non-uniform thermal loading equivalent situation. In this case it is non-uniform deformations due to thermal loading. Therefore, stresses are induced. Unlike the through thickness expansion case, there are no incompatibility issues to address in the longitudinal expansion case (however the compatibility relation will be used to help solve for the X-direction stresses).

To ascertain the stresses in the X-direction in the curved beam utilizing the two segments and their internal boundary interface interactions, a pseudo mechanical load is created- see Figure 35. This pseudo mechanical load is exactly its namesake, a mechanical load that does not exist in reality. However, it would emulate the effect that the variances in the coefficients of linear thermal expansion have concerning the non-uniform deformations in the X-direction with respect to the boundary interface between two adjacent segments. Therefore, this pseudo-mechanical load will be statically equivalent to the actual system. This is a technique that is readily and often used in mechanics and will equally be valid in its application here.

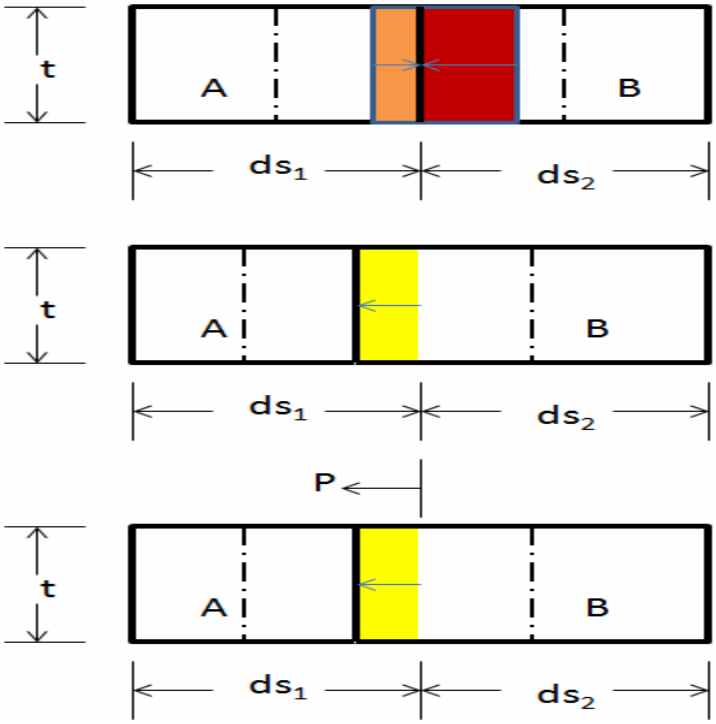

Figure 35. Representative model of two consecutive segment experiencing differential expansion due to variance in effective coefficient of linear thermal expansion in the Z-direction and a statically equivalent system using a pseudo mechanical load P.

The pseudo mechanical load is defined as P. Since it is used, a pseudo force-displacement relationship is needed to relate this force to the displacements that it causes. Of course, this displacement would be the cumulative displacement due to the non-uniform deformations due to the thermal loadings. Therefore, the temperature-displacement relations will be used to relate the thermal load to the real displacements. For congruency, the real displacement from the temperature-displacement relationship has to be equal to the pseudo displacement from the force-displacement relationship. By defining a pseudo load P that could independently create the deformation created by the thermal loading in the curved beam, the stress in the beam can be ascertain indirectly by using a statically equivalent pseudo system.

For a statically equivalent system to be a valid system, it must be compatible system and in equilibrium. By arranging the loading correctly (a trivial job) and assuming displacements are very small for each extremely infinitesimal interface region (inherently so by definition of these segments as defined

earlier and for small deformation theory which would apply here), any potential incompatibility issues that could arise are bounded and eliminated- see Figure 35. Equilibrium is not established locally. However, equilibrium is established globally for the whole beam. As mentioned earlier, the loading conditions, deformations, and effective coefficients of thermal expansion are antisymmetrical about the mid span of the curved beam- see Figure 28,

Figure 29, and Figure 31. Hence the pseudo loads will cancel themselves out and the sum of the forces in the X-direction will be zero. Furthermore, this equilibrium necessarily has the pseudo loads vanishing from the system globally. Hence, the non-uniform deformations due to the variances of the effective coefficients of linear thermal expansion are left.

Temperature-displacement:

$$\delta_{ORANGE} = \alpha_A(\Delta T)ds \tag{61}$$

$$\delta_{RED} = \alpha_B(\Delta T)ds \tag{62}$$

Force-displacement:

$$\delta_{YELLOW} = \frac{Pds}{EA} \tag{63}$$

Compatibility equation:

$$\begin{aligned} \delta_{YELLOW} &= \delta_{ORANGE} - \delta_{RED} \\ \frac{Pds}{EA} &= \alpha_A(\Delta T)ds - \alpha_B(\Delta T)ds \end{aligned} \tag{64}$$

Taking Equation (64), the characteristic length ds of the segments of the beam can be cancelled out of the compatibility equation since it is common in all terms on both sides of the equality. Since the beam is homogeneous and isotropic, the Young's modulus E_B and E_A for segments B and A respectively, was replaced by an equivalent Young's modulus E in Equation (63) as a matter of fact. The areas A_B and

A_A that the mechanical load P acts on for both segments A and B are equal and were replaced by an equivalent area A in Equation (63). After the latter changes, Equation (64) reduces to:

$$\frac{P}{EA} = \alpha_A(\Delta T) - \alpha_B(\Delta T) \tag{65}$$

Rearranging terms…

$$\frac{\sigma}{E} = (\alpha_A - \alpha_B)(\Delta T) \tag{66}$$

Solving for the stress σ …

$$\sigma_X = E(\alpha_A - \alpha_B)(\Delta T) \tag{67}$$

The α_A and α_B in Equation (67) are the effective coefficients of linear thermal expansion in the X-direction for segments A and B, respectively. These coefficients are defined by Equation (48) and Equation (51).

MATLAB was used to calculate the stress variations in the X and Z directions for a simply curved beam that swept 180 degrees. The material used was 6061-T6 Aluminum- see

. The thermal loading condition was $\Delta T = 100\ ^oF$. The stresses were plotted and shown in Figure 36 and Figure 37.

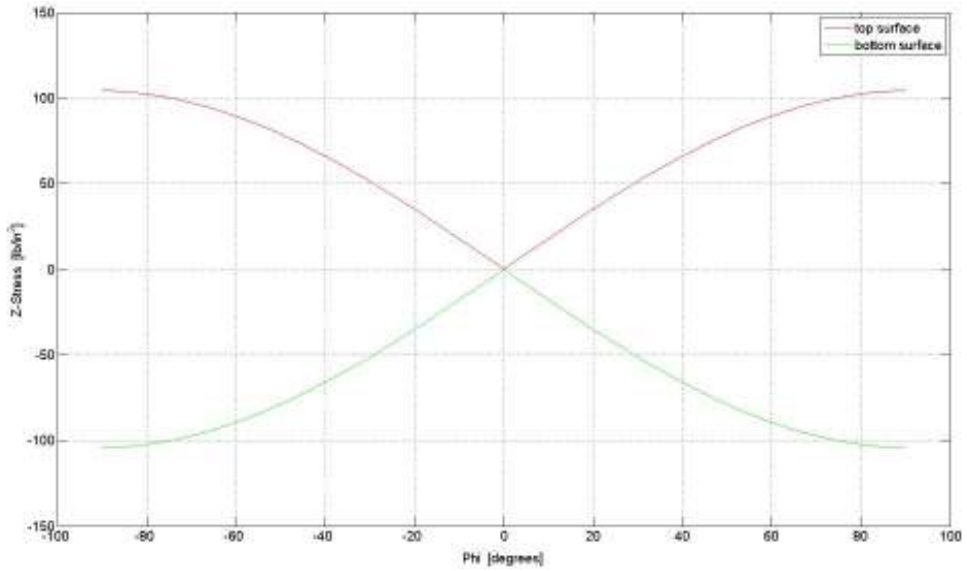

Figure 36. Z-direction stresses for a curved beam under a temperature change of 100 degrees Fahrenheit.

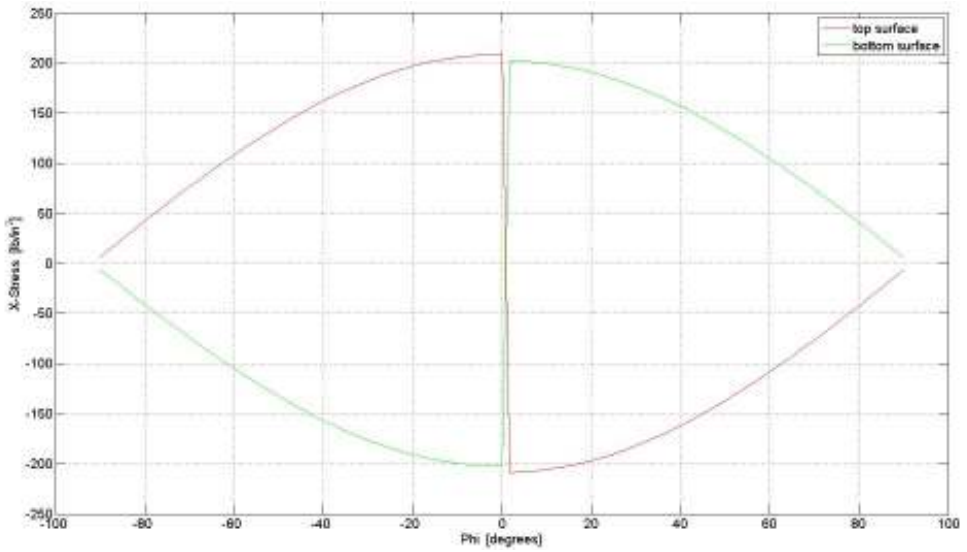

Figure 37. X-direction stresses for a curved beam under a temperature change of 100 degrees Fahrenheit.

The net result of adding curvature into a beam is that a free-free beam (free to expand) will generate stresses under thermal loading. For flat beams that are free-free (free to expand), it is well known that no stresses are generated. The magnitude of the stresses that are generated are small compared to

stresses that generally develop in constrain structures of the same material under the same thermal loading conditions. It should be noted that the stresses that show up as negative or positive in Figure 36 and Figure 37 aren't necessarily compressive or tensile, respectively. The sign of these stresses aren't calculated using the sign convention of compressive stress is negative and tensile stress is positive. They are based on the coordinate systems define in Figure 26 and Figure 27.

From Figure 36, it can be seen that the stresses in the Z-direction on the top surface are all positive. The stresses in the Z-direction on the bottom surface are all negative. With the top surface under positive stresses and the bottom surface under negative stresses of equal magnitude for every segmental span of the curved beam, the Z-direction thermal stresses do not deform the shape of the simply curved beam. The deflections caused by the positive stresses (forces) above the midline of the simply curved beam are cancelled out by equal magnitude but opposite direction negative stresses (forces) below the midline at the same X-point in the beam. The midline of the simply curved beam is stress free. In terms of the conventional nomenclature and sign convention for stresses, the simply curved beam is under tensile stresses of equal magnitude for both its top and bottom surfaces for every X-point in the beam.

From Figure 37, it can be seen that the stresses in the X-direction on the top surface on the left side of the curved beam are all positive. The stresses in the X-direction on the top surface on the right side of the curved beam are all negative. The stresses in the X-direction on the bottom surface on the left side of the curved beam are all negative. The stresses in the X-direction on the bottom surface on the right side of the curved beam are all positive. The effect of the stresses on the top surface of the curved beam is to cause the curved beam to *spring-in*. The effect of the stresses on the bottom surface of the curved beam is to cause the curved beam to *spring-out*. However, the stresses on the top surface of the beam are slightly higher than those on the bottom surface. Therefore, the net effect on the beam is a *spring-in* effect due to the thermal stresses in the simply curved beam in the X-direction. At the midline of the beam, the stresses in the X-direction are non-zero. They tend to cause the simply curved beam's shape to collapse on itself or *spring-in*.

The *spring-in* effect is a well documented phenomenon in beams with appreciably curved sections that are thermally loaded. This effect is rarely noticed in isotropic, homogeneous metals because the stresses are so small that the specimen experience negligible, reversible deformation that is hardly noticeable during a given thermal loading process. Hence, after reverse the cooling, the deformation reverses as well and the original shape is *recovered*. However, for composite materials, the mismatch in thermal expansion coefficient, anisotropic material properties in stiffnesses, Poisson's ratio mismatches, and particular stacking sequences leads to readily noticeable *spring-in* effects that are sometimes irreversible.

It should be noted that this *spring-in* effect is extremely small. First, in Figure 38 the sum of the stresses (the stress resultant at the mid-arc of the simply curved beam) in the global Cartesian coordinate system are shown. As mentioned earlier, the stress resultant in the Z-direction is zero throughout the span of the arc. The stress resultant in the X-direction is non-zero throughout the span of the arc except at the part of the beam where the segment is at a zero angle. Note: The abscissa is slightly shifted to the right. This is due to the nature of the MATLAB code used to numerically calculate the stress resultants. The X-direction stress resultants are extremely small in magnitude. Hence, the *spring-in* effect is hardly noticeable for isotropic material metals such as aluminum.

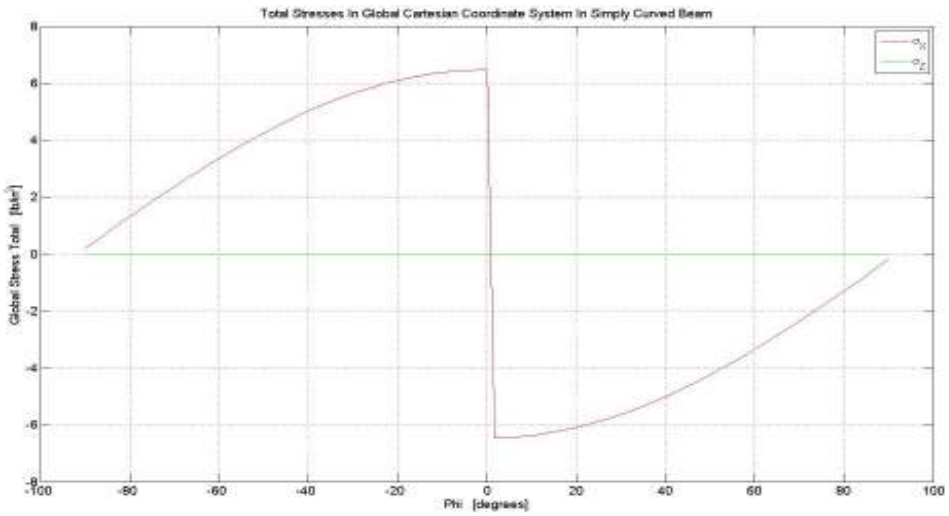

Figure 38. Stress resultants for simply curved beam in the global Cartesian Coordinate system.

To solve the statically indeterminant problem, the Author developed the fixed-fixed case for the simply curved beam. That is, the statically indeterminant problem is a fixed beam problem where the beam is simply curved. However, the reaction forces from the fixed ends are added to the solution. The stress resultants for the free-free case at the mid-arc of the beam are zero or negligible, these will be neglected in this derivation.

This solution is a variation in the fixed-fixed case for a flat beam, see Section 2.2.1. In this case the end of the beam is at an angle. The wall is still parallel to the face of the beam; yet, this surface (the wall and the face of the beam) is at an angle to the global Cartesian coordinate system. This means there is a reaction from the wall perpendicular to the face of the beam in contact with the wall. This face is at an angle lying in the XZ-plane. Therefore, there is a reaction from the wall in both the X- and Z-directions. However, to facilitate the solution, the original reference frame will be that local to the differential segment that is adjacent to the wall. This reference frame will change for each differential segment because each segment is oriented at a slightly different angle than the previous and seceding segment- see Figure 24 and Figure 25. As a result, the reaction force from the wall (whose orientation does not and cannot change) has a different effect on each segment- see Figure 39.

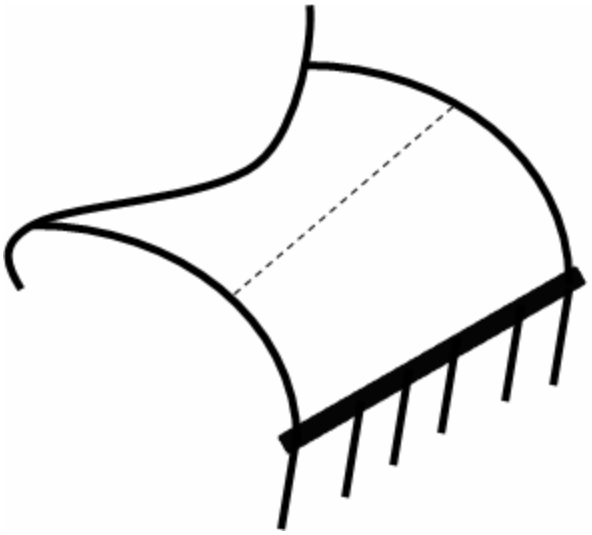

Figure 39. Representative section of one end of a simply curved beam that is fixed.

If the wall is removed from Figure 39 and the reaction due the thermal expansion (contraction), the reaction force from the wall will be perpendicular to the segment of the curved beam that is adjacent to the wall- see Figure 40.

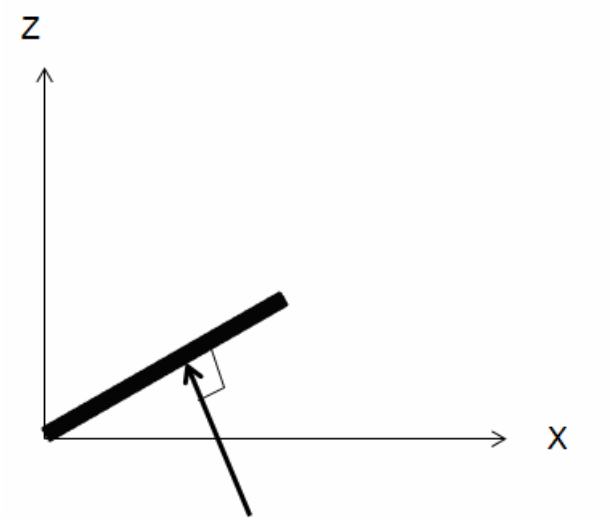

Figure 40. Representative reaction on curved beam section adjacent to wall.

The next infinitesimally small segment of the curved beam to the left of the section of the curved beam adjacent to the wall is at a slightly different angle with respect to the wall. Figure 39 gives a representative view of this where the dotted line represents the next infinitesimally small segment of the curved beam. Of course, Figure 39 is not to scale and is exaggerated to make it easier to visualize. Since the wall doesn't change it orientation and the section of the curved beam adjacent to the wall doesn't change its orientation, the next infinitesimally small segment will be at an angle to the reaction force. That is the reaction force will no longer be perpendicular to the face of that segment as the adjacent face is in Figure 40.

With straight, fixed-beams, the beam can be cut along any section and the internal force resultant due to the reaction from a wall will be equal in magnitude to the reaction and equivalent in direction. This is gained by using a free-body diagram of the overall beam (Figure 41) and the cut-section beam (Figure 42).

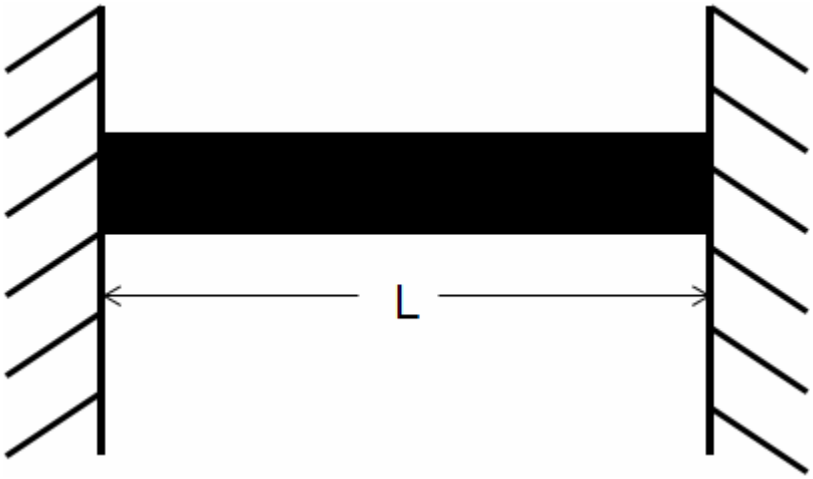

Figure 41. Representative view of a flat, fixed-beam.

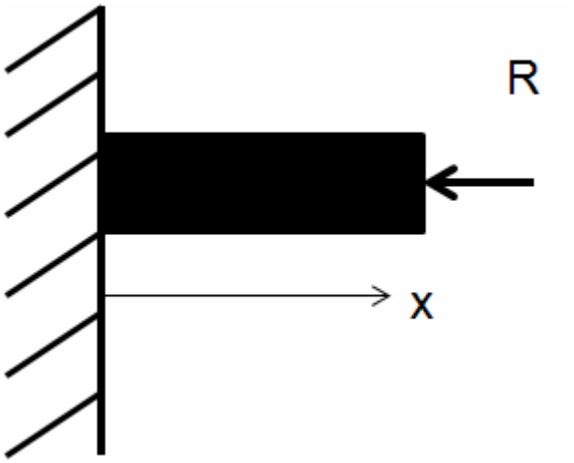

Figure 42. Representative view of flat, fixed beam with a section cut at beam length x. The internal force resultant (R) from the reaction force is shown.

With the curved beam the orientation of the exposed face with respect to the internal force resultant shown in Figure 40 will not be the same for every section cut as it would be for the case shown in Figure 42. The internal force resultant will have two components; one component perpendicular to the exposed face and one component tangential to the exposed face- see Figure 43.

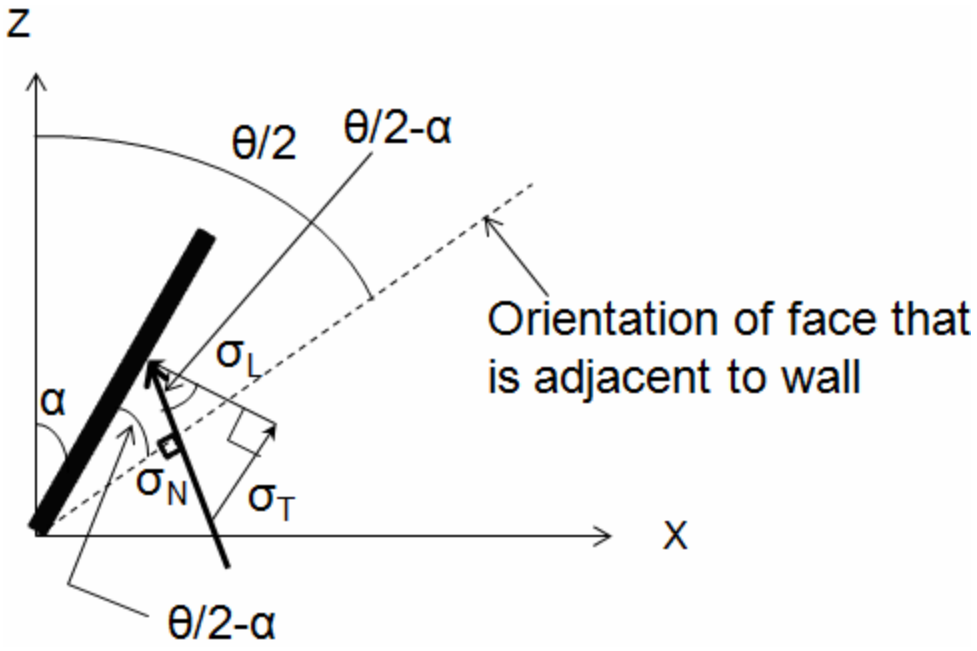

Figure 43. Representative view of a section of the curved beam with internal stress resultants.

For this schematic's purpose, the angle θ is the angle spanned by the simply curved beam. Therefore, the section shown in Figure 43 is the right half of the curved beam. The sectioning of the beam goes from left to right. The angle formed by this section with respect to the section of the beam that is always horizontal (like a flat beam), the mid-span section, is α. σ_N is the internal stress for a flat beam. This solution must be ascertained first just as was shown in Section 2.2.1. σ_T is the tangential component of σ_N along the face of the given section. σ_L is the longitudinal component of σ_N along the face of the given section. As the section increments from the mid-span of the simply curved beam to the end of the beam, the tangential and normal stress on the exposed face of a given section varies trigonometrically with the given arc location.

From Figure 43, the relationship for σ_L and σ_T are as follow:

$$\sigma_L = \sigma_N \cos\left(\frac{\theta}{2} - \alpha\right) \qquad \sigma_T = \sigma_N \sin\left(\frac{\theta}{2} - \alpha\right)$$

A model of a simply curved beam was used that was fixed on either longitudinal end. That material was 6061-T6 Aluminum- see

. It was subjected to a thermal loading of $\Delta T=100\ ^{o}F$. The above equations for the segment longitudinal and tangential stresses were numerically calculated in MATLAB. The length of the model was 1.5 inches. The angle spanned of the model was 120^{o}. The following plots are the tangential and longitudinal stresses throughout the internal segments of the simply curved, fixed-fixed beam.

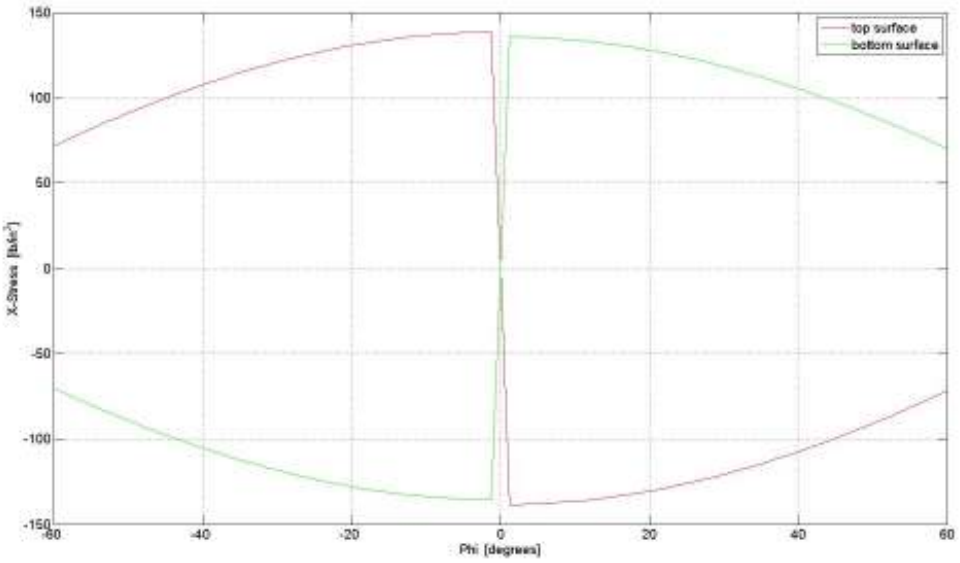

Figure 44. Global Cartesian X-stresses for the isotropic curved beam with a 120^{o} arc for top and bottom surfaces under free-free expansion.

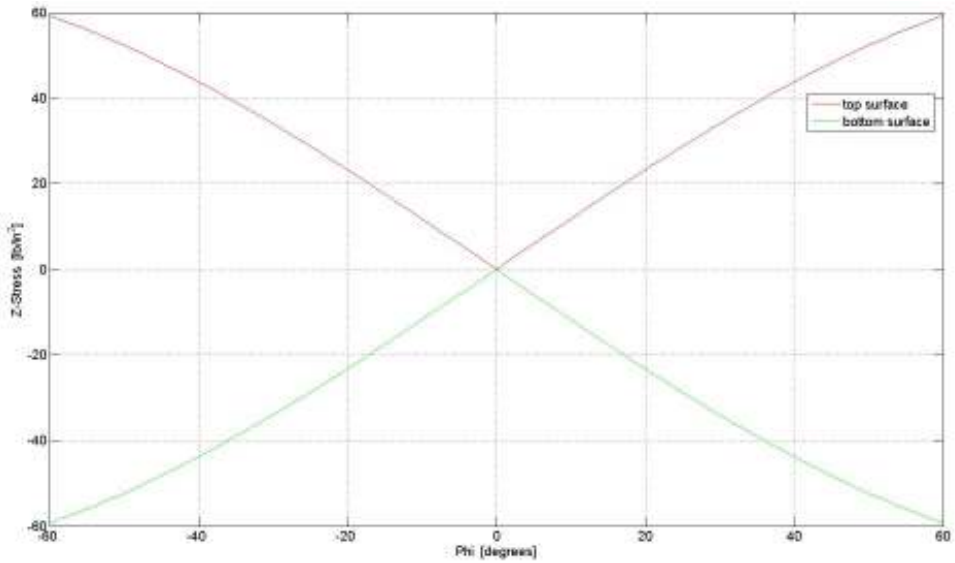

Figure 45. Global Cartesian Z-stresses for the isotropic curved beam with a 120^{o} arc for top and bottom surfaces under free-free expansion.

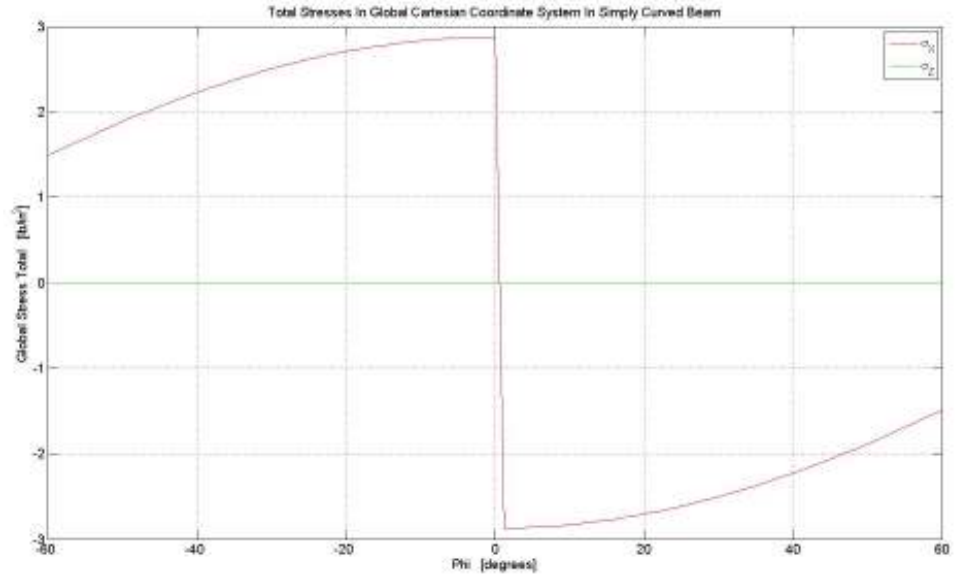

Figure 46. Global Cartesian total stresses for the isotropic curved beam with a 120^{o} arc for top and bottom surfaces under free-free expansion.

It can be seen from Figure 44 and Figure 45 that the X-stresses and the Z-stresses follow the same trend as discussed earlier. The overall result of this stresses, the sum at each given segment, is shown in Figure 46. As previously stated, the Z-stresses are zero at the mid arc surface (the mid-plane equivalent for curved surfaces). However, the X-stresses are non-zero. The stresses at the mid-arc surface are small, yet they would generate some very small deflections in the simply curved beam. On the left side of the curved beam, the X-stress resultants are in the positive (rightward) direction. On the right side of the curved beam, the X-stress resultants are in the negative (leftward) direction. The result is the beam is pushed *inward.* This inward motion is generally referred to as the *spring-in* effect. It is mainly characterized for composites since the anisotropic nature of the material and the unique stresses that generate in curved specimen amplifies the *spring-in* effect to a point where it is readily noticeable to a careful discerning eye. However, as this analytical solution shows, this is not readily noticeable for isotropic material because of the extremely small forces and the resulting extremely small deformation. Hence, it is not often recognized or discussed. These deformations are negligible in magnitude.

Figure 47 shows the *local* stresses for each differential segment of the beam in that segment's longitudinal and tangential direction. These stresses are in the general sign convention for stresses, that is negative stress is compressive and positive stresses is tensile. The longitudinal stresses at the face adjacent to the wall are equivalent to that in a flat fixed-fixed beam under similar thermal loadings that is isotropic and of the same material. These stresses decrease in magnitude at an increasing rate until they reach a minimum at the mid-span of the simply curved beam. The rate is non-linear. The tangential stresses at the face adjacent to the wall are equivalent to that in a fixed-fixed beam under similar thermal loadings that is isotropic and of the same material. These stresses increase in magnitude until they reach a maximum at the mid-span of the simply curved beam. The stresses increase in magnitude at decreasing rate. The rate is non-linear but is extremely close to a linear rate.

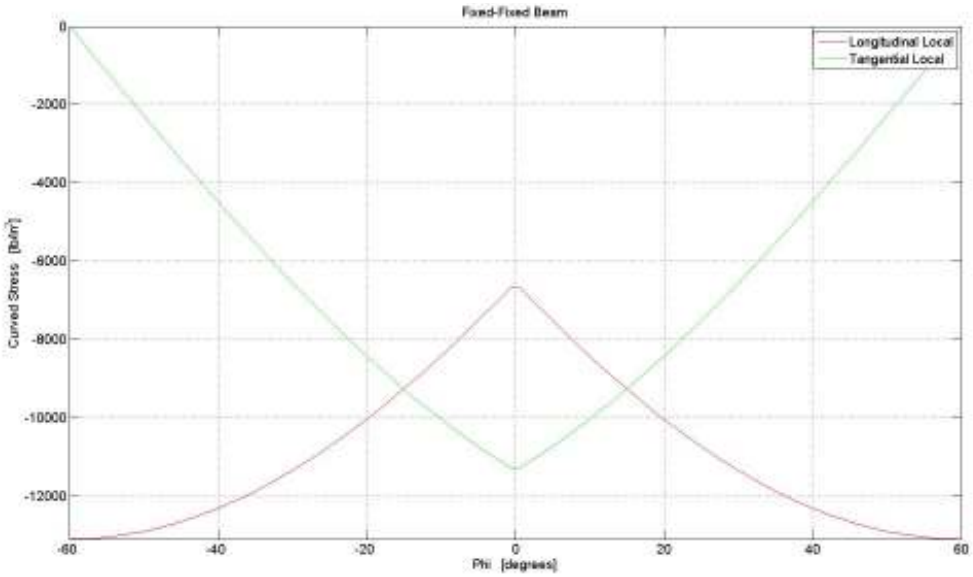

Figure 47. Global Cartesian curved stresses for the isotropic curved beam with a 120^{o} arc for top and bottom surfaces under fixed-fixed constraint.

2.2.6 Classical Lamination Theory (CLT) Solution For Curved Model

CLT has been used to take laminate level analysis to the structural level. This is done by shifting and rotating a number of laminates in space such that a structure consisting of a finite number of laminates is formed. Behind this physical action, there is a mechanical (solid mechanics) action as well. This requires the shifting and rotating of a number of stiffness matrices of the laminates in space such that the overall stiffness for the structures is emulated. For curved structures, the physical action consists of bending the laminate into an arc section, circular section, or an elliptical section. For curved structures, the mechanical action consists of laminate stiffnesses that are *continuously rotated* and shifted in space to form an effective curve section where the overall stiffness for that structure is emulated. Of course for this to be exact, an infinite number of laminates that are truly continuously rotated in space would have to be used. However, the laminates are *shrunk* in width to a sufficient size and rotated in space to a sufficient fineness such that a smooth curved structure can be approximated to a high degree of accuracy. Geometrically, this is a sound principal and is valid.

A number of students, engineers, and researchers have used this method to define composite structures with laminates of different orientations and locations that define a given structural shape. However, the results of this work are erroneous. The reason is because the basic, traditional, non-modified classical lamination theory is incapable of representing stiffnesses and compliances in directions perpendicular to the XY-plane (where the XY-plane is where the laminate stiffness and compliances are defined). This is necessary to represent these types of structures that are no longer plane.

The key to understanding this is rudimentary. The first problem arises in how traditional one-dimensional beam problems are solved for displacements, strains, forces, moments, and stresses in the plane of the beam (or in the plane of the paper upon which the given solution is ascertained). At the beginning of mechanics of material and deformable-bodies books, the problems are stated to be three-dimensional. However, to facilitate solutions using one-dimensional formulations for parameters in the plane of the structure (or paper), it is assumed that the problem has unit depth. This allows the whole problem to be drawn in a plane (which would be a piece of paper). Yet assuming unit depth into or out of the plane (paper) does not collapse the problem geometry from three-dimensional to two-dimensional. It basically allows representation (not actuation) of the problem two-dimensionally to facilitate solving the problem by hand on paper. Of course, the mechanics are still one-dimensional. This assumes variations of parameters into or out of the plane are zero or the parameters are constant through the depth of the plane. Therefore, the one-dimensional beam mechanics is often used on a two-dimensional representation that applies to a three-dimensional problem (assuming no variation through the depth of the plane- into or out of).

Thus, when beam is rotated or shifted in space with these problems, using traditional displacement relationships and rotation matrices suffices to accurately describe these problems. The rotations are always three-dimensional (geometrically). However, all the parameters for a problem as defined in the previous paragraph have no variation through the depth are zero. This allows the collapsing of the rotation matrices for these problems to 3x3 and 2x2 matrices depending on the particular type of formulation, parameter being modified, and type of problem. Yet, these problems are still geometrically three-dimensional. For

solving by hand, the method existing when the solutions for these problems were formulated before the age of the digital computer, the two-dimensional representation of the problem was sufficient assuming no variation through the depth (into or out of the paper). For isotropic problems, in light of the previous two sentences and based on the assumptions found in almost all mechanics of deformable bodies and mechanics of material textbook, the one-dimensional mechanics to ascertain parameters in two dimensions (in the plane of the paper) was sufficient. That is, all parameters (with appropriate reservations) in the plane of the problem could be defined using one-dimensional mechanics. The solution was visibly assisted by taking two-dimensional representations of the problem on paper, assuming unit depth for a three-dimensional geometry.

The key fact here is that rotations out of the plane are equally valid for these problems because the one-dimensional mechanics and the parameters that are a function of it will not change. The three-dimensional nature of the problem doesn't change either. That is, rotating the geometry about three axes and translating in three directions doesn't change the shape of the specimen being examined. The only difficulty comes in visual picturing of the problem on paper (two-dimensional) to facilitate the solution of the problem for complex geometries under a complex set of rotations and translations. Because of this and confusing transformations vectors or matrices with getting components of vectors (two completely different things that utilize trigonometric functions), many have also applied three-dimensional rotations to plane problems too.

This is where the first problem arises. It is easiest to think of a two dimension problem (not one that is a three-dimensional problem that has been characterized with unit depth, it is still three-dimensional and not two dimensional) as a system like planet earth that is flat, a plane. This plane is so because in the plane of the two dimensional problem, the two orthogonal directions extend to infinity. Therefore, no matter how thick the domain is, relative to infinity it will always be a plane. Everywhere outside this system is empty space like outer space, the environment. Both the environment and the system exist in a volumetric realm that is infinite in length, width, and height. The entities can only exist in the system (flat-earth). Outside this system they are not define and cannot exist (outer space/the environment). When the

system is rotated in its plane, its entities have not transcended to a realm where they aren't defined and where they cannot exist. Remember, this domain is infinite in length and width inside a volumetric realm that is infinite in length, size, and height. However, when the system is rotated outside of its plane, its entities now exist in a realm (the environment) where they are not define and cannot exist- see Figure 48.

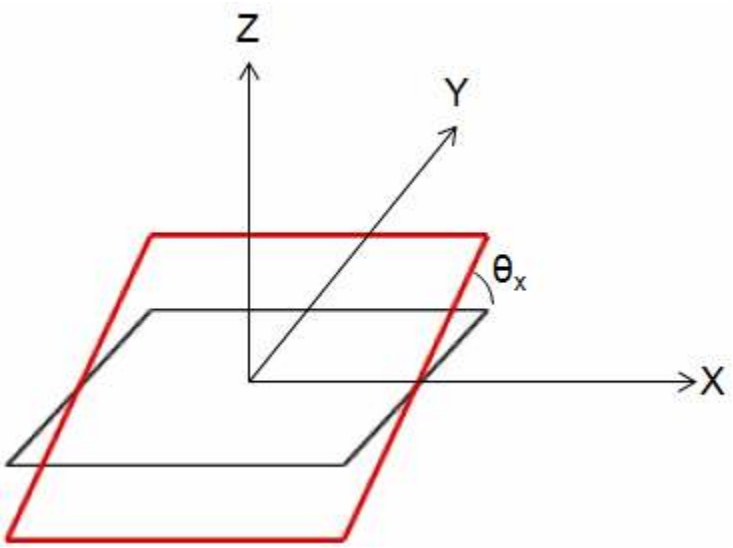

Figure 48. XY-plane and a plane rotated about the X-direction.

The black plane is the XY-plane and is defined as the system; this is where all the entities are defined and exists. Take the ply stiffness matrix in the laminate coordinate system defined in Section 2.2.2 as an example. By its derivation and essence, it is only defined in the XY-plane. Its components are all in terms of X and/or Y. Nothing is defined for any other plane, and nothing is in terms of Z. The red plane is some plane that *exists* once the XY-plane has been rotated by some angle θ_X about the X-axis. It can be readily seen from inspection that some of the parameters defined in the XY-plane will now have components in the Z-direction whereas before they didn't. This is what happens when a plane stress, plane strain, etc. problem is rotated out of its plane. It is a two-dimensional problem that is rotated in-part into a third dimension where its parameters don't exist. Once defined explicitly in terms of two-dimensions, the

definition is set. They cannot be defined in terms of the third dimension. This is the case for the whole plane. This isn't mathematically sound or mechanically sound. Hence, it is not valid and not possible. All results gained from this process are erroneous.

Another example whose trivial nature leads to errors in its use is the vector and its components. Take a vector $\overrightarrow{F_1}$ that is defined in three-space. This vector is shown to be $\overrightarrow{F_1} = r\bar{i} + s\bar{j} + t\bar{k}$. The components (r,s,t) of the vector $\overrightarrow{F_1}$ are some arbitrary values that can be either zero or non-zero. This vector can be rotated about any axis or set of axes for more than rotation in any combination. The resulting vector would be a valid vector, its components would be defined in third-space, and that vector would exist. Take a vector $\overrightarrow{F_2}$ that is defined in two-space. This vector is shown to be $\overrightarrow{F_2} = r\bar{i} + s\bar{j}$. The components (r,s) of the vector $\overrightarrow{F_2}$ are some arbitrary values that can be either zero or non-zero. This vector can be rotated about the axis that is perpendicular to this particular two-space only. The resulting vector would be a valid vector, its components would be defined in two-space, and that vector would exist. Now take the vector $\overrightarrow{F_1}$ and set the $\bar{k}$ component coefficient to 0. Now $\overrightarrow{F_1}$ is defined as $\overrightarrow{F_1} = r\bar{i} + s\bar{j} + 0\bar{k}$. Here is where the errors began to occur. At face value it would seem from inspection that the new $\overrightarrow{F_1}$ is the exact same as $\overrightarrow{F_2}$: $\overrightarrow{F_1} = r\bar{i} + s\bar{j} + 0\bar{k} \equiv \overrightarrow{F_2} = r\bar{i} + s\bar{j}$. This is assumed because traditionally $\overrightarrow{F_1} = r\bar{i} + s\bar{j} + 0\bar{k} = r\bar{i} + s\bar{j}$ is taken as fact. This is sort of *correct* but with a two important caveats.

First, new $\overrightarrow{F_1}$ is not the exact same as $\overrightarrow{F_2}$. The first reason is the first caveat. $\overrightarrow{F_1}$ exists only in three-space, and $\overrightarrow{F_2}$ exists only in two-space. These spaces are different dimensional essences. They can share all the same properties and characteristics save that those concerning the missing dimension in two-space with respect to three-space. Imagine trying to fit the Al-Khalifa Tower into an urban car garage of at least the same width and length but obviously different height. The Al-Khalifa Tower's size relative to an urban car garage can be assumed to be three-dimensional (in three-space), and the typical urban car garage

can be assumed to be two-dimensional (in two-space, plane) relative to the Al-Khalifa Tower. If one were to try to fit the Al-Khalifa Tower building into car garage, it would be an utter failure. It would be ludicrous to even think about such much less try it. Likewise for trying to fit $\overrightarrow{F_1} = r\bar{i} + s\bar{j} + t\bar{k}$ into $\overrightarrow{F_2} = r\bar{i} + s\bar{j}$, even though r and s are the same for both vectors. There are no mechanisms to enable such to happen without absolutely destroying the three-space entity, in this case the Al-Khalifa Tower. After such destruction, it would not be possible to reverse the process and recover the three-space entity- the Al-Khalifa Tower. Even though the new $\overrightarrow{F}_1$ has the same image and span as $\overrightarrow{F}_2$, they exist in different systems. Each system is an environment relative to the other system where that system's entities aren't defined and cannot exist. This leads to the second caveat.

At face value $\overrightarrow{F_1} = r\bar{i} + s\bar{j} + 0\bar{k} = r\bar{i} + s\bar{j}$ appears to be identical to $\overrightarrow{F_2} = r\bar{i} + s\bar{j}$. They have the same image and span. In part, they are identical. However, they exist in different realms. For an entity to exist, it must be defined first. However it is defined determines its essence and its behavior. $\overrightarrow{F}_1$ was define in three-space, and $\overrightarrow{F}_2$ was defined in two-space. So even though they may be identical in appearance, they are in two incompatible spaces. This fundamental definition of vectors and spaces can be (and generally is… out of ignorance) ignored. For problems that are inherently three-dimensional but use unit depth concepts, etc. to resolve the problem into a visually two-dimensional problem to facilitate the solution process, this equating of the two is inconsequential. This is because the new $\overrightarrow{F}_1$ and $\overrightarrow{F}_2$ have the same image and space; but, the problem hasn't actually changed from three-space to two-space. Its appearance for the solutions sake (appearance as one writes on paper, a two-space too) is two-dimensional because the writing on paper and visualizing what is own paper is a mapping to a two-space system, the paper. However, this is often incorrectly seen as a two-dimensional (two-space) problem. But unless explicitly defined as such, it generally isn't two-dimensional but three-dimensional. This error is exacerbated because for simplicity, $\overrightarrow{F_1} = r\bar{i} + s\bar{j} + 0\bar{k} = r\bar{i} + s\bar{j}$.

This expression for $\overrightarrow{F_1}$ is wrong. This is actually saying that the third component and its direction have vanished. Does a three dimensional coordinate system lose one of its axes if the coefficient of a vector that exists in that three-space goes to zero? Of course not! So $\overrightarrow{F_1} = r\bar{i} + s\bar{j} + 0\bar{k} = r\bar{i} + s\bar{j}$ is technically wrong. When this is done, the three-space entity is defined as a two-space entity because one of the coefficients along a given direction is zero. This is as ludicrous as defining a three-space vector as a vector that exists in infinite-space because one of its coefficients has a magnitude that approaches infinity. An infinite number of components cannot be added to the vector F since one of the coefficients of a given component is near or at infinity. Likewise, the deletion of one of the components of a vector since one of the coefficients of a given component along a given direction is zero is incorrect and impermissible: The upshot $\rightarrow \overrightarrow{F_1} = r\bar{i} + s\bar{j} + 0\bar{k} = r\bar{i} + s\bar{j} \neq \overrightarrow{F_2} = r\bar{i} + s\bar{j}$.

Refer back to Figure 48: The problems shown with the vector example are exacerbated by transforming a plane problem (two-dimensional) in such a way that it is transformed out of its plane. No problems exist if the plane problem is translated in its plane or translated perpendicular to its plane as long as it stays parallel to the plane in which it was defined. This condition is satisfied for only one rotation for a plane problem, rotation about the axis perpendicular to the plane that the problem is defined in.

The Author derived a relationship for displacements in three-space- see Appendix C. Interpreting the derivation process and the results thereof shows something that is generally ignored but is self-evident. Displacements in the X-direction can only exist in planes for which X is defined; that is, displacements in the X-direction can only exist in the XY- and XZ-planes. Displacements in the Y-direction can only exist in planes for which Y is defined; that is, displacements in the Y-direction can only exist in the XY- and YZ-planes. Displacements in the Z-direction can only exist in planes for which Z is defined; that is, displacements in the Z-direction can only exist in the XZ- and YZ-planes. This hearkens back to the essence of what was stated earlier. This means displacements fundamentally exist in a plane (two-space), not in volume (three-space).

For a displacement to occur in volume (three-space), it must be defined by two mutually orthogonal planes both independently and mutually at the same time and space. This allows the displacements to occur in the planes (a fundamental must) and for the displacement that exist in one plane to be coupled to another mutually perpendicular plane without violating the latter arguments concerning the connection between two-space and three-space.

$$u(x,y,z) = u_0(x,y,z) + \alpha_x(x,y)|_z\ z = \left[\varepsilon_x^0(x,y,z)x + \frac{\gamma_{xy}^0(x,y)|_z}{2}y\right] + \left[\kappa_x(x,y)|_z\ x + \frac{\kappa_{xy}(x,y)|_z}{2}y\right]z$$
$$= u_0(x,y,z) + \beta_x(x,z)|_y\ y = \left[\varepsilon_x^0(x,y,z)x + \frac{\gamma_{zx}^0(x,z)|_y}{2}z\right] + \left[\kappa_x(x,z)|_y\ x + \frac{\kappa_{zx}(x,z)|_y}{2}z\right]y$$

(68)

$$v(x,y,z) = v_0(x,y,z) + \alpha_y(x,y)|_Z\ z = \left[\varepsilon_y^0(x,y,z)y + \frac{\gamma_{xy}^0(x,y)|_z}{2}x\right] + \left[\kappa_y(x,y)|_z\ y + \frac{\kappa_{xy}(x,y)|_Z}{2}x\right]z$$
$$= v_0(x,y,z) + \beta_y(y,z)|_x\ x = \left[\varepsilon_y^0(x,y,z)y + \frac{\gamma_{yz}^0(y,z)|_x}{2}z\right] + \left[\kappa_y(y,z)|_x\ y + \frac{\kappa_{yz}(y,z)|_x}{2}z\right]x$$

(69)

$$w(x,y,z) = w_0(x,y,z) + \alpha_z(x,z)|_y\ y = \left[\varepsilon_z^0(x,y,z)z + \frac{\gamma_{zx}^0(x,z)|_y}{2}x\right] + \left[\kappa_z(x,z)|_y\ z + \frac{\kappa_{zx}(x,z)|_y}{2}x\right]y$$
$$= w_0(x,y,z) + \beta_z(y,z)|_x\ x = \left[\varepsilon_z^0(x,y,z)z + \frac{\gamma_{yz}^0(y,z)|_x}{2}y\right] + \left[\kappa_z(y,z)|_x\ z + \frac{\kappa_{yz}(y,z)|_x}{2}y\right]x$$

(70)

It can be seen in Equation (68), Equation (69), and Equation (70) that displacement u = u(x,y) = u(x,z), v = v(x,y) = v(y,z), w = w(y,z) = w(x,z). Inside the brackets the later functional dependence is obvious. Outside the second bracket for each displacement there is a variable distributed against the bracket that is not in the plane that the given displacement is defined in. That is that variable is in a

direction perpendicular to the plane defined by the variables in the brackets. This variable is the conduit that allows the displacement to be realized in three-space even though it is defined in two-space (on a plane). This can happen because each displacement is defined by two mutually perpendicular planes. These two two-space systems are unionized by the variable that is in a direction perpendicular to those variables. That variable in one equation for a given displacement on a plane is the conduit to the other equation for the same displacement direction on the second plane. This is the case for the second variable in the counterpart equation.

Since each displacement is defined on a plane and each plane is define within itself in the infinite volumetric space, it is permissible for these planes to be shifted such that they intersect each other. The points in this union of planes where (x,y,z) are defined are the permissible locations for the displacement to be realized in three-space even though it is defined in two separate two-space systems. Looking at Equation (68), Equation (69), and Equation (70), the mid-plane strains are equivalent for each expression for a given displacement. This is a must. If they were different, it would be self-evident that there would be two different locations for a given displacement; this, of course, is not possible and is an incompatible deformation. These mid-plane displacements are about a mutually common direction for two mutually orthogonal planes. This is the second mechanism (besides the distributed variable in the direction that is perpendicular to the plane upon which the displacement is defined). As it is with the mid-plane strains, so it is with the out of plane deformations- the curvatures.

Note: Even though the curvatures are out-of-plane, the latter arguments aren't violated since CLT is also compatible with small strain theory. These curvatures are thus still in a space that is defined as the plane because the deformations are assumed to be very small. For very large strains or large deformations, a completely different set of relationships exist while still maintaining the latter arguments.

For these displacements to be potentially permissible displacement, strain-displacement compatibility relationships must be satisfied. These were shown to be satisfied by using MATLAB- see Appendix D. The following relationships that were satisfied are:

Strain-displacement compatibility:

$$\varepsilon_{X_1} = \frac{\partial u|_{XY-PLANE}(x,y,z)}{\partial x} \qquad \varepsilon_{Y_1} = \frac{\partial v|_{XY-PLANE}(x,y,z)}{\partial y} \qquad \varepsilon_{Z_1} = \frac{\partial w|_{XZ-PLANE}(x,y,z)}{\partial z}$$

$$\varepsilon_{X_2} = \frac{\partial u|_{XZ-PLANE}(x,y,z)}{\partial x} \qquad \varepsilon_{Y_2} = \frac{\partial v|_{YZ-PLANE}(x,y,z)}{\partial y} \qquad \varepsilon_{Z_2} = \frac{\partial w|_{YZ-PLANE}(x,y,z)}{\partial z}$$

$$\gamma_{XY_1} = \frac{\partial u|_{XY-PLANE}(x,y,z)}{\partial y} + \frac{\partial v|_{XY-PLANE}(x,y,z)}{\partial x}$$

$$\gamma_{YZ_1} = \frac{\partial w|_{YZ-PLANE}(x,y,z)}{\partial y} + \frac{\partial v|_{YZ-PLANE}(x,y,z)}{\partial z}$$

$$\gamma_{XZ_1} = \frac{\partial u|_{XZ-PLANE}(x,y,z)}{\partial z} + \frac{\partial w|_{XZ-PLANE}(x,y,z)}{\partial x}$$

Second order (curvature) compatibility between normal strains and shear strains:

$$\frac{\partial^2 \varepsilon_{X_1}}{\partial y^2} + \frac{\partial^2 \varepsilon_{Y_1}}{\partial x^2} = \frac{\partial^2 \gamma_{XY_1}}{\partial x \partial y} \qquad \frac{\partial^2 \varepsilon_{Y_2}}{\partial z^2} + \frac{\partial^2 \varepsilon_{Z_2}}{\partial y^2} = \frac{\partial^2 \gamma_{YZ_1}}{\partial y \partial z} \qquad \frac{\partial^2 \varepsilon_{Z_1}}{\partial x^2} + \frac{\partial^2 \varepsilon_{X_2}}{\partial z^2} = \frac{\partial^2 \gamma_{XZ_1}}{\partial x \partial z}$$

By showing compatibility of Equation (68), Equation (69), and Equation (70), these deformations are compatible and permissible. No other caveats or assumptions were used in the derivation of these three equations. Hence, it is valid for all materials and material compositions. No gaps, wholes, etc. will develop in the structure due to any type of loading because of the deformations save such situations were failure due to material strength is concerned.

What the derivation of Equation (68), Equation (69), and Equation (70) and the previous arguments shows is that a rotation of a plane system (in this case a problem developed from CLT) out of its plane is not permissible and all deformations, strains, stiffness, etc., defined after such a process are invalid and erroneous. Vishal Sanghavi (my lab partner under Dr. Wen Chan) examined this problem with a

composite I-beam. The parameter that was being analyzed was the shear center for Vishal's Thesis [12]. Below is the result he formulated which provides an example to show all above latter assertions and arguments (the following is the verbatim argument):

Reasons for the failure of complete/overall ABD matrix approach to predict shear center:

It was observed that the shear center predicted by complete or overall ABD matrix approach presented by Syed [11] failed to predict the shear center for the I beam (isotropic and composite) and the error was huge. According to Syed [11], the overall ABD for the I-Beam structure is calculated by the following method:

$$\left[\overline{A}\right] = h_w[A]_w + b_{f1}[A]_{f1} + b_{f2}[A]_{f2}$$

$$\left[\overline{B}\right] = h_w[B]_w + b_{f1}\left([B]_{f1} + \rho_{f1}[A]_{f1}\right) + b_{f2}\left([B]_{f2} + \rho_{f2}[A]_{f2}\right)$$

$$\left[\overline{D}\right] = \left(h_w[D]_w + \frac{h_w^3}{12}[A]_w\right) + b_{f1}\left([D]_{f1} + 2\rho_{f1}[B]_{f1} + (\rho_{f1})^2[A]_{f1}\right) + b_{f2}\left([D]_{f2} - 2\rho_{f2}[B]_{f2} + (\rho_{f2}2)^2[A]_{f2}\right)$$

where,

$$[A]_W = \sum_{k=1}^{n}\left[\overline{Q}''_{x-y}\right]_k (h_k - h_{k-1})$$

$$[B]_W = \frac{1}{2}\sum_{k=1}^{n}\left[\overline{Q}''_{x-y}\right]_k \left(h_k^2 - h_{k-1}^2\right)$$

$$[D]_W = \frac{1}{3}\sum_{k=1}^{n}\left[\overline{Q}''_{x-y}\right]_k \left(h_k^3 - h_{k-1}^3\right)$$

$$\left[\overline{Q}''_{x-y}\right]_k = [T_\sigma(-\theta)]_z [T_\sigma(-\beta)]_z [Q]_{1-2} [T_\varepsilon(-\beta)]_x [T_\varepsilon(\theta)]_z$$

$$\theta = \textit{fiber orientation}$$

$$\beta = \textit{orientation of web with respect to the } x-y \textit{ plane},$$
$$\textit{in case of } I-\textit{beam } \beta = 90^o \textit{ as web is vertical to flange}$$

$$[T_\sigma(\beta)]_x = \begin{bmatrix} 1 & 0 & 0 \\ 0 & \cos^2(\beta) & 0 \\ 0 & 0 & \cos(\beta) \end{bmatrix} = [T_\varepsilon(\beta)]_x$$

for the I-beam web $\cos(\beta) = \cos^2(\beta) = \cos(90) = \cos^2(90) = 0$

$$\therefore [T_\sigma(\beta)]_x = \begin{bmatrix} 1 & 0 & 0 \\ 0 & 0 & 0 \\ 0 & 0 & 0 \end{bmatrix} = [T_\varepsilon(\beta)]_x$$

$$\rho_{f1} = \left(\frac{h_w}{2} + \frac{t_{f1}}{2}\right); \quad \rho_{f2} = \left(\frac{h_w}{2} + \frac{t_{f2}}{2}\right)$$

Thus, for web the ABD matrix will have only 4 non-zero terms and will be as follows:

$$[ABD]_W = \begin{bmatrix} A_{11,W} & 0 & 0 & B_{11,W} & 0 & 0 \\ 0 & 0 & 0 & 0 & 0 & 0 \\ 0 & 0 & 0 & 0 & 0 & 0 \\ B_{11,W} & 0 & 0 & D_{11,W} & 0 & 0 \\ 0 & 0 & 0 & 0 & 0 & 0 \\ 0 & 0 & 0 & 0 & 0 & 0 \end{bmatrix}$$

On investigating, the following reasons were found because of which the overall ABD matrix theory fails to predict the correct or comparable shear center:

Reason 1:

In I-Beam the bending loads are resisted by the flanges and the shear loads by the web. Thus web contributes for the major percentage of the shear stiffness while the flanges contribute for the major part of the bending stiffness. In composites the different stiffness are given by the following elements of the ABD matrix;

A_{11} = Axial Stiffness per unit width; A_{66} = Shear Stiffness per unit width;

D_{11} = Bending Stiffness per unit width; D_{66} = Twisting Stiffness per unit width;

From the rotated laminate stiffness of the web $[ABD]_W$ we observe that the web has only axial stiffness and bending stiffness while the shear stiffness and twisting stiffness are equal to zero. Thus there are some major errors in the method proposed by Syed [11].

Reason 2:

When the web ABD matrix is rotated by $(-90)^o$ with respect to x-axis, the original (un-rotated) ABD matrix of the laminate should be achieved, but that is not the case with this method.

Reason 3:

As proposed the shear center depends on b_{66} and d_{66} elements but as the web does not contribute to the b_{66} and d_{66} element, the shear center predicted is not correct.

$$shear\ center \equiv \bar{z}_{sc} = -\frac{\bar{b}_{66}}{\bar{d}_{66}}$$

But centroid depends on the b_{11} and d_{11} elements of the overall ABD matrix, and web and flanges both are contributing for the b_{11} and d_{11} elements and hence the overall ABD matrix approach gives comparable centroid location with centroid location equation shown below. Also as the logic of shifting the ABD matrix of flanges are correct and as flanges contribute the major percentage of the bending stiffness and the axial stiffness, the overall ABD matrix approach gives comparable results for both of them too.

$$centroid\ location \equiv z_c = \frac{b_{f1}A^*_{1,f1}z_1 + b_{f2}A^*_{1,f2}z_2 + h_wA^*_{1,w}z_w}{b_{f1}A^*_{1,f1} + b_{f2}A^*_{1,f2} + h_wA^*_{1,w}}$$

$$centroid = -\frac{\bar{b}_{11}}{\bar{d}_{11}}$$

$$EA = \frac{\overline{d_{11}}}{a_{11}\overline{d_{11}} - \overline{b^2}_{11}}; \quad EI = \frac{\overline{a_{11}}}{a_{11}\overline{d_{11}} - \overline{b^2}_{11}};$$

Reason 4:

If we carefully observe $[ABD]_w$ for the rotated laminate stiffness matrix for the web we can deduce that the matrix is a singular matrix and hence we cannot have the constitutive relationship shown below:

$$\begin{bmatrix} \varepsilon^o \\ \kappa \end{bmatrix} = \begin{bmatrix} a & b \\ b^T & d \end{bmatrix} \begin{bmatrix} N \\ M \end{bmatrix}$$

where,

$$\begin{bmatrix} a & b \\ b^T & d \end{bmatrix}_w = \begin{bmatrix} \overline{A} & \overline{B} \\ \overline{B} & \overline{D} \end{bmatrix}_w \textit{ not possible due to singularity of } \begin{bmatrix} \overline{A} & \overline{B} \\ \overline{B} & \overline{D} \end{bmatrix}_w$$

Reason 5:

Web should possess plane stress properties i.e. 2D properties as CLT is based on plane stress assumption. But looking at the $[ABD]_w$ we derive that web only has properties in global x-direction. Even though the web laminate is made of composite material, it losses all its coupling effects with the other direction which in our case is global z- axis.

End of Vishal Sanghavi's argument.

From the examples, arguments, and assertions the Author listed and the example provided by Vishal Sanghavi, it is now self-evident that the previous methods of taking the standard, non-modified, CLT from the laminate level to the structural level by rotating laminates out of their planes is incorrect and would provide incorrect results. A simply curved beam would require shifting the laminates in space and continuously rotating them along an arc (which would require rotating the laminates out of their planes) to appropriately alter their stiffnesses and compliances in a way that is commensurate with the given geometry; CLT cannot be used to evaluate such structures. Therefore, there is no CLT formulation for a simply curved beam whose curvature requires extension of the laminates into a plane perpendicular to the plane in which the laminate is defined. This is the case for the standard CLT without extensive alterations in both the shear, stiffness, and compliance terms.

Furthermore, for each per unit length segment of the simply curved beam, the axial, bending and twisting stiffness will change continuously throughout the structure. These stiffnesses at each unit span of the curved beam would be inherently coupled to the stiffnesses of the other unit spans. Since the traditional methods of developing a structural stiffness (and compliance) matrix requires stiffnesses for a laminate to

be constant throughout the span and the width of the said laminate, it is not possible to express an ABD or abd matrix for a simply curved beam and be mechanically and mathematically correct using standard classical lamination theory.

2.2.7 Finite Element Method Solution For Isotropic Curved Model

In order to develop a comparable finite element method solution for the isotropic curved model, particular care must be taken. The first reason for this is that with all comparisons in mechanics, the most relevant, meaningful, and accurate comparisons are those in which the systems have equivalent geometry, equivalent material properties, equivalent loading conditions, and equivalent states. One of the key comparisons that aren't readily obvious if equivalency is met is the state comparison. The analytical solution derived by the Author is a solution in which the simply curved, isotropic beam is in a state of plane stress. The plane that the plane stress condition exists in is the XZ-plane. It is not possible or mechanically correct to compare a plane stress problem with a non-plane stress problem in order to validate mechanical behavior or methods. The material response, stress and strain results, will be different.

For instance, take a beam that is fixed at each longitudinal end, is isotropic, and under thermal loading. There is a need to validate a given method for a flat beam. One method of verification is to use a plane stress method (2D), such as CLT. Another method of verification is to use a method that is not a plane stress method but one that has the potential to express stresses out of the given plane (3D), such as finite element method programs. If the given loading conditions are such that the finite element model shows 3D stresses, those results that are in the plane of interest of (for instance the XY-plane) CLT will not match. The only way those stresses would match is if the loading conditions are such that the finite element model shows 2D stresses in the plane of interest of CLT. That is both problems must be XY-plane stress problems. This is quite different from taking the solutions from a 1D analytical beam problem and using the knowledge of the Poisson's ratio effect on the strains due to mechanical loads to utilize a 3D stress solution as was done in Section 2.2.1.

Furthermore, take two models. One model doesn't account for some given type of shear. The second model does. These models are being used to ascertain a given stiffness parameter for a structure. If the shear is not present in the structure being modeled, both models (assuming all else was derived and built correctly) should give equivalent or very near comparable stiffnesses. This is because the shear term in the second model goes to zero, and the model then reduces to a form that is equal or equivalent to the first model. However, if the shear is present (especially if it is significantly present), the second model will generally give stiffnesses that are lower than the first model that doesn't account for shear. Therefore, it is important to have problems of the same state and correct model (all other things being equal) in order to correctly ascertain the behavior a structure. It is very easy to use a model and get results. However, even though the solution form may be correct, its ignorant usage can lead to erroneous results. When comparing distinct models of different natures, this equivalency is a must or the results will diverge. With this divergence, it is nearly impossible to ascertain which model is giving the correct results without some reference solution.

The same situation occurs for the finite element method solution for the curved beam. The purpose is to validate the MATLAB finite element code and verify that it produces correct results. It will then be used for further analysis with the confidence that it is robust. This is done by comparing its results with existing analytical theory, ANSYS, and personally developed analytical solutions. However, there must be a known solution that can serve as the reference point that is generic and can be applied to a number of cases successfully. As stated in the introduction, no such solution is known to exist to the Author or any professors to whom the Author has spoken to concerning such. There isn't an analytical isotropic solution that is free-expansion or fixed-fixed for simply curved beams under thermal loadings. Hence, the Author derived a form of an analytical solution for the isotropic, simply curved beam under free-expansion and under fixed-fixed constraint; but, this solution is a plane (XZ) stress solution. Any isotropic curved beam under any type of load will experience some type of uniform or non-uniform bending that will create appreciable 3D stresses once that beam is under a statically indeterminate configuration. The situation is even worse for composite, simply curved beams.

When researchers approach this problem, they have tried to develop analytical solutions but have failed to completely encapsulate all the necessary mechanics and give accurate solutions. The solution developed by the Author is the most involved solution to His best knowledge put can only handle isotropic cases that are in simple XZ-plane stress conditions. The unique thermal loading condition for a statically indeterminate (isotropic or composite) structure that results in only plane (XZ) stresses would have to be that which is non-uniform. That is, since this thesis is on uniform thermal loading of a simply curved composite, it is not possible to compare any finite element results from the MATLAB program to that of the analytical solution. This will be explored further during the composite flat beam validation process. Therefore, most researchers resort to finite element analysis from commercial software or use modified shape functions, stiffness and compliance parameters, functional multiples against strains and stresses, etc. to model isotropic and composite simply curved beams. However, all results must be verified by some known solution (either analytical or experimental). Also, finite element programs and models are only as accurate as the type and validity of the model built.

2.2.8 Validation Of Finite Element Analysis Program For Isotropic Curved Model

It suffices at this point to say that any curved specimen under any type of loading at any location of that specimen will experience bending and shear. These two will undoubtedly lead to stress conditions that are not XZ-plane as the analytical solution derived by the Author. This situation is even more complicated if the specimen is statically indeterminate. Therefore, it is not possible to use the finite element analysis (either from MATLAB, ANSYS, or any other program) to verify the validity of the analytical solution developed by the Author. The analytical solution meets the necessary conditions for validity but it can't be verified whether it meets the sufficient conditions. This is doable only with experimentation which can create a solution baseline that can be used as a reference point. These results are repeatable, and sufficient conditions can be define explicitly in term of stress, strain, or displacement results for a given configuration under a certain type of loading condition. This situation arises for composite structures as well and will be visited in detail in Section 2.2.11 and Section 2.2.12.

2.2.9 *Proof of Isotropic Curved Model Reducing To Isotropic Flat Model As Radius Of Curvature Goes To Infinity*

For the simply curved beam formulation for the effective coefficient of linear thermal expansion, the elongations, and the stresses, they must reduce to the flat beam solution as the radius of curvature goes to infinity. This condition is necessary for having a correct simply curved beam parameter formulation but is not sufficient. That is reducing to the flat beam solution as the radius of curvature goes to infinity is mandatory but not necessarily all that is required. In order to see if this minimum, mandatory standard is reached Equation (48) and Equation (51) have the arguments modified to reflect a radius of curvature that tends to infinity. This is done by setting the phi angles to zero. That is, as the radius of curvature tends to infinity, each segment is parallel to its neighbors- flat beam.

It can be seen that the effective coefficient of linear thermal expansion for the upper and lower halves of the segments reduces to that for a flat beam when the angles ϕ_B and ϕ_A go to zero.

$$\begin{Bmatrix} \overline{\alpha}_{T_X} \\ \overline{\alpha}_{T_Z} \end{Bmatrix}_{UPPER} = \frac{1}{4}\begin{bmatrix} \cos(0)-\cos(0) & \sin(0)+\sin(0) \\ \sin(0)-\sin(0) & \cos(0)+\cos(0) \end{bmatrix}\begin{Bmatrix} \alpha_{T_X} \\ \alpha_{T_Z} \end{Bmatrix} = \frac{1}{4}\begin{bmatrix} 0 & 0 \\ 0 & 2 \end{bmatrix}\begin{Bmatrix} \alpha_{T_X} \\ \alpha_{T_Z} \end{Bmatrix} \Rightarrow \begin{matrix} \overline{\alpha}_{T_X} = 0 \\ \overline{\alpha}_{T_Z} = \frac{1}{2}\alpha_{T_Z} \end{matrix}$$

$$\begin{Bmatrix} \overline{\alpha}_{T_X} \\ \overline{\alpha}_{T_Z} \end{Bmatrix}_{LOWER} = \frac{1}{4}\begin{bmatrix} \cos(0)-\cos(0) & -\sin(0)-\sin(0) \\ \sin(0)-\sin(0) & -\cos(0)-\cos(0) \end{bmatrix}\begin{Bmatrix} \alpha_{T_X} \\ \alpha_{T_Z} \end{Bmatrix} = \frac{1}{4}\begin{bmatrix} 0 & 0 \\ 0 & -2 \end{bmatrix}\begin{Bmatrix} \alpha_{T_X} \\ \alpha_{T_Z} \end{Bmatrix} \Rightarrow \begin{matrix} \overline{\alpha}_{T_X} = 0 \\ \overline{\alpha}_{T_Z} = -\frac{1}{2}\alpha_{T_Z} \end{matrix}$$

These results coincide exactly with what Figure 19 and Figure 22 show should occur for the flat beam. For the elongation, it is a rudimentary exercise in finding the product between the coefficient of linear thermal expansion, the change in temperature, and the reference dimension. This shows that there are no internal expansions in the longitudinal direction in a flat beam. Hence, there are no internal strains or stresses. This also shows that all internal expansions in the thickness direction above the midline of the segments of a flat beam are positive and below the midline of the segments of a flat beam are negative. Note the sign of the effective coefficient of linear thermal expansion are not with respect to the traditional sign convention

where positive expands and negative contracts. It is with respect to the global Cartesian system coordinates defined in Figure 26 and Figure 27.

This derivation was based on the fundamental geometry of a curved section, a one-dimensional isotropic beam that has free-free ends, and fundamental thermal expansion principals. Hence, there is no need for any special type of verification of this method since it fall within all the norms typically used in mechanics of materials that have already been proven and verified. The effective coefficient of thermal expansion reduces correctly to the case of a flat beam as the angle between consecutive segments/elements goes to zero. This derivation fulfills the necessary conditions for a curved beam under thermal loading.

MATLAB was used to verify analytically the method developed for ascertaining the effective coefficient of thermal expansion in curved beams- see Appendix E. The test material was 6061-T6 Aluminum- see

and Figure 49, Figure 50, Figure 51, and Figure 52. In Figure 52, it may originally appear that X-direction elongations aren't zero. However, they are to the power of -15. That is six orders of magnitude smaller than that of the Z-direction elongations. Hence, due to the numerical precision in MATLAB these are shown as non-zero but are practically zero.

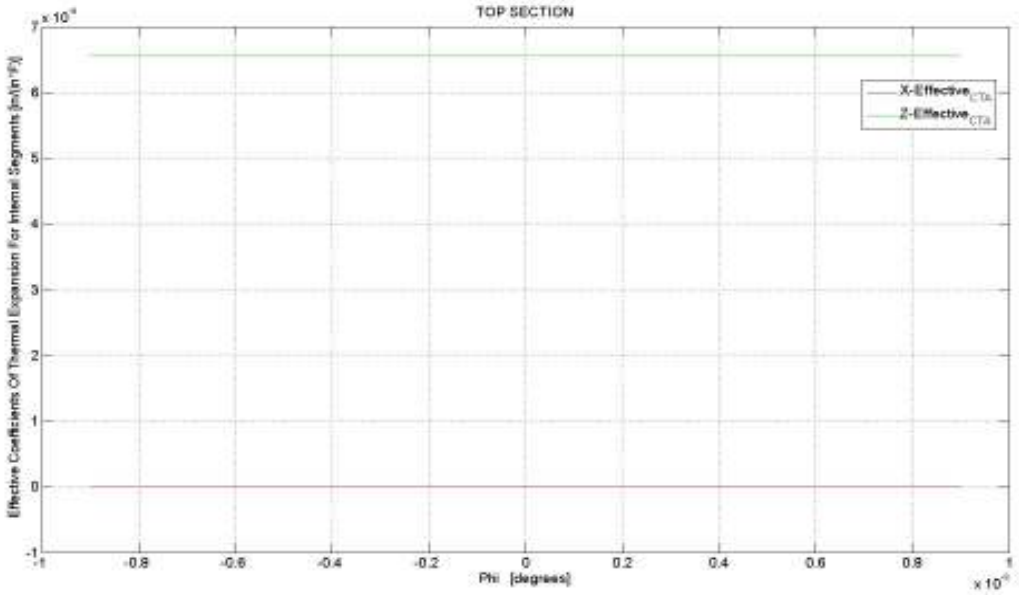

Figure 49. Effective coefficient of linear thermal expansion for internal segments for the top section of consecutive segments.

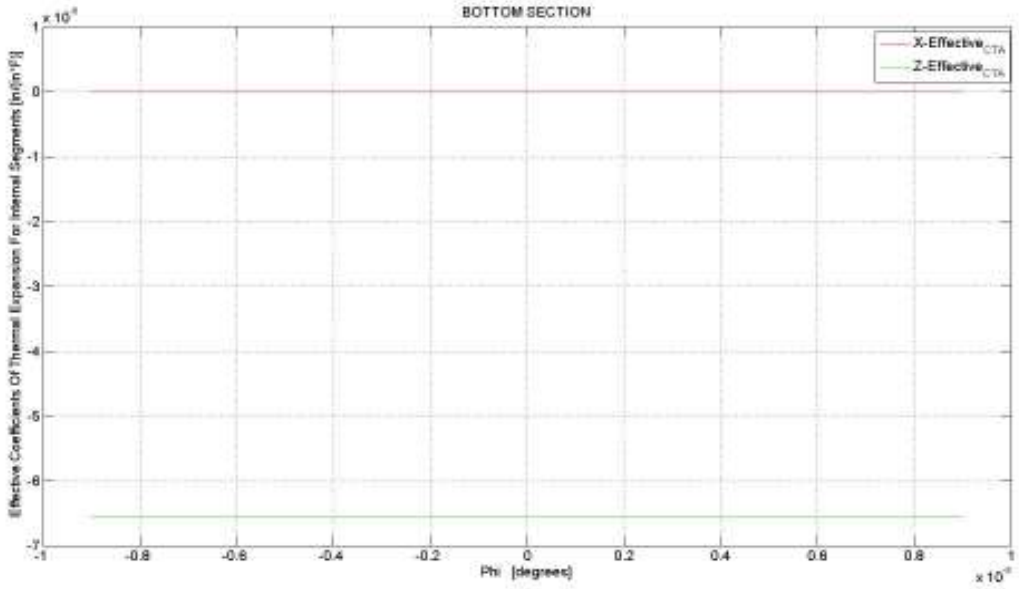

Figure 50. Effective coefficient of linear thermal expansion for internal segments for the bottom section of consecutive segments.

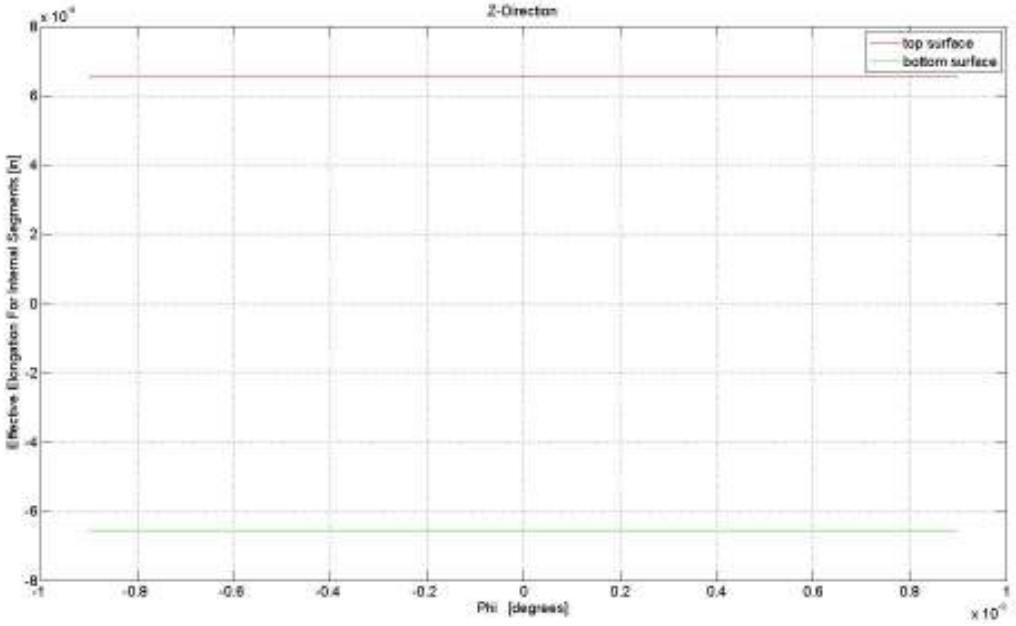

Figure 51. Effective elongation for internal segments for the bottom and top surfaces using a unit change in temperature and a unit reference dimension. Z-Direction.

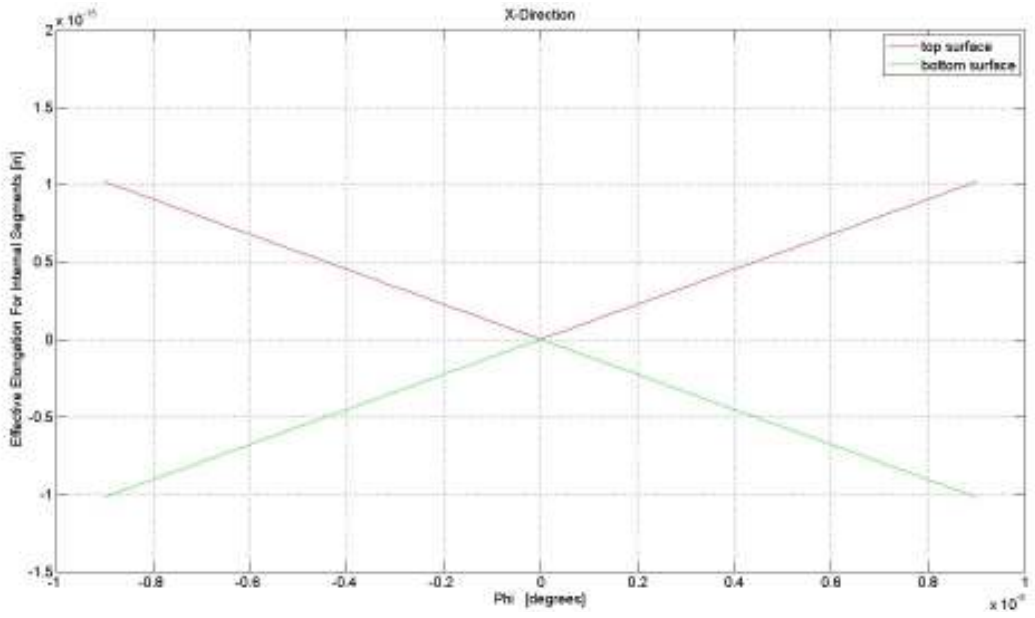

Figure 52. Effective elongation for internal segments for the bottom and top surfaces using a unit change in temperature and a unit reference dimension. X-Direction.

The stresses for the approximately flat beam in the Z-direction are shown by Figure 53. Looking at Figure 53, it can be seen that the bottom surface stresses are zero. The top surface stresses don't appear on the graph because they are plotted first. Since they are the exact same value throughout the domain, the bottom surface stresses cover them up since they are plotted last. Therefore, the top surface stresses are also zero throughout the domain. This confirms the case for flat beams under thermal loading. There are no stresses in the Z-direction. These stresses were calculated using Equation (60).

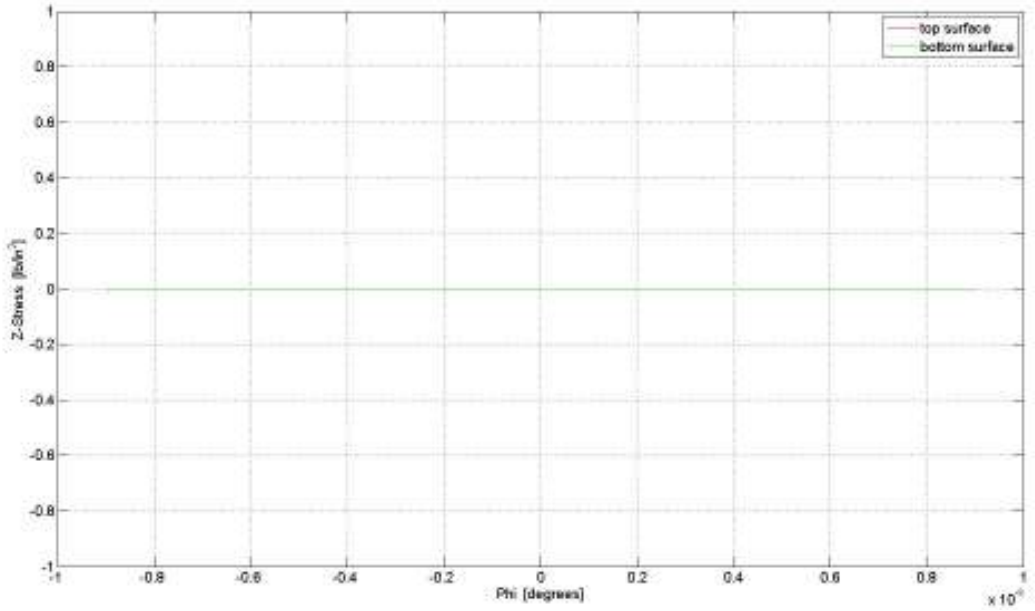

Figure 53. Stresses in the flat beam due to thermal loading for the top and bottom surfaces. Z-Direction.

The stresses for the approximately flat beam in the X-direction are shown by Figure 54. Looking at Figure 54, it can be seen that the bottom surface stresses on the left side of the approximately flat beam are approximately zero and positive. The bottom surface stresses on the right side of the approximately flat beam are approximately zero and negative. The top surface stresses on the left side of the approximately flat beam are approximately zero and negative. The top surface stresses on the right side of the approximately flat beam are approximately zero and positive. The situation here parallels that shown and explained earlier in Figure 44. The major difference is that the stresses are approximately zero (to the hundred-millionths place). This evidently means that the approximately flat beam, the radius of curvature isn't at infinity but tends to infinity for this beam, has zero stresses in the X-direction. This is what is exactly to be expected for a very well known and understood case of a flat, free-free beam that is under uniform thermal loading. It is also interesting to note that in Figure 44, the top surface stresses where similarly distributed but of slightly higher magnitude than the bottom surface stresses. This resulted in a *spring-in* effect. However, for the approximately flat beam the X-direction stresses for the top and bottom

surface are of identical magnitude. That is as the radius of curvature tends to infinity, the *spring-in* effect vanishes. These stresses were calculated using Equation (67).

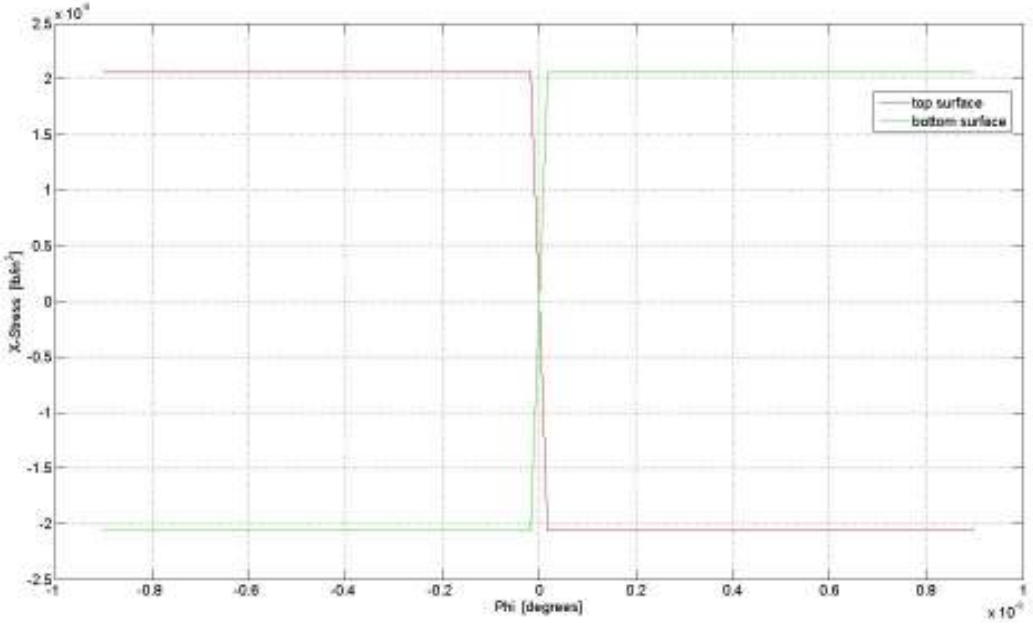

Figure 54. Stresses in the flat beam due to thermal loading for the top and bottom surfaces. X-Direction.

2.2.10 Proof of Finite Element Method Solution Reducing To Isotropic Flat Model As Radius Of Curvatures Goes to Infinity

The curved geometry of the laminate is achieved by orienting the elements in space along an arc. This is achieved not by physically rotating the element but its representative. This representative is not a physical quantity but a parameter of mechanics of solids, the stiffness matrix. This parameter's orientation and location in space defines where the physical construct (the differential segment) is oriented and located in space, and the physical construct's (the differential segment) orientation and location in space defines where the parameter is oriented and located in space. Therefore, by rotating the stiffness matrix about the Y-axis in a continuous, regular manner such that a simply curved arc is formed effectively achieves a

simply curved beam- see Figure 3, Figure 24, and Figure 25. The transformation matrix for the rotation about the Y-axis is given below:

$$[T_{ij}] = \begin{bmatrix} m_1^2 & n_1^2 & p_1^2 & 2n_1p_1 & 2p_1m_1 & 2m_1n_1 \\ m_2^2 & n_2^2 & p_2^2 & 2n_2p_2 & 2p_2m_2 & 2m_2n_2 \\ m_3^2 & n_3^2 & p_3^2 & 2n_3p_3 & 2p_3m_3 & 2m_3n_3 \\ m_2m_3 & n_2n_3 & p_2p_3 & n_2p_3+n_3p_2 & p_2m_3+p_3m_2 & m_2n_3+m_3n_2 \\ m_3m_1 & n_3n_1 & p_3p_1 & n_3p_1+n_1p_3 & p_3m_1+p_1m_3 & m_3n_1+m_1n_3 \\ m_1m_2 & n_1n_2 & p_1p_2 & n_1p_2+n_2p_1 & p_1m_2+p_2m_1 & m_1n_2+m_2n_1 \end{bmatrix}$$

$$m_1 = \cos(\phi_{x1}) = \phi_Y \qquad n_1 = \cos(\phi_{y1}) = -\frac{\pi}{2} \qquad p_1 = \cos(\phi_{z1}) = \left(\frac{\pi}{2} + \phi_Y\right)$$

$$m_2 = \cos(\phi_{x2}) = \frac{\pi}{2} \qquad n_2 = \cos(\phi_{y2}) = 0 \qquad p_2 = \cos(\phi_{z2}) = -\frac{\pi}{2}$$

$$m_3 = \cos(\phi_{x3}) = -\left(\frac{\pi}{2} - \phi_Y\right) \qquad n_3 = \cos(\phi_{y3}) = \frac{\pi}{2} \qquad p_3 = \cos(\phi_{z3}) = \phi_Y$$

ϕ_Y is the rotated angle of a given element about its local Y-axis. The inverse of $[T_{ij}]$ is achieved by taking the inverse of $[T_{ij}]$ or changing the sign of the angle argument.

For this transformation to give the pattern of orientations that would occur for a flat beam, $[T_{ij}]$'s argument should be zero: $\phi_Y = 0$. Evaluating $[T_{ij}]$ at $\phi_Y = 0$ yields:

$$[T_{ij}]_Y = \begin{bmatrix} 1 & 0 & 0 & 0 & 0 & 0_1 \\ 0 & 1 & 0 & 0 & 0 & 0 \\ 0 & 0 & 1 & 0 & 0 & 0 \\ 0 & 0 & 0 & 1 & 0 & 0 \\ 0 & 0 & 0 & 0 & 1 & 0 \\ 0 & 0 & 0 & 0 & 0 & 1 \end{bmatrix}$$

where $m_1 = 0$, $m_2 = \pi/2$, $m_3 = -\pi/2$, $n_1 = -\pi/2$, $n_2 = 0$, $n_3 = \pi/2$, $p_1 = \pi/2$, $p_2 = -\pi/2$, $p_3 = 0$

The inverse of $[T_{ij}]$ is the identity matrix as well. Therefore, the stiffness matrix is multiplied by the $[T_{ij}]$ matrix with the $[T_{ij}]$ on the right hand side. The resulting matrix is multiplied by the inverse of $[T_{ij}]$ with

the inverse of $[T_{ij}]$ on the left hand side. The identity matrix multiplied by any matrix [R] yields the same matrix, [R]. This is the case no matter the combination multiplication. This is synonymous with multiplying any given scalar by 1. Therefore, as ϕ_Y goes to zero, the modification of the stiffness matrix by transformation vanishes and the flat beam case with only a rotation of the stiffness matrix in the XY-plane is obtained.

2.2.11 Classical Lamination Theory Solution For Flat Composite Model

In Section 2.2.2, the assumptions for CLT were listed. The Author has found from personal experience that the accuracy of the results gained from CLT are highly sensitive to how faithful a model is to the given assumptions. In order to build a CLT model (2D) model that would be equivalent to the MATLAB FE (3D) model and the ANSYS FE (3D) model, the three-dimensional models must have the following:

(a) same stacking sequence

(b) width and length must be sufficiently larger than the thickness of the beam

(c) plane stress conditions: $\sigma_z = \tau_{xz} = \tau_{yz} = 0$

(d) near to fully uniform stress distribution through the width and length of the beam, save those areas where Saint Venant's principle dominates.

Simply taking a 3D model with the same stacking sequence as the 2D CLT model, same loading conditions, and the same boundary conditions is not sufficient to produce accurate results from the 3D models. Because CLT is inherently two-dimensional, it has no way to account for non-plane stress conditions. Therefore, when comparing models for verification purposes, CLT becomes the limiting factor. It is the limiting factor to which the other two models must conform to in order to provide consistent, repeatable, and accurate results that can be used for verification purposes.

Various stacking sequences produce different results. For the statically indeterminate problem under thermal loading, only a few set of stacking sequences will produce results that satisfy plane stress conditions. All other stacking sequences will produce some combination of $\sigma_z \neq 0$, $\tau_{yz} \neq 0$, and/or $\tau_{xz} \neq 0$. The stacking sequences that produce a plane stress condition for flat, fixed beam under uniform thermal loading are those that are symmetric and balanced that consist of only 0^o and/or 90^o : $[0^o]_n$, $[90^o]_n$, and $[(0^o/90^o)_n]_s$ where n = some positive integer. This family of stacking sequences is called the specially orthotropic family. Any other combination of plies and stacking sequences will produce out-of-plane loads (which CLT assumes will not occur, hence giving results that diverge from CLT). For these select few cases the A_{is} (where i = x, y) {extensional-shear coupling stiffness}, [B] = [b] = $[b^T]$ {the coupling stiffnesses for in-plane/flexure and coupling compliances for in-plane/flexure, respectively}, and D_{is} (where i = x, y) {bending or flexural/twisting stiffness} are all zero.

If the width of the beam is equivalent to the thickness, the conditions for the width and length of the beam being sufficiently larger than the thickness of the beam for CLT is violated. When this is the case, significant shear stresses (in- and out-of-plane) occur. The plane stress condition is clearly violated by having out-of-plane stresses. Also, the *additional* in-plane shear stresses aren't present with the CLT formulation. If the width of the beam and the length is too large compared to the thickness of the beam, the shear stresses (in- and out-of-plane) will tend to zero; however the longitudinal, transverse, and through thickness stresses will appreciably increase in magnitude versus that for a traditional beam- whether it is isotropic or composite. This too, leads to errors with respect to a beam.

The stress distributions must not only be in the XY-plane, but uniform in that plane (except where Saint Venant's principle applies). Classical lamination theory (implicitly) assumes uniform stress distributions. As a matter of fact, it cannot calculate stresses that aren't uniform. Therefore, any stress distributions that aren't uniform (as ascertained from ANSYS and MATLAB FE three-dimensional) will not be compatible with CLT. It would also result in stresses that diverge from CLT. ANSYS FE is less sensitive than MATLAB FE for statically indeterminate problems. This is because ANSYS departs from

the traditional methods of FE analysis for statically indeterminate problems. The standard solution method of isotropic beams that are fixed (statically indeterminate) that was used in Section 2.2.1., is used by ANSYS. This tends to *smooth* out the results and make it more *stable* when analyzing laminates that have a high degree of anisotropy due to stacking sequence geometry and stacking sequence material properties. All of the above cases are satisfied from using stacking sequences that are specially orthotropic. The width to thickness ratio for the beam used for validation was 10 to 1. The length to width ratio for the beam was 10 to 1.

The loading array must have an induced mechanical force N_x. This induced mechanical force is found by setting the mid-plane strain in the X-direction equal to zero (the beam is fixed in the X-direction and is not allowed to elongate or contract). The first row (equation) of the abd matrix is solved for the unknown N_x in terms of the compliances and the in- and out-of-plane deformations. The expression for N_x is:

$$N_X = -N_X^T - \frac{a_{12}}{a_{11}} N_Y^T$$

The material used for this test was AS4/3501-6 Carbon Epoxy- see Table 10. The thermal loading is $\Delta T = 100\ ^oF$. The stacking sequence is [0/90/0].

Table 10. Material properties of AS4/3501-6 Carbon Epoxy.

Material	Property	Value
AS4/3501-6 Carbon Epoxy		
	E_1	2.13E+07
	E_2	1.50+06
	E_3	1.50E+06
	G_23	0.54E+06
	G_13	1.00E+06

Table 10. – *Continued*

G_12	1.00E+06
v_23	0.54
v_13	0.27
v_12	0.27
alpha_1	-0.05E-05
alpha_2	1.50E-05
alpha_3	1.50E-05

ABD					
2.2164E5	6.106E3	0	0	0	0
6.106E3	1.2213E5	0	0	0	0
0	0	1.5E4	0	0	0
0	0	0	5.8412	1.145E-1	0
0	0	0	1.145E-1	6.314E-1	0
0	0	0	0	0	2.812E-1

abd					
4.52E-06	-2.26E-07	0	0	0	0
-2.26E-07	8.20E-06	0	0	0	0
0	0	6.67E-05	0	0	0
0	0	0	1.726E-1	-3.13E-2	0
0	0	0	-3.13E-2	1.5895	0
0	0	0	0	0	3.5556

Table 11. In- and out-of-plane loads.

Loadings		
N_x	1.0057	lb
Ny	20.1133	lb
Ns	0	lb
Mx	0	lb*in
My	0	lb*in
Ms	0	lb*in

Table 12. In- and out-of-plane deformations

Mid-Plane Strains & Curvatures	
0	in/in
0.000165	in/in
0	in/in
0	1/in
0	1/in
0	1/in

Table 13. Stress results from CLT

	Stresses			Units
	Layer 1	**Layer 2**	**Layer 3**	lb/in^2
σ_x	527	-2174	527	
σ_y	-1993	3986	-1993	
τ_s	0	0	0	

2.2.12 Finite Element Method Solution For Flat Composite Model

ANSYS was used to provide another check, along with CLT, of the MATLAB finite element analysis program developed by the Author. A flat beam model under the same loading conditions of the problem solved in Section 2.2.12 is analyzed. The following stresses were ascertained:

Table 14. Stress results from ANSYS.

	Stresses			Units
	Layer 1	**Layer 2**	**Layer 3**	lb/in^2
σ_x	513	-2174	546	
σ_y	-1993	3988	-1993	
τ_s	3.00E-03	3.00E-03	3.00E-03	

The following figures visually confirm the uniform nature of the stress distributions that are required for this model to match with CLT. The first figure is the deformations of the fixed, flat composite beam under the given thermal loading conditions- see Figure 55. Observe Figure 56, Figure 57, Figure 58, Figure 59, and Figure 60.

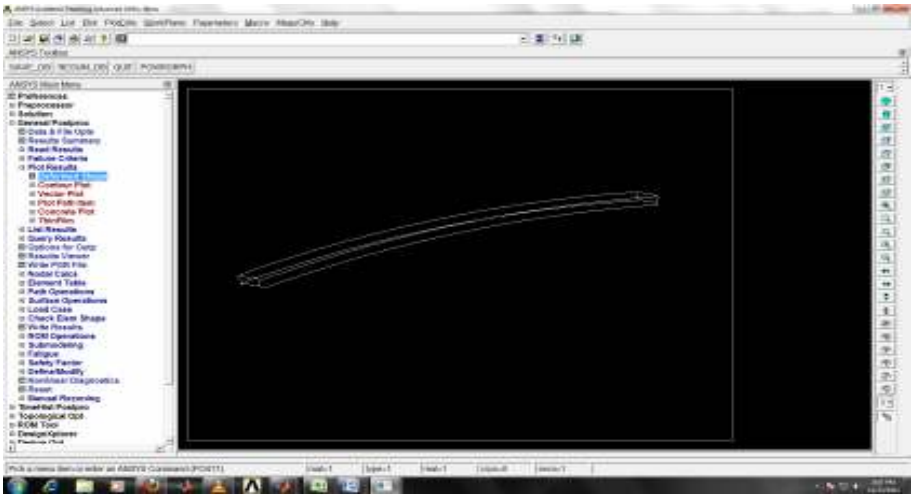

Figure 55. An exaggerated scale of the deformations of the given fixed, flat composite beam under thermal loading.

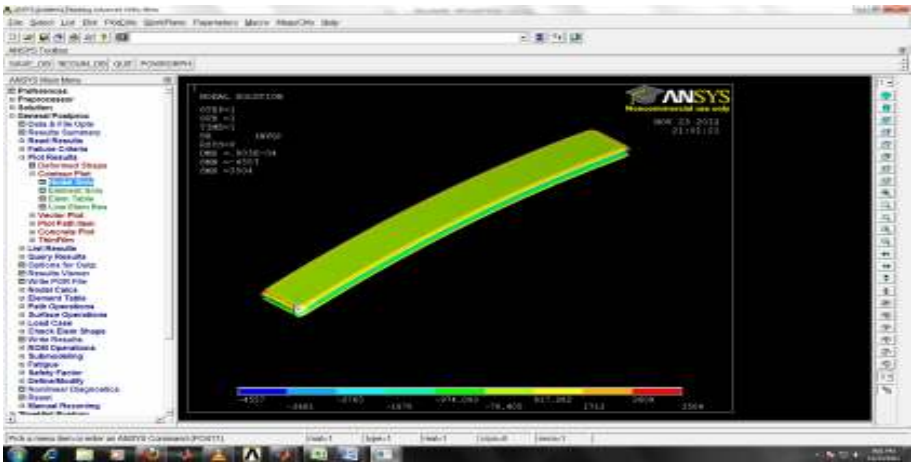

Figure 56. An exaggerated scale of the deformations of the given fixed, flat composite beam under thermal loading with an overlap of the σ_X stresses.

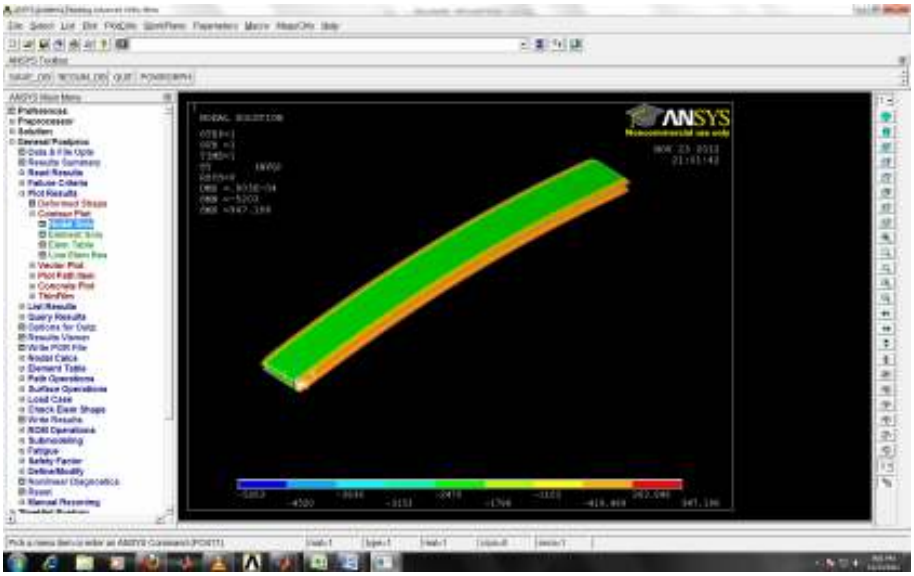

Figure 57. An exaggerated scale of the deformations of the given fixed, flat composite beam under thermal loading with an overlap of the σ_Y stresses.

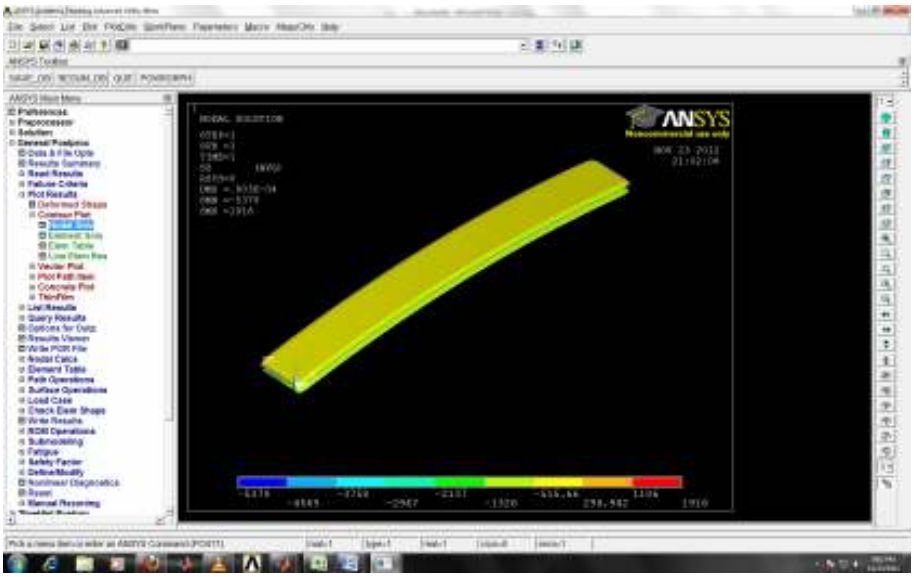

Figure 58. An exaggerated scale of the deformations of the given fixed, flat composite beam under thermal loading with an overlap of the σ_Z stresses.

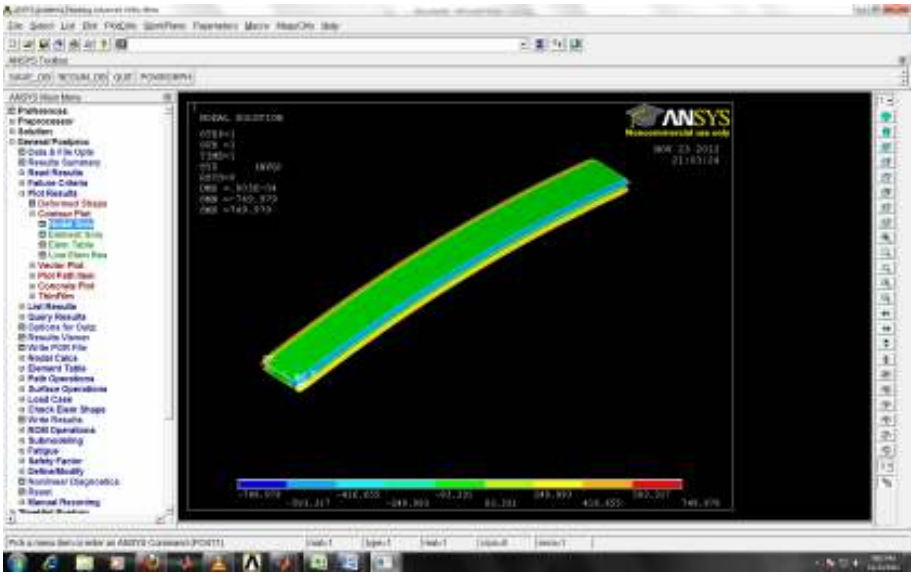

Figure 59. An exaggerated scale of the deformations of the given fixed, flat composite beam under thermal loading with an overlap of the τ_{YZ} stresses.

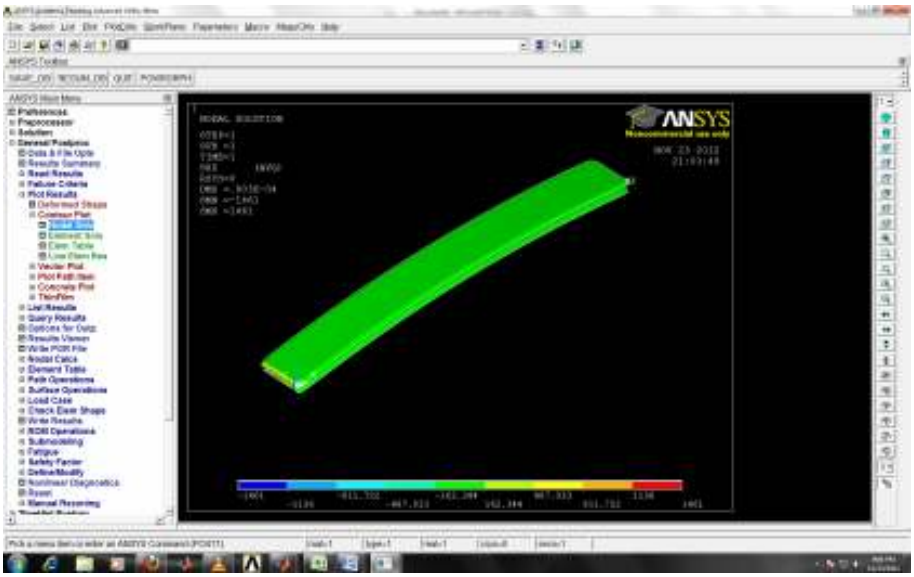

Figure 60. An exaggerated scale of the deformations of the given fixed, flat composite beam under thermal loading with an overlap of the τ_{XZ} stresses.

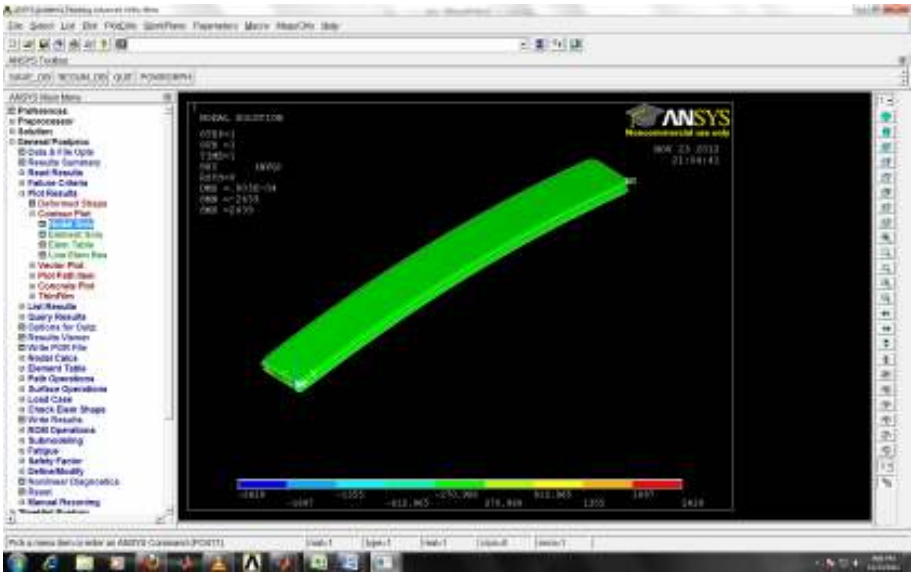

Figure 61. An exaggerated scale of the deformations of the given fixed, flat composite beam under thermal loading with an overlap of the τ_{XY} stresses.

It can be seen in Figure 55, Figure 56, Figure 57, Figure 58, Figure 59, Figure 60 and Figure 61, that the stresses are in fact fairly uniform throughout the beam. It can also be seen that the out-of-plane stresses are necessarily zero so that comparison of stress results with CLT would be possible and valid.

The MATLAB finite element analysis program used the same loading conditions, stacking sequence, material, etc. as the ANSYS finite element model and the CLT model. As mentioned in Section 2.1, the finite element analysis program in MATLAB uses a tri-linear, isoparametric element. This element and the MATLAB FE program are very sensitive to strains of an order higher than the interpolation functions of the element. The magnitude of the strains only exacerbates this sensitivity. If the variation of the strains is of a higher order than the interpolation functions of the element, then the elements would generate spurious strain modes. Isoparametric elements are notorious for this behavior. Nevertheless, these modes negligibly affect the accuracy of the solutions for this case. The variations are due to the fact that the Saint Venant's stresses aren't smoothed out as they are in ANSYS by treating the statically indeterminant problem similar to that shown in Section 2.2.1 and previously discussed. This problem is generally solved by making the beam very long so that Saint Venant's stresses don't come into play. That is with this particular program, the MATLAB FE analysis smoothes the strains to a linear order so that the spurious strain modes are suppressed if the length to width ratio of the beam is sufficiently high. This generally takes noticeable effect when this ratio is at least 30 to 1. Nevertheless, the mean of the stresses are slightly affected by these modes (since this beam has a length to width ratio of 10 to 1). Nevertheless, the most accurate representative of these stresses is the mode (not the mean) of the stresses. Therefore, the mode (which is very near the mean value) of the stresses is shown in the table below.

Table 15. Stress results from MATLAB.

	Stresses			Units
	Layer 1	**Layer 2**	**Layer 3**	lb/in^2
σ_x	508	-2176	508	
σ_y	-1993	3987	-1993	
τ_s	-5.70E-13	2.71E-14	5.42E-13	

The latter detailed effects combined with the anisotropic nature of the laminate gave final results showing spurious stresses.

The first check show that the beam is in fact in plane (XY-plane) stress conditions. For plane stress conditions, σ_z, τ_{xz}, and τ_{yz} are all equal to zero (that is the mean and mode are zero). This can be seen in Figure 62, Figure 63, Figure 64, Figure 65, Figure 66, Figure 67, Figure 68, Figure 69, and Figure 70:

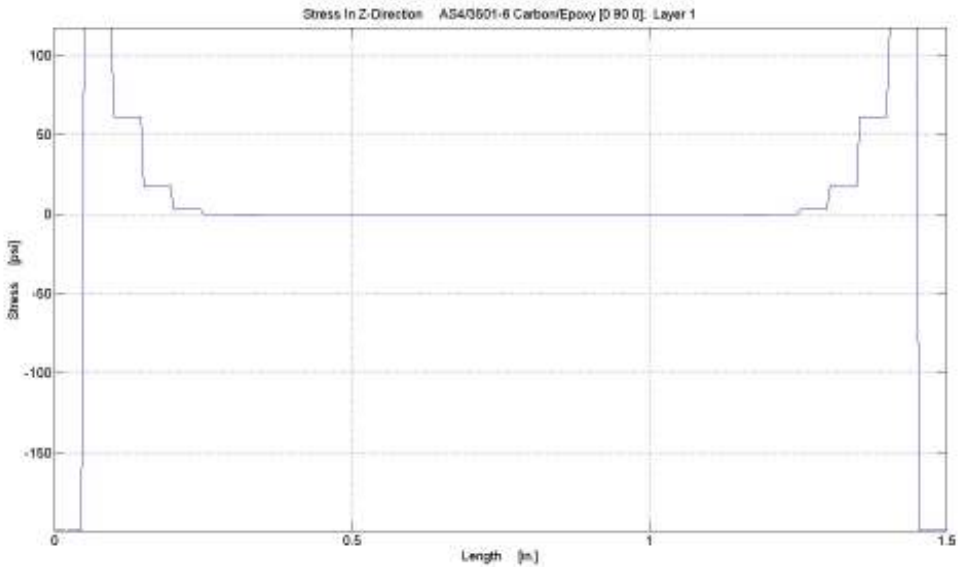

Figure 62. Stress σ_z plot for layer 1 (bottom layer).

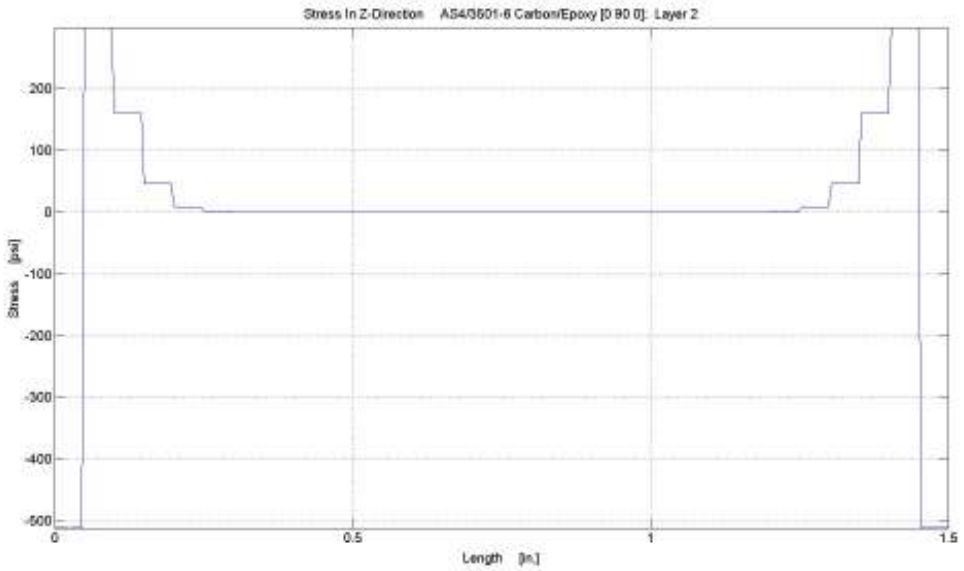

Figure 63. Stress σ_z plot for layer 2 (middle layer).

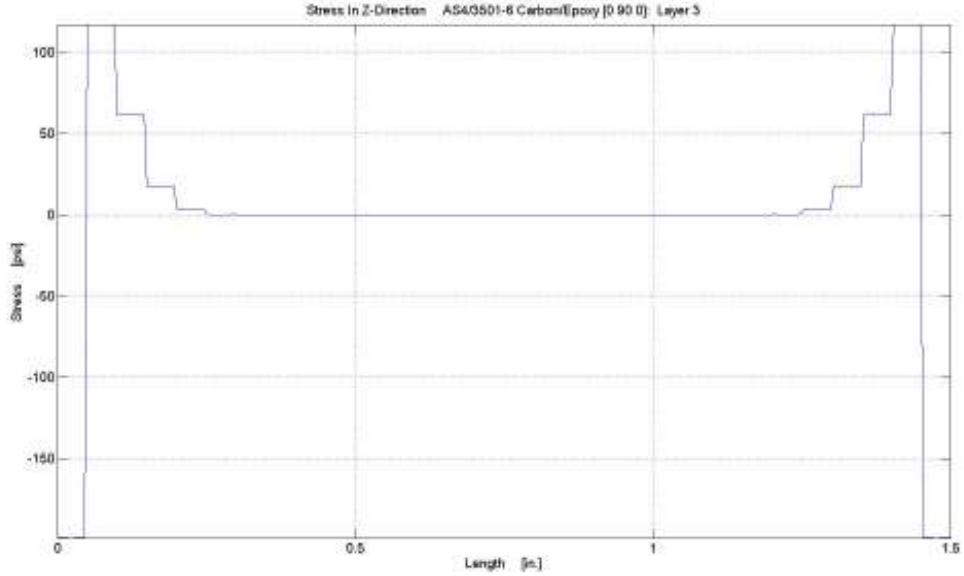

Figure 64. Stress σ_z plot for layer 3 (top layer).

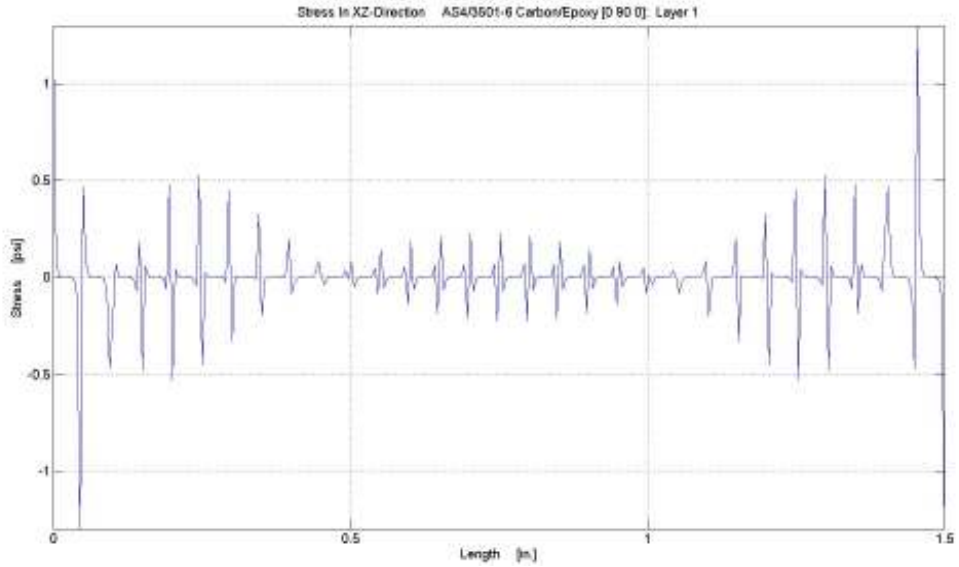

Figure 65. Stress τ_{xz} plot for layer 1 (bottom layer).

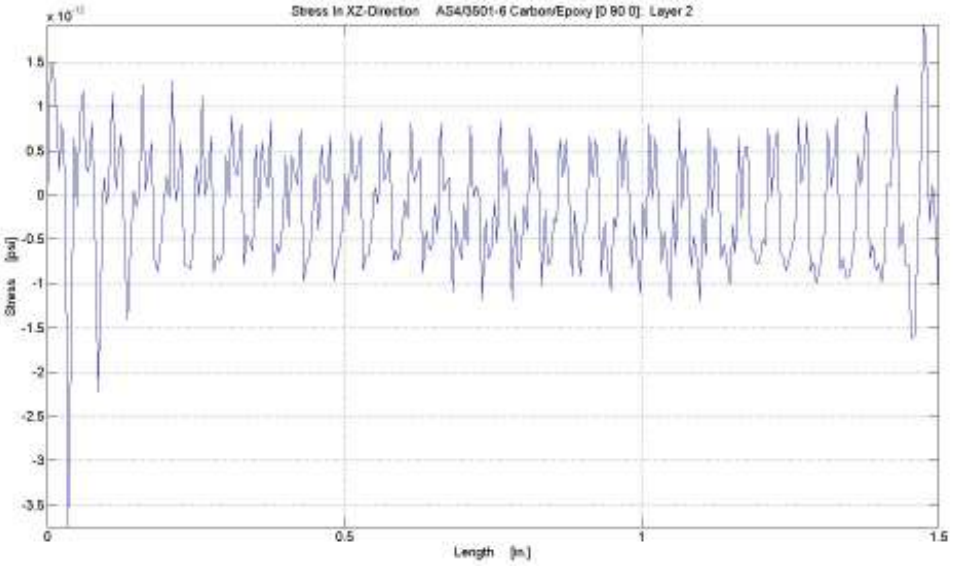

Figure 66. Stress τ_{xz} plot for layer 2 (middle layer).

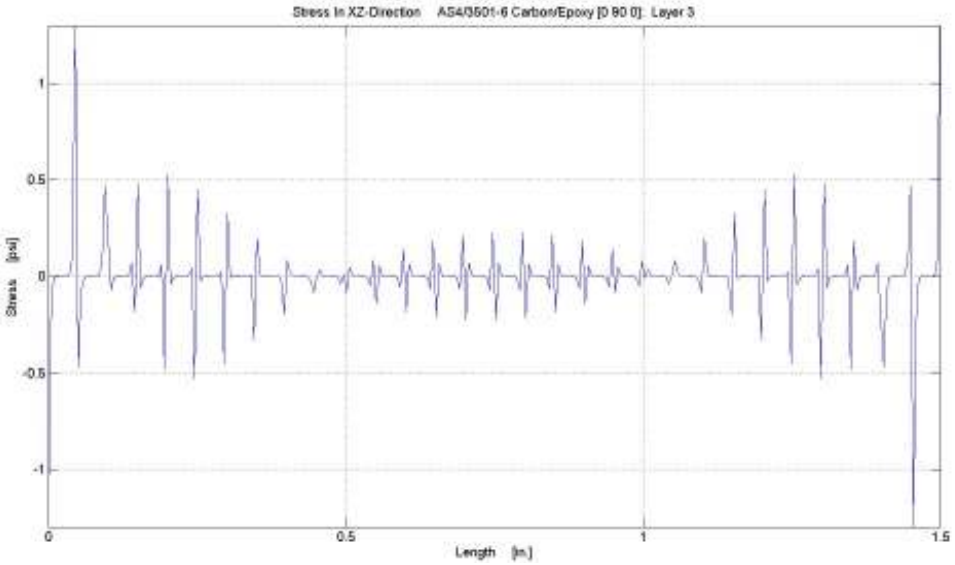

Figure 67. Stress τ_{xz} plot for layer 3 (top layer).

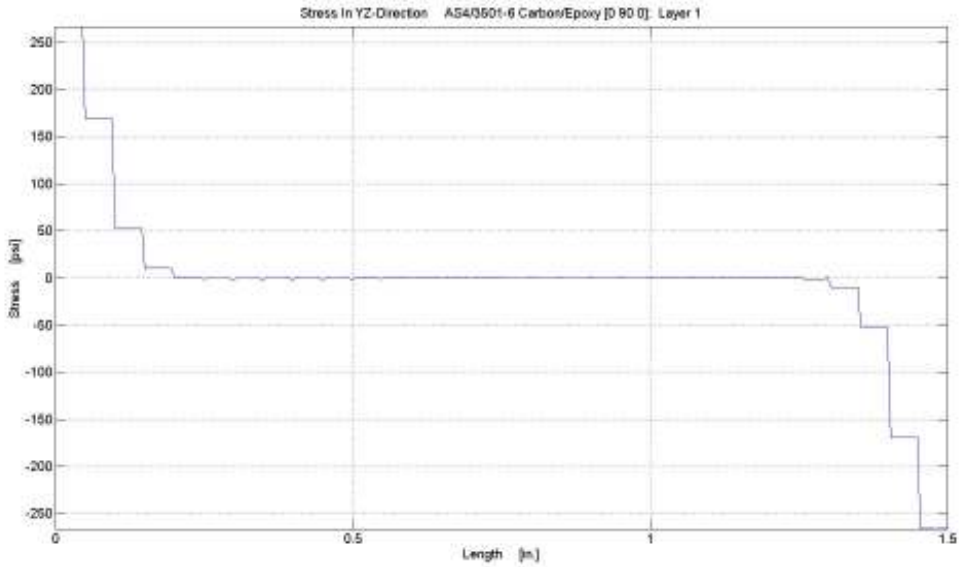

Figure 68. Stress τ_{yz} a plot for layer 1 (bottom layer).

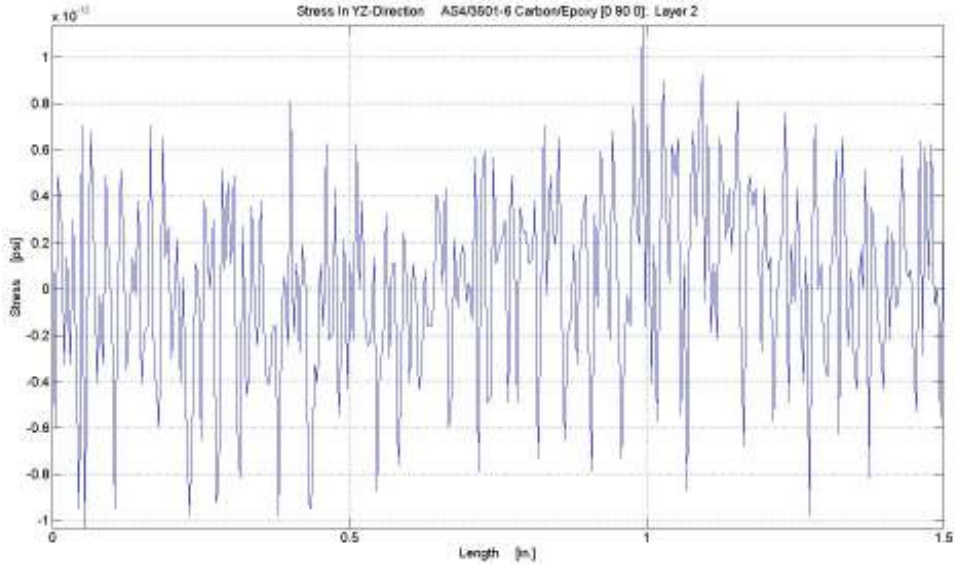

Figure 69. Stress τ_{yz} a plot for layer 2 (middle layer).

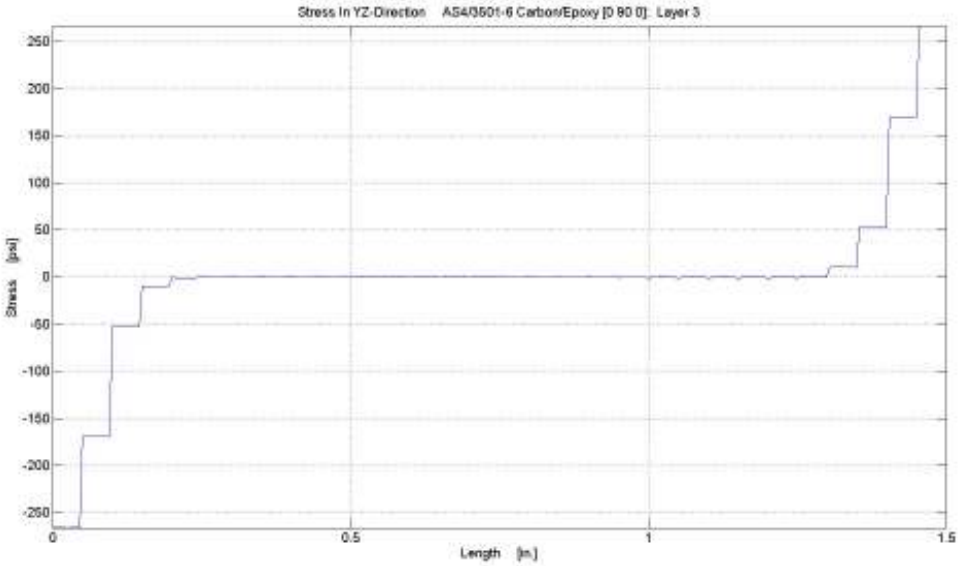

Figure 70. Stress τ_{yz} a plot for layer 3 (top layer).

The stress results for σ_x, σ_y, and τ_{xy} are in Figure 71, Figure 72, Figure 73, Figure 74, Figure 75, Figure 76, Figure 77, Figure 78, and Figure 79. For these stresses, spurious modes are more prevalent. Therefore, the median is plotted as a red-dotted line. This value is extremely close to the mean but tends to negate the spurious stresses that are generated.

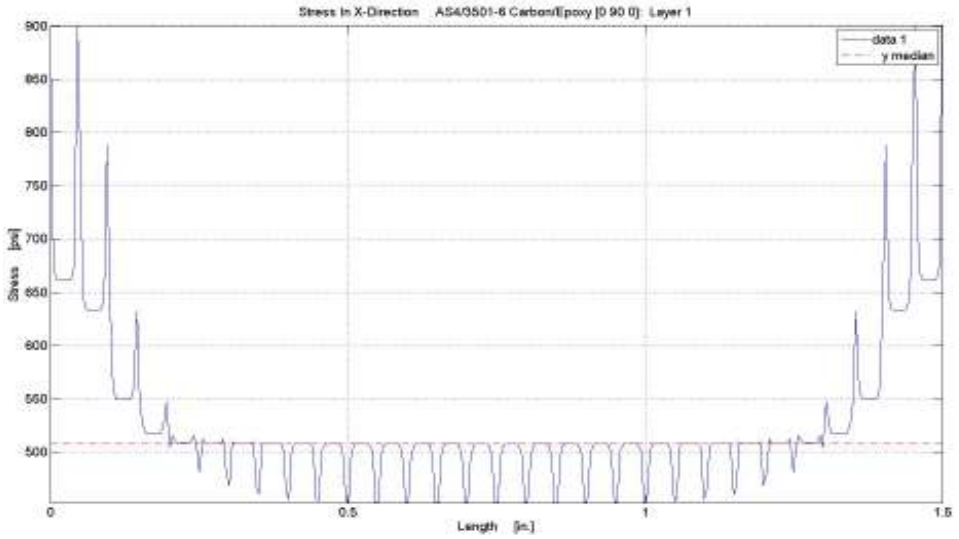

Figure 71. Stress σ_x a plot for layer 1 (bottom layer).

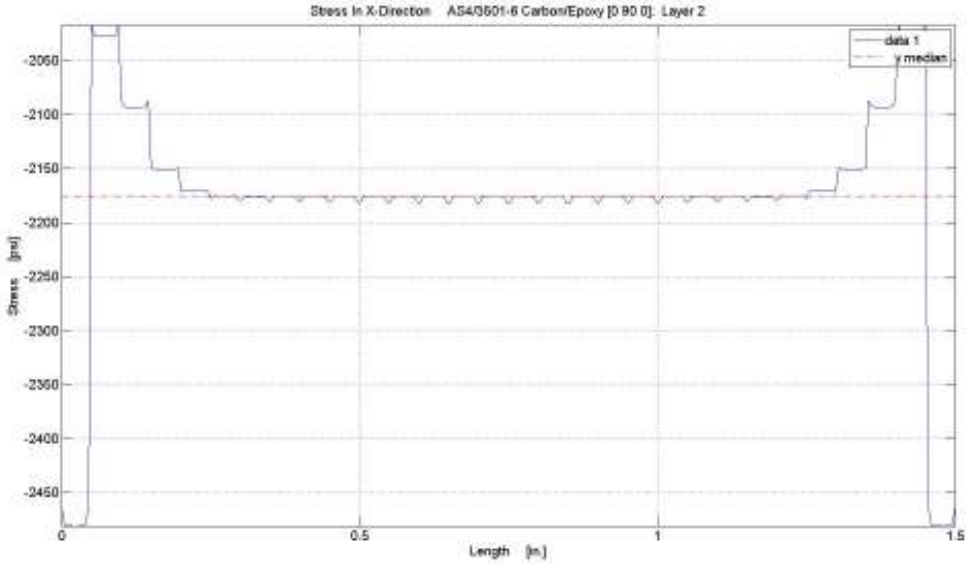

Figure 72. Stress σ_x a plot for layer 2 (middle layer).

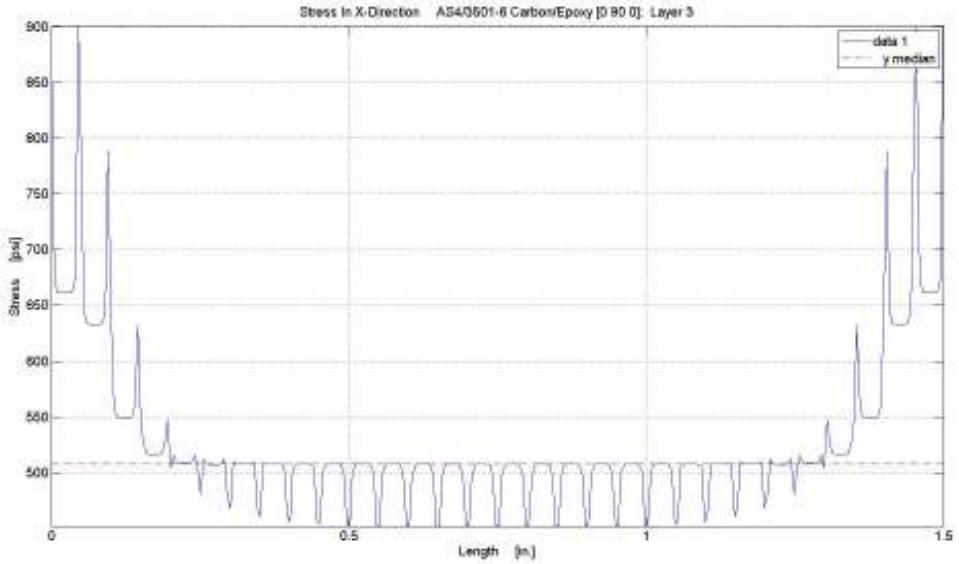

Figure 73. Stress σ_x a plot for layer 3 (top layer).

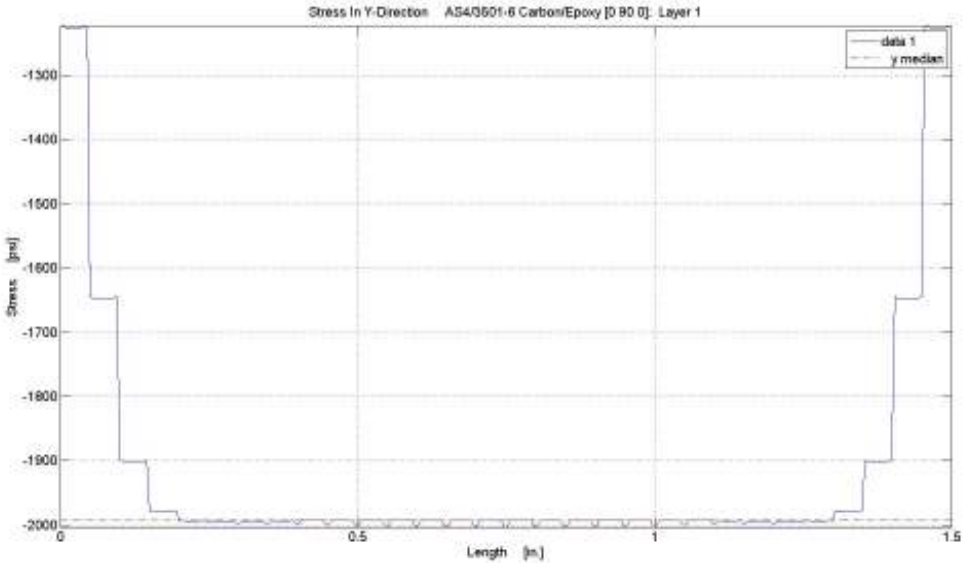

Figure 74. Stress σ_y a plot for layer 1 (bottom layer).

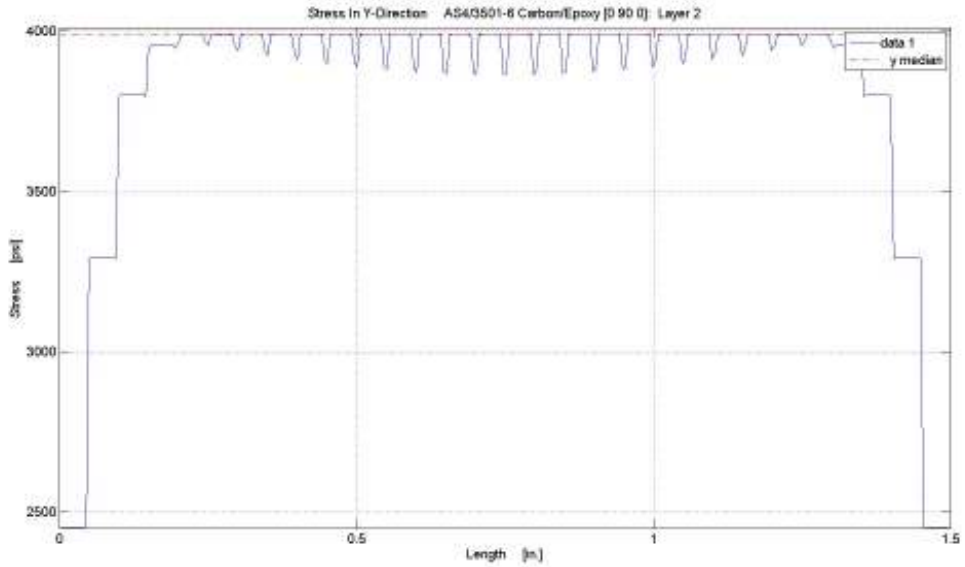

Figure 75. Stress σ_y a plot for layer 2 (middle layer).

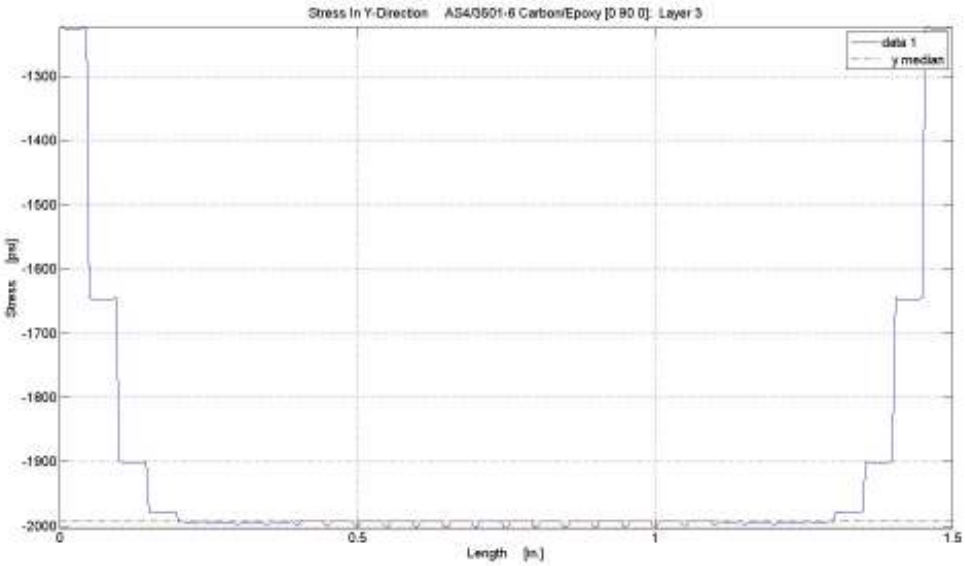

Figure 76. Stress σ_y a plot for layer 3 (top layer).

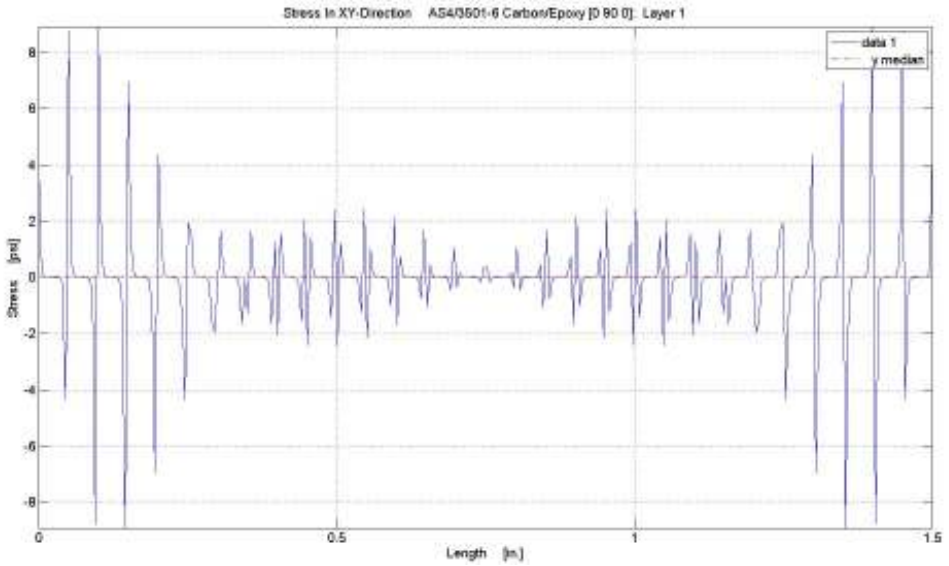

Figure 77. Stress τ_{xy} a plot for layer 1 (bottom layer).

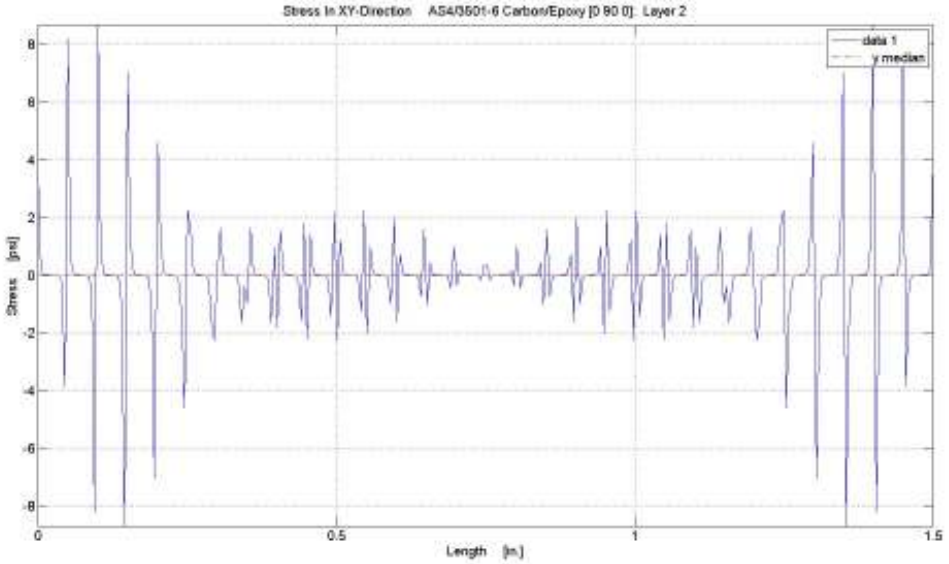

Figure 78. Stress τ_{xy} a plot for layer 2 (middle layer).

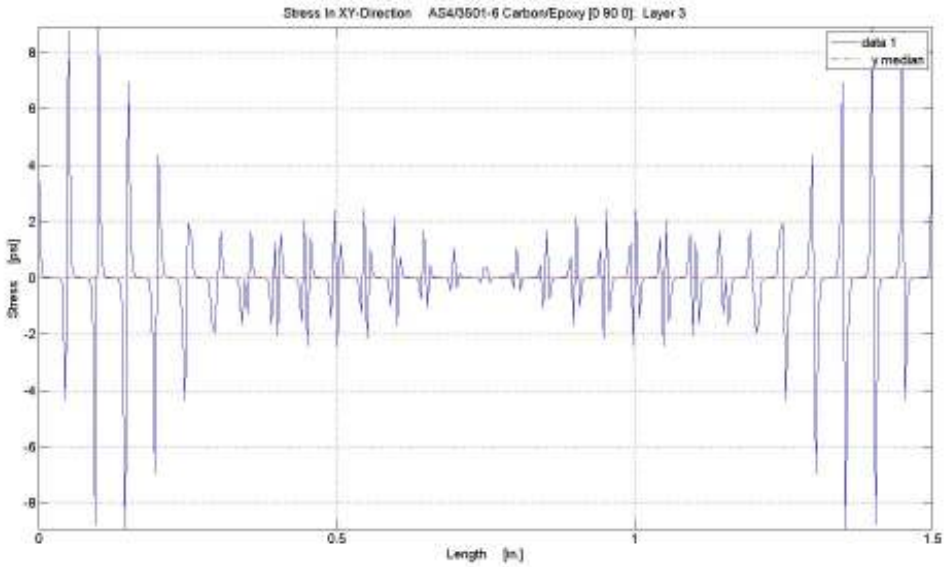

Figure 79. Stress τ_{xy} a plot for layer 3 (top player).

2.2.13 Model Validation Conclusions

The results from CLT (2D) analytical, ANSYS (3D) finite element, and MATLAB program (3D) finite element are shown in the following table:

Table 16. Stress results from CLT, ANSYS (FE), and MATLAB (FE).

$[0\ 90\ 0]_T$				
	Layer	**CLT**	**ANSYS (FE)**	**MATLAB (FE)**
σ_x	3	527	546	508
	2	-2174	-2174	-2176
	1	527	513	508
σ_y	3	-1993	-1993	-1993
	2	3986	3988	3987
	1	-1993	-1993	-1993
τ_{xy}	3	0	3.00E-03	5.42E-13
	2	0	3.00E-03	2.71E-14
	1	0	3.00E-03	-5.70E-13

From Section 2.2.11 and 2.2.12 and Table 16, it can be seen that the MATLAB program is successful in accurately modeling a composite laminate that is anisotropic in geometric stacking sequence and anisotropic in material stacking sequence. With all finite element analysis programs, careful modeling is the key to correct solutions. Verification of the model must occur with a known solution serving as a reference point. All verifications must be with parallel counterparts. After correctly verifying (to the fullest extent possible, that is without experimentation) and developing the MATLAB finite element program, it will now be used to model simply curved composite laminates that are fixed on either longitudinal end.

CHAPTER 3

CURVATURE AND STACKING SEQUENCE EFFECT ON STRESSES

The purpose of this chapter is to ascertain the relationship between the curvature of a laminate under thermal loading and the resulting stresses and how these stresses vary with a particular family of stacking sequences.

3.1 Geometry and Material Used

3.1.1 Geometry of Curved Laminates

Four unique geometries were chosen for modeling the curved laminates. The thickness and arc-length of the geometries are the same. The distinguishing parameters were the radius of curvature or curvature of the geometries. The five different radii of curvature were chosen to represent a zero curvature (flat), distinguishably small curvatures, moderately curved laminates, and distinctly large curvature beams. These curved laminates were simply curved laminates; they have a unique curvature (semi-circular). A representative model of the curved beam is shown in Figure 3.

Table 17. Geometrical configurations for trade study.

	Arc Length	Thickness	Width	Radius of Curvature	Curvature	Angle Spanned
Model 1	0.9 in	0.030 in	0.12 in	Infinity	0	0^{o}
Model 2	0.9 in	0.030 in	0.12 in	1.72 in	0.58 1/in.	30^{o}
Model 3	0.9 in	0.030 in	0.12 in	1.15 in	0.87 1/in.	45^{o}
Model 4	0.9 in	0.030 in	0.12 in	0.86 in	1.16 1/in.	60^{o}
Model 5	0.9 in	0.030 in	0.12 in	0.57 in	1.75 1/in.	90^{o}

3.1.2 Material of Curve Laminates

See Table 18 for material properties the E-Glass/Epoxy that was used in the models for the trade study.

Table 18. Material properties of E-Glass/Epoxy.

Material	Property	Value
E-Glass/Epoxy		
	E_1	6.00E+06
	E_2	1.50E+06
	E_3	1.50E+06
	G_23	5.00E+05
	G_13	6.20E+05
	G_12	6.20E+05
	v_23	0.5
	v_13	0.28
	v_12	0.28
	alpha_1	3.90E-06
	alpha_2	1.44E-05
	alpha_3	1.44E-05

3.2 Curvature Effect

3.2.1 General Curvature Effect

For a flat beam, there are many coupling behaviors that can be ignored because the infinite radius of curvature (zero curvature) decouples the normal loading & shear deformation and shear loading & normal deformation coupling that exist in materials. This coupling behavior is generally ignored for most mechanics problems because those problems concern flat beams. Even for some variously curved beam, this stiffness coupling behavior is generally ignored. Most of analytical solutions for the variously curved beam under certain types of loadings and boundary conditions have errors in the results with respect to experimental observations. Those analytical solutions generally involve derivations that are analogs to the

geometry of the beam and whether an internal shear may or may not exist, whether an internal moment may or may not exist, etcetera. However, these analytical solutions generally leave out the extremely important effect of the coupling of the stiffnesses due to the geometry of the problem. These couplings are through the off-diagonal terms that are zero for flat beams as shown in Equation (10). As curvature is added to these beams, depending on their anisotropic nature, these zero terms become non-zero. Also the other traditionally non-zero terms that are diagonal and off diagonal will change with curvature and anisotropic character of the beam.

The ignorance of these couplings that exist for curved beam (and for this thesis' purpose: simply curved beams) and the lack of accounting for these effect, is the main reason all of the analytical solutions discussed in Section 2.2.5 have some type of inherent error in their results. Regardless of how faithful various internal normal or shear forces and bending moments are accounted for, if the stiffness are unaccounted for completely or completely disregarded, error will result just as those analytical solutions show. These solutions are well known to have error that tends to zero as the beam's radius of curvature tends to infinity. These solutions are also well known to have error that tends to larger and larger values as the beam's radius of curvature tends to zero. Interestingly, the stiffness couplings that are traditionally zero (as discussed earlier) for beams that are flat goes to zero and hence the major source of error goes to zero. The stiffness couplings that are traditionally zero but become non-zero to increasing extents as the radius of curvature of the beam reduces (the beam acquires more curvature). Since these analytical models don't account for these couplings, the error likewise increases as these coupling terms become larger as the curvature increases. Furthermore, more coupling stiffnesses go from zero to non-zero values depending on the anisotropic character of the laminate. This effect is then exacerbated by the extent of the curvature in the beam. The following sections will examine the effect that the curvature has (via these stiffnesses) on the finite elements' x- and z-directions (globally: tangential and radial directions, respectively) with stacking sequences.

6061-T6 Aluminum is used as a baseline for the results. All of the following laminates consist of 6 plies, are under a thermal loading of $\Delta T = 100\ ^{o}F$, and are fixed along each *longitudinal end* as a fixed-

fixed (statically indeterminate) beam. That is, they are fixed along the X-direction- see Figure 6. The other three laminates are as follows:

Balanced and symmetrical laminate: $[+45/-45/0]_S$

Antisymmetrical (balanced and unsymmetrical) laminate: $[+45/-45/0/0/45/-45]_T$

Unbalanced and unsymmetrical laminate: $[+45/+45/0]_S$

It should also be noted that the length to width ratio of the beams are 7.5. Generally for beams, if the length to width ratio is less than 10, internal shear will exist in the beams. The variations of these shears are generally of a quadratic order or higher. Since the MATLAB finite element program uses tri-linear isoparametric elements (whose notorious spurious strain modes issues were addressed earlier), spurious shear and consequently spurious normal stresses will exist.

The average stress for the beam on layer 4 (0^o ply) of each laminate for each Model case- see Table 17- was ascertained. This stress was at the mid-width (Y-direction) of each laminate and was the element stress. Therefore, the following analysis is based on the average effect in the beam. Since every point in the beam has its own stress for each stress component and that stress varies according to stacking sequence, geometry, etc., it is best to use some overall result (the mean) to compare the mean behaviors of different geometries.

3.2.2 Detail Curvature And Stacking Sequence Effect For Mean Stress At (Near) Mid-Point Of Laminate

It can be seen from Figure 80 that the curvature of a beam has appreciable effects on the finite element longitudinal stresses σ_x. This stress is the local x-direction stress for each finite element. Hence, it is the global tangential stress for the curved beam at each differential segment (*finite element*). For the isotropic aluminum laminate all the tangential stresses are negative (note: the traditional stress sign convention is used here) for all five curvature cases. Hence, the curved laminate is tangentially under compression. However, for the glass/epoxy laminates this is not the case.

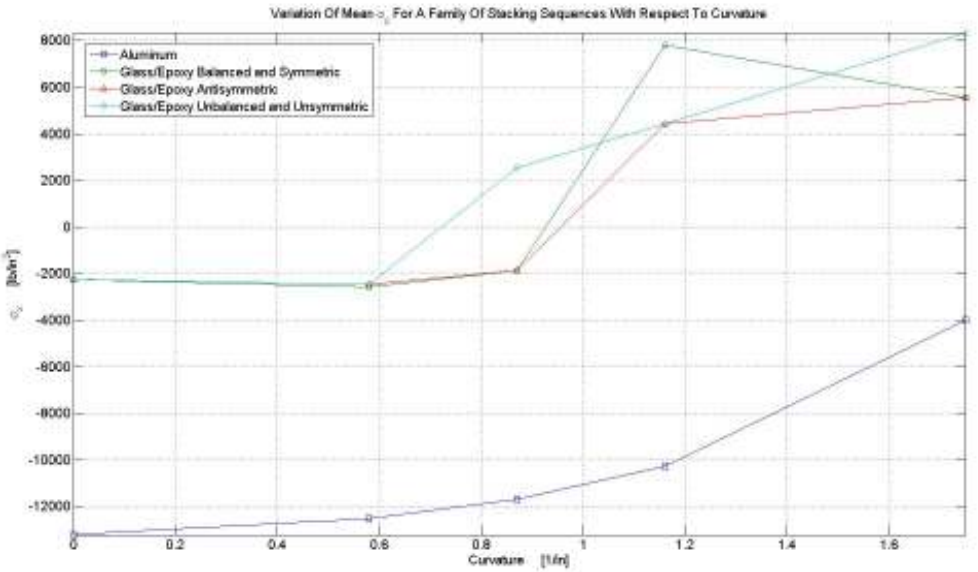

Figure 80. Stacking sequence trade study on σ_x as the curvature varies increasingly from 0.

The laminates initially have a similar compressive tangential stresses for the zero curvature case, Model 1 (see Table 17). This is due to the close similarity between the stacking sequences. For the Model 2 case, the laminates still have similar compressive tangential stresses; however, the unsymmetrical & unbalanced laminate begins to diverge from the symmetrical & balanced laminate and the antisymmetrical laminate. For the Model 2 cases, all of the laminates have a compressive tangential stress that is slightly higher in magnitude than that for the Model 1 case. For the Model 3 case, the unsymmetrical & unbalanced laminate completely diverges from the symmetrical & balanced laminate and the antisymmetrical laminate. The unsymmetrical & unbalanced laminate is now under tensile tangential stress. The symmetrical & balanced laminate and the antisymmetrical laminate still have similar compressive tangential stresses. For the Model 4 case, the symmetrical & balanced laminate and the antisymmetrical laminate tangential stress values diverge. However, the antisymmetrical and unsymmetrical & unbalanced laminates converge to a similar tensile tangential stress. For the Model 5 case, the balanced & symmetric and the antisymmetrical laminates converge to a similar tensile tangential stress. The unbalanced & unsymmetrical laminate

diverges from the balanced & symmetric and the antisymmetrical laminates to a unique tensile tangential stress.

It can be seen from Figure 81 that the curvature of a beam has appreciable effects on the finite element longitudinal stresses σ_z. This stress is the local z-direction stress for each finite element. Hence, it is the global radial stress for the curved beam at each differential segment (*finite element*). For the isotropic aluminum laminate all the radial stresses are negative (note: the traditional stress sign convention is used here) for all five curvature cases. Hence, the curved laminate is under compression in the radial direction. However, for the glass/epoxy laminates this is not the case.

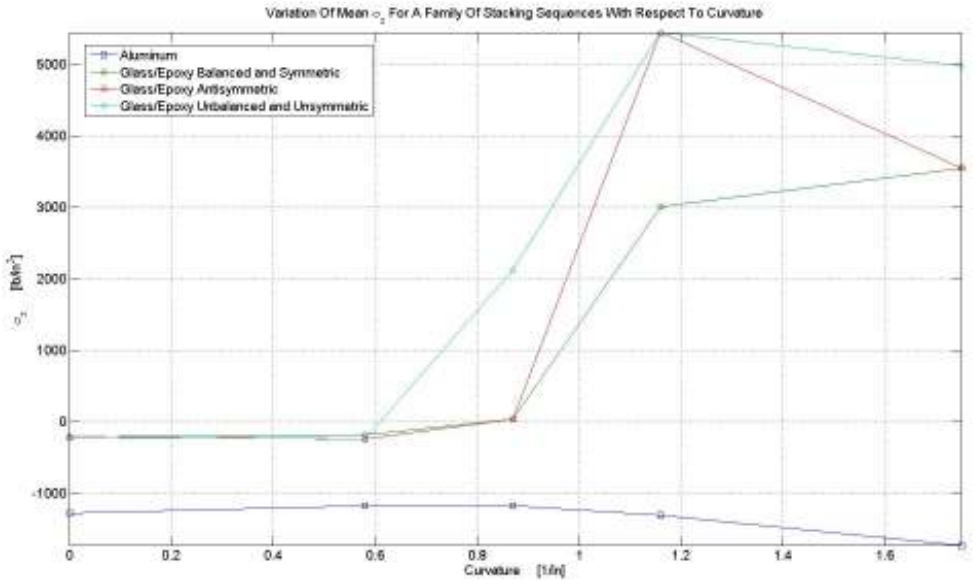

Figure 81. Stacking sequence trade study on σ_z as the curvature varies increasingly from 0.

The laminates initially have a similar compressive radial stresses for the zero curvature case, Model 1 (see Table 17). This is due to the close similarity between the stacking sequences. For the Model 2 case, the laminates still have similar compressive tangential stresses; however, the symmetrical & balanced laminate begins to diverge from the unsymmetrical & unbalanced laminate and the antisymmetrical laminate. For the Model 2 cases, all of the laminates have a compressive radial stress that is slightly higher in magnitude than that for the Model 1 case. For the Model 3 case, the unsymmetrical &

unbalanced laminate completely diverges from the symmetrical & balanced laminate and the antisymmetrical laminate. The unsymmetrical & unbalanced laminate is now under tensile radial stress. The symmetrical & balanced laminate and the antisymmetrical laminate still have similar approximately zero radial stresses. For the Model 4 case, the symmetrical & balanced laminate and the antisymmetrical laminate radial stress values diverge. However, the antisymmetrical and unsymmetrical & unbalanced laminates converge to a similar tensile tangential stress. All stresses are now tensile radial stresses. For the Model 5 case, the balanced & symmetric and the antisymmetrical laminates converge to a similar tensile radial stress. The unbalanced & unsymmetrical laminate diverges from the balanced & symmetric and the antisymmetrical laminates to a unique tensile radial stress.

3.2.3 Curvature And Stacking Sequence Effect For Mean Stress At (Near) Mid-Point Of Laminate Conclusions

The pattern of laminates diverging and converging in groups of two is the exact same pattern (not necessarily magnitude) for the radial stresses as it is for the tangential stresses. That is, the only difference in Figure 80 and Figure 81 is the magnitude of the stresses and similarity of the pattern of stresses. However, the trend between groups of two laminates for all the model cases is the same. Furthermore, only for the isotropic aluminum laminate does the radial and tangential stresses remain compressive for all five curvature cases.

The reason for the variations in the stresses from compressive to tensile in both the radial and tangential directions for the composite laminates while the isotropic aluminum laminate maintains compressive radial and tangential stresses is shown in Appendix G. The coupling stiffnesses that are normally zero for a flat beam (as discussed in Section 3.2.1) become non-zero for curved beams. The magnitude and the type of coupling stiffness that becomes non-zero vary with the radius of curvature and the anisotropic nature of the laminate. These coupling stiffness manifest because the finite element is rotated about the laminate Y-direction (see Figure 6) with the transformation matrix shown in Section 2.2.10. When these coupling stiffnesses come into effect, they effectively *transfer* the stresses in the beam

to other directions. That is, the stresses are redistributed from normal stresses to shear stresses. This redistribution of stresses is what causes the changes in the radial and tangential stresses in Figure 80 and Figure 81.

As the curvature increases, the stresses redistribute from the Model 1 case as is shown in Figure 80, Figure 81, and Appendix G. The magnitude and direction of the other four stresses other than the tangential and radial stresses are modified significantly so that the behavior of the laminate under thermal loading *changes*. For the glass/epoxy laminates, under a positive thermal loading, the material should expand in the longitudinal, transverse, and thickness directions. The fixed ends of the wall should react by *pushing* against the laminate created compressive stresses. However, as the curvature increases, the changes in the other stress components mentioned earlier begins to actually pull the laminate away from the wall. This can be easily imagine by visualizing a sufficient curved beam. Imagine the top of the arc of the beam expanding in the positive thickness direction. This would have a tendency to *pull* the fixed-ends of the beam away from the wall. The wall would tend to *pull* back on the beam creating tensile (positive) stresses in the longitudinal direction. As the curvature becomes more pronounced, this effect becomes more pronounced. As the curvature becomes less pronounced, this effect becomes less pronounced. There is a certain point where the curvature reaches a sufficient magnitude such that the combined effect of all the stresses result in a normal compressive effect from the wall becoming a tensile effect. This is caused by the shear-normal coupling stiffness becoming non-zero with a curved beam. This is the effect shown in Figure 80, Figure 81, and Appendix G. Each stress component has its own unique coupled behavior similar to the explanation above due to curvature. For the aluminum beam, this effect is not pronounced. Hence, it is shown that this is both an effect of the geometry of the beam and the anisotropic character of the beam as well.

If the goal is to reduce the tangential stresses in a beam, it is advantageous to use a composite beam rather than in isotropic beam. The curvature effect with a composite beam would redistribute the tangential stresses to other stress components and result in an overall smaller magnitude tangential stress- see Appendix G. If the curvature of the beam is further increased, the magnitude grows but is still less than

that of an isotropic beam (such as 6061-T6 aluminum in this case) for all cases except for the Model 5 case. For this case, all the composite laminates have higher magnitude tangential stresses than the isotropic laminate. The tangential stresses also change from compressive to tensile as the curvature increases for the composite laminates.

If the goal is to reduce the radial stresses in a beam, it is advantageous to use an isotropic beam rather than a composite beam. The curvature effect with a composite beam would redistribute the stresses such that the radial stresses have an overall larger magnitude- see Appendix G. If the curvature of the beam is further increased, the magnitude grows significantly larger than that of an isotropic beam (such as 6061-T6 aluminum in this case) for Models 4 and 5. This trend begins with the Model 3 for the unbalanced and unsymmetrical laminate. The tangential stresses also change from compressive to tensile as the curvature increases for the composite laminates.

The design of a curved beam must iteratively and concurrently take into account both the geometry of the beam (in particular the curvature) and the anisotropic character of the beam. Changes in the material properties of a beam can significantly effect not only the stress distribution, but also the stress magnitude and direction. Changes in the curvature of a beam can significantly effect not only the stress distribution, but also the magnitude and direction. These two parameter sets (curvature and anisotropic character) have a coupled relationship that determines the stress distribution, stress magnitude, and stress direction for a given curvature and given set of material properties.

3.2.4 Detail Curvature And Stacking Sequence Effect For Actual Stress Along Longitudinal Span Of Laminate

The tangential stresses along layer 4 (0^0) of the symmetrical and balanced laminate were plotted along the mid-width of the laminate with respect to its longitudinal (arc) span. These stresses are the element stresses. As mentioned before, the X-direction stresses are with respect to the finite elements. Hence, they are the global tangential stresses. Two model cases are analyzed, Model 3 and Model 5. The isotropic aluminum laminate is used as a baseline comparison for the symmetrical and balanced laminate.

The first case analyzed is the Model 3 case for the isotropic aluminum and the composite glass/epoxy beams. The second case analyzed is the Model 5 case for the isotropic aluminum and the composite glass/epoxy beams.

From Figure 82, it can be seen that the tri-linear, isoparametric elements are experiencing non-constant strains (in particular shear). This propagates to the tangential and radial stresses as "spikes." Beyond these spikes it can be seen that the curved beam doesn't have significant variances in tangential stresses with respect to the longitudinal (arc) span of the beam.

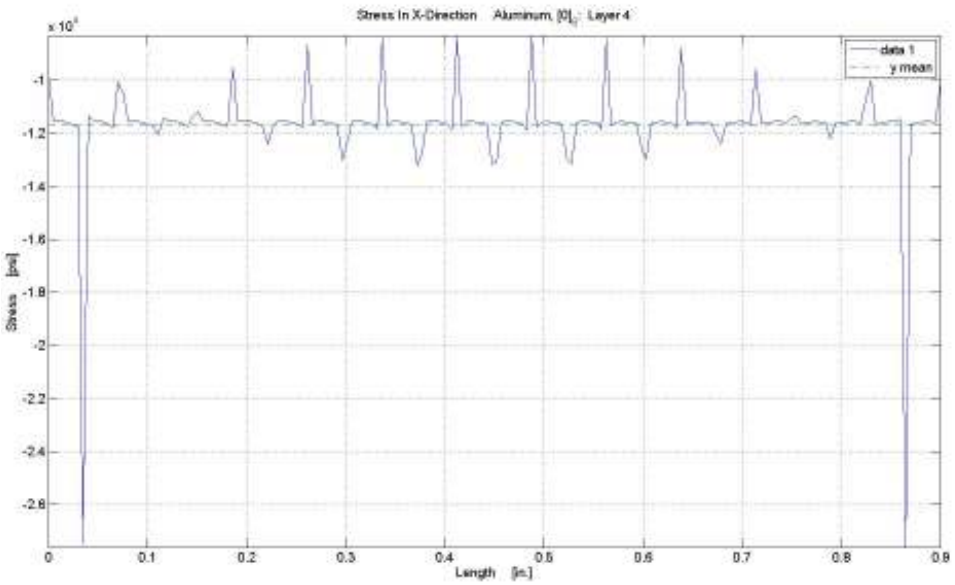

Figure 82. Longitudinal span of tangential stresses (local X-direction for finite elements) for isotropic aluminum laminate with Model 3 geometry. Element stresses.

This is primarily due to the type of loading the simply curved beam is experiencing. The beam is under an uniform thermal loading. That is the thermal load at every point of the beam is the same. The coupling stiffnesses effectively redistributes the tangential stresses at each point in the beam to other stress components, in particular the shear components. Each span of the beam has a particular orientation due to the rotation of a given finite element about the laminate's Y-direction. The magnitude of this rotation determines the amount of redistributing of the tangential stresses that occur. Hence, for a given flat beam

solution, the internal tangential (normal) stresses in the beam are all within a similar, small range for a fixed-fixed constrained beam. With curvature, this tangential stress is *altered* an amount commensurate with the rotation of the given segment about the laminate's Y-direction. This redistribution of the flat beam tangential stress result with the segment rotation tends to deliver fairly similar stress results through the longitudinal (arc) span of the isotropic aluminum beam.

This is not in line with the trend of the results shown in the analytical derivation of Section 2.2.5. This is because the analytical solution of Section 2.2.5 is a plane stress (XZ-plane) solution and the solution from the MATLAB FEA code (see Appendix F) is a three-dimension stress solution- see Appendix G. The importance of this commonality was previously discussed. Furthermore, the analytical solution of Section 2.2.5 did not account for the three-dimensional shear-normal coupling stiffness that are non-zero for curved beams and varies for every segment of the beam along the curve. Hence, the importance of stiffness couplings and stress conditions are highlighted.

From Figure 83, it can be seen that the tri-linear, isoparametric elements are experience non-constant strains of a higher order than those experience by the isotropic aluminum beam. This can be seen through the more spurious nature of the tangential stress plots. The variances of the stresses along the longitudinal (arc) span of the beam do not vary significantly either. The stresses don't vary significantly from the mean at the *near* mid-point of the beam either, as was noticed for the case of the mean stress at the *near* mid-point of the laminates in Sections 3.2.2 and 3.2.3. The reasons for this are the same as was listed for the isotropic aluminum beam. The stress magnitudes are lower as was discussed in Sections 3.2.2 and 3.2.3.

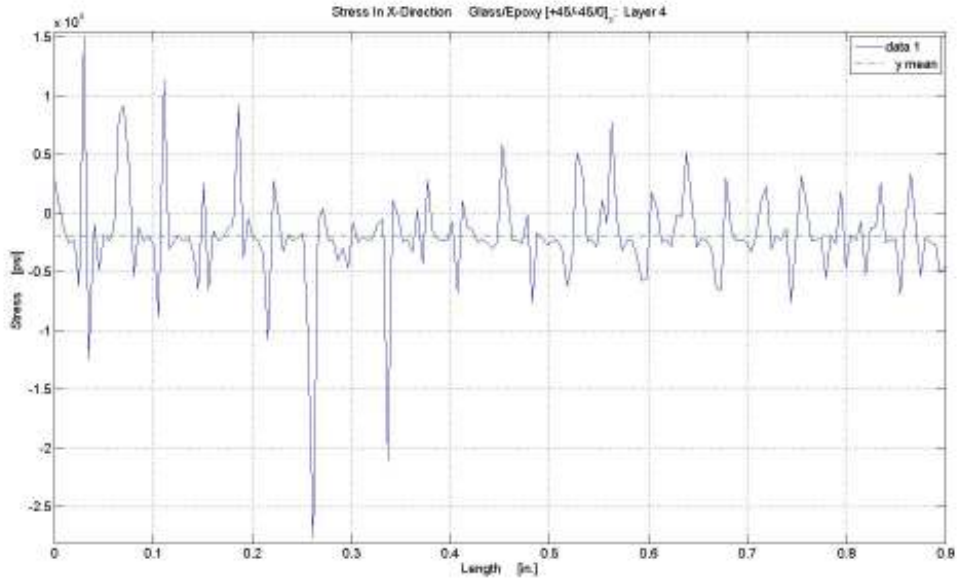

Figure 83. Longitudinal span of tangential stresses (local X-direction for finite elements) for glass/epoxy laminate with Model 3 geometry. Element stresses.

From Figure 84, the magnitude of the variations of the tangential stresses are much larger for the Model 5 case than for the Model 3 case for the isotropic aluminum beam. The spurious strain modes combined with the greater degree of coupling for the Model 5 case leads to the results shown in Figure 84. For the Model 5 case, only the tangential stresses reduce in magnitude. All other stress components increase in magnitude. The amount of coupling due to the highly curved geometry is significant- see Appendix G. Yet, if one *cancels* out the effect of the spurious strain modes due solely to the type of element used, then it can be readily seen that the tangential stresses actually vary very little with respect to the longitudinal (arc) span.

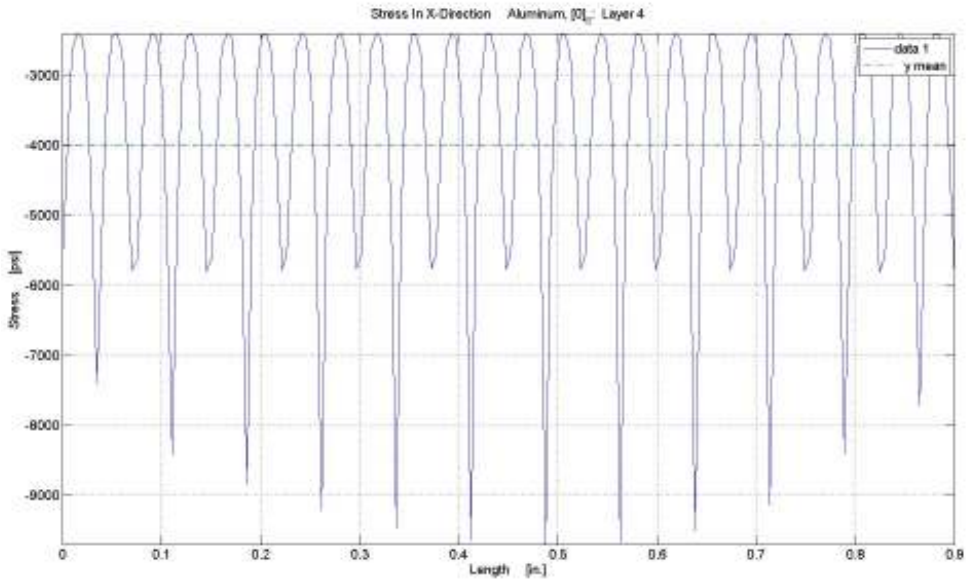

Figure 84. Longitudinal span of tangential stresses (local X-direction for finite elements) for isotropic aluminum laminate with Model 5 geometry. Element stresses.

From Figure 85, the magnitude of the variations of the tangential stresses are much larger for the Model 5 case than for the Model 3 case for the composite glass/epoxy beam. The spurious strain modes combined with the greater degree of coupling for the Model 5 case leads to the results shown in Figure 85. For the Model 5 case, the tangential stresses have an increasing trend in magnitude. All other stress components generally increase in magnitude. The amount of coupling due to the highly curved geometry is significant- see Appendix G. Yet, if one *cancels* out the effect of the spurious strain modes due solely to the type of element used, then it can be readily seen that the tangential stresses actually vary somewhat more than the isotropic aluminum beam with respect to the longitudinal (arc) span.

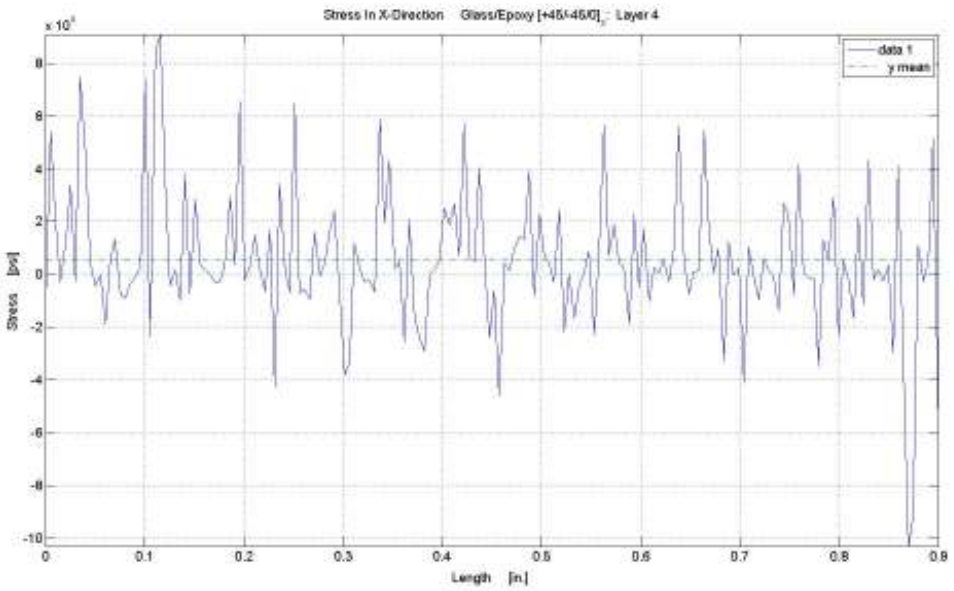

Figure 85. Longitudinal span of tangential stresses (local X-direction for finite elements) for glass/epoxy laminate with Model 5 geometry. Element stresses.

The nodal stresses for these 4 cases were calculated as well. Since these stresses are calculated at the nodes and the interpolation functions for the tri-linear, isoparametric element are defined at the nodes, these stresses are exact. The element stresses are the interpolated result of setting (r,s,t) = (0,0,0). The following four nodal plots show the tangential stresses (local X-direction for the finite elements) for the top and bottom surfaces only for each layer. The space in between each surface represents the thickness of each layer. The plots are not to geometric scale. That is, they will appear thicker and shorter than the actual geometry. This is to facilitate the ease of viewing of the nodal, tangential stress results. Unlike ANSYS and other FEA software, this MATLAB FEA program written by the Author assigns each stress value a unique RGB color from the Jet color map. Therefore, the stresses may seem to have more gradients and variation in them than *normal*. However, it is just each stress value has its own unique color. ANSYS would generally blend a range of stresses into one color- see Figure 56, Figure 57, Figure 58, Figure 59,

Figure 60, and Figure 61. This technique adopted by ANSYS and other programs can actually be a detriment if care isn't taken.

The nodal stresses are defined at the intersection of line segments in the following four plots. These intersections are the nodes. The line segments are the nodal connectivity lines that form the boundary for each single element as described in Section 2.1.3. The exact colors for the exact nodal stresses are assign to each node. The interpolation of the faces (surface area between the nodes) is based on an color interpolation scheme defined by the MATLAB function *patch*. That is, the face color is the interpolated result of the surrounding four nodes. The internal elements share the same surfaces at all times as described in Section 2.1.2. The nodal stress results for two surfaces that are adjacent are numerically averaged and the result becomes the nodal stress for mutually shared nodes between elements. Note: The element stresses that were previous calculated exist in the *white space* in between the colored surfaces. The element stresses are the interpolated results between two surfaces, the one directly above and the one directly below. Furthermore, due to the spurious strains modes in the results due to the inability of the linear elements to successfully map the non-linear strains (characteristic of sub-order isoparametric elements), the nodal stress results are "spiked" in magnitude. However, this "spiking" is smoothed and cancelled out by the nature of the interpolation functions for the element stress calculated at (r,s,t) = (0,0,0) for each element. Hence, they (the element stresses) *generally are smaller* in magnitude because it is the average effect of generally different magnitude and direction nodal stresses. Finally, the nodal stresses are plotted on the non-deformed view of the laminate to facilitate viewing nodal stress variations.

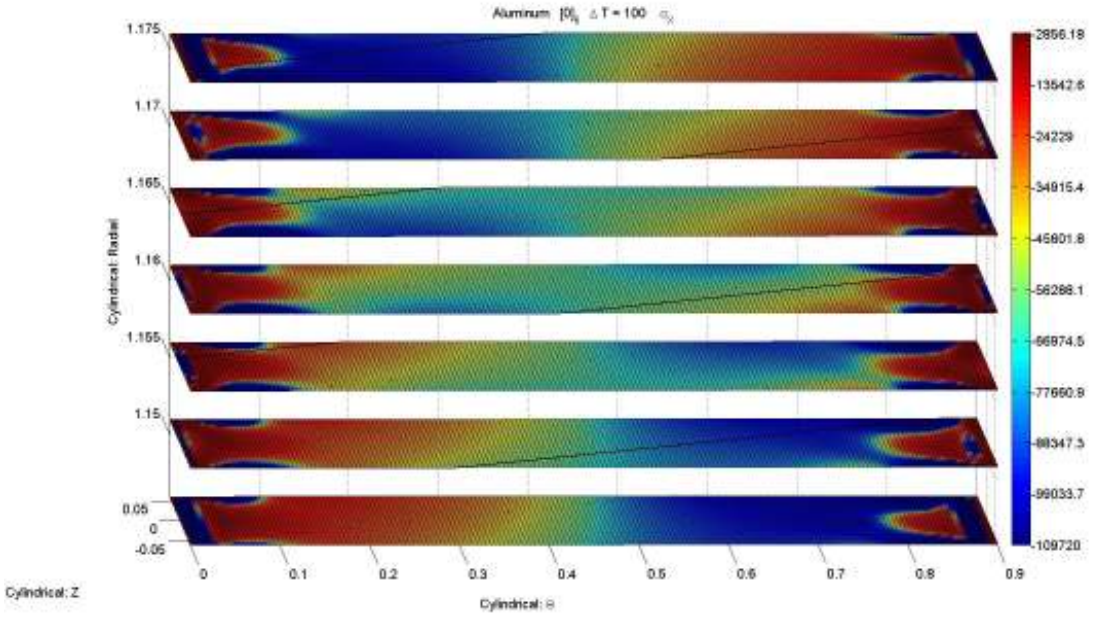

Figure 86. Longitudinal span of tangential stresses (local X-direction for finite elements) for isotropic aluminum laminate with Model 3 geometry. Nodal stresses.

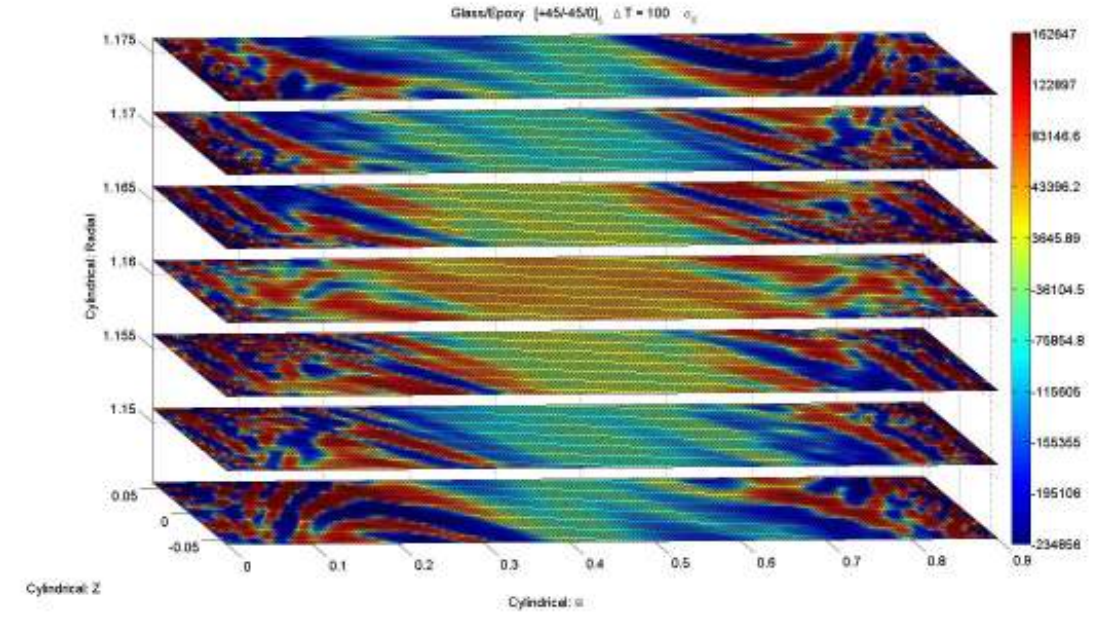

Figure 87. Longitudinal span of tangential stresses (local X-direction for finite elements) for glass/epoxy laminate with Model 3 geometry. Nodal stresses.

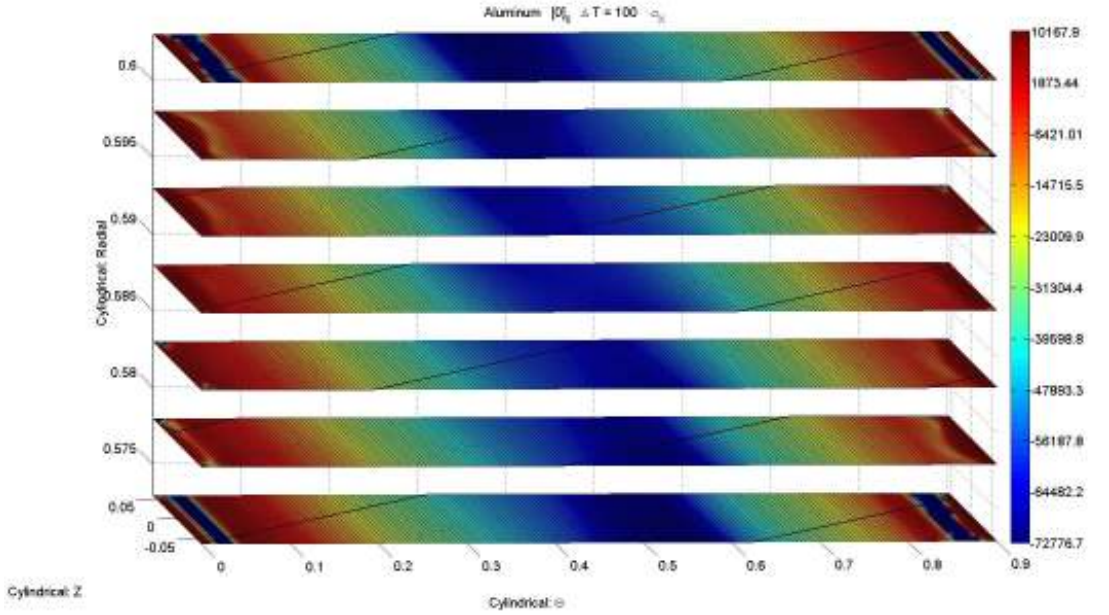

Figure 88. Longitudinal span of tangential stresses (local X-direction for finite elements) for isotropic aluminum laminate with Model 5 geometry. Nodal stresses.

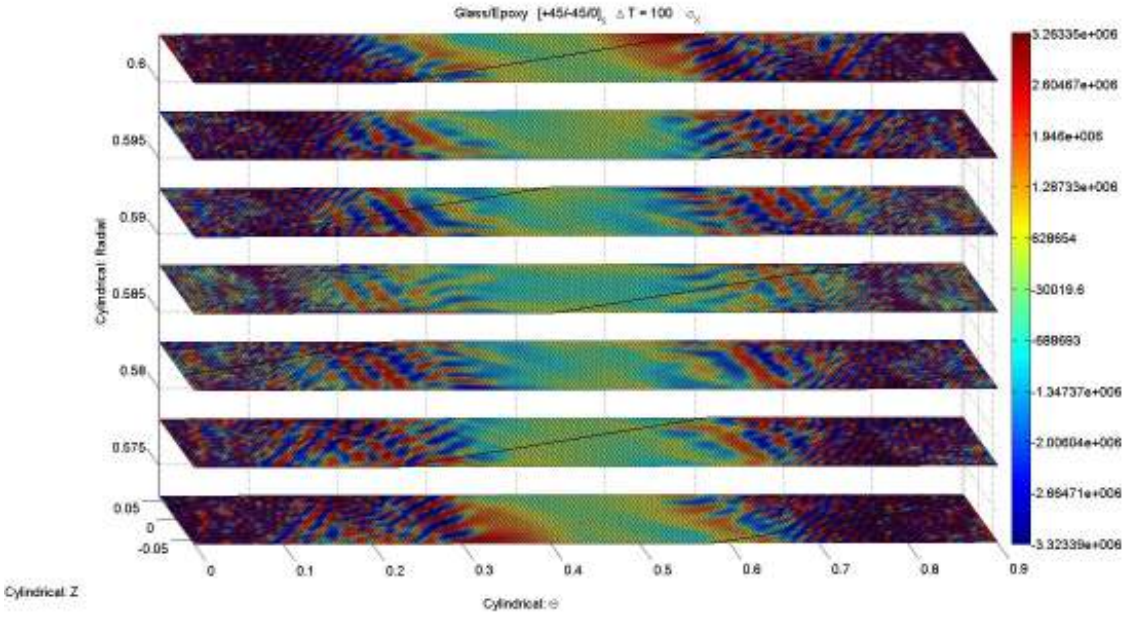

Figure 89. Longitudinal span of tangential stresses (local X-direction for finite elements) for glass/epoxy laminate with Model 5 geometry. Nodal stresses.

It can be seen from Figure 86, Figure 87, Figure 88, and Figure 89 that the stress distributions are far smoother and regular for the isotropic aluminum beams. The stress distributions are far more rougher and irregular for the composite glass/epoxy beams. The effect of the shear stress and their antisymmetrical effect on the stress distributions through the thickness (Radial) and transverse (Z) directions of the laminate can bee seen in all four plots. The edge effect and Saint Venant's stresses can also be readily seen. However, it must be noted again that they do not propagate as far into the middle of the beams as shown in the plots. This is so because the plots are not to scale.

The fourth surface of each plot is the representative behavior of the laminates where the shear effects *cancel* each other out. The previous element stress plots were about the Z-coordinate Z = 0. However, looking at the nodal surface plots shows that the stress distributions also vary in the Z-coordinate direction (transverse direction). The complex stress variations reveal the difficulty in stress analysis of composite beams. Nevertheless, looking at the fourth surface of each plot using nodal plots doesn't provide acceptably precise information on stress values. Take for instance the fourth surface of Figure 89. If one looks towards the middle of the surface, it cannot be ascertained whether the stresses are positive or negative. This is the downfall of such plots, especially if the stresses vary through the thickness of the element. However, useful information can be gained on the stress variation behavior from these plots.

3.2.5 Detail Curvature And Stacking Sequence Effect For Actual Stress Along Longitudinal Span Of Laminate Conclusions

According to material science mechanics, when a specimen is thermally loaded, approximately half the energy from the thermal load goes into increasing the temperature of the specimen- generally. The other half of the energy goes into deforming the specimen. All the conclusions observed from Section 3.2.3 are the same here. However, this trend varies through the transverse direction of the laminates. That is, for each transverse slice of the laminate, the trends of Section 3.2.3 have the same behavior but are of a different magnitude. Section 3.2.3 results are the average laminate results. Sometimes the average result can be extremely useful. Sometimes the average result can be extremely deceptive. Take for instance the

stress range of 495 psi to 505 psi. The average stress is 500 psi. Now take the stress range of 50 psi to 950 psi. The average stress is 500 psi. Care should be taken in using either average results from element stresses alone or nodal stress results in surface plots. Both must be used to gain a more complete understanding in the complex, non-linear stress variation in statically indeterminant, composite, simply curved beams.

CHAPTER 4

CONCLUSIONS AND FUTURE WORK

The purpose of this chapter is to discuss the conclusions of the work conducted in this thesis and to discuss future work.

Conclusions

Curved beams results in numerous coupling behaviors between shear deformations & normal stresses, normal deformation & shear stresses, and complex in-plane & out-of-plane cross coupling between deformations and stresses that vary continually and uniquely in the radial and tangential directions for differential segments that aren't in the same plane in space. These couplings vary continuously throughout the beam. There is no one coupling behavior that can describe the whole beam. As the radius of curvature changes, so does the extent of coupling behavior changes. As the material properties of the beam changes so does type of coupling behavior changes. This coupling behavior results in highly complex and irregular stress variations depending on the radius of curvature, that family of stacking sequences, and the anisotropic material properties. If the material properties are isotropic, the variation of the stresses are smoother and more regular.

For isotropic, simply curved beams, compressive stresses will still be compressive stresses for arc spans of up to 90^{o}. Tensile stresses will also stay tensile. For composite, simply curved beams, compressive stresses can become tensile stresses and tensile stresses can become compressive stresses depending on the stacking sequence and most important the radius of curvature. Care must be taken in designing curved composite parts that will experience appreciable thermal loading. If a part is not to experience significant tensile stresses under positive thermal loading (assuming the material properties have all positive thermal expansion coefficients), having too much curvature in the part can result in failure

in that part or even the system that the part is a component of. Composite, simply curved beams can reverse the state (compressive or tensile) of the stress direction depending on the curvature of the beam. How much curvature is required for this reversal depends overall on the amount of thermal loading, the family of stacking sequence that the laminate is in, and specifically to the actual stacking sequence within a family of laminates. Uniquely, these types of beams will also have a curvature of a given stacking sequence where the stresses will transition from compressive (negative) to tensile (positive). This transition must by definition pass through the zero stress mark. Hence, a composite curved beam of a particular radius of curvature will have an average element stress of zero for a given thermal loading condition. Therefore, if an engineer knows that a given stress component is most important and knows the thermal loading conditions typical for that given part, that engineer can potentially design a simply curved laminate that will experience zero average stress for that given component of stress under those given thermal loading conditions.

Curvature in a composite laminate results in redistribution of stresses in the laminate. For a fixed-fixed constraint beam where the constraints are on the longitudinal ends, this redistribution can be used to reduce the magnitude of stresses in the laminate for a direction(s) or interest. This can be done by varying the curvature of the laminate. However, care must be taken as some stress components will have higher stresses if the curvature is too pronounced. Furthermore, curved laminates must be able to handle very complex, three-dimensional states of shear stress. The curvature has a tendency to redistribute the normal stresses to shear stresses. Generally, this redistribution of stresses results in the magnitude of the traction at any given point in a simply, curved composite laminate being lower than that of an isotropic homogenous metal (e.g. aluminum)- see Appendix G.

The results from Section 3.2.3 combined with the nodal surface plots of Section 3.2.4 shows that complex behavior of simply curved composite beams that are statically indeterminant varies in very complex manners not only in overall behavior but in magnitude and direction as well. It is not advisable to utilize only the average stresses at the mid-point of the beam alone or just the surface nodal stresses of the

beam alone. Both must be used in a trade study with material properties and curvature for the most successful design experience.

In simply curved, composite beams, stresses vary non-linearly in the radial, tangential, and transverse directions in different orders. Each point in the laminate is generally in some varying degree three dimensional state of stress.

Future Work

Simply curved, composite beams that are statically indeterminate are very well understudied. Much work needs to be done in order to gather a fuller understanding of the complex mechanical behavior of these beams. Trade studies on how the normal and shear strains vary in the radial, tangential, and transverse directions need to be conducted. Any trends or patterns can be useful in understanding how the beams deform and how they *spring-in* while in surface life conditions.

Most work on these types of beams is done using finite element analysis. This is a great tool but can be costly in terms of capital and time. An analytical solution or set of solutions needs to be developed that can reduced to the flat beam case as the radius of curvature tends to infinity. It must be able to handle both isotropic and anisotropic laminates. Error cannot be induced in the solution due to the extent of the curvature or the ratio of key geometric parameters. Hence, all coupling behaviors due to geometry, orientation, and material properties must be accounted for. This can be done explicitly or using some average factor (not correction factor). Invariably, the solutions will most likely have to be broken down into tangential stress solution or solution sets, radial stress solution or solutions sets, and transverse solution or solutions sets.

APPENDIX A

DERIVATION OF THE TANGENTIAL STRAIN DUE TO A SIMPLE CURVATURE

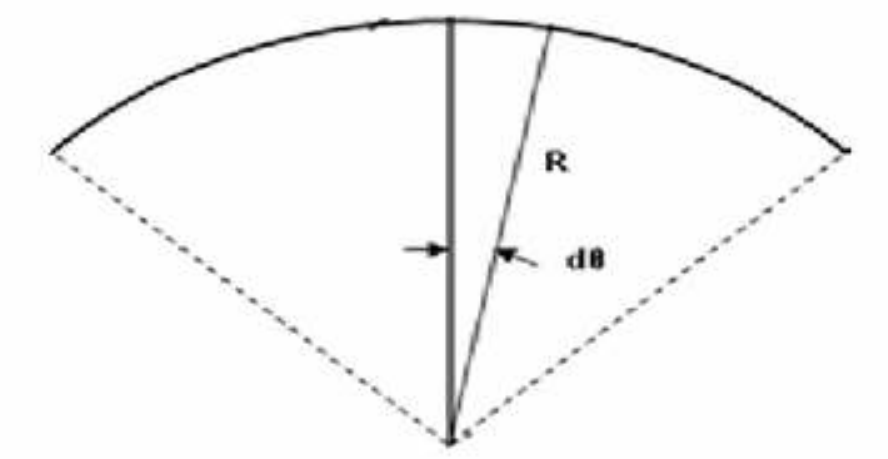

Figure 90. Representative view of a simply curved beam.

From the standard arc length relationship:

$$S = R\theta \rightarrow dS = Rd\theta \tag{A-1}$$

where S = arc length, dS = infinitesimal arc length, R = radius of curvature, θ = angle spanned by arc length S, dθ = infinitesimal angle spanned by dS.

From the standard strain relationship:

$$L = \frac{\delta}{\varepsilon} \rightarrow dL = \frac{d\delta}{\varepsilon} \tag{A-2}$$

where L = characteristic length, dL = infinitesimal characteristic length, ε = stain, δ = elongation, dδ = infinitesimal elongation.

Combining Equation (A-1) and Equation (A-2) yields:

$$dL = \frac{d\delta}{\varepsilon} \rightarrow dS = \frac{d\delta_\theta}{\varepsilon_\theta} = rd\theta \tag{A-3}$$

where r = radius of curvature from a given reference, δ_θ = tangential elongation, $d\delta_\theta$ = infinitesimal tangential elongation, ε_θ = tangential strain.

The infinitesimal tangential elongation ($d\delta_\theta$), with respect to the center of curvature is as follow:

r = R+z z = height above/below the mid plane of the laminate.

substituting the expression for r into Equation (A-3) yields:

$$dS = \frac{d\delta_\theta}{\varepsilon_\theta} = rd\theta \Rightarrow \frac{d\delta_\theta}{\varepsilon_\theta} = \left(R + z\right)d\theta \tag{A-4}$$

solving for the infinitesimal elongation…

$$d\delta_\theta = \varepsilon_\theta\left(R + z\right)d\theta \tag{A-5}$$

The infinitesimal tangential elongation ($d\delta_\theta$), with respect to the mid plane of the laminate is as follow:

r = R

strains with respect to the mid plane are

$$\varepsilon_\theta = \varepsilon_x^o + z\kappa_x$$

where κ_x = curvature along x-direction about the y-axis, ε_x^o = mid plane strain in the x-direction

substituting the expression for r and the expression for ε_θ into Equation (A-3) yields:

$$dS = \frac{d\delta_\theta}{\varepsilon_\theta} = rd\theta \Rightarrow \frac{d\delta_\theta}{\left(\varepsilon_x^o + z\kappa_x\right)} = Rd\theta \tag{A-6}$$

solving for the infinitesimal elongation…

$$d\delta_\theta = \left(\varepsilon_x^o + z\kappa_x\right)Rd\theta \tag{A-7}$$

The infinitesimal tangential elongation ($d\delta_\theta$) must be equal whether with respect to the center of curvature or with respect to the mid plane of the laminate. Therefore, equating Equation (A-5) and Equation (A-7) yields:

$$\varepsilon_\theta\left(R+z\right)d\theta = \left(\varepsilon_x^o + z\kappa_x\right)Rd\theta \tag{A-8}$$

Solving for the tangential strain.

$$\varepsilon_\theta = \frac{R}{R+z}\left(\varepsilon_x^o + z\kappa_x\right) \tag{A-9}$$

factoring the thermal strain e_x into the tangential strain yields:

$$\varepsilon_\theta = \frac{R}{R+z}\left(\varepsilon_x^o + z\kappa_x - e_x\right) \tag{A-10}$$

APPENDIX B

DERIVATION OF THE TANGENTIAL STRESS FOR A BEAM WITH SOME CURVATURE BY HETNARSKI, NODA, AND TANIGAWA DUE TO A THERMAL LOADING

The center line lies in one of the centroidal principal planes. If the element of the curved beam with curvature $\frac{1}{R}$ and angle $d\theta$ before thermal loading deforms to the curvature $\frac{1}{\rho}$ and angle $d\theta + \Delta d\theta$ after the temperature change ΔT, the strain ε_0 at the center line is given by

$$\varepsilon_0 = \frac{\overline{n'm'} - \overline{nm}}{\overline{nm}} = \frac{\rho(d\theta + \Delta d\theta) - Rd\theta}{Rd\theta} = \frac{\rho - R}{R} + \frac{\rho}{R}\frac{\Delta d\theta}{d\theta} = \frac{\rho - R}{R} + \frac{\rho}{R}\omega_0 \qquad \text{(B-1)}$$

where $\omega_0 = \frac{\Delta d\theta}{d\theta}$.

The strain ε at a distance y from the center line is given by

$$\varepsilon_0 = \frac{\overline{A'B'} - \overline{AB}}{\overline{AB}} = \frac{\left[\rho + y + \int_0^y \alpha(\Delta T)\right](d\theta + \Delta d\theta) - (R + y)d\theta}{(R + y)d\theta} \cong \frac{1}{R + y}\left[\varepsilon_0 R + \omega_0 y + \int_0^y \alpha(\Delta T)dy\right] \qquad \text{(B-2)}$$

In the last expression, the term $\omega_0 \int_0^y \alpha(\Delta T)dy$ was neglected as being small compared to $\int_0^y \alpha(\Delta T)dy$.

The final strain ε in the beam is expressed as the sum of the free thermal strain and the strain due to stress $\sigma_{\theta\theta}$:

$$\varepsilon = \alpha(\Delta T) + \frac{\sigma_{\theta\theta}}{E} = \frac{1}{R + y}\left[\varepsilon_0 R + \omega_0 y + \int_0^y \alpha(\Delta T)dy\right] \qquad \text{(B-3)}$$

The stress can, therefore, be expressed by

$$\sigma_{\theta\theta} = -\alpha E(\Delta T) + \frac{E}{R + y}\left[\varepsilon_0 R + \omega_0 y + \int_0^y \alpha(\Delta T)dy\right] \qquad \text{(B-4)}$$

Since the curved beam is not subjected to external forces and moments, we have

$$\int_A \sigma_{\theta\theta} dA = 0$$

$$\int_A \sigma_{\theta\theta} y dA = 0$$

We can obtain the normal strain ε_0 and the curvature ω_0 at the center surface y = 0 as follows:

$$\varepsilon_0 = \frac{N}{EA} + \frac{M}{EAR} \tag{B-5}$$

$$\omega_0 = \frac{N}{EA} + \frac{M}{EAR}\left(1 + \frac{1}{\kappa}\right) \tag{B-6}$$

where

$$\kappa = -\frac{1}{A}\int_A \frac{y}{R+y} dA$$

$$N = \int_A \alpha E(\Delta T) dA - \int_A \frac{E}{R+y}\left[\int_0^y \alpha(\Delta T) dy\right] dA \tag{B-7}$$

$$M = \int_A \alpha E(\Delta T) y dA - \int_A \frac{Ey}{R+y}\left[\int_0^y \alpha(\Delta T) dy\right] dA \tag{B-8}$$

The curvature is obtained after thermal loading at the center surface y=0 from the following two sets of equations:

$$\varepsilon_0 = \frac{\overline{n'm'} - \overline{nm}}{\overline{nm}} = \frac{\rho(d\theta + \Delta d\theta) - Rd\theta}{Rd\theta} = \frac{\rho - R}{R} + \frac{\rho}{R}\frac{\Delta d\theta}{d\theta} = \frac{\rho - R}{R} + \frac{\rho}{R}\omega_0$$

$$\varepsilon_0 = \frac{N}{EA} + \frac{M}{EAR} \quad \omega_0 = \frac{N}{EA} + \frac{M}{EAR}\left(1 + \frac{1}{\kappa}\right)$$

As…

$$\rho = \left(\frac{1+\varepsilon_0}{1+\omega_0}\right)R = \left[1 - \frac{\frac{M}{EAR}\frac{1}{\kappa}}{1+\frac{N}{EA}+\frac{M}{EAR}\left(1+\frac{1}{\kappa}\right)}\right]R \tag{B-9}$$

Substituting of

$$\varepsilon_0 = \frac{N}{EA}+\frac{M}{EAR} \quad \omega_0 = \frac{N}{EA}+\frac{M}{EAR}\left(1+\frac{1}{\kappa}\right)$$

Into

$$\sigma_{\theta\theta} = -\alpha E(\Delta T) + \frac{E}{R+y}\left[\varepsilon_0 R + \omega_0 y + \int_0^y \alpha(\Delta T)dy\right]$$

Yields:

$$\sigma_{\theta\theta} = -\alpha E(\Delta T) + \frac{1}{A}\left\{N + \frac{M}{R}\left[1+\frac{y}{\kappa(R+y)}\right]\right\} + \frac{E}{R+y}\int_0^y \alpha(\Delta T)dy \tag{B-10}$$

APPENDIX C

THREE-DIMENSIONAL DISPLACEMENT DERIVATION

The origin is equidistant from the top and bottom surfaces, the left and right surfaces, and front and rear surfaces. It is referred to as the *reference point*.

Displacements and strains parallel to a given direction, *normal actions*, are referenced as $(*)_0$ and $(*)^0$ respectively.

It is assumed that the displacements that are through *normal actions* are a function of (x,y,z). That is, each point in the volume can potentially have its own unique displacement. Since the displacements are functions of (x,y,z), the corresponding normal strains are also functions of (x,y,z).

$$\varepsilon_x^0(x,y,z) = \frac{\partial u_0(x,y,z)}{\partial x} \rightarrow \int \varepsilon_x^0(x,y,z)dx = \int \frac{\partial u_0(x,y,z)}{\partial x} dx = u_0(x,y,z) = \varepsilon_x^0(x,y,z)x + f(y,z)$$

$$\varepsilon_y^0(x,y,z) = \frac{\partial v_0(x,y,z)}{\partial y} \rightarrow \int \varepsilon_y^0(x,y,z)dy = \int \frac{\partial v_0(x,y,z)}{\partial y} dy = v_0(x,y,z) = \varepsilon_y^0(x,y,z)y + g(x,z)$$

$$\varepsilon_z^0(x,y,z) = \frac{\partial w_0(x,y,z)}{\partial z} \rightarrow \int \varepsilon_z^0(x,y,z)dz = \int \frac{\partial w_0(x,y,z)}{\partial z} dz = w_0(x,y,z) = \varepsilon_z^0(x,y,z)z + h(x,y)$$

$$\gamma_{xy}^0(x,y)|_z = \frac{\partial u_0(x,y,z)}{\partial y} + \frac{\partial v_0(x,y,z)}{\partial x} = \frac{\partial f(y,z)}{\partial y} + \frac{\partial g(x,z)}{\partial x}$$

$$\gamma_{yz}^0(y,z)|_x = \frac{\partial v_0(x,y,z)}{\partial z} + \frac{\partial w_0(x,y,z)}{\partial y} = \frac{\partial g(x,z)}{\partial z} + \frac{\partial h(x,y)}{\partial y}$$

$$\gamma_{zx}^0(x,z)|_y = \frac{\partial u_0(x,y,z)}{\partial z} + \frac{\partial w_0(x,y,z)}{\partial x} = \frac{\partial f(y,z)}{\partial z} + \frac{\partial h(x,y)}{\partial x}$$

Note:

*To define displacements on the xy-plane or planes parallel to the xy-plane, set z to a constant value as (x,y) is varied.

*To define displacements on the yz-plane or planes parallel to the yz-plane, set x to a constant value as (y,z) is varied.

*To define displacements on the zx-plane or planes parallel to the zx-plane, set y to a constant value as (x,z) is varied.

This forces a reduction to a given plane instead of a volume.

- Rigid body motion: $rotation \equiv \omega_z = \omega_y = \omega_x = 0$

$$\omega_z = \frac{\partial u_0(x,y,z)}{\partial y} - \frac{\partial v_0(x,y,z)}{\partial x} = \frac{\partial f(y,z)}{\partial y} - \frac{\partial g(x,z)}{\partial x} = 0 \Rightarrow \frac{\partial f(y,z)}{\partial y} = \frac{\partial g(x,z)}{\partial x}$$

$$\omega_y = \frac{\partial v_0(x,y,z)}{\partial z} - \frac{\partial w_0(x,y,z)}{\partial y} = \frac{\partial f(y,z)}{\partial z} - \frac{\partial h(x,y)}{\partial x} = 0 \Rightarrow \frac{\partial f(y,z)}{\partial z} = \frac{\partial h(x,y)}{\partial x}$$

$$\omega_x = \frac{\partial u_0(x,y,z)}{\partial z} - \frac{\partial w_0(x,y,z)}{\partial x} = \frac{\partial g(x,z)}{\partial z} - \frac{\partial h(x,y)}{\partial y} = 0 \Rightarrow \frac{\partial g(x,z)}{\partial z} = \frac{\partial h(x,y)}{\partial y}$$

for the given partial derivatives of f, g, and h to be equal… they must be equal to a constant.

$$\gamma^0_{xy}(x,y)|_z = \frac{\partial f(y,z)}{\partial y} + \frac{\partial g(x,z)}{\partial x} = \frac{\partial f(y,z)}{\partial y} + \frac{\partial f(y,z)}{\partial y} = 2\frac{\partial f(y,z)}{\partial y}$$

$$\frac{\partial f(y,z)}{\partial y} = \frac{\gamma^0_{xy}(x,y,z)}{2}$$

$$\frac{\partial g(x,z)}{\partial x} = \frac{\gamma^0_{xy}(x,y,z)}{2}$$

$$\gamma^0_{yz}(y,z)\,|_x = \frac{\partial g(x,z)}{\partial z} + \frac{\partial h(x,y)}{\partial y} = \frac{\partial g(x,z)}{\partial z} + \frac{\partial g(x,z)}{\partial z} = 2\frac{\partial g(x,z)}{\partial z}$$

$$\frac{\partial g(x,z)}{\partial z} = \frac{\gamma^0_{yz}(x,y,z)}{2}$$

$$\frac{\partial h(x,y)}{\partial y} = \frac{\gamma^0_{yz}(x,y,z)}{2}$$

$$\gamma^0_{zx}(x,z)\,|_y = \frac{\partial f(y,z)}{\partial z} + \frac{\partial h(x,y)}{\partial x} = \frac{\partial f(y,z)}{\partial z} + \frac{\partial f(y,z)}{\partial z} = 2\frac{\partial f(y,z)}{\partial z}$$

$$\frac{\partial f(y,z)}{\partial z} = \frac{\gamma^0_{zx}(x,y,z)}{2}$$

$$\frac{\partial h(x,y)}{\partial x} = \frac{\gamma^0_{zx}(x,y,z)}{2}$$

$$\frac{\partial f(y,z)}{\partial y}: \quad f(y,z) = \int \frac{\partial f(y,z)}{\partial y}\,dy = \int \frac{\gamma^0_{xy}(x,y)\,|_z}{2}\,dy = \frac{\gamma^0_{xy}(x,y)\,|_z}{2}\,y + F_A(z)$$

$$\frac{\partial g(x,z)}{\partial x}: \quad g(x,z) = \int \frac{\partial g(x,z)}{\partial x}\,dx = \int \frac{\gamma^0_{xy}(x,y)\,|_z}{2}\,dx = \frac{\gamma^0_{xy}(x,y)\,|_z}{2}\,x + G_A(z)$$

$$\frac{\partial g(x,z)}{\partial z}: \quad g(x,z) = \int \frac{\partial g(x,z)}{\partial z}\,dz = \int \frac{\gamma^0_{yz}(y,z)\,|_x}{2}\,dz = \frac{\gamma^0_{yz}(y,z)\,|_x}{2}\,z + G_B(x)$$

$$\frac{\partial h(x,y)}{\partial y}: \quad h(x,y) = \int \frac{\partial h(x,y)}{\partial y}\,dy = \int \frac{\gamma^0_{yz}(y,z)\,|_x}{2}\,dy = \frac{\gamma^0_{yz}(y,z)\,|_x}{2}\,y + H_A(x)$$

$$\frac{\partial f(y,z)}{\partial z}: \quad f(y,z) = \int \frac{\partial f(y,z)}{\partial z}\,dz = \int \frac{\gamma^0_{zx}(x,z)\,|_y}{2}\,dz = \frac{\gamma^0_{zx}(x,z)\,|_y}{2}\,z + F_B(y)$$

$$\frac{\partial h(x,y)}{\partial x}: \quad h(x,y) = \int \frac{\partial h(x,y)}{\partial x}\,dx = \int \frac{\gamma^0_{zx}(x,z)\,|_y}{2}\,dx = \frac{\gamma^0_{zx}(x,z)\,|_y}{2}\,x + H_B(y)$$

$$u_0(x,y,z) = \varepsilon_x^0(x,y,z)x + \frac{\gamma_{xy}^0(x,y)|_z}{2} y + F_A(z)$$
$$= \varepsilon_x^0(x,y,z)x + \frac{\gamma_{zx}^0(x,z)|_y}{2} z + F_B(y)$$

$$v_0(x,y,z) = \varepsilon_y^0(x,y,z)y + \frac{\gamma_{xy}^0(x,y)|_z}{2} x + G_A(z)$$
$$= \varepsilon_y^0(x,y,z)y + \frac{\gamma_{yz}^0(y,z)|_x}{2} z + G_B(x)$$

$$w_0(x,y,z) = \varepsilon_z^0(x,y,z)z + \frac{\gamma_{yz}^0(y,z)|_x}{2} y + H_A(x)$$
$$= \varepsilon_z^0(x,y,z)z + \frac{\gamma_{zx}^0(x,z)|_y}{2} x + H_B(y)$$

- Reference point displacement:

$$u_0(x,y,z) \Rightarrow u_0(0,0,0) = 0$$
$$v_0(x,y,z) \Rightarrow v_0(0,0,0) = 0$$
$$w_0(x,y,z) \Rightarrow w_0(0,0,0) = 0$$

$$u_0(0,0,0) = F_A(z) = 0 \quad = F_B(y) = 0$$

$$v_0(0,0,0) = G_A(z) = 0 \quad = G_B(x) = 0$$

$$w_0(0,0,0) = H_A(x) = 0 \quad = H_B(y) = 0$$

$$u_0(x,y,z) = \varepsilon_x^0(x,y,z)x + \frac{\gamma_{xy}^0(x,y)|_z}{2} y$$
$$= \varepsilon_x^0(x,y,z)x + \frac{\gamma_{zx}^0(x,z)|_y}{2} z$$

$$v_0(x,y,z) = \varepsilon_y^0(x,y,z)y + \frac{\gamma_{xy}^0(x,y)|_z}{2} x$$
$$= \varepsilon_y^0(x,y,z)y + \frac{\gamma_{yz}^0(y,z)|_x}{2} z$$

$$w_0(x,y,z) = \varepsilon_z^0(x,y,z)z + \frac{\gamma_{yz}^0(y,z)|_x}{2} y$$
$$= \varepsilon_z^0(x,y,z)z + \frac{\gamma_{zx}^0(x,z)|_y}{2} x$$

(C-1)

---

xy-plane:

$$\kappa_x(x,y)|_z = -\frac{\partial^2 w_0(x,y,z)}{\partial x^2} \rightarrow \int \kappa_x(x,y)|_z \, dx = \int -\frac{\partial^2 w_0(x,y,z)}{\partial x^2} dx = \kappa_x(x,y)|_z \; x + a_1(y,z) = \alpha_x(x,y)|_z = -\frac{\partial w_0(x,y,z)}{\partial x}$$

$$\kappa_y(x,y)|_z = -\frac{\partial^2 w_0(x,y,z)}{\partial y^2} \rightarrow \int \kappa_y(x,y)|_z \, dy = \int -\frac{\partial^2 w_0(x,y,z)}{\partial y^2} dy = \kappa_y(x,y)|_z \; y + b_1(y,z) = \alpha_y(x,y)|_z = -\frac{\partial w_0(x,y,z)}{\partial y}$$

$$\kappa_{xy}(x,y)\,|_z = -2\frac{\partial^2 w_0(x,y,z)}{\partial x \partial y}$$

$$2\frac{\partial}{\partial y}\left[-\frac{\partial w_0(x,y,z)}{\partial x}\right] = 2\frac{\partial}{\partial y}\left[\alpha_x(x,y)\,|_z\right] = 2\frac{\partial}{\partial y}\left[\kappa_x(x,y)\,|_z\ x + a_1(y,z)\right] = 2\frac{\partial}{\partial y}a_1(y,z) = -2\frac{\partial^2 w_0(x,y,z)}{\partial x \partial y} = \kappa_{xy}(x,y)\,|_z$$

$$2\frac{\partial}{\partial x}\left[-\frac{\partial w_0(x,y,z)}{\partial y}\right] = 2\frac{\partial}{\partial x}\left[\alpha_y(x,y)\,|_z\right] = 2\frac{\partial}{\partial x}\left[\kappa_y(x,y)\,|_z\ y + b_1(x,z)\right] = 2\frac{\partial}{\partial x}b_1(x,z) = -2\frac{\partial^2 w_0(x,y,z)}{\partial x \partial y} = \kappa_{xy}(x,y)\,|_z$$

yz-plane:

$$\kappa_y(y,z)\,|_x = -\frac{\partial^2 u_0(x,y,z)}{\partial y^2} \rightarrow \int \kappa_y(y,z)\,|_x\ dy = \int -\frac{\partial^2 u_0(x,y,z)}{\partial y^2}dy = \kappa_y(y,z)\,|_x\ y + b_2(x,z) = \beta_y(y,z)\,|_x = -\frac{\partial u_0(x,y,z)}{\partial y}$$

$$\kappa_z(y,z)\,|_x = -\frac{\partial^2 u_0(x,y,z)}{\partial z^2} \rightarrow \int \kappa_z(y,z)\,|_x\ dz = \int -\frac{\partial^2 u(x,y,z)}{\partial z^2}dz = \kappa_z(y,z)\,|_x\ z + c_1(x,y) = \beta_z(y,z)\,|_x = -\frac{\partial u_0(x,y,z)}{\partial z}$$

$$\kappa_{yz}(y,z)\,|_x = -2\frac{\partial^2 u_0(x,y,z)}{\partial y \partial z}$$

$$2\frac{\partial}{\partial y}\left[-\frac{\partial u_0(x,y,z)}{\partial z}\right] = 2\frac{\partial}{\partial y}\left[\beta_z(y,z)\,|_x\right] = 2\frac{\partial}{\partial y}\left[\kappa_z(y,z)\,|_x\ z + c_1(x,y)\right] = 2\frac{\partial}{\partial y}c_1(x,y) = -2\frac{\partial^2 u_0(x,y,z)}{\partial y \partial z} = \kappa_{yz}(y,z)\,|_x$$

$$2\frac{\partial}{\partial z}\left[-\frac{\partial u_0(x,y,z)}{\partial y}\right] = 2\frac{\partial}{\partial z}\left[\beta_y(y,z)\,|_x\right] = 2\frac{\partial}{\partial z}\left[\kappa_y(y,z)\,|_x\ y + b_2(x,z)\right] = 2\frac{\partial}{\partial z}b_2(x,z) = -2\frac{\partial^2 u_0(x,y,z)}{\partial y \partial z} = \kappa_{yz}(y,z)\,|_x$$

zx-plane:

$$\kappa_x(x,z)\,|_y = -\frac{\partial^2 v_0(x,y,z)}{\partial x^2} \rightarrow \int \kappa_x(x,z)\,|_y\ dx = \int -\frac{\partial^2 v_0(x,y,z)}{\partial x^2}dx = \kappa_x(x,z)\,|_y\ x + a_2(y,z) = \beta_x(x,z)\,|_y = -\frac{\partial v_0(x,y,z)}{\partial x}$$

$$\kappa_z(x,z)\,|_y = -\frac{\partial^2 v_0(x,y,z)}{\partial z^2} \rightarrow \int \kappa_z(x,z)\,|_y\ dz = \int -\frac{\partial^2 v_0(x,y,z)}{\partial z^2}dz = \kappa_z(x,z)\,|_y\ z + c_2(x,y) = \alpha_z(x,z)\,|_y = -\frac{\partial v_0(x,y,z)}{\partial z}$$

$$\kappa_{zx}(x,z)\,|_y = -2\frac{\partial^2 v_0(x,y,z)}{\partial z \partial x}$$

$$2\frac{\partial}{\partial z}\left[-\frac{\partial v_0(x,y,z)}{\partial x}\right] = 2\frac{\partial}{\partial z}\left[\beta_x(x,z)\,|_y\right] = 2\frac{\partial}{\partial z}\left[\kappa_x(x,z)\,|_y\ x + a_2(y,z)\right] = 2\frac{\partial}{\partial z}a_2(y,z) = -2\frac{\partial^2 v_0(x,y,z)}{\partial z \partial x} = \kappa_{zx}(x,z)\,|_y$$

$$2\frac{\partial}{\partial x}\left[-\frac{\partial v_0(x,y,z)}{\partial z}\right] = 2\frac{\partial}{\partial x}\left[\alpha_z(x,z)\,|_y\right] = 2\frac{\partial}{\partial x}\left[\kappa_z(x,z)\,|_y\ z + c_2(x,y)\right] = 2\frac{\partial}{\partial x}c_2(x,y) = -2\frac{\partial^2 v_0(x,y,z)}{\partial z \partial x} = \kappa_{zx}(x,z)\,|_y$$

From the xy-plane:

$$\kappa_{xy}(x,y,z) \equiv \kappa_{xy}(x,y,z) \rightarrow 2\frac{\partial}{\partial y}a_1(y,z) = 2\frac{\partial}{\partial x}b_1(x,z) \Rightarrow \frac{\partial}{\partial y}a_1(y,z) = \frac{\partial}{\partial x}b_1(x,z) = \frac{\kappa_{xy}(x,y)|_z}{2}$$

From the yz-plane:

$$\kappa_{yz}(x,y,z) \equiv \kappa_{yz}(x,y,z) \rightarrow 2\frac{\partial}{\partial y}c_1(x,y) = 2\frac{\partial}{\partial z}b_2(x,z) \Rightarrow \frac{\partial}{\partial y}c_1(x,y) = \frac{\partial}{\partial z}b_2(x,z) = \frac{\kappa_{yz}(y,z)|_x}{2}$$

From the zx-plane:

$$\kappa_{zx}(x,y,z) \equiv \kappa_{zx}(x,y,z) \rightarrow 2\frac{\partial}{\partial z}a_2(y,z) = 2\frac{\partial}{\partial x}c_2(x,y) \Rightarrow \frac{\partial}{\partial z}a_2(y,z) = \frac{\partial}{\partial x}c_2(x,y) = \frac{\kappa_{zx}(x,z)|_y}{2}$$

$$\int \frac{\partial}{\partial y}a_1(y,z)dy = a_1(y,z) = \frac{\kappa_{xy}(x,y)|_z}{2}y + a_{11}(z)$$

$$\int \frac{\partial}{\partial x}b_1(x,z)dx = b_1(x,z) = \frac{\kappa_{xy}(x,y)|_z}{2}x + b_{11}(z)$$

$$\int \frac{\partial}{\partial y}c_1(x,y)dy = c_1(x,y) = \frac{\kappa_{yz}(y,z)|_x}{2}y + c_{11}(x)$$

$$\int \frac{\partial}{\partial z}b_2(x,z)dz = b_2(x,z) = \frac{\kappa_{yz}(y,z)|_x}{2}z + b_{22}(x)$$

$$\int \frac{\partial}{\partial z}a_2(y,z)dz = a_2(y,z) = \frac{\kappa_{zx}(x,z)|_y}{2}z + a_{22}(y)$$

$$\int \frac{\partial}{\partial x}c_2(x,y)dx = c_2(x,y) = \frac{\kappa_{zx}(x,z)|_y}{2}x + c_{22}(y)$$

$$\alpha_x(x,y)|_z = \kappa_x(x,y)|_z\ x + \frac{\kappa_{xy}(x,y)|_z}{2}y + a_{11}(z)$$

$$\beta_x(x,z)|_y = \kappa_x(x,z)|_y\ x + \frac{\kappa_{zx}(x,z)|_y}{2} z + a_{22}(y)$$

$$\alpha_y(x,y)|_z = \kappa_y(x,y)|_z\ y + \frac{\kappa_{xy}(x,y)|_z}{2} x + b_{11}(z)$$

$$\beta_y(y,z)|_x = \kappa_y(y,z)|_x\ y + \frac{\kappa_{yz}(y,z)|_x}{2} z + b_{22}(x)$$

$$\alpha_z(x,z)|_y = \kappa_z(x,z)|_y\ z + \frac{\kappa_{zx}(x,z)|_y}{2} x + c_{22}(y)$$

$$\beta_z(y,z)|_x = \kappa_z(y,z)|_x\ z + \frac{\kappa_{yz}(y,z)|_x}{2} y + c_{11}(x)$$

- Slope At Reference Point:

$$\alpha_x(x,y)|_z \Rightarrow \alpha_x(0,0)|_z = a_{11}(z) = 0$$
$$\beta_x(x,z)|_y \Rightarrow \beta_x(0,0)|_y = a_{22}(y) = 0$$
$$\alpha_y(x,y)|_Z \Rightarrow \alpha_y(0,0)|_Z = b_{11}(z) = 0$$
$$\beta_y(y,z)|_x \Rightarrow \beta_y(0,0)|_x = b_{22}(x) = 0$$
$$\alpha_z(x,z)|_y \Rightarrow \alpha_z(0,0)|_y = c_{22}(y) = 0$$
$$\beta_z(y,z)|_x \Rightarrow \beta_z(0,0)|_x = c_{11}(x) = 0$$

$$\alpha_x(x,y)|_z = \kappa_x(x,y)|_z\ x + \frac{\kappa_{xy}(x,y)|_z}{2} y$$

$$\beta_x(x,z)|_y = \kappa_x(x,z)|_y\ x + \frac{\kappa_{zx}(x,z)|_y}{2} z$$

$$\alpha_y(x,y)|_Z = \kappa_y(x,y)|_z\ y + \frac{\kappa_{xy}(x,y)|_Z}{2} x$$

$$\beta_y(y,z)|_x = \kappa_y(y,z)|_x\ y + \frac{\kappa_{yz}(y,z)|_x}{2} z$$

$$\alpha_z(x,z)|_y = \kappa_z(x,z)|_y\ z + \frac{\kappa_{zx}(x,z)|_y}{2} x$$

$$\beta_z(y,z)|_x = \kappa_z(y,z)|_x\ z + \frac{\kappa_{yz}(y,z)|_x}{2} y$$

$$u(x,y,z) = u_0(x,y,z) + \alpha_x(x,y)|_z\ z = \left[\varepsilon_x^0(x,y,z)x + \frac{\gamma_{xy}^0(x,y)|_z}{2} y\right] + \left[\kappa_x(x,y)|_z\ x + \frac{\kappa_{xy}(x,y)|_z}{2} y\right] z$$

$$= u_0(x,y,z) + \beta_x(x,z)|_y\ y = \left[\varepsilon_x^0(x,y,z)x + \frac{\gamma_{zx}^0(x,z)|_y}{2} z\right] + \left[\kappa_x(x,z)|_y\ x + \frac{\kappa_{zx}(x,z)|_y}{2} z\right] y$$

$$v(x,y,z) = v_0(x,y,z) + \alpha_y(x,y)|_Z\ z = \left[\varepsilon_y^0(x,y,z)y + \frac{\gamma_{xy}^0(x,y)|_z}{2} x\right] + \left[\kappa_y(x,y)|_z\ y + \frac{\kappa_{xy}(x,y)|_Z}{2} x\right] z$$

$$= v_0(x,y,z) + \beta_y(y,z)|_x\ x = \left[\varepsilon_y^0(x,y,z)y + \frac{\gamma_{yz}^0(y,z)|_x}{2} z\right] + \left[\kappa_y(y,z)|_x\ y + \frac{\kappa_{yz}(y,z)|_x}{2} z\right] x$$

$$w(x,y,z) = w_0(x,y,z) + \alpha_z(x,z)|_y\ y = \left[\varepsilon_z^0(x,y,z)z + \frac{\gamma_{zx}^0(x,z)|_y}{2} x\right] + \left[\kappa_z(x,z)|_y\ z + \frac{\kappa_{zx}(x,z)|_y}{2} x\right] y$$

$$= w_0(x,y,z) + \beta_z(y,z)|_x\ x = \left[\varepsilon_z^0(x,y,z)z + \frac{\gamma_{yz}^0(y,z)|_x}{2} y\right] + \left[\kappa_z(y,z)|_x\ z + \frac{\kappa_{yz}(y,z)|_x}{2} y\right] x$$

(C-2)

APPENDIX D

MATLAB CODE FOR COMPATIBILITY VERIFICATION OF DISPLACEMENTS DERIVED IN APPENDIX C

```
%Jared C. Polk
%Master's Thesis
%Compatibility

clc
clear


syms x y z epsilon_x0 epsilon_y0 epsilon_z0 gamma_xy0_z gamma_zx0_y gamma_yz0_x kappa_x_z
kappa_x_y  kappa_y_z kappa_y_x kappa_z_x kappa_z_y kappa_xy_z kappa_zx_y kappa_yz_x

u_xy = ((epsilon_x0*x)+(0.5*gamma_xy0_z*y))+(((kappa_x_z*x)+(0.5*kappa_xy_z*y))*z);
u_zx = ((epsilon_x0*x)+(0.5*gamma_zx0_y*z))+(((kappa_x_y*x)+(0.5*kappa_zx_y*z))*y);

v_xy = ((epsilon_y0*y)+(0.5*gamma_xy0_z*x))+(((kappa_y_z*y)+(0.5*kappa_xy_z*x))*z);
v_yz = ((epsilon_y0*y)+(0.5*gamma_yz0_x*z))+(((kappa_y_x*y)+(0.5*kappa_yz_x*z))*x);

w_zx = ((epsilon_z0*z)+(0.5*gamma_zx0_y*x))+(((kappa_z_y*z)+(0.5*kappa_zx_y*x))*y);
w_yz = ((epsilon_z0*z)+(0.5*gamma_yz0_x*y))+(((kappa_z_x*z)+(0.5*kappa_yz_x*y))*x);


%Strain displacement compatibility:
epsilon_x1 = diff(u_xy,x);
epsilon_x2 = diff(u_zx,x);

epsilon_y1 = diff(v_xy,y);
epsilon_y2 = diff(v_yz,y);

epsilon_z1 = diff(w_zx,z);
epsilon_z2 = diff(w_yz,z);

gamma_xy1 = diff(u_xy,y)+diff(v_xy,x);

gamma_yz1 = diff(v_yz,z)+diff(w_yz,y);

gamma_zx1 = diff(u_zx,z)+diff(w_zx,x);


%Second order (curvature) compatibility between normal and shear strains

%A1=A2
A1 = diff(epsilon_x1,y,2)+diff(epsilon_y1,x,2);
A2 = diff(diff(gamma_xy1,y),x);

if A1-A2 == 0
   disp('XY Second order (curvature) IS compatibility between normal and shear strains')
else
   disp('XY Second order (curvature) NOT compatibility between normal and shear strains')
end

%B1=B2
B1 = diff(epsilon_y2,z,2)+diff(epsilon_z2,y,2);
B2 = diff(diff(gamma_yz1,z),y);
```

```
if B1-B2 == 0
   disp('YZ Second order (curvature) IS compatibility between normal and shear strains')
else
   disp('YZ Second order (curvature) NOT compatibility between normal and shear strains')
end

%C1=C2
C1 = diff(epsilon_z1,x,2)+diff(epsilon_x2,z,2);
C2 = diff(diff(gamma_zx1,x),z);

if C1-C2 == 0
   disp('ZX Second order (curvature) IS compatibility between normal and shear strains')
else
   disp('ZX Second order (curvature) NOT compatibility between normal and shear strains')
```

APPENDIX E

MATLAB CODE FOR CLASSICAL LAMINATION THEORY ANALYSIS

```
%Jared Polk
%Master Thesis
%Classical Lamination Theory (CLT)

clc
clear


%%% Input %%%
plies = 6;
Theta = [45 45 0 45 45 0];   %top -> bottom
z = [0.015 0.010 0.005 0.000 -0.005 -0.010 -0.015];   %top -> bottom
z_bar = [0.0125 0.0075 0.0025 -0.0025 -0.0075 -0.0125];       %above -> below
%%% Glass Epoxy
E_1 = 6.00e6;
E_2 = 1.50e6;
G_12 = 0.62e6;
v_12 = 0.28;
delta_T = 100;
alpha_1 = 3.9e-6;
alpha_2 = 14.4e-6;



%%%%%%%%%%%%%%%%%%%%%%%%%%%%%%%%%%%%%%%%%%%%%%%%%%%%%%%%%%%%%%%%%%%%%%%%%%%%
%%%%%%%%%%%%%%%%%%%%%%%%%%%%%%%%%%%%%%%%%%%%%%%%%%%%%%%%%%%%%%%%%%%%%%%%%%%%

v_21 = (E_2/E_1)*v_12;
Q_11 = E_1/(1-(v_12*v_21));
Q_22 = E_2/(1-(v_12*v_21));
Q_12 = (v_12*E_2)/(1-(v_12*v_21));
Q_66 = G_12;


A=zeros(3,3);
B=zeros(3,3);
D=zeros(3,3);
alphas=zeros(3,1,plies);
THERMAL_LOADINGS_CLT_IP=zeros(3,1);
THERMAL_LOADINGS_CLT_OP=zeros(3,1);
count=0;
for i=1:plies
    count=count+1;
    theta = Theta(count);
     m = cos(theta*(pi/180));  %material coordinate rotation
     n = sin(theta*(pi/180));  %material coordinate rotation

    Q_xx = (Q_11*m^4)+(Q_22*n^4)+(2*Q_12*m^2*n^2)+(4*Q_66*m^2*n^2);
    Q_yy = (Q_11*n^4)+(Q_22*m^4)+(2*Q_12*m^2*n^2)+(4*Q_66*m^2*n^2);
    Q_xy = (Q_11*m^2*n^2)+(Q_22*m^2*n^2)+(Q_12*(m^4+n^4))-(4*Q_66*m^2*n^2);
    Q_xs = (Q_11*m^3*n^1)-(Q_22*m^1*n^3)-(Q_12*(m^2-n^2)*m*n)-(2*Q_66*(m^2-n^2)*m*n);
    Q_ys = (Q_11*m^1*n^3)-(Q_22*m^3*n^1)+(Q_12*(m^2-n^2)*m*n)+(2*Q_66*(m^2-n^2)*m*n);
    Q_ss = (Q_11*m^2*n^2)+(Q_22*m^2*n^2)-(2*Q_12*m^2*n^2)+(Q_66*(m^2-n^2)^2);
```

```
    Q_yx = Q_xy;
    Q_sx = Q_xs;
    Q_sy = Q_ys;
    Q_XY(:,:,count) = [Q_xx  Q_xy  Q_xs
                    Q_yx  Q_yy  Q_ys
                    Q_sx  Q_sy  Q_ss];

      %Rotating laminate about y-axis

    A = A+(Q_XY(:,:,count)*(z(count)-z(count+1)));
    B = B+(Q_XY(:,:,count)*(z(count)^2-z(count+1)^2));
    D = D+(Q_XY(:,:,count)*(z(count)^3-z(count+1)^3));

    alpha_x = ((alpha_1*m^2)+(alpha_2*n^2));
    alpha_y = ((alpha_1*n^2)+(alpha_2*m^2));
    alpha_s = (2*(alpha_1-alpha_2)*m*n);
    alphas(:,:,count) = [alpha_x;alpha_y;alpha_s];

    thermal_loading_CLT_IP(:,:,count) = Q_XY(:,:,count)*alphas(:,:,count)*delta_T*0.005;
    THERMAL_LOADINGS_CLT_IP =
THERMAL_LOADINGS_CLT_IP+thermal_loading_CLT_IP(:,:,count);
    thermal_loading_CLT_OP(:,:,count) = Q_XY(:,:,count)*alphas(:,:,count)*delta_T*0.005*z_bar(count);
    THERMAL_LOADINGS_CLT_OP =
THERMAL_LOADINGS_CLT_OP+thermal_loading_CLT_OP(:,:,count);
end

B = (1/2)*B;
D = (1/3)*D;

ABD = [A B
     B D];
abd = inv(ABD);
%%%%%%%%%%%%%%%%%%%%%%%%%%%%%%%%%%%%%%%%%%%%%%%%%%%%%%%%%%%%%%%%%%%%%%%%
%%%%%%%%%%%%%%%%%%%%%%%%%%%%%%%%%%%%%%%%%%%%%%%%%%

%%% Input %%%%
    %solve for:  Input
    Nx_induced = -
(abd(1,1)*THERMAL_LOADINGS_CLT_IP(1)+abd(1,2)*THERMAL_LOADINGS_CLT_IP(2)+abd(1,3
)*THERMAL_LOADINGS_CLT_IP(3)+abd(1,4)*THERMAL_LOADINGS_CLT_OP(1)+abd(1,5)*THE
RMAL_LOADINGS_CLT_OP(2)+abd(1,6)*THERMAL_LOADINGS_CLT_OP(3))/abd(1,1)  ;
%%%%%%%%%%%%%%%%%%%%%%%%%%%%%%%%%%%%%%%%%%%%%%%%%%%%%%%%%%%%%%%%%%%%%%%%
%%%%%%%%%%%%%%%%%%%%%%%%%%%%%%%%%%%%%%%%%%%%%%%%%%%%%%%%%%%%%%%%%%%%

LOADINGS =
[THERMAL_LOADINGS_CLT_IP(1)+Nx_induced;THERMAL_LOADINGS_CLT_IP(2);THERMAL_L
OADINGS_CLT_IP(3)+Ns_induced;THERMAL_LOADINGS_CLT_OP(1);THERMAL_LOADINGS_C
LT_OP(2);THERMAL_LOADINGS_CLT_OP(3)];
strain_curvatures = abd*LOADINGS;

count=0;
stress_induced_strains=zeros(3,1,plies);
stresses_xy=zeros(3,1,plies);
```

```
for i=1:plies
   count=count+1;

   stress_induced_strains(:,:,count) = strain_curvatures(1:3)+z_bar(count)*strain_curvatures(4:6)-
alphas(:,:,count)*delta_T;    %calculates strain at mid-plane of each ply
   stresses_xy(:,:,count) = Q_XY(:,:,count)*stress_induced_strains(:,:,count);
end



%%% AS4/3501-6 Carbon Epoxy
%E_1 = 21.3e6;
%E_2 = 1.5e6;
%G_12 = 1.00e6;
%v_12 = 0.27;
%delta_T = 100;
%alpha_1 = -0.5e-6;
%alpha_2 = 15.0e-6;

%%% Aluminum %%%%
%E_1 = 10e6;
%E_2 = 10e6;
%G_12 = 3.77e6;
%v_12 = 0.33;
%delta_T = 100;
%alpha_1 = 13.1e-6;
%alpha_2 = 13.1e-6;

%%% Glass Epoxy
%E_1 = 6.00e6;
%E_2 = 1.50e6;
%G_12 = 0.62e6;
%v_12 = 0.28;
%delta_T = 100;
%alpha_1 = 3.9e-6;
%alpha_2 = 14.4e-6;


%%% Nx_induced for different family of stacking sequences %%%
%symmetric and balanced:       Nx_induced = -
(abd(1,1)*THERMAL_LOADINGS_CLT_IP(1)+abd(1,2)*THERMAL_LOADINGS_CLT_IP(2))/abd(1,1
)
%unsymmetric and balanced:     Nx_induced = -
(abd(1,1)*THERMAL_LOADINGS_CLT_IP(1)+abd(1,2)*THERMAL_LOADINGS_CLT_IP(2)+abd(1,4
)*THERMAL_LOADINGS_CLT_OP(1)+abd(1,5)*THERMAL_LOADINGS_CLT_OP(2)+abd(1,6)*THE
RMAL_LOADINGS_CLT_OP(3))/abd(1,1)
%symmetric and unbalanced:     Nx_induced = -
(abd(1,1)*THERMAL_LOADINGS_CLT_IP(1)+abd(1,2)*THERMAL_LOADINGS_CLT_IP(2)+abd(1,3
)*THERMAL_LOADINGS_CLT_IP(3))/abd(1,1)
%unsymmetric and unbalanced:   Nx_induced = -
(abd(1,1)*THERMAL_LOADINGS_CLT_IP(1)+abd(1,2)*THERMAL_LOADINGS_CLT_IP(2)+abd(1,3
)*THERMAL_LOADINGS_CLT_IP(3)+abd(1,4)*THERMAL_LOADINGS_CLT_OP(1)+abd(1,5)*THE
RMAL_LOADINGS_CLT_OP(2)+abd(1,6)*THERMAL_LOADINGS_CLT_OP(3))/abd(1,1)
```

APPENDIX F

MATLAB CODE FOR FINITE ELEMENT ANALYSIS OF CURVED AND FLAT COMPOSITE LAMINATES

Main File: filename: TCLAP_8nodeISO

```
%Jared C. Polk
%Master Thesis
%Thermal Curved Laminate Analysis Program (TCLAP)

%%%%%%%%%%%%%%%%%%%%%%%%%%%%   PURPOSE
%%%%%%%%%%%%%%%%%%%%%%%%%%%%%%%%%%%%%%%%%%%%%%%%%%%%%%%%%%%%%%%%%%%%%%%%%%%%
%  Stress analysis on thermally loaded, axi-symmetric, simple curvature
%  laminates
%%%%%%%%%%%%%%%%%%%%%%%%%%%%%%%%%%%%%%%%%%%%%%%%%%%%%%%%%%%%%%%%%%%%%%%%%%%%
%%%%%%%%%%%%%%%%%%%%%%%%%%%%


tic %%%'" T I M E R "'%%%
%-----------------------------Inputs----------------------------------------%
%%%    Aluminum      %%%%
%*** Material Properties ***
E1 = 10e6;
E2 = 10e6;
E3 = 10e6;
G13 = 3.77e6;
G23 = 3.77e6;
G12 = 3.77e6;
v12 = 0.33;
v13 = 0.33;
v23 = 0.33;
%.....................................................................
%*** Thermal Conditions and Properties ***
T_final = 100;
T_initial = 0;
alpha_1 = 13.1e-6;
alpha_2 = 13.1e-6;
alpha_3 = 13.1e-6;
%.....................................................................
%*** Laminate Stacking Sequence Data ***
plies = 6;
Theta = [0 0 0 0 0 0];  %list direction: Theta = [bottom laminate -> top laminate]
z = linspace(-0.5*plies*0.005,0.5*plies*0.005,plies+1);  %list direction: z = [bottom laminate -> top
laminate]
laminate_Z = [-0.015 -0.010 -0.005 0 0.005 0.010 0.015];   %list direction:  laminate_Z = [bottom laminate
-> top laminate]

%.....................................................................
%*** Model Element Configuration ***
Number_Of_Elements__THETA = 180;
Number_Of_Elements__Z = 24;
Number_Of_Elements__RADIAL = plies;
%.....................................................................
%*** Model Geometry Configuration ***
thickness_ply = 0.005;

Angle_Spanned = (30)*(pi/180);  %Angle_Spanned = Angle{degrees}*{conversion to radians}
```

```
Arc_Length = Number_Of_Elements__THETA*thickness_ply;
if Angle_Spanned == 0
   Radius_Of_Curvature = 0;
else
   Radius_Of_Curvature = Arc_Length/Angle_Spanned;  % Radius_Of_Curvature = Arc
Length/Angle_Spanned
end

%.....................................................................
%*** Boundary Conditions ***
Right_Boundary = 1;
Left_Boundary = 1;
Top_Boundary = 0;
Bottom_Boundary = 0;
Front_Boundary = 0;
Rear_Boundary = 0;
%.....................................................................

%---------------------------------------------------------------------%




%-------------------Material Constants and Parameters----------------------%
v21 = (E2/E1)*v12;
v31 = (E3/E1)*v13;
v32 = (E3/E2)*v23;
triangle = 1/E1/E2/E3*(1-v32*v23-v12*v21-v12*v31*v23-v13*v21*v32-v13*v31);
C11 = (1-(v23*v32))/(E2*E3*triangle);
C22 = (1-(v13*v31))/(E1*E3*triangle);
C33 = (1-(v12*v21))/(E1*E2*triangle);
C12 = (v21+(v31*v23))/(E2*E3*triangle);
C23 = (v32+(v12*v31))/(E1*E3*triangle);
C13 = (v13+(v12*v23))/(E1*E2*triangle);
C21 = C12;
C32 = C23;
C31 = C13;
C44 = G23;
C55 = G13;
C66 = G12;
delta_T = T_final-T_initial;
alpha_12 = transpose([alpha_1 alpha_2 alpha_3 0 0 0]);
%.....................................................................
ne = Number_Of_Elements__THETA*Number_Of_Elements__RADIAL*Number_Of_Elements__Z;
nn_THETA = Number_Of_Elements__THETA+1;
nn_RADIAL = Number_Of_Elements__RADIAL+1;
nn_Z = Number_Of_Elements__Z+1;
nn = nn_RADIAL*nn_Z*nn_THETA;
ndof=3*nn;
%.....................................................................
%.....................................................................
%---------------------------------------------------------------------%
```

```
%------------------Laminate Rotation-----------------------------------%
Phi = linspace(-0.5*Angle_Spanned,0.5*Angle_Spanned,(2*Number_Of_Elements__THETA)+1);
i_master=0;
i_servant=0;
for RADIAL_master = 1:Number_Of_Elements__RADIAL

   for Z_master = 1:Number_Of_Elements__Z

      for THETA_master = 1:Number_Of_Elements__THETA
         i_master = i_master+1;
         i_servant = i_servant+1;
         phi_y(i_servant) = Phi(i_master*2);    %#ok<AGROW>
      end
      i_master=0;

   end

end
%-------------------------------------------------------------------------%
%_____________________________________________________________________________%
t_input_initialization=toc   %#ok<NOPTS>  %%%''' T I M E R '''%%%


tic   %%%''' T I M E R '''%%%
[elements] =
funct_element_connectivity_8nodeISO(Number_Of_Elements__THETA,Number_Of_Elements__RADIA
L,Number_Of_Elements__Z,ne,nn_THETA,nn_Z);
[k_element_sym] = funct_symbolic_stiffness_matrix_8nodeISO();
[B_FEA_SYM,N] = funct_b_matrix_integral_8nodeISO();
[thermal_load_sym] = funct_symbolic_thermal_load_matrix_8nodeISO();
t_symbolic_set_up=toc %#ok<NOPTS>   %%%''' T I M E R '''%%%

tic   %%%''' T I M E R '''%%%
fid = fopen('k_element_symbolic_2_numeric.m','w');

 fprintf(fid,'k_element_numeric = [ ');
   SIZE_k_element_sym = size(k_element_sym);
   for row = 1:SIZE_k_element_sym(1)
      for col = 1:SIZE_k_element_sym(2)
         fprintf(fid,'%s',char(k_element_sym(row,col)),',');
      end
      fprintf(fid,';...\n');
   end
   fprintf(fid,' ];');
t_function_for_k_element=toc %#ok<NOPTS>   %%%''' T I M E R '''%%%

tic   %%%''' T I M E R '''%%%
fid = fopen('thermal_strain_symbolic_2_numeric.m','w');

 fprintf(fid,'thermal_load_numeric = [ ');
   SIZE_thermal_load_sym = size(thermal_load_sym);
   for row = 1:SIZE_thermal_load_sym(1)
```

```
        for col = 1:SIZE_thermal_load_sym(2)
            fprintf(fid,'%s',char(thermal_load_sym(row,col)),',');
        end
        fprintf(fid,';...\n');
    end
    fprintf(fid,' ];');
t_function_for_thermal_load=toc %#ok<NOPTS>   %%%''' T I M E R '''%%%

tic   %%%''' T I M E R '''%%%
%Calculation of element stiffness matrices and thermal nodal forces
layer_check=1;
layer_check_index=1;
i_master=0;
for I_master = 1:ne
    i_master=i_master+1;
        PHI_Y = phi_y(i_master);

[C] =
funct_C_matrices_8nodeISO(layer_check,Theta,PHI_Y,C11,C12,C13,C21,C22,C23,C31,C32,C33,C44,C5
5,C66);
        D_FEA(:,:,i_master) = C; %#ok<AGROW>
        A11=C(1,1);
        A12=C(1,2);
        A16=C(1,3);
        B11=C(1,4);
        B12=C(1,5);
        B16=C(1,6);
        A21=C(2,1);
        A22=C(2,2);
        A26=C(2,3);
        B21=C(2,4);
        B22=C(2,5);
        B26=C(2,6);
        A61=C(3,1);
        A62=C(3,2);
        A66=C(3,3);
        B61=C(3,4);
        B62=C(3,5);
        B66=C(3,6);
        D11=C(4,4);
        D12=C(4,5);
        D16=C(4,6);
        D21=C(5,4);
        D22=C(5,5);
        D26=C(5,6);
        D61=C(6,4);
        D62=C(6,5);
        D66=C(6,6);
    [Determinant_Jacobian] = funct_jacobian_8nodeISO(PHI_Y);
    run('k_element_symbolic_2_numeric')
    k_element_num = Determinant_Jacobian*k_element_numeric;
    k_element(:,:,i_master) = k_element_numeric; %#ok<AGROW>
```

```
  [THERMAL_STRAIN] =
funct_thermal_strains_8nodeISO(layer_check,Theta,PHI_Y,delta_T,alpha_12);
      THERMAL_STRAIN_FEA(:,:,i_master) = THERMAL_STRAIN;  %#ok<AGROW>
      thermal_strain_r = THERMAL_STRAIN(1,1);
      thermal_strain_s = THERMAL_STRAIN(2,1);
      thermal_strain_t = THERMAL_STRAIN(3,1);
      thermal_strain_st = THERMAL_STRAIN(4,1);
      thermal_strain_rt = THERMAL_STRAIN(5,1);
      thermal_strain_rs = THERMAL_STRAIN(6,1);
  run('thermal_strain_symbolic_2_numeric')

  thermal_load(:,:,i_master) = thermal_load_numeric; %#ok<AGROW>

  if i_master == layer_check_index*Number_Of_Elements__THETA*Number_Of_Elements__Z;
   layer_check = layer_check+1;
   layer_check_index = layer_check_index+1;
  end
end
t_processing=toc %#ok<NOPTS>   %%%''' T I M E R '''%%%


tic   %%%''' T I M E R '''%%%
[K_global] = funct_global_stiffness_matrix_8nodeISO(ne,elements,k_element,ndof);
[bottom_face_nodes,top_face_nodes,right_face_nodes,left_face_nodes,front_face_nodes,rear_face_nodes]
=
funct_boundary_conditions_8nodeISO(elements,Number_Of_Elements__THETA,Number_Of_Elements_
_RADIAL,Number_Of_Elements__Z,ne,nn_THETA,nn_Z);
[K_global_reduced] =
funct_reduced_stiffness_matrix_8nodeISO(bottom_face_nodes,top_face_nodes,right_face_nodes,left_face
_nodes,front_face_nodes,rear_face_nodes,K_global,Right_Boundary,Left_Boundary,Top_Boundary,Botto
m_Boundary,Front_Boundary,Rear_Boundary,ndof);
[thermal_load_Array,thermal_load_Array_Reduced] =
funct_nodal_force_array_8nodeISO(thermal_load,elements,ne,ndof,bottom_face_nodes,top_face_nodes,rig
ht_face_nodes,left_face_nodes,front_face_nodes,rear_face_nodes,Right_Boundary,Left_Boundary,Top_Bo
undary,Bottom_Boundary,Front_Boundary,Rear_Boundary);

[Reduced_Displacement_Array] =
funct_reduced_displacement_array_8nodeISO(K_global_reduced,thermal_load_Array_Reduced);

[Displacements] = funct_displacements_8nodeISO(elements,ne,Reduced_Displacement_Array);

[Displacement_Function] = funct_displacement_function_8nodeISO(ne,Displacements,N);
t_solving1=toc %#ok<NOPTS>   %%%''' T I M E R '''%%%




tic   %%%''' T I M E R '''%%%
[Element_Strain,Nodal_Strain] =
funct_strain_8nodeISO(Displacements,B_FEA_SYM,ne,Radius_Of_Curvature,laminate_Z,Number_Of_El
ements__THETA,Number_Of_Elements__Z,Number_Of_Elements__RADIAL,plies);
```

```
[Element_Stress,Nodal_Stress] =
funct_stress_8nodeISO(Element_Strain,Nodal_Strain,ne,D_FEA,THERMAL_STRAIN_FEA);

[Forces,FORCES] = funct_forces_8nodeISO(Displacements,k_element,ne,thermal_load);
t_solving2=toc   %#ok<NOPTS>   %%%''' T I M E R '''%%%


t_total_seconds=t_solving2+t_solving1+t_processing+t_function_for_k_element+t_symbolic_set_up+t_inp
ut_initialization %#ok<NOPTS>
t_total_minutes=t_total_seconds/60 %#ok<NOPTS>


%%%     Aluminum       %%%%
%*** Material Properties ***
%E1 = 10e6;
%E2 = 10e6;
%E3 = 10e6;
%G13 = 3.77e6;
%G23 = 3.77e6;
%G12 = 3.77e6;
%v12 = 0.33;
%v13 = 0.33;
%v23 = 0.33;
%.....................................................................
%*** Thermal Conditions and Properties ***
%T_final = 100;
%T_initial = 0;
%alpha_1 = 13.1e-6;
%alpha_2 = 13.1e-6;
%alpha_3 = 13.1e-6;



%%%     AS4/3501-6 Carbon Epoxy       %%%%
%*** Material Properties ***
%E1 = 21.3e6;
%E2 = 1.50e6;
%E3 = 1.50e6;
%G13 = 1.00e6;
%G23 = 0.54e6;
%G12 = 1.00e6;
%v12 = 0.27;
%v13 = 0.27;
%v23 = 0.54;
%.....................................................................
%*** Thermal Conditions and Properties ***
%T_final = 100;
%T_initial = 0;
%alpha_1 = -0.5e-6;
%alpha_2 = 15.0e-6;
%alpha_3 = 15.0e-6;
```

```
%%%    E-Glass/Epoxy      %%%%
%*** Material Properties ***
%E1 = 6.00e6;
%E2 = 1.50e6;
%E3 = 1.50e6;
%G13 = 0.62e6;
%G23 = 0.50e6;
%G12 = 0.62e6;
%v12 = 0.28;
%v13 = 0.28;
%v23 = 0.50;
%.....................................................................
%*** Thermal Conditions and Properties ***
%T_final = 100;
%T_initial = 0;
%alpha_1 = 3.9e-6;
%alpha_2 = 14.4e-6;
%alpha_3 = 14.4e-6;
```

Element Connectivity File: filename: funct_element_connectivity_8nodeISO

```
function    [elements] =
funct_element_connectivity_8nodeISO(Number_Of_Elements__THETA,Number_Of_Elements__RADIA
L,Number_Of_Elements__Z,ne,nn_THETA,nn_Z)

%%%%%%%%%%%%%%%%%%%%%%%%%%   PURPOSE
%%%%%%%%%%%%%%%%%%%%%%%%%%%%%%%%%%%%%%%%%%%%%
%  Defines element connectivity.  Definition of connectivity is done one
%  element at a time.  The sequence in which the elements are addressed is
%  at a given Theta & R, elements are addressed from Z=0 to Z=Z_final.  The
%  indexing progresses to a new Theta with the same R until the domain of
%  Theta is transversed.  Then the indexing cycles to a new R position and
%  the latter processes repeat until all elements have been addressed.
%%%%%%%%%%%%%%%%%%%%%%%%%%%%%%%%%%%%%%%%%%%%%%%%%%%%%%%%%%%%%
%%%%%%%%%%%%%%%%%%%%%%%%%%




elements = zeros(ne,8);

 ii=1:1:nn_THETA;
 iii=0;
jj=linspace(1,Number_Of_Elements__THETA,Number_Of_Elements__THETA);
 j=1; %#ok<NASGU>
 jjj=0;
k=0;
 kk=0;


for J=1:Number_Of_Elements__THETA
   iii=iii+1;
   i=ii(iii);
   jjj=jjj+1;
   j=jj(jjj);

   for I=1:Number_Of_Elements__Z

      elements(j,1:2) = [i i+1];
      elements(j,3:4) = [i+nn_THETA+1 i+nn_THETA];
      elements(j,5:6) = [i+(nn_THETA*nn_Z) i+(nn_THETA*nn_Z)+1];
      elements(j,7:8) = [i+(nn_THETA*nn_Z)+nn_THETA+1 i+(nn_THETA*nn_Z)+nn_THETA];

      i=i+nn_THETA;
      j=j+Number_Of_Elements__THETA;
   end

end

if Number_Of_Elements__RADIAL > 1

   k=0;
```

```
   for K=2:Number_Of_Elements__RADIAL
      k=k+1;

elements((((Number_Of_Elements__THETA*Number_Of_Elements__Z)*k)+1):((Number_Of_Elements_
_THETA*Number_Of_Elements__Z)*(k+1)),:) =
[elements(1:(Number_Of_Elements__THETA*Number_Of_Elements__Z),1:4)+(k*nn_THETA*nn_Z)
elements(1:(Number_Of_Elements__THETA*Number_Of_Elements__Z),5:8)+(k*nn_THETA*nn_Z)];
   end

end
```

Symbolic Stiffness Matrix File: filename: funct_symbolic_stiffness_matrix_8nodeISO

```
function [k_element_sym] = funct_symbolic_stiffness_matrix_8nodeISO()

%%%%%%%%%%%%%%%%%%%%%%%%   PURPOSE
%%%%%%%%%%%%%%%%%%%%%%%%%%%%%%%%%%%%%%%%%%%%%
% Generates the symbolic element stiffness matrix (with respect to) the
% laminates constitutive relationship
%%%%%%%%%%%%%%%%%%%%%%%%%%%%%%%%%%%%%%%%%%%%%%%%%%%%%%%%%%%%%%
%%%%%%%%%%%%%%%%%%%%%%%%

syms A11 A12 A16 B11 B12 B16 A21 A22 A26 B21 B22 B26 A61 A62 A66 B61 B62 B66 B11 B12 B16
D11 D12 D16 B21 B22 B26 D21 D22 D26 B61 B62 B66 D61 D62 D66


k_element_sym = [      [
2/9*A11+2/9*D66+1/6*B61+1/6*B16+2/9*D22+1/6*B21+1/6*D26+1/6*B12+1/6*D62,
2/9*B62+1/6*A12+2/9*B16+1/6*D66+1/6*D26+1/6*B22+2/9*D21+1/6*B11+1/6*D61,
2/9*D61+1/6*B11+2/9*B12+1/6*D62+1/6*D22+1/6*D21+1/6*A16+2/9*B26+1/6*B66,        1/9*D66-
2/9*A11-1/6*B61+1/6*B16+1/9*D22-1/6*B21+1/12*D62+1/12*D26+1/6*B12,        1/9*B62+1/6*A12-
2/9*B16-1/6*D66-1/6*D26+1/12*D61+1/9*D21+1/6*B11+1/12*B22,        1/9*D61+1/6*B11-2/9*B12-
1/6*D62-1/6*D22+1/12*D21+1/6*A16+1/9*B26+1/12*B66,     -1/9*A11-1/9*D66-1/6*B61-
1/6*B16+1/18*D22-1/12*B21-1/12*D26+1/12*B12+1/12*D62,     -1/9*B62-1/6*A12-1/9*B16-1/6*D66-
1/12*D26-1/12*B22+1/18*D21+1/12*B11+1/12*D61,     -1/9*D61-1/6*B11-1/9*B12-1/6*D62-
1/12*D22-1/12*D21+1/12*A16+1/18*B26+1/12*B66,       -2/9*D66+1/9*A11+1/6*B61-
1/6*B16+1/9*D22+1/12*B21+1/6*D62-1/6*D26+1/12*B12,       -2/9*B62-
1/6*A12+1/9*B16+1/6*D66+1/12*D26-1/6*B22+1/9*D21+1/12*B11+1/6*D61,       -2/9*D61-
1/6*B11+1/9*B12+1/6*D62+1/12*D22-1/6*D21+1/12*A16+1/9*B26+1/6*B66,
1/9*D66+1/9*A11+1/12*B61+1/12*B16-2/9*D22+1/6*B21-1/6*D62+1/6*D26-1/6*B12,
1/9*B62+1/12*A12+1/9*B16+1/12*D66+1/6*D26-1/6*D61-2/9*D21-1/6*B11+1/6*B22,
1/9*D61+1/12*B11+1/9*B12+1/12*D62+1/6*D22-2/9*B26+1/6*D21-1/6*A16-1/6*B66,     -
1/9*A11+1/18*D66-1/12*B61+1/12*B16-1/9*D22-1/6*B21+1/12*D26-1/6*B12-1/12*D62,
1/18*B62+1/12*A12-1/9*B16-1/12*D66-1/6*D26-1/12*D61-1/9*D21-1/6*B11+1/12*B22,
1/18*D61+1/12*B11-1/9*B12-1/12*D62-1/6*D22+1/12*D21-1/6*A16-1/9*B26-1/12*B66, -1/18*D66-
1/18*A11-1/12*B61-1/12*B16-1/18*D22-1/12*B21-1/12*D62-1/12*D26-1/12*B12, -1/18*B62-
1/12*A12-1/18*B16-1/12*D66-1/12*D26-1/12*D61-1/18*D21-1/12*B11-1/12*B22, -1/18*D61-
1/12*B11-1/18*B12-1/12*D62-1/12*D22-1/18*B26-1/12*D21-1/12*A16-1/12*B66,      1/18*A11-
1/9*D66+1/12*B61-1/12*B16-1/9*D22+1/12*B21-1/6*D26-1/12*B12-1/6*D62,     -1/9*B62-
1/12*A12+1/18*B16+1/12*D66+1/12*D26-1/6*B22-1/9*D21-1/12*B11-1/6*D61,     -1/9*D61-
1/12*B11+1/18*B12+1/12*D62+1/12*D22-1/9*B26-1/6*D21-1/12*A16-1/6*B66]
                    [
2/9*B61+2/9*B26+1/6*A21+1/6*D66+2/9*D12+1/6*B11+1/6*D16+1/6*B22+1/6*D62,
2/9*A22+1/6*B62+2/9*D66+1/6*B26+1/6*D16+1/6*B12+2/9*D11+1/6*D61+1/6*B21,
2/9*B21+1/6*D61+2/9*D62+1/6*B22+1/6*D12+1/6*D11+2/9*B16+1/6*B66+1/6*A26,        1/9*B26-
1/6*A21-2/9*B61+1/6*D66+1/9*D12-1/6*B11+1/12*B22+1/12*D16+1/6*D62,        1/9*A22+1/6*B62-
2/9*D66-1/6*B26-1/6*D16+1/12*B21+1/9*D11+1/6*D61+1/12*B12,        1/9*B21+1/6*D61-2/9*D62-
1/6*B22-1/6*D12+1/12*D11+1/9*B16+1/6*B66+1/12*A26,     -1/9*B61-1/9*B26-1/6*A21-
1/6*D66+1/18*D12-1/12*B11-1/12*D16+1/12*B22+1/12*D62,     -1/9*A22-1/6*B62-1/9*D66-1/6*B26-
1/12*D16-1/12*B12+1/18*D11+1/12*D61+1/12*B21,     -1/9*B21-1/6*D61-1/9*D62-1/6*B22-
1/12*D12-1/12*D11+1/18*B16+1/12*B66+1/12*A26,       -2/9*B26+1/6*A21+1/9*B61-
1/6*D66+1/9*D12+1/12*B11+1/6*B22-1/6*D16+1/12*D62,       -2/9*A22-
1/6*B62+1/9*D66+1/6*B26+1/12*D16-1/6*B12+1/9*D11+1/12*D61+1/6*B21,       -2/9*B21-
```

1/6*D61+1/9*D62+1/6*B22+1/12*D12-1/6*D11+1/9*B16+1/12*B66+1/6*A26,
1/9*B61+1/9*B26+1/12*A21+1/12*D66-2/9*D12+1/6*B11-1/6*B22+1/6*D16-1/6*D62,
1/9*A22+1/12*B62+1/9*D66+1/12*B26+1/6*D16-1/6*B21-2/9*D11-1/6*D61+1/6*B12,
1/9*B21+1/12*D61+1/9*D62+1/12*B22+1/6*D12+1/6*D11-2/9*B16-1/6*B66-1/6*A26, -
1/9*B61+1/18*B26-1/12*A21+1/12*D66-1/9*D12-1/6*B11+1/12*D16-1/12*B22-1/6*D62,
1/18*A22+1/12*B62-1/9*D66-1/12*B26-1/6*D16-1/12*B21-1/9*D11-1/6*D61+1/12*B12,
1/18*B21+1/12*D61-1/9*D62-1/12*B22-1/6*D12+1/12*D11-1/9*B16-1/6*B66-1/12*A26, -1/18*B26-
1/12*A21-1/18*B61-1/12*D66-1/18*D12-1/12*B11-1/12*B22-1/12*D16-1/12*D62, -1/18*A22-
1/12*B62-1/18*D66-1/12*B26-1/12*D16-1/12*B21-1/18*D11-1/12*D61-1/12*B12, -1/18*B21-
1/12*D61-1/18*D62-1/12*B22-1/12*D12-1/12*D11-1/18*B16-1/12*B66-1/12*A26, 1/18*B61-
1/9*B26+1/12*A21-1/12*D66-1/9*D12+1/12*B11-1/6*D16-1/6*B22-1/12*D62, -1/9*A22-
1/12*B62+1/18*D66+1/12*B26+1/12*D16-1/6*B12-1/9*D11-1/12*D61-1/6*B21, -1/9*B21-
1/12*D61+1/18*D62+1/12*B22+1/12*D12-1/6*D11-1/9*B16-1/12*B66-1/6*A26]
[
2/9*B21+2/9*D16+1/6*B11+1/6*D26+2/9*B62+1/6*A61+1/6*B66+1/6*D12+1/6*D22,
2/9*B12+1/6*B22+2/9*D26+1/6*D16+1/6*B66+1/6*A62+2/9*B61+1/6*D21+1/6*D11,
2/9*D11+1/6*D21+2/9*D22+1/6*D12+1/6*B62+1/6*B61+2/9*A66+1/6*B26+1/6*B16, 1/9*D16-
1/6*B11-2/9*B21+1/6*D26+1/9*B62-1/6*A61+1/12*D12+1/12*B66+1/6*D22, 1/9*B12+1/6*B22-
2/9*D26-1/6*D16-1/6*B66+1/12*D11+1/9*B61+1/6*D21+1/12*A62, 1/9*D11+1/6*D21-2/9*D22-
1/6*D12-1/6*B62+1/12*B61+1/9*A66+1/6*B26+1/12*B16, -1/9*B21-1/9*D16-1/6*B11-
1/6*D26+1/18*B62-1/12*A61-1/12*B66+1/12*D12+1/12*D22, -1/9*B12-1/6*B22-1/9*D26-1/6*D16-
1/12*B66-1/12*A62+1/18*B61+1/12*D21+1/12*D11, -1/9*D11-1/6*D21-1/9*D22-1/6*D12-
1/12*B62-1/12*B61+1/18*A66+1/12*B26+1/12*B16, -2/9*D16+1/6*B11+1/9*B21-
1/6*D26+1/9*B62+1/12*A61+1/6*D12-1/6*B66+1/12*D22, -2/9*B12-
1/6*B22+1/9*D26+1/6*D16+1/12*B66-1/6*A62+1/9*B61+1/12*D21+1/6*D11, -2/9*D11-
1/6*D21+1/9*D22+1/6*D12+1/12*B62-1/6*B61+1/9*A66+1/12*B26+1/6*B16,
1/9*B21+1/9*D16+1/12*B11+1/12*D26-2/9*B62+1/6*A61-1/6*D12+1/6*B66-1/6*D22,
1/9*B12+1/12*B22+1/9*D26+1/12*D16+1/6*B66-1/6*D11-2/9*B61-1/6*D21+1/6*A62,
1/9*D11+1/12*D21+1/9*D22+1/12*D12+1/6*B62+1/6*B61-2/9*A66-1/6*B26-1/6*B16, -
1/9*B21+1/18*D16-1/12*B11+1/12*D26-1/9*B62-1/6*A61+1/12*B66-1/12*D12-1/6*D22,
1/18*B12+1/12*B22-1/9*D26-1/12*D16-1/6*B66-1/12*D11-1/9*B61-1/6*D21+1/12*A62,
1/18*D11+1/12*D21-1/9*D22-1/12*D12-1/6*B62+1/12*B61-1/9*A66-1/6*B26-1/12*B16, -1/18*D16-
1/12*B11-1/18*B21-1/12*D26-1/18*B62-1/12*A61-1/12*D12-1/12*B66-1/12*D22, -1/18*B12-
1/12*B22-1/18*D26-1/12*D16-1/12*B66-1/12*D11-1/18*B61-1/12*D21-1/12*A62, -1/18*D11-
1/12*D21-1/18*D22-1/12*D12-1/12*B62-1/12*B61-1/18*A66-1/12*B26-1/12*B16, 1/18*B21-
1/9*D16+1/12*B11-1/12*D26-1/9*B62+1/12*A61-1/6*B66-1/6*D12-1/12*D22, -1/9*B12-
1/12*B22+1/18*D26+1/12*D16+1/12*B66-1/6*A62-1/9*B61-1/12*D21-1/6*D11, -1/9*D11-
1/12*D21+1/18*D22+1/12*D12+1/12*B62-1/6*B61-1/9*A66-1/12*B26-1/6*B16]
[-2/9*A11+1/6*B61+1/9*D66-1/6*B16+1/9*D22+1/6*B21+1/12*D62+1/12*D26-
1/6*B12, -2/9*B16-1/6*A12+1/9*B62+1/6*D66+1/6*D26+1/12*B22+1/12*D61+1/9*D21-1/6*B11,
-2/9*B12-1/6*B11+1/9*D61+1/6*D62+1/6*D22+1/9*B26+1/12*D21-1/6*A16+1/12*B66,
2/9*A11-1/6*B61+2/9*D66-1/6*B16+2/9*D22-1/6*B21+1/6*D62+1/6*D26-1/6*B12, 2/9*B16-
1/6*A12+2/9*B62-1/6*D66-1/6*D26+1/6*B22+1/6*D61+2/9*D21-1/6*B11, 2/9*B12-
1/6*B11+2/9*D61-1/6*D62-1/6*D22+2/9*B26+1/6*D21-1/6*A16+1/6*B66, 1/9*A11-1/6*B61-
2/9*D66+1/6*B16+1/9*D22-1/12*B21+1/6*D62-1/6*D26-1/12*B12, 1/9*B16+1/6*A12-2/9*B62-
1/6*D66-1/12*D26-1/6*B22+1/6*D61+1/9*D21-1/12*B11, 1/9*B12+1/6*B11-2/9*D61-1/6*D62-
1/12*D22+1/9*B26-1/6*D21-1/12*A16+1/6*B66, -1/9*A11+1/6*B61-
1/9*D66+1/6*B16+1/18*D22+1/12*B21+1/12*D62-1/12*D26-1/12*B12, -1/9*B16+1/6*A12-
1/9*B62+1/6*D66+1/12*D26-1/12*B22+1/12*D61+1/18*D21-1/12*B11, -1/9*B12+1/6*B11-
1/9*D61+1/6*D62+1/12*D22+1/18*B26-1/12*D21-1/12*A16+1/12*B66, -
1/9*A11+1/12*B61+1/18*D66-1/12*B16-1/9*D22+1/6*B21-1/12*D62+1/12*D26+1/6*B12, -
1/9*B16-1/12*A12+1/18*B62+1/12*D66+1/6*D26+1/12*B22-1/12*D61-1/9*D21+1/6*B11, -
1/9*B12-1/12*B11+1/18*D61+1/12*D62+1/6*D22-1/9*B26+1/12*D21+1/6*A16-1/12*B66,

1/9*A11-1/12*B61+1/9*D66-1/12*B16-2/9*D22-1/6*B21-1/6*D62+1/6*D26+1/6*B12, 1/9*B16-
1/12*A12+1/9*B62-1/12*D66-1/6*D26+1/6*B22-1/6*D61-2/9*D21+1/6*B11, 1/9*B12-
1/12*B11+1/9*D61-1/12*D62-1/6*D22-2/9*B26+1/6*D21+1/6*A16-1/6*B66, 1/18*A11-1/12*B61-
1/9*D66+1/12*B16-1/9*D22-1/12*B21-1/6*D62-1/6*D26+1/12*B12, 1/18*B16+1/12*A12-1/9*B62-
1/12*D66-1/12*D26-1/6*B22-1/6*D61-1/9*D21+1/12*B11, 1/18*B12+1/12*B11-1/9*D61-1/12*D62-
1/12*D22-1/9*B26-1/6*D21+1/12*A16-1/6*B66, -1/18*A11+1/12*B61-1/18*D66+1/12*B16-
1/18*D22+1/12*B21-1/12*D62-1/12*D26+1/12*B12, -1/18*B16+1/12*A12-
1/18*B62+1/12*D66+1/12*D26-1/12*B22-1/12*D61-1/18*D21+1/12*B11, -1/18*B12+1/12*B11-
1/18*D61+1/12*D62+1/12*D22-1/18*B26-1/12*D21+1/12*A16-1/12*B66]

[1/6*A21-2/9*B61+1/9*B26-1/6*D66+1/9*D12+1/6*B11+1/12*B22+1/12*D16-
1/6*D62, -2/9*D66+1/9*A22-1/6*B62+1/6*B26+1/6*D16+1/12*B12+1/12*B21+1/9*D11-1/6*D61,
-2/9*D62+1/9*B21-1/6*D61+1/6*B22+1/6*D12+1/12*A26+1/12*D11+1/9*B16-1/6*B66, -
1/6*A21+2/9*B61+2/9*B26-1/6*D66+2/9*D12-1/6*B11+1/6*B22+1/6*D16-1/6*D62,
2/9*D66+2/9*A22-1/6*B62-1/6*B26-1/6*D16+1/6*B12+1/6*B21+2/9*D11-1/6*D61,
2/9*D62+2/9*B21-1/6*D61-1/6*B22-1/6*D12+1/6*A26+1/6*D11+2/9*B16-1/6*B66, -
1/6*A21+1/9*B61-2/9*B26+1/6*D66+1/9*D12-1/12*B11+1/6*B22-1/6*D16-1/12*D62, 1/9*D66-
2/9*A22+1/6*B62-1/6*B26-1/12*D16-1/6*B12+1/6*B21+1/9*D11-1/12*D61, 1/9*D62-
2/9*B21+1/6*D61-1/6*B22-1/12*D12+1/6*A26-1/6*D11+1/9*B16-1/12*B66, 1/6*A21-1/9*B61-
1/9*B26+1/6*D66+1/18*D12+1/12*B11+1/12*B22-1/12*D16-1/12*D62, -1/9*D66-
1/9*A22+1/6*B62+1/6*B26+1/12*D16-1/12*B12+1/12*B21+1/18*D11-1/12*D61, -1/9*D62-
1/9*B21+1/6*D61+1/6*B22+1/12*D12+1/12*A26-1/12*D11+1/18*B16-1/12*B66, 1/12*A21-
1/9*B61+1/18*B26-1/12*D66-1/9*D12+1/6*B11-1/12*B22+1/12*D16+1/6*D62, -
1/9*D66+1/18*A22-1/12*B62+1/12*B26+1/6*D16+1/12*B12-1/12*B21-1/9*D11+1/6*D61, -
1/9*D62+1/18*B21-1/12*D61+1/12*B22+1/6*D12-1/12*A26+1/12*D11-1/9*B16+1/6*B66, -
1/12*A21+1/9*B61+1/9*B26-1/12*D66-2/9*D12-1/6*B11-1/6*B22+1/6*D16+1/6*D62,
1/9*D66+1/9*A22-1/12*B62-1/12*B26-1/6*D16+1/6*B12-1/6*B21-2/9*D11+1/6*D61,
1/9*D62+1/9*B21-1/12*D61-1/12*B22-1/6*D12-1/6*A26+1/6*D11-2/9*B16+1/6*B66, -
1/12*A21+1/18*B61-1/9*B26+1/12*D66-1/9*D12-1/12*B11-1/6*B22-1/6*D16+1/12*D62,
1/18*D66-1/9*A22+1/12*B62-1/12*B26-1/12*D16-1/6*B12-1/6*B21-1/9*D11+1/12*D61, 1/18*D62-
1/9*B21+1/12*D61-1/12*B22-1/12*D12-1/6*A26-1/6*D11-1/9*B16+1/12*B66, 1/12*A21-1/18*B61-
1/18*B26+1/12*D66-1/18*D12+1/12*B11-1/12*B22-1/12*D16+1/12*D62, -1/18*D66-
1/18*A22+1/12*B62+1/12*B26+1/12*D16-1/12*B12-1/12*B21-1/18*D11+1/12*D61, -1/18*D62-
1/18*B21+1/12*D61+1/12*B22+1/12*D12-1/12*A26-1/12*D11-1/18*B16+1/12*B66]

[1/6*B11-2/9*B21+1/9*D16-1/6*D26+1/9*B62+1/6*A61+1/12*D12+1/12*B66-
1/6*D22, -2/9*D26+1/9*B12-1/6*B22+1/6*D16+1/6*B66+1/12*A62+1/12*D11+1/9*B61-1/6*D21,
-2/9*D22+1/9*D11-1/6*D21+1/6*D12+1/6*B62+1/12*B16+1/12*B61+1/9*A66-1/6*B26, -
1/6*B11+2/9*B21+2/9*D16-1/6*D26+2/9*B62-1/6*A61+1/6*D12+1/6*B66-1/6*D22,
2/9*D26+2/9*B12-1/6*B22-1/6*D16-1/6*B66+1/6*A62+1/6*D11+2/9*B61-1/6*D21,
2/9*D22+2/9*D11-1/6*D21-1/6*D12-1/6*B62+1/6*B16+1/6*B61+2/9*A66-1/6*B26, -
1/6*B11+1/9*B21-2/9*D16+1/6*D26+1/9*B62-1/12*A61+1/6*D12-1/6*B66-1/12*D22, 1/9*D26-
2/9*B12+1/6*B22-1/6*D16-1/12*B66-1/6*A62+1/6*D11+1/9*B61-1/12*D21, 1/9*D22-
2/9*D11+1/6*D21-1/6*D12-1/12*B62+1/6*B16-1/6*B61+1/9*A66-1/12*B26, 1/6*B11-1/9*B21-
1/9*D16+1/6*D26+1/18*B62+1/12*A61+1/12*D12-1/12*B66-1/12*D22, -1/9*D26-
1/9*B12+1/6*B22+1/6*D16+1/12*B66-1/12*A62+1/12*D11+1/18*B61-1/12*D21, -1/9*D22-
1/9*D11+1/6*D21+1/6*D12+1/12*B62+1/12*B16-1/12*B61+1/18*A66-1/12*B26, 1/12*B11-
1/9*B21+1/18*D16-1/12*D26-1/9*B62+1/6*A61-1/12*D12+1/12*B66+1/6*D22, -
1/9*D26+1/18*B12-1/12*B22+1/12*D16+1/6*B66+1/12*A62-1/12*D11-1/9*B61+1/6*D21, -
1/9*D22+1/18*D11-1/12*D21+1/12*D12+1/6*B62-1/12*B16+1/12*B61-1/9*A66+1/6*B26, -
1/12*B11+1/9*B21+1/9*D16-1/12*D26-2/9*B62-1/6*A61-1/6*D12+1/6*B66+1/6*D22,
1/9*D26+1/9*B12-1/12*B22-1/12*D16-1/6*B66+1/6*A62-1/6*D11-2/9*B61+1/6*D21,
1/9*D22+1/9*D11-1/12*D21-1/12*D12-1/6*B62-1/6*B16+1/6*B61-2/9*A66+1/6*B26, -
1/12*B11+1/18*B21-1/9*D16+1/12*D26-1/9*B62-1/12*A61-1/6*D12-1/6*B66+1/12*D22,
1/18*D26-1/9*B12+1/12*B22-1/12*D16-1/12*B66-1/6*A62-1/6*D11-1/9*B61+1/12*D21, 1/18*D22-

1/9*D11+1/12*D21-1/12*D12-1/12*B62-1/6*B16-1/6*B61-1/9*A66+1/12*B26, 1/12*B11-1/18*B21-1/18*D16+1/12*D26-1/18*B62+1/12*A61-1/12*D12-1/12*B66+1/12*D22, -1/18*D26-1/18*B12+1/12*B22+1/12*D16+1/12*B66-1/12*A62-1/12*D11-1/18*B61+1/12*D21, -1/18*D22-1/18*D11+1/12*D21+1/12*D12+1/12*B62-1/12*B16-1/12*B61-1/18*A66+1/12*B26]

[-1/9*D66-1/9*A11-1/6*B61-1/6*B16+1/18*D22+1/12*B21-1/12*D62+1/12*D26-1/12*B12, -1/9*B62-1/6*A12-1/9*B16-1/6*D66+1/12*D26-1/12*D61+1/18*D21-1/12*B11+1/12*B22, -1/9*D61-1/6*B11-1/9*B12-1/6*D62+1/12*D22+1/18*B26+1/12*D21-1/12*A16-1/12*B66, 1/9*A11-2/9*D66+1/6*B61-1/6*B16+1/9*D22-1/12*B21+1/6*D26-1/12*B12-1/6*D62, -2/9*B62-1/6*A12+1/9*B16+1/6*D66-1/12*D26+1/6*B22+1/9*D21-1/12*B11-1/6*D61, -2/9*D61-1/6*B11+1/9*B12+1/6*D62-1/12*D22+1/9*B26+1/6*D21-1/12*A16-1/6*B66, 2/9*D66+2/9*A11+1/6*B61+1/6*B16+2/9*D22-1/6*B21-1/6*D62-1/6*D26-1/6*B12, 2/9*B62+1/6*A12+2/9*B16+1/6*D66-1/6*D26-1/6*D61+2/9*D21-1/6*B11-1/6*B22, 2/9*D61+1/6*B11+2/9*B12+1/6*D62-1/6*D22+2/9*B26-1/6*D21-1/6*A16-1/6*B66, -2/9*A11+1/9*D66-1/6*B61+1/6*B16+1/9*D22+1/6*B21-1/12*D26-1/6*B12-1/12*D62, 1/9*B62+1/6*A12-2/9*B16-1/6*D66+1/6*D26-1/12*D61+1/9*D21-1/6*B11-1/12*B22, 1/9*D61+1/6*B11-2/9*B12-1/6*D62+1/6*D22-1/12*D21-1/6*A16+1/9*B26-1/12*B66, -1/18*A11-1/18*D66-1/12*B61-1/12*B16-1/18*D22+1/12*B21+1/12*D26+1/12*B12+1/12*D62, -1/18*B62-1/12*A12-1/18*B16-1/12*D66+1/12*D26+1/12*B22-1/18*D21+1/12*B11+1/12*D61, -1/18*D61-1/12*B11-1/18*B12-1/12*D62+1/12*D22+1/12*D21+1/12*A16-1/18*B26+1/12*B66, -1/9*D66+1/18*A11+1/12*B61-1/12*B16-1/9*D22-1/12*B21+1/6*D62+1/6*D26+1/12*B12, -1/9*B62-1/12*A12+1/18*B16+1/12*D66-1/12*D26+1/6*B22-1/9*D21+1/12*B11+1/6*D61, -1/9*D61-1/12*B11+1/18*B12+1/12*D62-1/12*D22-1/9*B26+1/6*D21+1/12*A16+1/6*B66, 1/9*A11+1/9*D66+1/12*B61+1/12*B16-2/9*D22-1/6*B21-1/6*D26+1/6*B12+1/6*D62, 1/9*B62+1/12*A12+1/9*B16+1/12*D66-1/6*D26-1/6*B22-2/9*D21+1/6*B11+1/6*D61, 1/9*D61+1/12*B11+1/9*B12+1/12*D62-1/6*D22-1/6*D21+1/6*A16-2/9*B26+1/6*B66, 1/18*D66-1/9*A11-1/12*B61+1/12*B16-1/9*D22+1/6*B21+1/12*D62-1/12*D26+1/6*B12, 1/18*B62+1/12*A12-1/9*B16-1/12*D66+1/6*D26+1/12*D61-1/9*D21+1/6*B11-1/12*B22, 1/18*D61+1/12*B11-1/9*B12-1/12*D62+1/6*D22-1/12*D21+1/6*A16-1/9*B26+1/12*B66]

[-1/9*B26-1/6*A21-1/9*B61-1/6*D66+1/18*D12+1/12*B11-1/12*B22+1/12*D16-1/12*D62, -1/9*A22-1/6*B62-1/9*D66-1/6*B26+1/12*D16+1/12*B12+1/18*D11-1/12*D61-1/12*B21, -1/9*B21-1/6*D61-1/9*D62-1/6*B22+1/12*D12+1/12*D11+1/18*B16-1/12*B66-1/12*A26, 1/9*B61-2/9*B26+1/6*A21-1/6*D66+1/9*D12-1/12*B11+1/6*D16-1/6*B22-1/12*D62, -2/9*A22-1/6*B62+1/9*D66+1/6*B26-1/12*D16+1/6*B12+1/9*D11-1/12*D61-1/6*B21, -2/9*B21-1/6*D61+1/9*D62+1/6*B22-1/12*D12+1/6*D11+1/9*B16-1/12*B66-1/6*A26, 2/9*B26+1/6*A21+2/9*B61+1/6*D66+2/9*D12-1/6*B11-1/6*B22-1/6*D16-1/6*D62, 2/9*A22+1/6*B62+2/9*D66+1/6*B26-1/6*D16-1/6*B12+2/9*D11-1/6*D61-1/6*B21, 2/9*B21+1/6*D61+2/9*D62+1/6*B22-1/6*D12-1/6*D11+2/9*B16-1/6*B66-1/6*A26, -2/9*B61+1/9*B26-1/6*A21+1/6*D66+1/9*D12+1/6*B11-1/12*D16-1/12*B22-1/6*D62, 1/9*A22+1/6*B62-2/9*D66-1/6*B26+1/6*D16-1/12*B21+1/9*D11-1/6*D61-1/12*B12, 1/9*B21+1/6*D61-2/9*D62-1/6*B22+1/6*D12-1/12*D11+1/9*B16-1/6*B66-1/12*A26, -1/18*B61-1/18*B26-1/12*A21-1/12*D66-1/18*D12+1/12*B11+1/12*D16+1/12*B22+1/12*D62, -1/18*A22-1/12*B62-1/18*D66-1/12*B26+1/12*D16+1/12*B21-1/18*D11+1/12*D61+1/12*B12, -1/18*B21-1/12*D61-1/18*D62-1/12*B22+1/12*D12+1/12*D11-1/18*B16+1/12*B66+1/12*A26, -1/9*B26+1/12*A21+1/18*B61-1/12*D66-1/9*D12-1/12*B11+1/6*B22+1/6*D16+1/12*D62, -1/9*A22-1/12*B62+1/18*D66+1/12*B26-1/12*D16+1/6*B12-1/9*D11+1/12*D61+1/6*B21, -1/9*B21-1/12*D61+1/18*D62+1/12*B22-1/12*D12+1/6*D11-1/9*B16+1/12*B66+1/6*A26, 1/9*B61+1/9*B26+1/12*A21+1/12*D66-2/9*D12-1/6*B11-1/6*D16+1/6*B22+1/6*D62, 1/9*A22+1/12*B62+1/9*D66+1/12*B26-1/6*D16+1/6*B21-2/9*D11+1/6*D61-1/6*B12, 1/9*B21+1/12*D61+1/9*D62+1/12*B22-1/6*D12-1/6*D11-2/9*B16+1/6*B66+1/6*A26, 1/18*B26-1/12*A21-1/9*B61+1/12*D66-1/9*D12+1/6*B11+1/12*B22-1/12*D16+1/6*D62, 1/18*A22+1/12*B62-1/9*D66-1/12*B26+1/6*D16+1/12*B21-1/9*D11+1/6*D61-1/12*B12, 1/18*B21+1/12*D61-1/9*D62-1/12*B22+1/6*D12-1/12*D11-1/9*B16+1/6*B66+1/12*A26]

[-1/9*D16-1/6*B11-1/9*B21-1/6*D26+1/18*B62+1/12*A61-1/12*D12+1/12*B66-
1/12*D22, -1/9*B12-1/6*B22-1/9*D26-1/6*D16+1/12*B66+1/12*A62+1/18*B61-1/12*D21-
1/12*D11, -1/9*D11-1/6*D21-1/9*D22-1/6*D12+1/12*B62+1/12*B61+1/18*A66-1/12*B26-
1/12*B16, 1/9*B21-2/9*D16+1/6*B11-1/6*D26+1/9*B62-1/12*A61+1/6*B66-1/6*D12-1/12*D22,
-2/9*B12-1/6*B22+1/9*D26+1/6*D16-1/12*B66+1/6*A62+1/9*B61-1/12*D21-1/6*D11, -2/9*D11-
1/6*D21+1/9*D22+1/6*D12-1/12*B62+1/6*B61+1/9*A66-1/12*B26-1/6*B16,
2/9*D16+1/6*B11+2/9*B21+1/6*D26+2/9*B62-1/6*A61-1/6*D12-1/6*B66-1/6*D22,
2/9*B12+1/6*B22+2/9*D26+1/6*D16-1/6*B66-1/6*A62+2/9*B61-1/6*D21-1/6*D11,
2/9*D11+1/6*D21+2/9*D22+1/6*D12-1/6*B62-1/6*B61+2/9*A66-1/6*B26-1/6*B16, -
2/9*B21+1/9*D16-1/6*B11+1/6*D26+1/9*B62+1/6*A61-1/12*B66-1/12*D12-1/6*D22,
1/9*B12+1/6*B22-2/9*D26-1/6*D16+1/6*B66-1/12*D11+1/9*B61-1/6*D21-1/12*A62,
1/9*D11+1/6*D21-2/9*D22-1/6*D12+1/6*B62-1/12*B61+1/9*A66-1/6*B26-1/12*B16, -1/18*B21-
1/18*D16-1/12*B11-1/12*D26-1/18*B62+1/12*A61+1/12*B66+1/12*D12+1/12*D22, -1/18*B12-
1/12*B22-1/18*D26-1/12*D16+1/12*B66+1/12*D11-1/18*B61+1/12*D21+1/12*A62, -1/18*D11-
1/12*D21-1/18*D22-1/12*D12+1/12*B62+1/12*B61-1/18*A66+1/12*B26+1/12*B16, -
1/9*D16+1/12*B11+1/18*B21-1/12*D26-1/9*B62-1/12*A61+1/6*D12+1/6*B66+1/12*D22, -
1/9*B12-1/12*B22+1/18*D26+1/12*D16-1/12*B66+1/6*A62-1/9*B61+1/12*D21+1/6*D11, -
1/9*D11-1/12*D21+1/18*D22+1/12*D12-1/12*B62+1/6*B61-1/9*A66+1/12*B26+1/6*B16,
1/9*B21+1/9*D16+1/12*B11+1/12*D26-2/9*B62-1/6*A61-1/6*B66+1/6*D12+1/6*D22,
1/9*B12+1/12*B22+1/9*D26+1/12*D16-1/6*B66+1/6*D11-2/9*B61+1/6*D21-1/6*A62,
1/9*D11+1/12*D21+1/9*D22+1/12*D12-1/6*B62-1/6*B61-2/9*A66+1/6*B26+1/6*B16, 1/18*D16-
1/12*B11-1/9*B21+1/12*D26-1/9*B62+1/6*A61+1/12*D12-1/12*B66+1/6*D22,
1/18*B12+1/12*B22-1/9*D26-1/12*D16+1/6*B66+1/12*D11-1/9*B61+1/6*D21-1/12*A62,
1/18*D11+1/12*D21-1/9*D22-1/12*D12+1/6*B62-1/12*B61-1/9*A66+1/6*B26+1/12*B16]
[1/9*A11-1/6*B61-2/9*D66+1/6*B16+1/9*D22+1/12*B21-
1/6*D62+1/6*D26+1/12*B12, 1/9*B16+1/6*A12-2/9*B62-1/6*D66+1/12*D26+1/6*B22-
1/6*D61+1/9*D21+1/12*B11, 1/9*B12+1/6*B11-2/9*D61-
1/6*D62+1/12*D22+1/9*B26+1/6*D21+1/12*A16-1/6*B66, -1/9*A11+1/6*B61-
1/9*D66+1/6*B16+1/18*D22-1/12*B21-1/12*D62+1/12*D26+1/12*B12, -1/9*B16+1/6*A12-
1/9*B62+1/6*D66-1/12*D26+1/12*B22-1/12*D61+1/18*D21+1/12*B11, -1/9*B12+1/6*B11-
1/9*D61+1/6*D62-1/12*D22+1/18*B26+1/12*D21+1/12*A16-1/12*B66, -
2/9*A11+1/6*B61+1/9*D66-1/6*B16+1/9*D22-1/6*B21-1/12*D62-1/12*D26+1/6*B12, -2/9*B16-
1/6*A12+1/9*B62+1/6*D66-1/6*D26-1/12*B22-1/12*D61+1/9*D21+1/6*B11, -2/9*B12-
1/6*B11+1/9*D61+1/6*D62-1/6*D22+1/9*B26-1/12*D21+1/6*A16-1/12*B66, 2/9*A11-
1/6*B61+2/9*D66-1/6*B16+2/9*D22+1/6*B21-1/6*D62-1/6*D26+1/6*B12, 2/9*B16-
1/6*A12+2/9*B62-1/6*D66+1/6*D26-1/6*B22-1/6*D61+2/9*D21+1/6*B11, 2/9*B12-
1/6*B11+2/9*D61-1/6*D62+1/6*D22+2/9*B26-1/6*D21+1/6*A16-1/6*B66, 1/18*A11-1/12*B61-
1/9*D66+1/12*B16-1/9*D22+1/12*B21+1/6*D62+1/6*D26-1/12*B12, 1/18*B16+1/12*A12-1/9*B62-
1/12*D66+1/12*D26+1/6*B22+1/6*D61-1/9*D21-1/12*B11, 1/18*B12+1/12*B11-1/9*D61-
1/12*D62+1/12*D22-1/9*B26+1/6*D21-1/12*A16+1/6*B66, -1/18*A11+1/12*B61-
1/18*D66+1/12*B16-1/18*D22-1/12*B21+1/12*D62+1/12*D26-1/12*B12, -1/18*B16+1/12*A12-
1/18*B62+1/12*D66-1/12*D26+1/12*B22+1/12*D61-1/18*D21-1/12*B11, -1/18*B12+1/12*B11-
1/18*D61+1/12*D62-1/12*D22-1/18*B26+1/12*D21-1/12*A16+1/12*B66, -
1/9*A11+1/12*B61+1/18*D66-1/12*B16-1/9*D22-1/6*B21+1/12*D62-1/12*D26-1/6*B12, -1/9*B16-
1/12*A12+1/18*B62+1/12*D66-1/6*D26-1/12*B22+1/12*D61-1/9*D21-1/6*B11, -1/9*B12-
1/12*B11+1/18*D61+1/12*D62-1/6*D22-1/9*B26-1/12*D21-1/6*A16+1/12*B66, 1/9*A11-
1/12*B61+1/9*D66-1/12*B16-2/9*D22+1/6*B21+1/6*D62-1/6*D26-1/6*B12, 1/9*B16-
1/12*A12+1/9*B62-1/12*D66+1/6*D26-1/6*B22+1/6*D61-2/9*D21-1/6*B11, 1/9*B12-
1/12*B11+1/9*D61-1/12*D62+1/6*D22-2/9*B26-1/6*D21-1/6*A16+1/6*B66]
[-1/6*A21+1/9*B61-2/9*B26+1/6*D66+1/9*D12+1/12*B11-
1/6*B22+1/6*D16+1/12*D62, 1/9*D66-2/9*A22+1/6*B62-1/6*B26+1/12*D16+1/6*B12-
1/6*B21+1/9*D11+1/12*D61, 1/9*D62-2/9*B21+1/6*D61-1/6*B22+1/12*D12-
1/6*A26+1/6*D11+1/9*B16+1/12*B66, 1/6*A21-1/9*B61-1/9*B26+1/6*D66+1/18*D12-1/12*B11-

1/12*B22+1/12*D16+1/12*D62, -1/9*D66-1/9*A22+1/6*B62+1/6*B26-1/12*D16+1/12*B12-
1/12*B21+1/18*D11+1/12*D61, -1/9*D62-1/9*B21+1/6*D61+1/6*B22-1/12*D12-
1/12*A26+1/12*D11+1/18*B16+1/12*B66, 1/6*A21-2/9*B61+1/9*B26-1/6*D66+1/9*D12-
1/6*B11-1/12*B22-1/12*D16+1/6*D62, -2/9*D66+1/9*A22-1/6*B62+1/6*B26-1/6*D16-1/12*B12-
1/12*B21+1/9*D11+1/6*D61, -2/9*D62+1/9*B21-1/6*D61+1/6*B22-1/6*D12-1/12*A26-
1/12*D11+1/9*B16+1/6*B66, -1/6*A21+2/9*B61+2/9*B26-1/6*D66+2/9*D12+1/6*B11-1/6*B22-
1/6*D16+1/6*D62, 2/9*D66+2/9*A22-1/6*B62-1/6*B26+1/6*D16-1/6*B12-
1/6*B21+2/9*D11+1/6*D61, 2/9*D62+2/9*B21-1/6*D61-1/6*B22+1/6*D12-1/6*A26-
1/6*D11+2/9*B16+1/6*B66, -1/12*A21+1/18*B61-1/9*B26+1/12*D66-
1/9*D12+1/12*B11+1/6*B22+1/6*D16-1/12*D62, 1/18*D66-1/9*A22+1/12*B62-
1/12*B26+1/12*D16+1/6*B12+1/6*B21-1/9*D11-1/12*D61, 1/18*D62-1/9*B21+1/12*D61-
1/12*B22+1/12*D12+1/6*A26+1/6*D11-1/9*B16-1/12*B66, 1/12*A21-1/18*B61-1/18*B26+1/12*D66-
1/18*D12-1/12*B11+1/12*B22+1/12*D16-1/12*D62, -1/18*D66-1/18*A22+1/12*B62+1/12*B26-
1/12*D16+1/12*B12+1/12*B21-1/18*D11-1/12*D61, -1/18*D62-1/18*B21+1/12*D61+1/12*B22-
1/12*D12+1/12*A26+1/12*D11-1/18*B16-1/12*B66, 1/12*A21-1/9*B61+1/18*B26-1/12*D66-
1/9*D12-1/6*B11+1/12*B22-1/12*D16-1/6*D62, -1/9*D66+1/18*A22-1/12*B62+1/12*B26-1/6*D16-
1/12*B12+1/12*B21-1/9*D11-1/6*D61, -1/9*D62+1/18*B21-1/12*D61+1/12*B22-
1/6*D12+1/12*A26-1/12*D11-1/9*B16-1/6*B66, -1/12*A21+1/9*B61+1/9*B26-1/12*D66-
2/9*D12+1/6*B11+1/6*B22-1/6*D16-1/6*D62, 1/9*D66+1/9*A22-1/12*B62-1/12*B26+1/6*D16-
1/6*B12+1/6*B21-2/9*D11-1/6*D61, 1/9*D62+1/9*B21-1/12*D61-1/12*B22+1/6*D12+1/6*A26-
1/6*D11-2/9*B16-1/6*B66]

[-1/6*B11+1/9*B21-2/9*D16+1/6*D26+1/9*B62+1/12*A61-
1/6*D12+1/6*B66+1/12*D22, 1/9*D26-2/9*B12+1/6*B22-1/6*D16+1/12*B66+1/6*A62-
1/6*D11+1/9*B61+1/12*D21, 1/9*D22-2/9*D11+1/6*D21-1/6*D12+1/12*B62-
1/6*B16+1/6*B61+1/9*A66+1/12*B26, 1/6*B11-1/9*B21-1/9*D16+1/6*D26+1/18*B62-1/12*A61-
1/12*D12+1/12*B66+1/12*D22, -1/9*D26-1/9*B12+1/6*B22+1/6*D16-1/12*B66+1/12*A62-
1/12*D11+1/18*B61+1/12*D21, -1/9*D22-1/9*D11+1/6*D21+1/6*D12-1/12*B62-
1/12*B16+1/12*B61+1/18*A66+1/12*B26, 1/6*B11-2/9*B21+1/9*D16-1/6*D26+1/9*B62-
1/6*A61-1/12*D12-1/12*B66+1/6*D22, -2/9*D26+1/9*B12-1/6*B22+1/6*D16-1/6*B66-1/12*A62-
1/12*D11+1/9*B61+1/6*D21, -2/9*D22+1/9*D11-1/6*D21+1/6*D12-1/6*B62-1/12*B16-
1/12*B61+1/9*A66+1/6*B26, -1/6*B11+2/9*B21+2/9*D16-1/6*D26+2/9*B62+1/6*A61-1/6*D12-
1/6*B66+1/6*D22, 2/9*D26+2/9*B12-1/6*B22-1/6*D16+1/6*B66-1/6*A62-
1/6*D11+2/9*B61+1/6*D21, 2/9*D22+2/9*D11-1/6*D21-1/6*D12+1/6*B62-1/6*B16-
1/6*B61+2/9*A66+1/6*B26, -1/12*B11+1/18*B21-1/9*D16+1/12*D26-
1/9*B62+1/12*A61+1/6*D12+1/6*B66-1/12*D22, 1/18*D26-1/9*B12+1/12*B22-
1/12*D16+1/12*B66+1/6*A62+1/6*D11-1/9*B61-1/12*D21, 1/18*D22-1/9*D11+1/12*D21-
1/12*D12+1/12*B62+1/6*B16+1/6*B61-1/9*A66-1/12*B26, 1/12*B11-1/18*B21-1/18*D16+1/12*D26-
1/18*B62-1/12*A61+1/12*D12+1/12*B66-1/12*D22, -1/18*D26-1/18*B12+1/12*B22+1/12*D16-
1/12*B66+1/12*A62+1/12*D11-1/18*B61-1/12*D21, -1/18*D22-1/18*D11+1/12*D21+1/12*D12-
1/12*B62+1/12*B16+1/12*B61-1/18*A66-1/12*B26, 1/12*B11-1/9*B21+1/18*D16-1/12*D26-
1/9*B62-1/6*A61+1/12*D12-1/12*B66-1/6*D22, -1/9*D26+1/18*B12-1/12*B22+1/12*D16-1/6*B66-
1/12*A62+1/12*D11-1/9*B61-1/6*D21, -1/9*D22+1/18*D11-1/12*D21+1/12*D12-
1/6*B62+1/12*B16-1/12*B61-1/9*A66-1/6*B26, -1/12*B11+1/9*B21+1/9*D16-1/12*D26-
2/9*B62+1/6*A61+1/6*D12-1/6*B66-1/6*D22, 1/9*D26+1/9*B12-1/12*B22-1/12*D16+1/6*B66-
1/6*A62+1/6*D11-2/9*B61-1/6*D21, 1/9*D22+1/9*D11-1/12*D21-1/12*D12+1/6*B62+1/6*B16-
1/6*B61-2/9*A66-1/6*B26]

[1/9*A11+1/9*D66+1/12*B61+1/12*B16-2/9*D22-1/6*B21-
1/6*D26+1/6*B12+1/6*D62, 1/9*B62+1/12*A12+1/9*B16+1/12*D66-1/6*D26-1/6*B22-
2/9*D21+1/6*B11+1/6*D61, 1/9*D61+1/12*B11+1/9*B12+1/12*D62-1/6*D22-1/6*D21+1/6*A16-
2/9*B26+1/6*B66, 1/18*D66-1/9*A11-1/12*B61+1/12*B16-1/9*D22+1/6*B21+1/12*D62-
1/12*D26+1/6*B12, 1/18*B62+1/12*A12-1/9*B16-1/12*D66+1/6*D26+1/12*D61-1/9*D21+1/6*B11-
1/12*B22, 1/18*D61+1/12*B11-1/9*B12-1/12*D62+1/6*D22-1/12*D21+1/6*A16-
1/9*B26+1/12*B66, -1/18*A11-1/18*D66-1/12*B61-1/12*B16-

1/18*D22+1/12*B21+1/12*D26+1/12*B12+1/12*D62, -1/18*B62-1/12*A12-1/18*B16-
1/12*D66+1/12*D26+1/12*B22-1/18*D21+1/12*B11+1/12*D61, -1/18*D61-1/12*B11-1/18*B12-
1/12*D62+1/12*D22+1/12*D21+1/12*A16-1/18*B26+1/12*B66, -1/9*D66+1/18*A11+1/12*B61-
1/12*B16-1/9*D22-1/12*B21+1/6*D62+1/6*D26+1/12*B12, -1/9*B62-
1/12*A12+1/18*B16+1/12*D66-1/12*D26+1/6*B22-1/9*D21+1/12*B11+1/6*D61, -1/9*D61-
1/12*B11+1/18*B12+1/12*D62-1/12*D22-1/9*B26+1/6*D21+1/12*A16+1/6*B66,
2/9*D66+2/9*A11+1/6*B61+1/6*B16+2/9*D22-1/6*B21-1/6*D62-1/6*D26-1/6*B12,
2/9*B62+1/6*A12+2/9*B16+1/6*D66-1/6*D26-1/6*D61+2/9*D21-1/6*B11-1/6*B22,
2/9*D61+1/6*B11+2/9*B12+1/6*D62-1/6*D22+2/9*B26-1/6*D21-1/6*A16-1/6*B66, -
2/9*A11+1/9*D66-1/6*B61+1/6*B16+1/9*D22+1/6*B21-1/12*D26-1/6*B12-1/12*D62,
1/9*B62+1/6*A12-2/9*B16-1/6*D66+1/6*D26-1/12*D61+1/9*D21-1/6*B11-1/12*B22,
1/9*D61+1/6*B11-2/9*B12-1/6*D62+1/6*D22-1/12*D21-1/6*A16+1/9*B26-1/12*B66, -1/9*D66-
1/9*A11-1/6*B61-1/6*B16+1/18*D22+1/12*B21-1/12*D62+1/12*D26-1/12*B12, -1/9*B62-1/6*A12-
1/9*B16-1/6*D66+1/12*D26-1/12*D61+1/18*D21-1/12*B11+1/12*B22, -1/9*D61-1/6*B11-1/9*B12-
1/6*D62+1/12*D22+1/18*B26+1/12*D21-1/12*A16-1/12*B66, 1/9*A11-2/9*D66+1/6*B61-
1/6*B16+1/9*D22-1/12*B21+1/6*D26-1/12*B12-1/6*D62, -2/9*B62-1/6*A12+1/9*B16+1/6*D66-
1/12*D26+1/6*B22+1/9*D21-1/12*B11-1/6*D61, -2/9*D61-1/6*B11+1/9*B12+1/6*D62-
1/12*D22+1/9*B26+1/6*D21-1/12*A16-1/6*B66]
[1/9*B61+1/9*B26+1/12*A21+1/12*D66-2/9*D12-1/6*B11-
1/6*D16+1/6*B22+1/6*D62, 1/9*A22+1/12*B62+1/9*D66+1/12*B26-1/6*D16+1/6*B21-
2/9*D11+1/6*D61-1/6*B12, 1/9*B21+1/12*D61+1/9*D62+1/12*B22-1/6*D12-1/6*D11-
2/9*B16+1/6*B66+1/6*A26, 1/18*B26-1/12*A21-1/9*B61+1/12*D66-1/9*D12+1/6*B11+1/12*B22-
1/12*D16+1/6*D62, 1/18*A22+1/12*B62-1/9*D66-1/12*B26+1/6*D16+1/12*B21-
1/9*D11+1/6*D61-1/12*B12, 1/18*B21+1/12*D61-1/9*D62-1/12*B22+1/6*D12-1/12*D11-
1/9*B16+1/6*B66+1/12*A26, -1/18*B61-1/18*B26-1/12*A21-1/12*D66-
1/18*D12+1/12*B11+1/12*D16+1/12*B22+1/12*D62, -1/18*A22-1/12*B62-1/18*D66-
1/12*B26+1/12*D16+1/12*B21-1/18*D11+1/12*D61+1/12*B12, -1/18*B21-1/12*D61-1/18*D62-
1/12*B22+1/12*D12+1/12*D11-1/18*B16+1/12*B66+1/12*A26, -1/9*B26+1/12*A21+1/18*B61-
1/12*D66-1/9*D12-1/12*B11+1/6*B22+1/6*D16+1/12*D62, -1/9*A22-
1/12*B62+1/18*D66+1/12*B26-1/12*D16+1/6*B12-1/9*D11+1/12*D61+1/6*B21, -1/9*B21-
1/12*D61+1/18*D62+1/12*B22-1/12*D12+1/6*D11-1/9*B16+1/12*B66+1/6*A26,
2/9*B26+1/6*A21+2/9*B61+1/6*D66+2/9*D12-1/6*B11-1/6*B22-1/6*D16-1/6*D62,
2/9*A22+1/6*B62+2/9*D66+1/6*B26-1/6*D16-1/6*B12+2/9*D11-1/6*D61-1/6*B21,
2/9*B21+1/6*D61+2/9*D62+1/6*B22-1/6*D12-1/6*D11+2/9*B16-1/6*B66-1/6*A26, -
2/9*B61+1/9*B26-1/6*A21+1/6*D66+1/9*D12+1/6*B11-1/12*D16-1/12*B22-1/6*D62,
1/9*A22+1/6*B62-2/9*D66-1/6*B26+1/6*D16-1/12*B21+1/9*D11-1/6*D61-1/12*B12,
1/9*B21+1/6*D61-2/9*D62-1/6*B22+1/6*D12-1/12*D11+1/9*B16-1/6*B66-1/12*A26, -1/9*B26-
1/6*A21-1/9*B61-1/6*D66+1/18*D12+1/12*B11-1/12*B22+1/12*D16-1/12*D62, -1/9*A22-1/6*B62-
1/9*D66-1/6*B26+1/12*D16+1/12*B12+1/18*D11-1/12*D61-1/12*B21, -1/9*B21-1/6*D61-1/9*D62-
1/6*B22+1/12*D12+1/12*D11+1/18*B16-1/12*B66-1/12*A26, 1/9*B61-2/9*B26+1/6*A21-
1/6*D66+1/9*D12-1/12*B11+1/6*D16-1/6*B22-1/12*D62, -2/9*A22-1/6*B62+1/9*D66+1/6*B26-
1/12*D16+1/6*B12+1/9*D11-1/12*D61-1/6*B21, -2/9*B21-1/6*D61+1/9*D62+1/6*B22-
1/12*D12+1/6*D11+1/9*B16-1/12*B66-1/6*A26]
[1/9*B21+1/9*D16+1/12*B11+1/12*D26-2/9*B62-1/6*A61-
1/6*B66+1/6*D12+1/6*D22, 1/9*B12+1/12*B22+1/9*D26+1/12*D16-1/6*B66+1/6*D11-
2/9*B61+1/6*D21-1/6*A62, 1/9*D11+1/12*D21+1/9*D22+1/12*D12-1/6*B62-1/6*B61-
2/9*A66+1/6*B26+1/6*B16, 1/18*D16-1/12*B11-1/9*B21+1/12*D26-1/9*B62+1/6*A61+1/12*D12-
1/12*B66+1/6*D22, 1/18*B12+1/12*B22-1/9*D26-1/12*D16+1/6*B66+1/12*D11-1/9*B61+1/6*D21-
1/12*A62, 1/18*D11+1/12*D21-1/9*D22-1/12*D12+1/6*B62-1/12*B61-
1/9*A66+1/6*B26+1/12*B16, -1/18*B21-1/18*D16-1/12*B11-1/12*D26-
1/18*B62+1/12*A61+1/12*B66+1/12*D12+1/12*D22, -1/18*B12-1/12*B22-1/18*D26-
1/12*D16+1/12*B66+1/12*D11-1/18*B61+1/12*D21+1/12*A62, -1/18*D11-1/12*D21-1/18*D22-
1/12*D12+1/12*B62+1/12*B61-1/18*A66+1/12*B26+1/12*B16, -1/9*D16+1/12*B11+1/18*B21-

1/12*D26-1/9*B62-1/12*A61+1/6*D12+1/6*B66+1/12*D22, -1/9*B12-
1/12*B22+1/18*D26+1/12*D16-1/12*B66+1/6*A62-1/9*B61+1/12*D21+1/6*D11, -1/9*D11-
1/12*D21+1/18*D22+1/12*D12-1/12*B62+1/6*B61-1/9*A66+1/12*B26+1/6*B16,
2/9*D16+1/6*B11+2/9*B21+1/6*D26+2/9*B62-1/6*A61-1/6*D12-1/6*B66-1/6*D22,
2/9*B12+1/6*B22+2/9*D26+1/6*D16-1/6*B66-1/6*A62+2/9*B61-1/6*D21-1/6*D11,
2/9*D11+1/6*D21+2/9*D22+1/6*D12-1/6*B62-1/6*B61+2/9*A66-1/6*B26-1/6*B16, -
2/9*B21+1/9*D16-1/6*B11+1/6*D26+1/9*B62+1/6*A61-1/12*B66-1/12*D12-1/6*D22,
1/9*B12+1/6*B22-2/9*D26-1/6*D16+1/6*B66-1/12*D11+1/9*B61-1/6*D21-1/12*A62,
1/9*D11+1/6*D21-2/9*D22-1/6*D12+1/6*B62-1/12*B61+1/9*A66-1/6*B26-1/12*B16, -1/9*D16-
1/6*B11-1/9*B21-1/6*D26+1/18*B62+1/12*A61-1/12*D12+1/12*B66-1/12*D22, -1/9*B12-1/6*B22-
1/9*D26-1/6*D16+1/12*B66+1/12*A62+1/18*B61-1/12*D21-1/12*D11, -1/9*D11-1/6*D21-1/9*D22-
1/6*D12+1/12*B62+1/12*B61+1/18*A66-1/12*B26-1/12*B16, 1/9*B21-2/9*D16+1/6*B11-
1/6*D26+1/9*B62-1/12*A61+1/6*B66-1/6*D12-1/12*D22, -2/9*B12-1/6*B22+1/9*D26+1/6*D16-
1/12*B66+1/6*A62+1/9*B61-1/12*D21-1/6*D11, -2/9*D11-1/6*D21+1/9*D22+1/6*D12-
1/12*B62+1/6*B61+1/9*A66-1/12*B26-1/6*B16]
[-1/9*A11+1/12*B61+1/18*D66-1/12*B16-1/9*D22-1/6*B21+1/12*D62-1/12*D26-
1/6*B12, -1/9*B16-1/12*A12+1/18*B62+1/12*D66-1/6*D26-1/12*B22+1/12*D61-1/9*D21-1/6*B11,
-1/9*B12-1/12*B11+1/18*D61+1/12*D62-1/6*D22-1/9*B26-1/12*D21-1/6*A16+1/12*B66,
1/9*A11-1/12*B61+1/9*D66-1/12*B16-2/9*D22+1/6*B21+1/6*D62-1/6*D26-1/6*B12, 1/9*B16-
1/12*A12+1/9*B62-1/12*D66+1/6*D26-1/6*B22+1/6*D61-2/9*D21-1/6*B11, 1/9*B12-
1/12*B11+1/9*D61-1/12*D62+1/6*D22-2/9*B26-1/6*D21-1/6*A16+1/6*B66, 1/18*A11-1/12*B61-
1/9*D66+1/12*B16-1/9*D22+1/12*B21+1/6*D62+1/6*D26-1/12*B12, 1/18*B16+1/12*A12-1/9*B62-
1/12*D66+1/12*D26+1/6*B22+1/6*D61-1/9*D21-1/12*B11, 1/18*B12+1/12*B11-1/9*D61-
1/12*D62+1/12*D22-1/9*B26+1/6*D21-1/12*A16+1/6*B66, -1/18*A11+1/12*B61-
1/18*D66+1/12*B16-1/18*D22-1/12*B21+1/12*D62+1/12*D26-1/12*B12, -1/18*B16+1/12*A12-
1/18*B62+1/12*D66-1/12*D26+1/12*B22+1/12*D61-1/18*D21-1/12*B11, -1/18*B12+1/12*B11-
1/18*D61+1/12*D62-1/12*D22-1/18*B26+1/12*D21-1/12*A16+1/12*B66, -
2/9*A11+1/6*B61+1/9*D66-1/6*B16+1/9*D22-1/6*B21-1/12*D62-1/12*D26+1/6*B12, -2/9*B16-
1/6*A12+1/9*B62+1/6*D66-1/6*D26-1/12*B22-1/12*D61+1/9*D21+1/6*B11, -2/9*B12-
1/6*B11+1/9*D61+1/6*D62-1/6*D22+1/9*B26-1/12*D21+1/6*A16-1/12*B66, 2/9*A11-
1/6*B61+2/9*D66-1/6*B16+2/9*D22+1/6*B21-1/6*D62-1/6*D26+1/6*B12, 2/9*B16-
1/6*A12+2/9*B62-1/6*D66+1/6*D26-1/6*B22-1/6*D61+2/9*D21+1/6*B11, 2/9*B12-
1/6*B11+2/9*D61-1/6*D62+1/6*D22+2/9*B26-1/6*D21+1/6*A16-1/6*B66, 1/9*A11-1/6*B61-
2/9*D66+1/6*B16+1/9*D22+1/12*B21-1/6*D62+1/6*D26+1/12*B12, 1/9*B16+1/6*A12-2/9*B62-
1/6*D66+1/12*D26+1/6*B22-1/6*D61+1/9*D21+1/12*B11, 1/9*B12+1/6*B11-2/9*D61-
1/6*D62+1/12*D22+1/9*B26+1/6*D21+1/12*A16-1/6*B66, -1/9*A11+1/6*B61-
1/9*D66+1/6*B16+1/18*D22-1/12*B21-1/12*D62+1/12*D26+1/12*B12, -1/9*B16+1/6*A12-
1/9*B62+1/6*D66-1/12*D26+1/12*B22-1/12*D61+1/18*D21+1/12*B11, -1/9*B12+1/6*B11-
1/9*D61+1/6*D62-1/12*D22+1/18*B26+1/12*D21+1/12*A16-1/12*B66]
[1/12*A21-1/9*B61+1/18*B26-1/12*D66-1/9*D12-1/6*B11+1/12*B22-1/12*D16-
1/6*D62, -1/9*D66+1/18*A22-1/12*B62+1/12*B26-1/6*D16-1/12*B12+1/12*B21-1/9*D11-1/6*D61,
-1/9*D62+1/18*B21-1/12*D61+1/12*B22-1/6*D12+1/12*A26-1/12*D11-1/9*B16-1/6*B66, -
1/12*A21+1/9*B61+1/9*B26-1/12*D66-2/9*D12+1/6*B11+1/6*B22-1/6*D16-1/6*D62,
1/9*D66+1/9*A22-1/12*B62-1/12*B26+1/6*D16-1/6*B12+1/6*B21-2/9*D11-1/6*D61,
1/9*D62+1/9*B21-1/12*D61-1/12*B22+1/6*D12+1/6*A26-1/6*D11-2/9*B16-1/6*B66, -
1/12*A21+1/18*B61-1/9*B26+1/12*D66-1/9*D12+1/12*B11+1/6*B22+1/6*D16-1/12*D62,
1/18*D66-1/9*A22+1/12*B62-1/12*B26+1/12*D16+1/6*B12+1/6*B21-1/9*D11-1/12*D61,
1/18*D62-1/9*B21+1/12*D61-1/12*B22+1/12*D12+1/6*A26+1/6*D11-1/9*B16-1/12*B66, 1/12*A21-
1/18*B61-1/18*B26+1/12*D66-1/18*D12-1/12*B11+1/12*B22+1/12*D16-1/12*D62, -1/18*D66-
1/18*A22+1/12*B62+1/12*B26-1/12*D16+1/12*B12+1/12*B21-1/18*D11-1/12*D61, -1/18*D62-
1/18*B21+1/12*D61+1/12*B22-1/12*D12+1/12*A26+1/12*D11-1/18*B16-1/12*B66, 1/6*A21-
2/9*B61+1/9*B26-1/6*D66+1/9*D12-1/6*B11-1/12*B22-1/12*D16+1/6*D62, -2/9*D66+1/9*A22-
1/6*B62+1/6*B26-1/6*D16-1/12*B12-1/12*B21+1/9*D11+1/6*D61, -2/9*D62+1/9*B21-

1/6*D61+1/6*B22-1/6*D12-1/12*A26-1/12*D11+1/9*B16+1/6*B66, -1/6*A21+2/9*B61+2/9*B26-
1/6*D66+2/9*D12+1/6*B11-1/6*B22-1/6*D16+1/6*D62, 2/9*D66+2/9*A22-1/6*B62-
1/6*B26+1/6*D16-1/6*B12-1/6*B21+2/9*D11+1/6*D61, 2/9*D62+2/9*B21-1/6*D61-
1/6*B22+1/6*D12-1/6*A26-1/6*D11+2/9*B16+1/6*B66, -1/6*A21+1/9*B61-
2/9*B26+1/6*D66+1/9*D12+1/12*B11-1/6*B22+1/6*D16+1/12*D62, 1/9*D66-2/9*A22+1/6*B62-
1/6*B26+1/12*D16+1/6*B12-1/6*B21+1/9*D11+1/12*D61, 1/9*D62-2/9*B21+1/6*D61-
1/6*B22+1/12*D12-1/6*A26+1/6*D11+1/9*B16+1/12*B66, 1/6*A21-1/9*B61-
1/9*B26+1/6*D66+1/18*D12-1/12*B11-1/12*B22+1/12*D16+1/12*D62, -1/9*D66-
1/9*A22+1/6*B62+1/6*B26-1/12*D16+1/12*B12-1/12*B21+1/18*D11+1/12*D61, -1/9*D62-
1/9*B21+1/6*D61+1/6*B22-1/12*D12-1/12*A26+1/12*D11+1/18*B16+1/12*B66]
[1/12*B11-1/9*B21+1/18*D16-1/12*D26-1/9*B62-1/6*A61+1/12*D12-1/12*B66-
1/6*D22, -1/9*D26+1/18*B12-1/12*B22+1/12*D16-1/6*B66-1/12*A62+1/12*D11-1/9*B61-1/6*D21,
-1/9*D22+1/18*D11-1/12*D21+1/12*D12-1/6*B62+1/12*B16-1/12*B61-1/9*A66-1/6*B26, -
1/12*B11+1/9*B21+1/9*D16-1/12*D26-2/9*B62+1/6*A61+1/6*D12-1/6*B66-1/6*D22,
1/9*D26+1/9*B12-1/12*B22-1/12*D16+1/6*B66-1/6*A62+1/6*D11-2/9*B61-1/6*D21,
1/9*D22+1/9*D11-1/12*D21-1/12*D12+1/6*B62+1/6*B16-1/6*B61-2/9*A66-1/6*B26, -
1/12*B11+1/18*B21-1/9*D16+1/12*D26-1/9*B62+1/12*A61+1/6*D12+1/6*B66-1/12*D22,
1/18*D26-1/9*B12+1/12*B22-1/12*D16+1/12*B66+1/6*A62+1/6*D11-1/9*B61-1/12*D21,
1/18*D22-1/9*D11+1/12*D21-1/12*D12+1/12*B62+1/6*B16+1/6*B61-1/9*A66-1/12*B26, 1/12*B11-
1/18*B21-1/18*D16+1/12*D26-1/18*B62-1/12*A61+1/12*D12+1/12*B66-1/12*D22, -1/18*D26-
1/18*B12+1/12*B22+1/12*D16-1/12*B66+1/12*A62+1/12*D11-1/18*B61-1/12*D21, -1/18*D22-
1/18*D11+1/12*D21+1/12*D12-1/12*B62+1/12*B16+1/12*B61-1/18*A66-1/12*B26, 1/6*B11-
2/9*B21+1/9*D16-1/6*D26+1/9*B62-1/6*A61-1/12*D12-1/12*B66+1/6*D22, -2/9*D26+1/9*B12-
1/6*B22+1/6*D16-1/6*B66-1/12*A62-1/12*D11+1/9*B61+1/6*D21, -2/9*D22+1/9*D11-
1/6*D21+1/6*D12-1/6*B62-1/12*B16-1/12*B61+1/9*A66+1/6*B26, -1/6*B11+2/9*B21+2/9*D16-
1/6*D26+2/9*B62+1/6*A61-1/6*D12-1/6*B66+1/6*D22, 2/9*D26+2/9*B12-1/6*B22-
1/6*D16+1/6*B66-1/6*A62-1/6*D11+2/9*B61+1/6*D21, 2/9*D22+2/9*D11-1/6*D21-
1/6*D12+1/6*B62-1/6*B16-1/6*B61+2/9*A66+1/6*B26, -1/6*B11+1/9*B21-
2/9*D16+1/6*D26+1/9*B62+1/12*A61-1/6*D12+1/6*B66+1/12*D22, 1/9*D26-2/9*B12+1/6*B22-
1/6*D16+1/12*B66+1/6*A62-1/6*D11+1/9*B61+1/12*D21, 1/9*D22-2/9*D11+1/6*D21-
1/6*D12+1/12*B62-1/6*B16+1/6*B61+1/9*A66+1/12*B26, 1/6*B11-1/9*B21-
1/9*D16+1/6*D26+1/18*B62-1/12*A61-1/12*D12+1/12*B66+1/12*D22, -1/9*D26-
1/9*B12+1/6*B22+1/6*D16-1/12*B66+1/12*A62-1/12*D11+1/18*B61+1/12*D21, -1/9*D22-
1/9*D11+1/6*D21+1/6*D12-1/12*B62-1/12*B16+1/12*B61+1/18*A66+1/12*B26]
[-1/18*D66-1/18*A11-1/12*B61-1/12*B16-1/18*D22-1/12*B21-1/12*D62-1/12*D26-
1/12*B12, -1/18*B62-1/12*A12-1/18*B16-1/12*D66-1/12*D26-1/12*D61-1/18*D21-1/12*B11-
1/12*B22, -1/18*D61-1/12*B11-1/18*B12-1/12*D62-1/12*D22-1/18*B26-1/12*D21-1/12*A16-
1/12*B66, 1/18*A11-1/9*D66+1/12*B61-1/12*B16-1/9*D22+1/12*B21-1/6*D26-1/12*B12-1/6*D62,
-1/9*B62-1/12*A12+1/18*B16+1/12*D66+1/12*D26-1/6*B22-1/9*D21-1/12*B11-1/6*D61, -1/9*D61-
1/12*B11+1/18*B12+1/12*D62+1/12*D22-1/9*B26-1/6*D21-1/12*A16-1/6*B66,
1/9*D66+1/9*A11+1/12*B61+1/12*B16-2/9*D22+1/6*B21-1/6*D62+1/6*D26-1/6*B12,
1/9*B62+1/12*A12+1/9*B16+1/12*D66+1/6*D26-1/6*D61-2/9*D21-1/6*B11+1/6*B22,
1/9*D61+1/12*B11+1/9*B12+1/12*D62+1/6*D22-2/9*B26+1/6*D21-1/6*A16-1/6*B66, -
1/9*A11+1/18*D66-1/12*B61+1/12*B16-1/9*D22-1/6*B21+1/12*D26-1/6*B12-1/12*D62,
1/18*B62+1/12*A12-1/9*B16-1/12*D66-1/6*D26-1/12*D61-1/9*D21-1/6*B11+1/12*B22,
1/18*D61+1/12*B11-1/9*B12-1/12*D62-1/6*D22+1/12*D21-1/6*A16-1/9*B26-1/12*B66, -1/9*A11-
1/9*D66-1/6*B61-1/6*B16+1/18*D22-1/12*B21-1/12*D26+1/12*B12+1/12*D62, -1/9*B62-1/6*A12-
1/9*B16-1/6*D66-1/12*D26-1/12*B22+1/18*D21+1/12*B11+1/12*D61, -1/9*D61-1/6*B11-1/9*B12-
1/6*D62-1/12*D22-1/12*D21+1/12*A16+1/18*B26+1/12*B66, -2/9*D66+1/9*A11+1/6*B61-
1/6*B16+1/9*D22+1/12*B21+1/6*D62-1/6*D26+1/12*B12, -2/9*B62-
1/6*A12+1/9*B16+1/6*D66+1/12*D26-1/6*B22+1/9*D21+1/12*B11+1/6*D61, -2/9*D61-
1/6*B11+1/9*B12+1/6*D62+1/12*D22-1/6*D21+1/12*A16+1/9*B26+1/6*B66,
2/9*A11+2/9*D66+1/6*B61+1/6*B16+2/9*D22+1/6*B21+1/6*D26+1/6*B12+1/6*D62,

2/9*B62+1/6*A12+2/9*B16+1/6*D66+1/6*D26+1/6*B22+2/9*D21+1/6*B11+1/6*D61,
2/9*D61+1/6*B11+2/9*B12+1/6*D62+1/6*D22+1/6*D21+1/6*A16+2/9*B26+1/6*B66, 1/9*D66-
2/9*A11-1/6*B61+1/6*B16+1/9*D22-1/6*B21+1/12*D62+1/12*D26+1/6*B12, 1/9*B62+1/6*A12-
2/9*B16-1/6*D66-1/6*D26+1/12*D61+1/9*D21+1/6*B11+1/12*B22, 1/9*D61+1/6*B11-2/9*B12-
1/6*D62-1/6*D22+1/12*D21+1/6*A16+1/9*B26+1/12*B66]

[-1/18*B26-1/12*A21-1/18*B61-1/12*D66-1/18*D12-1/12*B11-1/12*B22-1/12*D16-
1/12*D62, -1/18*A22-1/12*B62-1/18*D66-1/12*B26-1/12*D16-1/12*B21-1/18*D11-1/12*D61-
1/12*B12, -1/18*B21-1/12*D61-1/18*D62-1/12*B22-1/12*D12-1/12*D11-1/18*B16-1/12*B66-
1/12*A26, 1/18*B61-1/9*B26+1/12*A21-1/12*D66-1/9*D12+1/12*B11-1/6*D16-1/6*B22-1/12*D62,
-1/9*A22-1/12*B62+1/18*D66+1/12*B26+1/12*D16-1/6*B12-1/9*D11-1/12*D61-1/6*B21, -1/9*B21-
1/12*D61+1/18*D62+1/12*B22+1/12*D12-1/6*D11-1/9*B16-1/12*B66-1/6*A26,
1/9*B61+1/9*B26+1/12*A21+1/12*D66-2/9*D12+1/6*B11-1/6*B22+1/6*D16-1/6*D62,
1/9*A22+1/12*B62+1/9*D66+1/12*B26+1/6*D16-1/6*B21-2/9*D11-1/6*D61+1/6*B12,
1/9*B21+1/12*D61+1/9*D62+1/12*B22+1/6*D12+1/6*D11-2/9*B16-1/6*B66-1/6*A26, -
1/9*B61+1/18*B26-1/12*A21+1/12*D66-1/9*D12-1/6*B11+1/12*D16-1/12*B22-1/6*D62,
1/18*A22+1/12*B62-1/9*D66-1/12*B26-1/6*D16-1/12*B21-1/9*D11-1/6*D61+1/12*B12,
1/18*B21+1/12*D61-1/9*D62-1/12*B22-1/6*D12+1/12*D11-1/9*B16-1/6*B66-1/12*A26, -1/9*B61-
1/9*B26-1/6*A21-1/6*D66+1/18*D12-1/12*B11-1/12*D16+1/12*B22+1/12*D62, -1/9*A22-1/6*B62-
1/9*D66-1/6*B26-1/12*D16-1/12*B12+1/18*D11+1/12*D61+1/12*B21, -1/9*B21-1/6*D61-1/9*D62-
1/6*B22-1/12*D12-1/12*D11+1/18*B16+1/12*B66+1/12*A26, -2/9*B26+1/6*A21+1/9*B61-
1/6*D66+1/9*D12+1/12*B11+1/6*B22-1/6*D16+1/12*D62, -2/9*A22-
1/6*B62+1/9*D66+1/6*B26+1/12*D16-1/6*B12+1/9*D11+1/12*D61+1/6*B21, -2/9*B21-
1/6*D61+1/9*D62+1/6*B22+1/12*D12-1/6*D11+1/9*B16+1/12*B66+1/6*A26,
2/9*B61+2/9*B26+1/6*A21+1/6*D66+2/9*D12+1/6*B11+1/6*D16+1/6*B22+1/6*D62,
2/9*A22+1/6*B62+2/9*D66+1/6*B26+1/6*D16+1/6*B12+2/9*D11+1/6*D61+1/6*B21,
2/9*B21+1/6*D61+2/9*D62+1/6*B22+1/6*D12+1/6*D11+2/9*B16+1/6*B66+1/6*A26, 1/9*B26-
1/6*A21-2/9*B61+1/6*D66+1/9*D12-1/6*B11+1/12*B22+1/12*D16+1/6*D62, 1/9*A22+1/6*B62-
2/9*D66-1/6*B26-1/6*D16+1/12*B21+1/9*D11+1/6*D61+1/12*B12, 1/9*B21+1/6*D61-2/9*D62-
1/6*B22-1/6*D12+1/12*D11+1/9*B16+1/6*B66+1/12*A26]

[-1/18*D16-1/12*B11-1/18*B21-1/12*D26-1/18*B62-1/12*A61-1/12*D12-1/12*B66-
1/12*D22, -1/18*B12-1/12*B22-1/18*D26-1/12*D16-1/12*B66-1/12*D11-1/18*B61-1/12*D21-
1/12*A62, -1/18*D11-1/12*D21-1/18*D22-1/12*D12-1/12*B62-1/12*B61-1/18*A66-1/12*B26-
1/12*B16, 1/18*B21-1/9*D16+1/12*B11-1/12*D26-1/9*B62+1/12*A61-1/6*B66-1/6*D12-1/12*D22,
-1/9*B12-1/12*B22+1/18*D26+1/12*D16+1/12*B66-1/6*A62-1/9*B61-1/12*D21-1/6*D11, -1/9*D11-
1/12*D21+1/18*D22+1/12*D12+1/12*B62-1/6*B61-1/9*A66-1/12*B26-1/6*B16,
1/9*B21+1/9*D16+1/12*B11+1/12*D26-2/9*B62+1/6*A61-1/6*D12+1/6*B66-1/6*D22,
1/9*B12+1/12*B22+1/9*D26+1/12*D16+1/6*B66-1/6*D11-2/9*B61-1/6*D21+1/6*A62,
1/9*D11+1/12*D21+1/9*D22+1/12*D12+1/6*B62+1/6*B61-2/9*A66-1/6*B26-1/6*B16, -
1/9*B21+1/18*D16-1/12*B11+1/12*D26-1/9*B62-1/6*A61+1/12*B66-1/12*D12-1/6*D22,
1/18*B12+1/12*B22-1/9*D26-1/12*D16-1/6*B66-1/12*D11-1/9*B61-1/6*D21+1/12*A62,
1/18*D11+1/12*D21-1/9*D22-1/12*D12-1/6*B62+1/12*B61-1/9*A66-1/6*B26-1/12*B16, -1/9*B21-
1/9*D16-1/6*B11-1/6*D26+1/18*B62-1/12*A61-1/12*B66+1/12*D12+1/12*D22, -1/9*B12-1/6*B22-
1/9*D26-1/6*D16-1/12*B66-1/12*A62+1/18*B61+1/12*D21+1/12*D11, -1/9*D11-1/6*D21-1/9*D22-
1/6*D12-1/12*B62-1/12*B61+1/18*A66+1/12*B26+1/12*B16, -2/9*D16+1/6*B11+1/9*B21-
1/6*D26+1/9*B62+1/12*A61+1/6*D12-1/6*B66+1/12*D22, -2/9*B12-
1/6*B22+1/9*D26+1/6*D16+1/12*B66-1/6*A62+1/9*B61+1/12*D21+1/6*D11, -2/9*D11-
1/6*D21+1/9*D22+1/6*D12+1/12*B62-1/6*B61+1/9*A66+1/12*B26+1/6*B16,
2/9*B21+2/9*D16+1/6*B11+1/6*D26+2/9*B62+1/6*A61+1/6*B66+1/6*D12+1/6*D22,
2/9*B12+1/6*B22+2/9*D26+1/6*D16+1/6*B66+1/6*A62+2/9*B61+1/6*D21+1/6*D11,
2/9*D11+1/6*D21+2/9*D22+1/6*D12+1/6*B62+1/6*B61+2/9*A66+1/6*B26+1/6*B16, 1/9*D16-
1/6*B11-2/9*B21+1/6*D26+1/9*B62-1/6*A61+1/12*D12+1/12*B66+1/6*D22, 1/9*B12+1/6*B22-
2/9*D26-1/6*D16-1/6*B66+1/12*D11+1/9*B61+1/6*D21+1/12*A62, 1/9*D11+1/6*D21-2/9*D22-
1/6*D12-1/6*B62+1/12*B61+1/9*A66+1/6*B26+1/12*B16]

[1/18*A11-1/12*B61-1/9*D66+1/12*B16-1/9*D22-1/12*B21-1/6*D62-
1/6*D26+1/12*B12, 1/18*B16+1/12*A12-1/9*B62-1/12*D66-1/12*D26-1/6*B22-1/6*D61-
1/9*D21+1/12*B11, 1/18*B12+1/12*B11-1/9*D61-1/12*D62-1/12*D22-1/9*B26-
1/6*D21+1/12*A16-1/6*B66, -1/18*A11+1/12*B61-1/18*D66+1/12*B16-1/18*D22+1/12*B21-
1/12*D62-1/12*D26+1/12*B12, -1/18*B16+1/12*A12-1/18*B62+1/12*D66+1/12*D26-1/12*B22-
1/12*D61-1/18*D21+1/12*B11, -1/18*B12+1/12*B11-1/18*D61+1/12*D62+1/12*D22-1/18*B26-
1/12*D21+1/12*A16-1/12*B66, -1/9*A11+1/12*B61+1/18*D66-1/12*B16-1/9*D22+1/6*B21-
1/12*D62+1/12*D26+1/6*B12, -1/9*B16-1/12*A12+1/18*B62+1/12*D66+1/6*D26+1/12*B22-
1/12*D61-1/9*D21+1/6*B11, -1/9*B12-1/12*B11+1/18*D61+1/12*D62+1/6*D22-
1/9*B26+1/12*D21+1/6*A16-1/12*B66, 1/9*A11-1/12*B61+1/9*D66-1/12*B16-2/9*D22-1/6*B21-
1/6*D62+1/6*D26+1/6*B12, 1/9*B16-1/12*A12+1/9*B62-1/12*D66-1/6*D26+1/6*B22-1/6*D61-
2/9*D21+1/6*B11, 1/9*B12-1/12*B11+1/9*D61-1/12*D62-1/6*D22-2/9*B26+1/6*D21+1/6*A16-
1/6*B66, 1/9*A11-1/6*B61-2/9*D66+1/6*B16+1/9*D22-1/12*B21+1/6*D62-1/6*D26-1/12*B12,
1/9*B16+1/6*A12-2/9*B62-1/6*D66-1/12*D26-1/6*B22+1/6*D61+1/9*D21-1/12*B11,
1/9*B12+1/6*B11-2/9*D61-1/6*D62-1/12*D22+1/9*B26-1/6*D21-1/12*A16+1/6*B66, -
1/9*A11+1/6*B61-1/9*D66+1/6*B16+1/18*D22+1/12*B21+1/12*D62-1/12*D26-1/12*B12, -
1/9*B16+1/6*A12-1/9*B62+1/6*D66+1/12*D26-1/12*B22+1/12*D61+1/18*D21-1/12*B11, -
1/9*B12+1/6*B11-1/9*D61+1/6*D62+1/12*D22+1/18*B26-1/12*D21-1/12*A16+1/12*B66, -
2/9*A11+1/6*B61+1/9*D66-1/6*B16+1/9*D22+1/6*B21+1/12*D62+1/12*D26-1/6*B12, -2/9*B16-
1/6*A12+1/9*B62+1/6*D66+1/6*D26+1/12*B22+1/12*D61+1/9*D21-1/6*B11, -2/9*B12-
1/6*B11+1/9*D61+1/6*D62+1/6*D22+1/9*B26+1/12*D21-1/6*A16+1/12*B66, 2/9*A11-
1/6*B61+2/9*D66-1/6*B16+2/9*D22-1/6*B21+1/6*D62+1/6*D26-1/6*B12, 2/9*B16-
1/6*A12+2/9*B62-1/6*D66-1/6*D26+1/6*B22+1/6*D61+2/9*D21-1/6*B11, 2/9*B12-
1/6*B11+2/9*D61-1/6*D62-1/6*D22+2/9*B26+1/6*D21-1/6*A16+1/6*B66]
[-1/12*A21+1/18*B61-1/9*B26+1/12*D66-1/9*D12-1/12*B11-1/6*B22-
1/6*D16+1/12*D62, 1/18*D66-1/9*A22+1/12*B62-1/12*B26-1/12*D16-1/6*B12-1/6*B21-
1/9*D11+1/12*D61, 1/18*D62-1/9*B21+1/12*D61-1/12*B22-1/12*D12-1/6*A26-1/6*D11-
1/9*B16+1/12*B66, 1/12*A21-1/18*B61-1/18*B26+1/12*D66-1/18*D12+1/12*B11-1/12*B22-
1/12*D16+1/12*D62, -1/18*D66-1/18*A22+1/12*B62+1/12*B26+1/12*D16-1/12*B12-1/12*B21-
1/18*D11+1/12*D61, -1/18*D62-1/18*B21+1/12*D61+1/12*B22+1/12*D12-1/12*A26-1/12*D11-
1/18*B16+1/12*B66, 1/12*A21-1/9*B61+1/18*B26-1/12*D66-1/9*D12+1/6*B11-
1/12*B22+1/12*D16+1/6*D62, -1/9*D66+1/18*A22-1/12*B62+1/12*B26+1/6*D16+1/12*B12-
1/12*B21-1/9*D11+1/6*D61, -1/9*D62+1/18*B21-1/12*D61+1/12*B22+1/6*D12-
1/12*A26+1/12*D11-1/9*B16+1/6*B66, -1/12*A21+1/9*B61+1/9*B26-1/12*D66-2/9*D12-
1/6*B11-1/6*B22+1/6*D16+1/6*D62, 1/9*D66+1/9*A22-1/12*B62-1/12*B26-1/6*D16+1/6*B12-
1/6*B21-2/9*D11+1/6*D61, 1/9*D62+1/9*B21-1/12*D61-1/12*B22-1/6*D12-1/6*A26+1/6*D11-
2/9*B16+1/6*B66, -1/6*A21+1/9*B61-2/9*B26+1/6*D66+1/9*D12-1/12*B11+1/6*B22-1/6*D16-
1/12*D62, 1/9*D66-2/9*A22+1/6*B62-1/6*B26-1/12*D16-1/6*B12+1/6*B21+1/9*D11-1/12*D61,
1/9*D62-2/9*B21+1/6*D61-1/6*B22-1/12*D12+1/6*A26-1/6*D11+1/9*B16-1/12*B66, 1/6*A21-
1/9*B61-1/9*B26+1/6*D66+1/18*D12+1/12*B11+1/12*B22-1/12*D16-1/12*D62, -1/9*D66-
1/9*A22+1/6*B62+1/6*B26+1/12*D16-1/12*B12+1/12*B21+1/18*D11-1/12*D61, -1/9*D62-
1/9*B21+1/6*D61+1/6*B22+1/12*D12+1/12*A26-1/12*D11+1/18*B16-1/12*B66, 1/6*A21-
2/9*B61+1/9*B26-1/6*D66+1/9*D12+1/6*B11+1/12*B22+1/12*D16-1/6*D62, -2/9*D66+1/9*A22-
1/6*B62+1/6*B26+1/6*D16+1/12*B12+1/12*B21+1/9*D11-1/6*D61, -2/9*D62+1/9*B21-
1/6*D61+1/6*B22+1/6*D12+1/12*A26+1/12*D11+1/9*B16-1/6*B66, -
1/6*A21+2/9*B61+2/9*B26-1/6*D66+2/9*D12-1/6*B11+1/6*B22+1/6*D16-1/6*D62,
2/9*D66+2/9*A22-1/6*B62-1/6*B26-1/6*D16+1/6*B12+1/6*B21+2/9*D11-1/6*D61,
2/9*D62+2/9*B21-1/6*D61-1/6*B22-1/6*D12+1/6*A26+1/6*D11+2/9*B16-1/6*B66]
[-1/12*B11+1/18*B21-1/9*D16+1/12*D26-1/9*B62-1/12*A61-1/6*D12-
1/6*B66+1/12*D22, 1/18*D26-1/9*B12+1/12*B22-1/12*D16-1/12*B66-1/6*A62-1/6*D11-
1/9*B61+1/12*D21, 1/18*D22-1/9*D11+1/12*D21-1/12*D12-1/12*B62-1/6*B16-1/6*B61-
1/9*A66+1/12*B26, 1/12*B11-1/18*B21-1/18*D16+1/12*D26-1/18*B62+1/12*A61-1/12*D12-
1/12*B66+1/12*D22, -1/18*D26-1/18*B12+1/12*B22+1/12*D16+1/12*B66-1/12*A62-1/12*D11-

1/18*B61+1/12*D21, -1/18*D22-1/18*D11+1/12*D21+1/12*D12+1/12*B62-1/12*B16-1/12*B61-
1/18*A66+1/12*B26, 1/12*B11-1/9*B21+1/18*D16-1/12*D26-1/9*B62+1/6*A61-
1/12*D12+1/12*B66+1/6*D22, -1/9*D26+1/18*B12-1/12*B22+1/12*D16+1/6*B66+1/12*A62-
1/12*D11-1/9*B61+1/6*D21, -1/9*D22+1/18*D11-1/12*D21+1/12*D12+1/6*B62-
1/12*B16+1/12*B61-1/9*A66+1/6*B26, -1/12*B11+1/9*B21+1/9*D16-1/12*D26-2/9*B62-1/6*A61-
1/6*D12+1/6*B66+1/6*D22, 1/9*D26+1/9*B12-1/12*B22-1/12*D16-1/6*B66+1/6*A62-1/6*D11-
2/9*B61+1/6*D21, 1/9*D22+1/9*D11-1/12*D21-1/12*D12-1/6*B62-1/6*B16+1/6*B61-
2/9*A66+1/6*B26, -1/6*B11+1/9*B21-2/9*D16+1/6*D26+1/9*B62-1/12*A61+1/6*D12-1/6*B66-
1/12*D22, 1/9*D26-2/9*B12+1/6*B22-1/6*D16-1/12*B66-1/6*A62+1/6*D11+1/9*B61-1/12*D21,
1/9*D22-2/9*D11+1/6*D21-1/6*D12-1/12*B62+1/6*B16-1/6*B61+1/9*A66-1/12*B26, 1/6*B11-
1/9*B21-1/9*D16+1/6*D26+1/18*B62+1/12*A61+1/12*D12-1/12*B66-1/12*D22, -1/9*D26-
1/9*B12+1/6*B22+1/6*D16+1/12*B66-1/12*A62+1/12*D11+1/18*B61-1/12*D21, -1/9*D22-
1/9*D11+1/6*D21+1/6*D12+1/12*B62+1/12*B16-1/12*B61+1/18*A66-1/12*B26, 1/6*B11-
2/9*B21+1/9*D16-1/6*D26+1/9*B62+1/6*A61+1/12*D12+1/12*B66-1/6*D22, -2/9*D26+1/9*B12-
1/6*B22+1/6*D16+1/6*B66+1/12*A62+1/12*D11+1/9*B61-1/6*D21, -2/9*D22+1/9*D11-
1/6*D21+1/6*D12+1/6*B62+1/12*B16+1/12*B61+1/9*A66-1/6*B26, -
1/6*B11+2/9*B21+2/9*D16-1/6*D26+2/9*B62-1/6*A61+1/6*D12+1/6*B66-1/6*D22,
2/9*D26+2/9*B12-1/6*B22-1/6*D16-1/6*B66+1/6*A62+1/6*D11+2/9*B61-1/6*D21,
2/9*D22+2/9*D11-1/6*D21-1/6*D12-1/6*B62+1/6*B16+1/6*B61+2/9*A66-1/6*B26]];

Strain-Displacement Symbolic Operator Matrix File: filename: funct_b_matrix_integral_8nodeISO

```
function    [B_FEA_SYM,N] = funct_b_matrix_integral_8nodeISO()
%%%%%%%%%%%%%%%%%%%%%%%%%%%   PURPOSE
%%%%%%%%%%%%%%%%%%%%%%%%%%%%%%%%%%%%%%%%%%%%
%  Calculation of the strain-displacment matrix (operator) that is symbolic
%  in variables r, s, and t
%%%%%%%%%%%%%%%%%%%%%%%%%%%%%%%%%%%%%%%%%%%%%%%%%%%%%%%%%%%%%%%%%%
%%%%%%%%%%%%%%%%%%%%%%%%%%%


syms r s t


N1 = (1/8)*(1-r)*(1-s)*(1-t);
N2 = (1/8)*(1+r)*(1-s)*(1-t);
N3 = (1/8)*(1+r)*(1+s)*(1-t);
N4 = (1/8)*(1-r)*(1+s)*(1-t);
N5 = (1/8)*(1-r)*(1-s)*(1+t);
N6 = (1/8)*(1+r)*(1-s)*(1+t);
N7 = (1/8)*(1+r)*(1+s)*(1+t);
N8 = (1/8)*(1-r)*(1+s)*(1+t);

N = [N1*eye(3)   N2*eye(3)   N3*eye(3)   N4*eye(3)   N5*eye(3)   N6*eye(3)   N7*eye(3)   N8*eye(3)];


B1 = [diff(N1,r)       0              0
      0              diff(N1,s)       0
      0              0              diff(N1,t)
      0              diff(N1,t)      diff(N1,s)
      diff(N1,t)       0             diff(N1,r)
      diff(N1,s)       diff(N1,r)      0        ];

B2 = [diff(N2,r)       0              0
      0              diff(N2,s)       0
      0              0              diff(N2,t)
      0              diff(N2,t)      diff(N2,s)
      diff(N2,t)       0             diff(N2,r)
      diff(N2,s)       diff(N2,r)      0        ];

B3 = [diff(N3,r)       0              0
      0              diff(N3,s)       0
      0              0              diff(N3,t)
      0              diff(N3,t)      diff(N3,s)
      diff(N3,t)       0             diff(N3,r)
      diff(N3,s)       diff(N3,r)      0        ];

B4 = [diff(N4,r)       0              0
      0              diff(N4,s)       0
      0              0              diff(N4,t)
      0              diff(N4,t)      diff(N4,s)
      diff(N4,t)       0             diff(N4,r)
      diff(N4,s)       diff(N4,r)      0        ];
```

```
B5 = [diff(N5,r)       0              0
     0             diff(N5,s)      0
     0             0             diff(N5,t)
     0             diff(N5,t)      diff(N5,s)
     diff(N5,t)      0             diff(N5,r)
     diff(N5,s)      diff(N5,r)      0        ];

B6 = [diff(N6,r)       0              0
     0             diff(N6,s)      0
     0             0             diff(N6,t)
     0             diff(N6,t)      diff(N6,s)
     diff(N6,t)      0             diff(N6,r)
     diff(N6,s)      diff(N6,r)      0        ];

B7 = [diff(N7,r)       0              0
     0             diff(N7,s)      0
     0             0             diff(N7,t)
     0             diff(N7,t)      diff(N7,s)
     diff(N7,t)      0             diff(N7,r)
     diff(N7,s)      diff(N7,r)      0        ];

B8 = [diff(N8,r)       0              0
     0             diff(N8,s)      0
     0             0             diff(N8,t)
     0             diff(N8,t)      diff(N8,s)
     diff(N8,t)      0             diff(N8,r)
     diff(N8,s)      diff(N8,r)      0        ];


B_FEA_SYM = [B1 B2 B3 B4 B5 B6 B7 B8];
```

Symbolic Thermal Load Matrix File: filename: funct_symbolic_thermal_load_matrix_8nodeISO

```
function [thermal_load_sym] = funct_symbolic_thermal_load_matrix_8nodeISO()


%%%%%%%%%%%%%%%%%%%%%%%%%   PURPOSE
%%%%%%%%%%%%%%%%%%%%%%%%%%%%%%%%%%%%%%%%
% Generates the symbolic element thermal load matrix (with respect to) the
% laminates constitutive relationship
%%%%%%%%%%%%%%%%%%%%%%%%%%%%%%%%%%%%%%%%%%%%%%%%%%%%%%%%%%%
%%%%%%%%%%%%%%%%%%%%%%%%%


syms A11 A12 A16 B11 B12 B16 A21 A22 A26 B21 B22 B26 A61 A62 A66 B61 B62 B66 B11 B12 B16
D11 D12 D16 B21 B22 B26 D21 D22 D26 B61 B62 B66 D61 D62 D66 thermal_strain_r thermal_strain_s
thermal_strain_t thermal_strain_st thermal_strain_rt thermal_strain_rs



 thermal_load_sym =     [   8*(-1/8*A11-1/8*B21-1/8*B61)*thermal_strain_r+8*(-1/8*A12-1/8*B22-
1/8*B62)*thermal_strain_s+8*(-1/8*A16-1/8*B26-1/8*B66)*thermal_strain_t+8*(-1/8*B11-1/8*D21-
1/8*D61)*thermal_strain_st+8*(-1/8*B12-1/8*D22-1/8*D62)*thermal_strain_rt+8*(-1/8*B16-1/8*D26-
1/8*D66)*thermal_strain_rs
                         8*(-1/8*A21-1/8*B11-1/8*B61)*thermal_strain_r+8*(-1/8*A22-1/8*B12-
1/8*B62)*thermal_strain_s+8*(-1/8*A26-1/8*B16-1/8*B66)*thermal_strain_t+8*(-1/8*B21-1/8*D11-
1/8*D61)*thermal_strain_st+8*(-1/8*B22-1/8*D12-1/8*D62)*thermal_strain_rt+8*(-1/8*B26-1/8*D16-
1/8*D66)*thermal_strain_rs
                         8*(-1/8*A61-1/8*B11-1/8*B21)*thermal_strain_r+8*(-1/8*A62-1/8*B12-
1/8*B22)*thermal_strain_s+8*(-1/8*A66-1/8*B16-1/8*B26)*thermal_strain_t+8*(-1/8*B61-1/8*D11-
1/8*D21)*thermal_strain_st+8*(-1/8*B62-1/8*D12-1/8*D22)*thermal_strain_rt+8*(-1/8*B66-1/8*D16-
1/8*D26)*thermal_strain_rs
                             8*(1/8*A11-1/8*B21-1/8*B61)*thermal_strain_r+8*(1/8*A12-1/8*B22-
1/8*B62)*thermal_strain_s+8*(1/8*A16-1/8*B26-1/8*B66)*thermal_strain_t+8*(1/8*B11-1/8*D21-
1/8*D61)*thermal_strain_st+8*(1/8*B12-1/8*D22-1/8*D62)*thermal_strain_rt+8*(1/8*B16-1/8*D26-
1/8*D66)*thermal_strain_rs
                         8*(-1/8*A21-1/8*B11+1/8*B61)*thermal_strain_r+8*(-1/8*A22-
1/8*B12+1/8*B62)*thermal_strain_s+8*(-1/8*A26-1/8*B16+1/8*B66)*thermal_strain_t+8*(-1/8*B21-
1/8*D11+1/8*D61)*thermal_strain_st+8*(-1/8*B22-1/8*D12+1/8*D62)*thermal_strain_rt+8*(-1/8*B26-
1/8*D16+1/8*D66)*thermal_strain_rs
                         8*(-1/8*A61-1/8*B11+1/8*B21)*thermal_strain_r+8*(-1/8*A62-
1/8*B12+1/8*B22)*thermal_strain_s+8*(-1/8*A66-1/8*B16+1/8*B26)*thermal_strain_t+8*(-1/8*B61-
1/8*D11+1/8*D21)*thermal_strain_st+8*(-1/8*B62-1/8*D12+1/8*D22)*thermal_strain_rt+8*(-1/8*B66-
1/8*D16+1/8*D26)*thermal_strain_rs
                             8*(1/8*A11-1/8*B21+1/8*B61)*thermal_strain_r+8*(1/8*A12-
1/8*B22+1/8*B62)*thermal_strain_s+8*(1/8*A16-1/8*B26+1/8*B66)*thermal_strain_t+8*(1/8*B11-
1/8*D21+1/8*D61)*thermal_strain_st+8*(1/8*B12-1/8*D22+1/8*D62)*thermal_strain_rt+8*(1/8*B16-
1/8*D26+1/8*D66)*thermal_strain_rs
                             8*(1/8*A21-1/8*B11+1/8*B61)*thermal_strain_r+8*(1/8*A22-
1/8*B12+1/8*B62)*thermal_strain_s+8*(1/8*A26-1/8*B16+1/8*B66)*thermal_strain_t+8*(1/8*B21-
1/8*D11+1/8*D61)*thermal_strain_st+8*(1/8*B22-1/8*D12+1/8*D62)*thermal_strain_rt+8*(1/8*B26-
1/8*D16+1/8*D66)*thermal_strain_rs
```

8*(-1/8*A61+1/8*B11+1/8*B21)*thermal_strain_r+8*(-1/8*A62+1/8*B12+1/8*B22)*thermal_strain_s+8*(-1/8*A66+1/8*B16+1/8*B26)*thermal_strain_t+8*(-1/8*B61+1/8*D11+1/8*D21)*thermal_strain_st+8*(-1/8*B62+1/8*D12+1/8*D22)*thermal_strain_rt+8*(-1/8*B66+1/8*D16+1/8*D26)*thermal_strain_rs

8*(-1/8*A11-1/8*B21+1/8*B61)*thermal_strain_r+8*(-1/8*A12-1/8*B22+1/8*B62)*thermal_strain_s+8*(-1/8*A16-1/8*B26+1/8*B66)*thermal_strain_t+8*(-1/8*B11-1/8*D21+1/8*D61)*thermal_strain_st+8*(-1/8*B12-1/8*D22+1/8*D62)*thermal_strain_rt+8*(-1/8*B16-1/8*D26+1/8*D66)*thermal_strain_rs

8*(1/8*A21-1/8*B11-1/8*B61)*thermal_strain_r+8*(1/8*A22-1/8*B12-1/8*B62)*thermal_strain_s+8*(1/8*A26-1/8*B16-1/8*B66)*thermal_strain_t+8*(1/8*B21-1/8*D11-1/8*D61)*thermal_strain_st+8*(1/8*B22-1/8*D12-1/8*D62)*thermal_strain_rt+8*(1/8*B26-1/8*D16-1/8*D66)*thermal_strain_rs

8*(-1/8*A61+1/8*B11-1/8*B21)*thermal_strain_r+8*(-1/8*A62+1/8*B12-1/8*B22)*thermal_strain_s+8*(-1/8*A66+1/8*B16-1/8*B26)*thermal_strain_t+8*(-1/8*B61+1/8*D11-1/8*D21)*thermal_strain_st+8*(-1/8*B62+1/8*D12-1/8*D22)*thermal_strain_rt+8*(-1/8*B66+1/8*D16-1/8*D26)*thermal_strain_rs

8*(-1/8*A11+1/8*B21-1/8*B61)*thermal_strain_r+8*(-1/8*A12+1/8*B22-1/8*B62)*thermal_strain_s+8*(-1/8*A16+1/8*B26-1/8*B66)*thermal_strain_t+8*(-1/8*B11+1/8*D21-1/8*D61)*thermal_strain_st+8*(-1/8*B12+1/8*D22-1/8*D62)*thermal_strain_rt+8*(-1/8*B16+1/8*D26-1/8*D66)*thermal_strain_rs

8*(-1/8*A21+1/8*B11-1/8*B61)*thermal_strain_r+8*(-1/8*A22+1/8*B12-1/8*B62)*thermal_strain_s+8*(-1/8*A26+1/8*B16-1/8*B66)*thermal_strain_t+8*(-1/8*B21+1/8*D11-1/8*D61)*thermal_strain_st+8*(-1/8*B22+1/8*D12-1/8*D62)*thermal_strain_rt+8*(-1/8*B26+1/8*D16-1/8*D66)*thermal_strain_rs

8*(1/8*A61-1/8*B11-1/8*B21)*thermal_strain_r+8*(1/8*A62-1/8*B12-1/8*B22)*thermal_strain_s+8*(1/8*A66-1/8*B16-1/8*B26)*thermal_strain_t+8*(1/8*B61-1/8*D11-1/8*D21)*thermal_strain_st+8*(1/8*B62-1/8*D12-1/8*D22)*thermal_strain_rt+8*(1/8*B66-1/8*D16-1/8*D26)*thermal_strain_rs

8*(1/8*A11+1/8*B21-1/8*B61)*thermal_strain_r+8*(1/8*A12+1/8*B22-1/8*B62)*thermal_strain_s+8*(1/8*A16+1/8*B26-1/8*B66)*thermal_strain_t+8*(1/8*B11+1/8*D21-1/8*D61)*thermal_strain_st+8*(1/8*B12+1/8*D22-1/8*D62)*thermal_strain_rt+8*(1/8*B16+1/8*D26-1/8*D66)*thermal_strain_rs

8*(-1/8*A21+1/8*B11+1/8*B61)*thermal_strain_r+8*(-1/8*A22+1/8*B12+1/8*B62)*thermal_strain_s+8*(-1/8*A26+1/8*B16+1/8*B66)*thermal_strain_t+8*(-1/8*B21+1/8*D11+1/8*D61)*thermal_strain_st+8*(-1/8*B22+1/8*D12+1/8*D62)*thermal_strain_rt+8*(-1/8*B26+1/8*D16+1/8*D66)*thermal_strain_rs

8*(1/8*A61-1/8*B11+1/8*B21)*thermal_strain_r+8*(1/8*A62-1/8*B12+1/8*B22)*thermal_strain_s+8*(1/8*A66-1/8*B16+1/8*B26)*thermal_strain_t+8*(1/8*B61-1/8*D11+1/8*D21)*thermal_strain_st+8*(1/8*B62-1/8*D12+1/8*D22)*thermal_strain_rt+8*(1/8*B66-1/8*D16+1/8*D26)*thermal_strain_rs

8*(1/8*A11+1/8*B21+1/8*B61)*thermal_strain_r+8*(1/8*A12+1/8*B22+1/8*B62)*thermal_strain_s+8*(1/8*A16+1/8*B26+1/8*B66)*thermal_strain_t+8*(1/8*B11+1/8*D21+1/8*D61)*thermal_strain_st+8*(1/8*B12+1/8*D22+1/8*D62)*thermal_strain_rt+8*(1/8*B16+1/8*D26+1/8*D66)*thermal_strain_rs

8*(1/8*A21+1/8*B11+1/8*B61)*thermal_strain_r+8*(1/8*A22+1/8*B12+1/8*B62)*thermal_strain_s+8*(1/8*A26+1/8*B16+1/8*B66)*thermal_strain_t+8*(1/8*B21+1/8*D11+1/8*D61)*thermal_strain_st+8*(1/8*B22+1/8*D12+1/8*D62)*thermal_strain_rt+8*(1/8*B26+1/8*D16+1/8*D66)*thermal_strain_rs

8*(1/8*A61+1/8*B11+1/8*B21)*thermal_strain_r+8*(1/8*A62+1/8*B12+1/8*B22)*thermal_strain_s+8*(1/8*A66+1/8*B16+1/8*B26)*thermal_strain_t+8*(1/8*B61+1/8*D11+1/8*D21)*thermal_strain_st+8*(1/8*B62+1/8*D12+1/8*D22)*thermal_strain_rt+8*(1/8*B66+1/8*D16+1/8*D26)*thermal_strain_rs

```
                    8*(-1/8*A11+1/8*B21+1/8*B61)*thermal_strain_r+8*(-
1/8*A12+1/8*B22+1/8*B62)*thermal_strain_s+8*(-1/8*A16+1/8*B26+1/8*B66)*thermal_strain_t+8*(-
1/8*B11+1/8*D21+1/8*D61)*thermal_strain_st+8*(-1/8*B12+1/8*D22+1/8*D62)*thermal_strain_rt+8*(-
1/8*B16+1/8*D26+1/8*D66)*thermal_strain_rs
                        8*(1/8*A21+1/8*B11-1/8*B61)*thermal_strain_r+8*(1/8*A22+1/8*B12-
1/8*B62)*thermal_strain_s+8*(1/8*A26+1/8*B16-1/8*B66)*thermal_strain_t+8*(1/8*B21+1/8*D11-
1/8*D61)*thermal_strain_st+8*(1/8*B22+1/8*D12-1/8*D62)*thermal_strain_rt+8*(1/8*B26+1/8*D16-
1/8*D66)*thermal_strain_rs
                        8*(1/8*A61+1/8*B11-1/8*B21)*thermal_strain_r+8*(1/8*A62+1/8*B12-
1/8*B22)*thermal_strain_s+8*(1/8*A66+1/8*B16-1/8*B26)*thermal_strain_t+8*(1/8*B61+1/8*D11-
1/8*D21)*thermal_strain_st+8*(1/8*B62+1/8*D12-1/8*D22)*thermal_strain_rt+8*(1/8*B66+1/8*D16-
1/8*D26)*thermal_strain_rs   ];
```

Element Stiffness Matrix File: filename: funct_C_matrices_8nodeISO

```
function    [C] =
funct_C_matrices_8nodeISO(layer_check,Theta,PHI_Y,C11,C12,C13,C21,C22,C23,C31,C32,C33,C44,C5
5,C66)

%%%%%%%%%%%%%%%%%%%%%%%%   PURPOSE
%%%%%%%%%%%%%%%%%%%%%%%%%%%%%%%%%%%%%%%%%
%  Calculates the Stiffness matrix of each element
%%%%%%%%%%%%%%%%%%%%%%%%%%%%%%%%%%%%%%%%%%%%%%%%%%%%%%%%%%%%%%%
%%%%%%%%%%%%%%%%%%%%%%%%%

%Rotation about the Z-axis:
theta = Theta(layer_check);

Theta_X1 = -1*(theta*(pi/180));
Theta_X2 = -1*((90+theta)*(pi/180));
Theta_X3 = -1*(-90*(pi/180));
Theta_Y1 = -1*(-(90-theta)*(pi/180));
Theta_Y2 = -1*(theta*(pi/180));
Theta_Y3 = -1*(90*(pi/180));
Theta_Z1 = -1*(90*(pi/180));
Theta_Z2 = -1*(-90*(pi/180));
Theta_Z3 = -1*(0*(pi/180));

T_ij_inverse = [(cos(Theta_X1)^2)                (cos(Theta_Y1)^2)                (cos(Theta_Z1)^2)
2*(cos(Theta_Y1)^2)*(cos(Theta_Z1)^2)
2*(cos(Theta_Z1)^2)*(cos(Theta_X1)^2)
2*(cos(Theta_X1)^2)*(cos(Theta_Y1)^2)
            (cos(Theta_X2)^2)                (cos(Theta_Y2)^2)                (cos(Theta_Z2)^2)
2*(cos(Theta_Y2)^2)*(cos(Theta_Z2)^2)
2*(cos(Theta_Z2)^2)*(cos(Theta_X2)^2)
2*(cos(Theta_X2)^2)*(cos(Theta_Y2)^2)
            (cos(Theta_X3)^2)                (cos(Theta_Y3)^2)                (cos(Theta_Z3)^2)
2*(cos(Theta_Y3)^2)*(cos(Theta_Z3)^2)
2*(cos(Theta_Z3)^2)*(cos(Theta_X3)^2)
2*(cos(Theta_X3)^2)*(cos(Theta_Y3)^2)
            (cos(Theta_X2)^2)*(cos(Theta_X3)^2)    (cos(Theta_Y2)^2)*(cos(Theta_Y3)^2)
(cos(Theta_Z2)^2)*(cos(Theta_Z3)^2)
((cos(Theta_Y2)^2)*(cos(Theta_Z3)^2))+((cos(Theta_Y3)^2)*(cos(Theta_Z2)^2))
((cos(Theta_Z2)^2)*(cos(Theta_X3)^2))+((cos(Theta_Z3)^2)*(cos(Theta_X2)^2))
((cos(Theta_X2)^2)*(cos(Theta_Y3)^2))+((cos(Theta_X3)^2)*(cos(Theta_Y2)^2))
            (cos(Theta_X3)^2)*(cos(Theta_X1)^2)    (cos(Theta_Y3)^2)*(cos(Theta_Y1)^2)
(cos(Theta_Z3)^2)*(cos(Theta_Z1)^2)
((cos(Theta_Y3)^2)*(cos(Theta_Z1)^2))+((cos(Theta_Y1)^2)*(cos(Theta_Z3)^2))
((cos(Theta_Z3)^2)*(cos(Theta_X1)^2))+((cos(Theta_Z1)^2)*(cos(Theta_X3)^2))
((cos(Theta_X3)^2)*(cos(Theta_Y1)^2))+((cos(Theta_X1)^2)*(cos(Theta_Y3)^2))
            (cos(Theta_X1)^2)*(cos(Theta_X2)^2)    (cos(Theta_Y1)^2)*(cos(Theta_Y2)^2)
(cos(Theta_Z1)^2)*(cos(Theta_Z2)^2)
((cos(Theta_Y1)^2)*(cos(Theta_Z2)^2))+((cos(Theta_Y2)^2)*(cos(Theta_Z1)^2))
((cos(Theta_Z1)^2)*(cos(Theta_X2)^2))+((cos(Theta_Z2)^2)*(cos(Theta_X1)^2))
((cos(Theta_X1)^2)*(cos(Theta_Y2)^2))+((cos(Theta_X2)^2)*(cos(Theta_Y1)^2))];
```

```
%Rotation about the Z-axis:
Theta_X1 = (theta*(pi/180));
Theta_X2 = ((90+theta)*(pi/180));
Theta_X3 = (-90*(pi/180));
Theta_Y1 = (-(90-theta)*(pi/180));
Theta_Y2 = (theta*(pi/180));
Theta_Y3 = (90*(pi/180));
Theta_Z1 = (90*(pi/180));
Theta_Z2 = (-90*(pi/180));
Theta_Z3 = (0*(pi/180));

T_ij = [(cos(Theta_X1)^2)                    (cos(Theta_Y1)^2)                    (cos(Theta_Z1)^2)
2*(cos(Theta_Y1)^2)*(cos(Theta_Z1)^2)
2*(cos(Theta_Z1)^2)*(cos(Theta_X1)^2)
2*(cos(Theta_X1)^2)*(cos(Theta_Y1)^2)
      (cos(Theta_X2)^2)                    (cos(Theta_Y2)^2)                    (cos(Theta_Z2)^2)
2*(cos(Theta_Y2)^2)*(cos(Theta_Z2)^2)
2*(cos(Theta_Z2)^2)*(cos(Theta_X2)^2)
2*(cos(Theta_X2)^2)*(cos(Theta_Y2)^2)
      (cos(Theta_X3)^2)                    (cos(Theta_Y3)^2)                    (cos(Theta_Z3)^2)
2*(cos(Theta_Y3)^2)*(cos(Theta_Z3)^2)
2*(cos(Theta_Z3)^2)*(cos(Theta_X3)^2)
2*(cos(Theta_X3)^2)*(cos(Theta_Y3)^2)
      (cos(Theta_X2)^2)*(cos(Theta_X3)^2)    (cos(Theta_Y2)^2)*(cos(Theta_Y3)^2)
(cos(Theta_Z2)^2)*(cos(Theta_Z3)^2)
((cos(Theta_Y2)^2)*(cos(Theta_Z3)^2))+((cos(Theta_Y3)^2)*(cos(Theta_Z2)^2))
((cos(Theta_Z2)^2)*(cos(Theta_X3)^2))+((cos(Theta_Z3)^2)*(cos(Theta_X2)^2))
((cos(Theta_X2)^2)*(cos(Theta_Y3)^2))+((cos(Theta_X3)^2)*(cos(Theta_Y2)^2))
      (cos(Theta_X3)^2)*(cos(Theta_X1)^2)    (cos(Theta_Y3)^2)*(cos(Theta_Y1)^2)
(cos(Theta_Z3)^2)*(cos(Theta_Z1)^2)
((cos(Theta_Y3)^2)*(cos(Theta_Z1)^2))+((cos(Theta_Y1)^2)*(cos(Theta_Z3)^2))
((cos(Theta_Z3)^2)*(cos(Theta_X1)^2))+((cos(Theta_Z1)^2)*(cos(Theta_X3)^2))
((cos(Theta_X3)^2)*(cos(Theta_Y1)^2))+((cos(Theta_X1)^2)*(cos(Theta_Y3)^2))
      (cos(Theta_X1)^2)*(cos(Theta_X2)^2)    (cos(Theta_Y1)^2)*(cos(Theta_Y2)^2)
(cos(Theta_Z1)^2)*(cos(Theta_Z2)^2)
((cos(Theta_Y1)^2)*(cos(Theta_Z2)^2))+((cos(Theta_Y2)^2)*(cos(Theta_Z1)^2))
((cos(Theta_Z1)^2)*(cos(Theta_X2)^2))+((cos(Theta_Z2)^2)*(cos(Theta_X1)^2))
((cos(Theta_X1)^2)*(cos(Theta_Y2)^2))+((cos(Theta_X2)^2)*(cos(Theta_Y1)^2))];



%Rotation about the Y-axis
Phi_X1 = -1*(PHI_Y);
Phi_X2 = -1*(pi/2);
Phi_X3 = -1*(-((pi/2)-PHI_Y));
Phi_Y1 = -1*(-(pi/2));
Phi_Y2 = -1*(0);
Phi_Y3 = -1*((pi/2));
Phi_Z1 = -1*(((pi/2)+PHI_Y));
Phi_Z2 = -1*(-(pi/2));
```

```
Phi_Z3 = -1*(PHI_Y);
T_ij_Y_inverse = [(cos(Phi_X1)^2)                (cos(Phi_Y1)^2)                (cos(Phi_Z1)^2)
2*(cos(Phi_Y1)^2)*(cos(Phi_Z1)^2)                                    2*(cos(Phi_Z1)^2)*(cos(Phi_X1)^2)
2*(cos(Phi_X1)^2)*(cos(Phi_Y1)^2)
            (cos(Phi_X2)^2)                (cos(Phi_Y2)^2)                (cos(Phi_Z2)^2)
2*(cos(Phi_Y2)^2)*(cos(Phi_Z2)^2)                                    2*(cos(Phi_Z2)^2)*(cos(Phi_X2)^2)
2*(cos(Phi_X2)^2)*(cos(Phi_Y2)^2)
            (cos(Phi_X3)^2)                (cos(Phi_Y3)^2)                (cos(Phi_Z3)^2)
2*(cos(Phi_Y3)^2)*(cos(Phi_Z3)^2)                                    2*(cos(Phi_Z3)^2)*(cos(Phi_X3)^2)
2*(cos(Phi_X3)^2)*(cos(Phi_Y3)^2)
            (cos(Phi_X2)^2)*(cos(Phi_X3)^2)    (cos(Phi_Y2)^2)*(cos(Phi_Y3)^2)
(cos(Phi_Z2)^2)*(cos(Phi_Z3)^2)
((cos(Phi_Y2)^2)*(cos(Phi_Z3)^2))+((cos(Phi_Y3)^2)*(cos(Phi_Z2)^2))
((cos(Phi_Z2)^2)*(cos(Phi_X3)^2))+((cos(Phi_Z3)^2)*(cos(Phi_X2)^2))
((cos(Phi_X2)^2)*(cos(Phi_Y3)^2))+((cos(Phi_X3)^2)*(cos(Phi_Y2)^2))
            (cos(Phi_X3)^2)*(cos(Phi_X1)^2)    (cos(Phi_Y3)^2)*(cos(Phi_Y1)^2)
(cos(Phi_Z3)^2)*(cos(Phi_Z1)^2)
((cos(Phi_Y3)^2)*(cos(Phi_Z1)^2))+((cos(Phi_Y1)^2)*(cos(Phi_Z3)^2))
((cos(Phi_Z3)^2)*(cos(Phi_X1)^2))+((cos(Phi_Z1)^2)*(cos(Phi_X3)^2))
((cos(Phi_X3)^2)*(cos(Phi_Y1)^2))+((cos(Phi_X1)^2)*(cos(Phi_Y3)^2))
            (cos(Phi_X1)^2)*(cos(Phi_X2)^2)    (cos(Phi_Y1)^2)*(cos(Phi_Y2)^2)
(cos(Phi_Z1)^2)*(cos(Phi_Z2)^2)
((cos(Phi_Y1)^2)*(cos(Phi_Z2)^2))+((cos(Phi_Y2)^2)*(cos(Phi_Z1)^2))
((cos(Phi_Z1)^2)*(cos(Phi_X2)^2))+((cos(Phi_Z2)^2)*(cos(Phi_X1)^2))
((cos(Phi_X1)^2)*(cos(Phi_Y2)^2))+((cos(Phi_X2)^2)*(cos(Phi_Y1)^2))];


%Rotation about the Y-axis
Phi_X1 = (PHI_Y);
Phi_X2 = ((pi/2));
Phi_X3 = (-((pi/2)-PHI_Y));
Phi_Y1 = (-(pi/2));
Phi_Y2 = (0);
Phi_Y3 = ((pi/2));
Phi_Z1 = (((pi/2)+PHI_Y));
Phi_Z2 = (-(pi/2));
Phi_Z3 = (PHI_Y);

T_ij_Y = [(cos(Phi_X1)^2)                (cos(Phi_Y1)^2)                (cos(Phi_Z1)^2)
2*(cos(Phi_Y1)^2)*(cos(Phi_Z1)^2)                                    2*(cos(Phi_Z1)^2)*(cos(Phi_X1)^2)
2*(cos(Phi_X1)^2)*(cos(Phi_Y1)^2)
        (cos(Phi_X2)^2)                (cos(Phi_Y2)^2)                (cos(Phi_Z2)^2)
2*(cos(Phi_Y2)^2)*(cos(Phi_Z2)^2)                                    2*(cos(Phi_Z2)^2)*(cos(Phi_X2)^2)
2*(cos(Phi_X2)^2)*(cos(Phi_Y2)^2)
        (cos(Phi_X3)^2)                (cos(Phi_Y3)^2)                (cos(Phi_Z3)^2)
2*(cos(Phi_Y3)^2)*(cos(Phi_Z3)^2)                                    2*(cos(Phi_Z3)^2)*(cos(Phi_X3)^2)
2*(cos(Phi_X3)^2)*(cos(Phi_Y3)^2)
        (cos(Phi_X2)^2)*(cos(Phi_X3)^2)    (cos(Phi_Y2)^2)*(cos(Phi_Y3)^2)
(cos(Phi_Z2)^2)*(cos(Phi_Z3)^2)
((cos(Phi_Y2)^2)*(cos(Phi_Z3)^2))+((cos(Phi_Y3)^2)*(cos(Phi_Z2)^2))
((cos(Phi_Z2)^2)*(cos(Phi_X3)^2))+((cos(Phi_Z3)^2)*(cos(Phi_X2)^2))
((cos(Phi_X2)^2)*(cos(Phi_Y3)^2))+((cos(Phi_X3)^2)*(cos(Phi_Y2)^2))
```

```
        (cos(Phi_X3)^2)*(cos(Phi_X1)^2)     (cos(Phi_Y3)^2)*(cos(Phi_Y1)^2)
(cos(Phi_Z3)^2)*(cos(Phi_Z1)^2)
((cos(Phi_Y3)^2)*(cos(Phi_Z1)^2))+((cos(Phi_Y1)^2)*(cos(Phi_Z3)^2))
((cos(Phi_Z3)^2)*(cos(Phi_X1)^2))+((cos(Phi_Z1)^2)*(cos(Phi_X3)^2))
((cos(Phi_X3)^2)*(cos(Phi_Y1)^2))+((cos(Phi_X1)^2)*(cos(Phi_Y3)^2))
        (cos(Phi_X1)^2)*(cos(Phi_X2)^2)     (cos(Phi_Y1)^2)*(cos(Phi_Y2)^2)
(cos(Phi_Z1)^2)*(cos(Phi_Z2)^2)
((cos(Phi_Y1)^2)*(cos(Phi_Z2)^2))+((cos(Phi_Y2)^2)*(cos(Phi_Z1)^2))
((cos(Phi_Z1)^2)*(cos(Phi_X2)^2))+((cos(Phi_Z2)^2)*(cos(Phi_X1)^2))
((cos(Phi_X1)^2)*(cos(Phi_Y2)^2))+((cos(Phi_X2)^2)*(cos(Phi_Y1)^2))];



C_rot=zeros(6,6);

C_12 = [C11 C12 C13   0     0     0
        C21 C22 C23   0     0     0
        C31 C32 C33   0     0     0
         0   0   0  2*C44   0     0
         0   0   0    0   2*C55   0
         0   0   0    0     0   2*C66];

C_XY = T_ij_inverse*C_12*T_ij;

C_XY_Y = T_ij_Y_inverse*C_XY*T_ij_Y;




C = C_XY_Y;
```

Jacobian File: filename: funct_jacobian_8nodeISO

```
function    [Determinant_Jacobian] = funct_jacobian_8nodeISO(PHI_Y)

%%%%%%%%%%%%%%%%%%%%%%%%%%%%   PURPOSE
%%%%%%%%%%%%%%%%%%%%%%%%%%%%%%%%%%%%%%%%%%%%%%%%%%%%%%%%%%%%%%%%%%%%%%%%%%%%
%  Calculates the Jacobian matrix and its determinant.
%%%%%%%%%%%%%%%%%%%%%%%%%%%%%%%%%%%%%%%%%%%%%%%%%%%%%%%%%%%%%%%%%%%%%%%%%%%%
%%%%%%%%%%%%%%%%%%%%%%%%%%%%%%%%%%%%%%%%%%%%%%%%%%%%%%%%%%%%%%%%%%%%%%%%%%%%


Jacobian = [cos(PHI_Y)      0      -sin(PHI_Y)
              0             1          0
            sin(PHI_Y)      0       cos(PHI_Y)];
Determinant_Jacobian = det(Jacobian);
```

Thermal Strain File: filename: funct_thermal_strains_8nodeISO

```
function   [THERMAL_STRAIN] =
funct_thermal_strains_8nodeISO(layer_check,Theta,PHI_Y,delta_T,alpha_12)

%%%%%%%%%%%%%%%%%%%%%%%%%%%  PURPOSE
%%%%%%%%%%%%%%%%%%%%%%%%%%%%%%%%%%%%%%%%%%%%%%%%%%%%%%%%%%%%%%%%%%%%%%%
%  Calculates the thermal stains in each element
%%%%%%%%%%%%%%%%%%%%%%%%%%%%%%%%%%%%%%%%%%%%%%%%%%%%%%%%%%%%%%%%%%%%%%%
%%%%%%%%%%%%%%%%%%%%%%%%%%%%%%%%%%%%%%%%%%%%%%%%%%%%%%%%%%%%%%%%%%%%%%%

%Rotation about the Z-axis:
theta = Theta(layer_check);

%Transformation matrix is for laminate coordinate system to material
% coordinate system;  Hence, the inverse of the transformation matrix has
% the cos arguments multiplied by negative one.

Theta_X1 = -1*(theta*(pi/180));
Theta_X2 = -1*((90+theta)*(pi/180));
Theta_X3 = -1*(-90*(pi/180));
Theta_Y1 = -1*(-(90-theta)*(pi/180));
Theta_Y2 = -1*(theta*(pi/180));
Theta_Y3 = -1*(90*(pi/180));
Theta_Z1 = -1*(90*(pi/180));
Theta_Z2 = -1*(-90*(pi/180));
Theta_Z3 = -1*(0*(pi/180));


T_ij_inverse = [(cos(Theta_X1)^2)                (cos(Theta_Y1)^2)                (cos(Theta_Z1)^2)
2*(cos(Theta_Y1)^2)*(cos(Theta_Z1)^2)
2*(cos(Theta_Z1)^2)*(cos(Theta_X1)^2)
2*(cos(Theta_X1)^2)*(cos(Theta_Y1)^2)
          (cos(Theta_X2)^2)              (cos(Theta_Y2)^2)              (cos(Theta_Z2)^2)
2*(cos(Theta_Y2)^2)*(cos(Theta_Z2)^2)
2*(cos(Theta_Z2)^2)*(cos(Theta_X2)^2)
2*(cos(Theta_X2)^2)*(cos(Theta_Y2)^2)
          (cos(Theta_X3)^2)              (cos(Theta_Y3)^2)              (cos(Theta_Z3)^2)
2*(cos(Theta_Y3)^2)*(cos(Theta_Z3)^2)
2*(cos(Theta_Z3)^2)*(cos(Theta_X3)^2)
2*(cos(Theta_X3)^2)*(cos(Theta_Y3)^2)
          (cos(Theta_X2)^2)*(cos(Theta_X3)^2)   (cos(Theta_Y2)^2)*(cos(Theta_Y3)^2)
(cos(Theta_Z2)^2)*(cos(Theta_Z3)^2)
((cos(Theta_Y2)^2)*(cos(Theta_Z3)^2))+((cos(Theta_Y3)^2)*(cos(Theta_Z2)^2))
((cos(Theta_Z2)^2)*(cos(Theta_X3)^2))+((cos(Theta_Z3)^2)*(cos(Theta_X2)^2))
((cos(Theta_X2)^2)*(cos(Theta_Y3)^2))+((cos(Theta_X3)^2)*(cos(Theta_Y2)^2))
          (cos(Theta_X3)^2)*(cos(Theta_X1)^2)   (cos(Theta_Y3)^2)*(cos(Theta_Y1)^2)
(cos(Theta_Z3)^2)*(cos(Theta_Z1)^2)
((cos(Theta_Y3)^2)*(cos(Theta_Z1)^2))+((cos(Theta_Y1)^2)*(cos(Theta_Z3)^2))
((cos(Theta_Z3)^2)*(cos(Theta_X1)^2))+((cos(Theta_Z1)^2)*(cos(Theta_X3)^2))
((cos(Theta_X3)^2)*(cos(Theta_Y1)^2))+((cos(Theta_X1)^2)*(cos(Theta_Y3)^2))
          (cos(Theta_X1)^2)*(cos(Theta_X2)^2)   (cos(Theta_Y1)^2)*(cos(Theta_Y2)^2)
(cos(Theta_Z1)^2)*(cos(Theta_Z2)^2)
```

```
((cos(Theta_Y1)^2)*(cos(Theta_Z2)^2))+((cos(Theta_Y2)^2)*(cos(Theta_Z1)^2))
((cos(Theta_Z1)^2)*(cos(Theta_X2)^2))+((cos(Theta_Z2)^2)*(cos(Theta_X1)^2))
((cos(Theta_X1)^2)*(cos(Theta_Y2)^2))+((cos(Theta_X2)^2)*(cos(Theta_Y1)^2))];


alpha_xy = T_ij_inverse*alpha_12;
THERMAL_STRAIN_xy = alpha_xy*delta_T;


%Rotation about the Y-axis
Phi_X1 = -1*(PHI_Y);
Phi_X2 = -1*(pi/2);
Phi_X3 = -1*(-((pi/2)-PHI_Y));
Phi_Y1 = -1*(-(pi/2));
Phi_Y2 = -1*(0);
Phi_Y3 = -1*((pi/2));
Phi_Z1 = -1*(((pi/2)+PHI_Y));
Phi_Z2 = -1*(-(pi/2));
Phi_Z3 = -1*(PHI_Y);
T_ij_Y_inverse = [(cos(Phi_X1)^2)                (cos(Phi_Y1)^2)                (cos(Phi_Z1)^2)
2*(cos(Phi_Y1)^2)*(cos(Phi_Z1)^2)                                    2*(cos(Phi_Z1)^2)*(cos(Phi_X1)^2)
2*(cos(Phi_X1)^2)*(cos(Phi_Y1)^2)
            (cos(Phi_X2)^2)                (cos(Phi_Y2)^2)                (cos(Phi_Z2)^2)
2*(cos(Phi_Y2)^2)*(cos(Phi_Z2)^2)                                    2*(cos(Phi_Z2)^2)*(cos(Phi_X2)^2)
2*(cos(Phi_X2)^2)*(cos(Phi_Y2)^2)
            (cos(Phi_X3)^2)                (cos(Phi_Y3)^2)                (cos(Phi_Z3)^2)
2*(cos(Phi_Y3)^2)*(cos(Phi_Z3)^2)                                    2*(cos(Phi_Z3)^2)*(cos(Phi_X3)^2)
2*(cos(Phi_X3)^2)*(cos(Phi_Y3)^2)
            (cos(Phi_X2)^2)*(cos(Phi_X3)^2)    (cos(Phi_Y2)^2)*(cos(Phi_Y3)^2)
(cos(Phi_Z2)^2)*(cos(Phi_Z3)^2)
((cos(Phi_Y2)^2)*(cos(Phi_Z3)^2))+((cos(Phi_Y3)^2)*(cos(Phi_Z2)^2))
((cos(Phi_Z2)^2)*(cos(Phi_X3)^2))+((cos(Phi_Z3)^2)*(cos(Phi_X2)^2))
((cos(Phi_X2)^2)*(cos(Phi_Y3)^2))+((cos(Phi_X3)^2)*(cos(Phi_Y2)^2))
            (cos(Phi_X3)^2)*(cos(Phi_X1)^2)    (cos(Phi_Y3)^2)*(cos(Phi_Y1)^2)
(cos(Phi_Z3)^2)*(cos(Phi_Z1)^2)
((cos(Phi_Y3)^2)*(cos(Phi_Z1)^2))+((cos(Phi_Y1)^2)*(cos(Phi_Z3)^2))
((cos(Phi_Z3)^2)*(cos(Phi_X1)^2))+((cos(Phi_Z1)^2)*(cos(Phi_X3)^2))
((cos(Phi_X3)^2)*(cos(Phi_Y1)^2))+((cos(Phi_X1)^2)*(cos(Phi_Y3)^2))
            (cos(Phi_X1)^2)*(cos(Phi_X2)^2)    (cos(Phi_Y1)^2)*(cos(Phi_Y2)^2)
(cos(Phi_Z1)^2)*(cos(Phi_Z2)^2)
((cos(Phi_Y1)^2)*(cos(Phi_Z2)^2))+((cos(Phi_Y2)^2)*(cos(Phi_Z1)^2))
((cos(Phi_Z1)^2)*(cos(Phi_X2)^2))+((cos(Phi_Z2)^2)*(cos(Phi_X1)^2))
((cos(Phi_X1)^2)*(cos(Phi_Y2)^2))+((cos(Phi_X2)^2)*(cos(Phi_Y1)^2))];

THERMAL_STRAIN = T_ij_Y_inverse*THERMAL_STRAIN_xy;
```

Global Stiffness Matrix File: filename: funct_global_stiffness_matrix_8nodeISO

```
function    [K_global] = funct_global_stiffness_matrix_8nodeISO(ne,elements,k_element,ndof)

%%%%%%%%%%%%%%%%%%%%%%%%   PURPOSE
%%%%%%%%%%%%%%%%%%%%%%%%%%%%%%%%%%%%%%
%  Assembles global stiffness matrix.
%%%%%%%%%%%%%%%%%%%%%%%%%%%%%%%%%%%%%%%%%%%%%%%%%%%
%%%%%%%%%%%%%%%%%%%%%%%%




ntriplets=ne*24^2;
I_SPARSE = (zeros(ntriplets,1));
J_SPARSE = (zeros(ntriplets,1));
X_SPARSE = (zeros(ntriplets,1));
ntriplets=0;



i=0;
j=0;
jj=0;
count=0;
krow=0;
kcol=0;
for II=1:ne
   i=i+1;
   count(i)=i;  %#ok<AGROW>
   sctr = elements(i,:);

   for JJ=1:8
      j=j+1;
      jj=jj+1;
      %Addresses DOFs as r_1,s_1,t_1,r_2,s_2,t_2,.......,r_nn,s_nn,t_nn
      %  where nn equals the total number of nodes in the model
      sctrVec(jj) = (sctr(j)*3)-2; %#ok<AGROW>    %r-DOF
      sctrVec(jj+1) = (sctr(j)*3)-1; %#ok<AGROW>  %s-DOF
      sctrVec(jj+2) = (sctr(j)*3); %#ok<AGROW>    %t-DOF
      jj=jj+2;
   end

         for KROW=1:24
            krow=krow+1;

               for KCOL=1:24
                  kcol=kcol+1;
                  ntriplets = ntriplets + 1 ;
                  I_SPARSE(ntriplets) = sctrVec(krow);
                  J_SPARSE(ntriplets) = sctrVec(kcol);
                  X_SPARSE(ntriplets) = k_element(krow,kcol,count(i));
               end
```

```
            kcol=0;
        end
        krow=0;
    j=0;
    jj=0;


end

K_global = sparse(I_SPARSE,J_SPARSE,X_SPARSE,ndof,ndof);
```

Boundary Condition File: filename: funct_boundary_conditions_8nodeISO

```
function
[bottom_face_nodes,top_face_nodes,right_face_nodes,left_face_nodes,front_face_nodes,rear_face_nodes]
=
funct_boundary_conditions_8nodeISO(elements,Number_Of_Elements__THETA,Number_Of_Elements_
_RADIAL,Number_Of_Elements__Z,ne,nn_THETA,nn_Z)

%%%%%%%%%%%%%%%%%%%%%%%%%   PURPOSE
%%%%%%%%%%%%%%%%%%%%%%%%%%%%%%%%%%%%%%%%
%  Defines element connectivity for boundary condtions.  Definition of
%  connectivity is done one element at a time.  Listing of all the unique
%  nodes on a given boundary face is created.
%%%%%%%%%%%%%%%%%%%%%%%%%%%%%%%%%%%%%%%%%%%%%%%%%%%%%%%%%%%%%%%%
%%%%%%%%%%%%%%%%%%%%%%%%%




bottom_face = elements(1:Number_Of_Elements__THETA*Number_Of_Elements__Z,1:4);
top_face =
elements((((Number_Of_Elements__THETA*Number_Of_Elements__Z)*(Number_Of_Elements__RADI
AL-1))+1):ne,5:8);

i=0;
ii=0;
iii=0;
for J=1:Number_Of_Elements__RADIAL

   for I=1:Number_Of_Elements__THETA
      i=i+1;
      iii=iii+1;
      front_face(iii,:) = [elements(i,1:2) elements(i,5:6)]; %#ok<AGROW>
      rear_face(iii,:) = [elements(i,1:2) elements(i,5:6)] + nn_THETA*(nn_Z-1); %#ok<AGROW>
   end
   ii=ii+1;
   i=ii*Number_Of_Elements__THETA*Number_Of_Elements__Z;
      if Number_Of_Elements__RADIAL == 1
         break
      end
end

i=1:Number_Of_Elements__THETA:ne-(Number_Of_Elements__THETA-1);
j=i+(Number_Of_Elements__THETA-1);
ii=0;
for I=1:Number_Of_Elements__RADIAL*Number_Of_Elements__Z
   ii=ii+1;
   left_face(ii,:) = [elements(i(ii),1) elements(i(ii),4) elements(i(ii),5) elements(i(ii),8)]; %#ok<AGROW>
   right_face(ii,:) = [elements(j(ii),2) elements(j(ii),3) elements(j(ii),6) elements(j(ii),7)]; %#ok<AGROW>
end
```

```
bottom_face_nodes = unique(bottom_face);
top_face_nodes = unique(top_face);
front_face_nodes = unique(front_face);
rear_face_nodes = unique(rear_face);
left_face_nodes = unique(left_face);
right_face_nodes = unique(right_face);
```

Reduced Stiffness Matrix File: filename: funct_reduced_stiffness_matrix_8nodeISO

```
function    [K_global_reduced] =
funct_reduced_stiffness_matrix_8nodeISO(bottom_face_nodes,top_face_nodes,right_face_nodes,left_face
_nodes,front_face_nodes,rear_face_nodes,K_global,Right_Boundary,Left_Boundary,Top_Boundary,Botto
m_Boundary,Front_Boundary,Rear_Boundary,ndof)

%%%%%%%%%%%%%%%%%%%%%%%%%   PURPOSE
%%%%%%%%%%%%%%%%%%%%%%%%%%%%%%%%%%%%%%%%%%%%
%  Reduction of the global stiffness matrix for removing the singularity
%  utilizing the boundary conditions to set all rows and columns that
%  correspond to zero displacement equal to zero except where it is on the
%  diagonal.
%%%%%%%%%%%%%%%%%%%%%%%%%%%%%%%%%%%%%%%%%%%%%%%%%%%%%%%%%%%%%%%
%%%%%%%%%%%%%%%%%%%%%%%%%



K_global_reduced = K_global;

if Right_Boundary == 1
  i=0;
   for I=1:length(right_face_nodes)
       i=i+1;
       K_global_reduced(:,(right_face_nodes(i)*3)-2) = 0;
       K_global_reduced(:,(right_face_nodes(i)*3)-1) = 0;
       K_global_reduced(:,(right_face_nodes(i)*3)) = 0;
       K_global_reduced((right_face_nodes(i)*3)-2,:) = 0;
       K_global_reduced((right_face_nodes(i)*3)-1,:) = 0;
       K_global_reduced((right_face_nodes(i)*3),:) = 0;
   end

end

if Left_Boundary == 1
   i=0;
   for I=1:length(left_face_nodes)
       i=i+1;
       K_global_reduced(:,(left_face_nodes(i)*3)-2) = 0;
       K_global_reduced(:,(left_face_nodes(i)*3)-1) = 0;
       K_global_reduced(:,(left_face_nodes(i)*3)) = 0;
       K_global_reduced((left_face_nodes(i)*3)-2,:) = 0;
       K_global_reduced((left_face_nodes(i)*3)-1,:) = 0;
       K_global_reduced((left_face_nodes(i)*3),:) = 0;
   end

end

if Top_Boundary == 1
   i=0;
   for I=1:length(top_face_nodes)
       i=i+1;
       K_global_reduced(:,(top_face_nodes(i)*3)-2) = 0;
```

```
        K_global_reduced(:,(top_face_nodes(i)*3)-1) = 0;
        K_global_reduced(:,(top_face_nodes(i)*3)) = 0;
        K_global_reduced((top_face_nodes(i)*3)-2,:) = 0;
        K_global_reduced((top_face_nodes(i)*3)-1,:) = 0;
        K_global_reduced((top_face_nodes(i)*3),:) = 0;
    end
end

if Bottom_Boundary == 1
    i=0;
    for I=1:length(bottom_face_nodes)
        i=i+1;
        K_global_reduced(:,(bottom_face_nodes(i)*3)-2) = 0;
        K_global_reduced(:,(bottom_face_nodes(i)*3)-1) = 0;
        K_global_reduced(:,(bottom_face_nodes(i)*3)) = 0;
        K_global_reduced((bottom_face_nodes(i)*3)-2,:) = 0;
        K_global_reduced((bottom_face_nodes(i)*3)-1,:) = 0;
        K_global_reduced((bottom_face_nodes(i)*3),:) = 0;
    end
end

if Front_Boundary == 1
    i=0;
    for I=1:length(front_face_nodes)
        i=i+1;
        K_global_reduced(:,(front_face_nodes(i)*3)-2) = 0;
        K_global_reduced(:,(front_face_nodes(i)*3)-1) = 0;
        K_global_reduced(:,(front_face_nodes(i)*3)) = 0;
        K_global_reduced((front_face_nodes(i)*3)-2,:) = 0;
        K_global_reduced((front_face_nodes(i)*3)-1,:) = 0;
        K_global_reduced((front_face_nodes(i)*3),:) = 0;
    end
end

if Rear_Boundary == 1
    i=0;
    for I=1:length(rear_face_nodes)
        i=i+1;
        K_global_reduced(:,(rear_face_nodes(i)*3)-2) = 0;
        K_global_reduced(:,(rear_face_nodes(i)*3)-1) = 0;
        K_global_reduced(:,(rear_face_nodes(i)*3)) = 0;
        K_global_reduced((rear_face_nodes(i)*3)-2,:) = 0;
        K_global_reduced((rear_face_nodes(i)*3)-1,:) = 0;
        K_global_reduced((rear_face_nodes(i)*3),:) = 0;
    end
end


i=0;
for I=1:ndof
    i=i+1;

     if K_global_reduced(i,i) == 0
```

```
        K_global_reduced(i,i) = 1;
    end
end
```

Nodal Force File: filename: funct_nodal_force_array_8nodeISO

```
function    [thermal_load_Array,thermal_load_Array_Reduced] =
funct_nodal_force_array_8nodeISO(thermal_load,elements,ne,ndof,bottom_face_nodes,top_face_nodes,rig
ht_face_nodes,left_face_nodes,front_face_nodes,rear_face_nodes,Right_Boundary,Left_Boundary,Top_Bo
undary,Bottom_Boundary,Front_Boundary,Rear_Boundary)

%%%%%%%%%%%%%%%%%%%%%%%%%   PURPOSE
%%%%%%%%%%%%%%%%%%%%%%%%%%%%%%%%%%%%
%  Assembles nodal force array in global coordinates
%%%%%%%%%%%%%%%%%%%%%%%%%%%%%%%%%%%%%%%%%%%%%%%%%%%%%
%%%%%%%%%%%%%%%%%%%%%%%%%


ntriplets=ne*24;
I_SPARSE = (zeros(ntriplets,1));
J_SPARSE = (zeros(ntriplets,1));
X_SPARSE = (zeros(ntriplets,1));
ntriplets=0;



i=0;
j=0;
jj=0;
count=0;
krow=0;
kcol=1;
for II=1:ne
  i=i+1;
  count(i)=i;
  sctr = elements(i,:);

  for JJ=1:8
    j=j+1;
    jj=jj+1;
    %Addresses DOFs as r_1,s_1,t_1,r_2,s_2,t_2,.......,r_nn,s_nn,t_nn
    %  where nn equals the total number of nodes in the model
    sctrVec(jj) = (sctr(j)*3)-2;    %r-DOF
    sctrVec(jj+1) = (sctr(j)*3)-1;  %s-DOF
    sctrVec(jj+2) = (sctr(j)*3);    %t-DOF
    jj=jj+2;
  end
  j=0;
  jj=0;

  for KROW=1:24
    krow=krow+1;
    ntriplets = ntriplets + 1 ;
    I_SPARSE(ntriplets) = sctrVec(krow);
    J_SPARSE(ntriplets) = 1;
    X_SPARSE(ntriplets) = thermal_load(krow,kcol,count(i));
  end
```

```
   krow=0;

end

thermal_load_Array_full_matrix = sparse(I_SPARSE,J_SPARSE,X_SPARSE,ndof,ndof);
thermal_load_Array = thermal_load_Array_full_matrix(:,1);



thermal_load_Array_Reduced =  thermal_load_Array;

if Right_Boundary == 1
  i=0;
   for I=1:length(right_face_nodes)
      i=i+1;
      thermal_load_Array_Reduced((right_face_nodes(i)*3)-2,1) = 0;
      thermal_load_Array_Reduced((right_face_nodes(i)*3)-1,1) = 0;
      thermal_load_Array_Reduced((right_face_nodes(i)*3),1) = 0;
   end
end

if Left_Boundary == 1
   i=0;
   for I=1:length(left_face_nodes)
      i=i+1;
      thermal_load_Array_Reduced((left_face_nodes(i)*3)-2,1) = 0;
      thermal_load_Array_Reduced((left_face_nodes(i)*3)-1,1) = 0;
      thermal_load_Array_Reduced((left_face_nodes(i)*3),1) = 0;
   end
end

if Top_Boundary == 1
   i=0;
   for I=1:length(top_face_nodes)
      i=i+1;
      thermal_load_Array_Reduced((top_face_nodes(i)*3)-2,1) = 0;
      thermal_load_Array_Reduced((top_face_nodes(i)*3)-1,1) = 0;
      thermal_load_Array_Reduced((top_face_nodes(i)*3),1) = 0;
   end
end

if Bottom_Boundary == 1
   i=0;
   for I=1:length(bottom_face_nodes)
      i=i+1;
      thermal_load_Array_Reduced((bottom_face_nodes(i)*3)-2,1) = 0;
      thermal_load_Array_Reduced((bottom_face_nodes(i)*3)-1,1) = 0;
      thermal_load_Array_Reduced((bottom_face_nodes(i)*3),1) = 0;
   end
end

if Front_Boundary == 1
   i=0;
```

```
    for I=1:length(front_face_nodes)
        i=i+1;
        thermal_load_Array_Reduced((front_face_nodes(i)*3)-2,1) = 0;
        thermal_load_Array_Reduced((front_face_nodes(i)*3)-1,1) = 0;
        thermal_load_Array_Reduced((front_face_nodes(i)*3),1) = 0;
    end
end

if Rear_Boundary == 1
    i=0;
    for I=1:length(rear_face_nodes)
        i=i+1;
        thermal_load_Array_Reduced((rear_face_nodes(i)*3)-2,1) = 0;
        thermal_load_Array_Reduced((rear_face_nodes(i)*3)-1,1) = 0;
        thermal_load_Array_Reduced((rear_face_nodes(i)*3),1) = 0;
    end
end
```

Displacement File: filename: funct_reduced_displacement_array_8nodeISO

```
function    [Reduced_Displacement_Array] =
funct_reduced_displacement_array_8nodeISO(K_global_reduced,thermal_load_Array_Reduced)


%%%%%%%%%%%%%%%%%%%%%%%%   PURPOSE
%%%%%%%%%%%%%%%%%%%%%%%%%%%%%%%%%%%%%%
%  Calculates global displacements in model at the nodes
%%%%%%%%%%%%%%%%%%%%%%%%%%%%%%%%%%%%%%%%%%%%%%%%%%%
%%%%%%%%%%%%%%%%%%%%%%%%


Reduced_Displacement_Array = K_global_reduced\thermal_load_Array_Reduced;
```

Element Displacement Collection File: filename: funct_displacements_8nodeISO

```
function    [Displacements] = funct_displacements_8nodeISO(elements,ne,Reduced_Displacement_Array)

%%%%%%%%%%%%%%%%%%%%%%%%%   PURPOSE
%%%%%%%%%%%%%%%%%%%%%%%%%%%%%%%%%%%%%%%
%  Collects the Displacements for each element
%%%%%%%%%%%%%%%%%%%%%%%%%%%%%%%%%%%%%%%%%%%%%%%%%%%%%%%%%%%%
%%%%%%%%%%%%%%%%%%%%%%%%%



i=0;
j=0;
jj=0;
for II=1:ne
   i=i+1;
   sctr = elements(i,:);

   for JJ=1:8
      j=j+1;
      jj=jj+1;
      sctrVec(jj) = (sctr(j)*3)-2; %#ok<AGROW>     %r-DOF
      sctrVec(jj+1) = (sctr(j)*3)-1; %#ok<AGROW>   %s-DOF
      sctrVec(jj+2) = (sctr(j)*3); %#ok<AGROW>     %t-DOF
      jj=jj+2;
   end
   j=0;
   jj=0;



   Displacements(i,1) = Reduced_Displacement_Array(sctrVec(1));
   Displacements(i,2) = Reduced_Displacement_Array(sctrVec(2));
   Displacements(i,3) = Reduced_Displacement_Array(sctrVec(3));
   Displacements(i,4) = Reduced_Displacement_Array(sctrVec(4));
   Displacements(i,5) = Reduced_Displacement_Array(sctrVec(5));
   Displacements(i,6) = Reduced_Displacement_Array(sctrVec(6));
   Displacements(i,7) = Reduced_Displacement_Array(sctrVec(7));
   Displacements(i,8) = Reduced_Displacement_Array(sctrVec(8));
   Displacements(i,9) = Reduced_Displacement_Array(sctrVec(9));
   Displacements(i,10) = Reduced_Displacement_Array(sctrVec(10));
   Displacements(i,11) = Reduced_Displacement_Array(sctrVec(11));
   Displacements(i,12) = Reduced_Displacement_Array(sctrVec(12));
   Displacements(i,13) = Reduced_Displacement_Array(sctrVec(13));
   Displacements(i,14) = Reduced_Displacement_Array(sctrVec(14));
   Displacements(i,15) = Reduced_Displacement_Array(sctrVec(15));
   Displacements(i,16) = Reduced_Displacement_Array(sctrVec(16));
   Displacements(i,17) = Reduced_Displacement_Array(sctrVec(17));
   Displacements(i,18) = Reduced_Displacement_Array(sctrVec(18));
   Displacements(i,19) = Reduced_Displacement_Array(sctrVec(19));
   Displacements(i,20) = Reduced_Displacement_Array(sctrVec(20));
```

```
    Displacements(i,21) = Reduced_Displacement_Array(sctrVec(21));
    Displacements(i,22) = Reduced_Displacement_Array(sctrVec(22));
    Displacements(i,23) = Reduced_Displacement_Array(sctrVec(23));
    Displacements(i,24) = Reduced_Displacement_Array(sctrVec(24));


end
```

Displacement Function File: filename: funct_displacement_function_8nodeISO

```
function    [Displacement_Function] = funct_displacement_function_8nodeISO(ne,Displacements,N)

%%%%%%%%%%%%%%%%%%%%%%%%%%%   PURPOSE
%%%%%%%%%%%%%%%%%%%%%%%%%%%%%%%%%%%%%%%%%%%%%%%%%%%%%%%%%%%%%%%%%%%%%%%%%%%
%  Calculates the Displacements for each element as a function of
%  the element's local coordinate system (r,s,t)
%%%%%%%%%%%%%%%%%%%%%%%%%%%%%%%%%%%%%%%%%%%%%%%%%%%%%%%%%%%%%%%%%%%%%%%%%%%
%%%%%%%%%%%%%%%%%%%%%%%%%%%%%%%%%%%%%%%%%%%%%%%%%%%%%%%%%%%%%%%%%%%%%%%%%%%



i=0;
for I=1:ne
   i=i+1;
   Displacement_Function(:,i) = N*transpose(Displacements(i,:));
end
```

Element and Nodal Strain File: filename: funct_strain_8nodeISO

```
function    [Element_Strain,Nodal_Strain] =
funct_strain_8nodeISO(Displacements,B_FEA_SYM,ne,Radius_Of_Curvature,laminate_Z,Number_Of_El
ements__THETA,Number_Of_Elements__Z,Number_Of_Elements__RADIAL,plies)

%%%%%%%%%%%%%%%%%%%%%%%%%   PURPOSE
%%%%%%%%%%%%%%%%%%%%%%%%%%%%%%%%%%%%%%%
% Calculates the strains for each element and node
%%%%%%%%%%%%%%%%%%%%%%%%%%%%%%%%%%%%%%%%%%%%%%%%%%%%%%%%%%%%
%%%%%%%%%%%%%%%%%%%%%%%%%%%%
fid = fopen('B_FEA_symbolic_2_numeric.m','w');

 fprintf(fid,'B_FEA_numeric = [ ');
   SIZE_B_FEA_SYM = size(B_FEA_SYM);
   for row = 1:SIZE_B_FEA_SYM(1)
      for col = 1:SIZE_B_FEA_SYM(2)
         fprintf(fid,'%s',char(B_FEA_SYM(row,col)),',');
      end
      fprintf(fid,';...\n');
   end
   fprintf(fid,' ];');


element_Z = zeros(ne,1);

k=0;
for K=1:plies
   k=k+1;

   if laminate_Z(k) < 0
      Plus_Minus_1 = 1;
   else
      Plus_Minus_1 = -1;
   end
   element_Z(1+(Number_Of_Elements__THETA*Number_Of_Elements__Z*(k-
1)):(Number_Of_Elements__THETA*Number_Of_Elements__Z)+(Number_Of_Elements__THETA*Nu
mber_Of_Elements__Z*(k-1)),1) = laminate_Z(k)+(Plus_Minus_1*0.0025);

end


Element_Strain = zeros(6,ne);
Element_Strain_curved = zeros(6,ne);
Nodal_Strain = zeros(6,8,ne);
Nodal_Strain_curved = zeros(6,8,ne);
i=0;
j=0;
for I=1:Number_Of_Elements__RADIAL
   j=j+1;

   for J=1:(Number_Of_Elements__THETA*Number_Of_Elements__Z)
      i=i+1;
```

```
%Element (at center)
r=0;s=0;t=0;
run('B_FEA_symbolic_2_numeric')
Element_Strain(:,i) = (B_FEA_numeric*transpose(Displacements(i,:))).*[1;1;1;0.5;0.5;0.5];


%Node 1
r=-1;s=-1;t=-1;
run('B_FEA_symbolic_2_numeric')
Nodal_Strain(:,1,i) = (B_FEA_numeric*transpose(Displacements(i,:))).*[1;1;1;0.5;0.5;0.5];


%Node 2
r=1;s=-1;t=-1;
run('B_FEA_symbolic_2_numeric')
Nodal_Strain(:,2,i) = (B_FEA_numeric*transpose(Displacements(i,:))).*[1;1;1;0.5;0.5;0.5];


%Node 3
r=1;s=1;t=-1;
run('B_FEA_symbolic_2_numeric')
Nodal_Strain(:,3,i) = (B_FEA_numeric*transpose(Displacements(i,:))).*[1;1;1;0.5;0.5;0.5];


%Node 4
r=-1;s=1;t=-1;
run('B_FEA_symbolic_2_numeric')
Nodal_Strain(:,4,i) = (B_FEA_numeric*transpose(Displacements(i,:))).*[1;1;1;0.5;0.5;0.5];


%Node 5
r=-1;s=-1;t=1;
run('B_FEA_symbolic_2_numeric')
Nodal_Strain(:,5,i) = (B_FEA_numeric*transpose(Displacements(i,:))).*[1;1;1;0.5;0.5;0.5];


%Node 6
r=1;s=-1;t=1;
run('B_FEA_symbolic_2_numeric')
Nodal_Strain(:,6,i) = (B_FEA_numeric*transpose(Displacements(i,:))).*[1;1;1;0.5;0.5;0.5];


%Node 7
r=1;s=1;t=1;
run('B_FEA_symbolic_2_numeric')
Nodal_Strain(:,7,i) = (B_FEA_numeric*transpose(Displacements(i,:))).*[1;1;1;0.5;0.5;0.5];


%Node 8
r=-1;s=1;t=1;
run('B_FEA_symbolic_2_numeric')
Nodal_Strain(:,8,i) = (B_FEA_numeric*transpose(Displacements(i,:))).*[1;1;1;0.5;0.5;0.5];
```

```
    end
end
```

Element and Nodal Stress File: filename: funct_stress_8nodeISO

```
function    [Element_Stress,Nodal_Stress] =
funct_stress_8nodeISO(Element_Strain,Nodal_Strain,ne,D_FEA,THERMAL_STRAIN_FEA)

%%%%%%%%%%%%%%%%%%%%%%%%%   PURPOSE
%%%%%%%%%%%%%%%%%%%%%%%%%%%%%%%%%%%%%%%%%
%  Calculates the stresses for each element and node
%%%%%%%%%%%%%%%%%%%%%%%%%%%%%%%%%%%%%%%%%%%%%%%%%%%%%%%%%%%%%%%%%%%%%%%%%%%%%%%%%%%%%%%%%%%%%%%%%%%%%%%%%%%%%%%%%%%%%%%%%%%%%%%%%%%%%%%%%%%%%
%%%%%%%%%%%%%%%%%%%%%%%%%



Element_Stress = zeros(6,ne);
Element_Stress_curved = zeros(6,ne);
Nodal_Stress = zeros(6,8,ne);
Nodal_Stress_curved = zeros(6,8,ne);
i=0;
for I=1:ne
   i=i+1;

   %Element (at center)
   Element_Stress(:,i) = (D_FEA(:,:,i)*Element_Strain(:,i)) -
(D_FEA(:,:,i)*THERMAL_STRAIN_FEA(:,:,i));


   %Node 1
   Nodal_Stress(:,1,i) = (D_FEA(:,:,i)*Nodal_Strain(:,1,i)) -
(D_FEA(:,:,i)*THERMAL_STRAIN_FEA(:,:,i));


   %Node 2
   Nodal_Stress(:,2,i) = (D_FEA(:,:,i)*Nodal_Strain(:,2,i)) -
(D_FEA(:,:,i)*THERMAL_STRAIN_FEA(:,:,i));


   %Node 3
   Nodal_Stress(:,3,i) = (D_FEA(:,:,i)*Nodal_Strain(:,3,i)) -
(D_FEA(:,:,i)*THERMAL_STRAIN_FEA(:,:,i));


   %Node 4
   Nodal_Stress(:,4,i) = (D_FEA(:,:,i)*Nodal_Strain(:,4,i)) -
(D_FEA(:,:,i)*THERMAL_STRAIN_FEA(:,:,i));


   %Node 5
   Nodal_Stress(:,5,i) = (D_FEA(:,:,i)*Nodal_Strain(:,5,i)) -
(D_FEA(:,:,i)*THERMAL_STRAIN_FEA(:,:,i));


   %Node 6
```

```
    Nodal_Stress(:,6,i) = (D_FEA(:,:,i)*Nodal_Strain(:,6,i)) -
(D_FEA(:,:,i)*THERMAL_STRAIN_FEA(:,:,i));


    %Node 7
    Nodal_Stress(:,7,i) = (D_FEA(:,:,i)*Nodal_Strain(:,7,i)) -
(D_FEA(:,:,i)*THERMAL_STRAIN_FEA(:,:,i));


    %Node 8
    Nodal_Stress(:,8,i) = (D_FEA(:,:,i)*Nodal_Strain(:,8,i)) -
(D_FEA(:,:,i)*THERMAL_STRAIN_FEA(:,:,i));

end
```

Mechanical Forces File: filename: funct_forces_8nodeISO

```
function    [Forces,FORCES] = funct_forces_8nodeISO(Displacements,k_element,ne,thermal_load)

%%%%%%%%%%%%%%%%%%%%%%%%%   PURPOSE
%%%%%%%%%%%%%%%%%%%%%%%%%%%%%%%%%%%%%%%%
%  Calculates global forces in model at the nodes
%%%%%%%%%%%%%%%%%%%%%%%%%%%%%%%%%%%%%%%%%%%%%%%%%%%%%%%%%%%%%%%%%%%%%%
%%%%%%%%%%%%%%%%%%%%%%%%%%%%%%%%%%%%%%%%%%%%%%%%%%%%%%%%


Stiffness_Forces = zeros(ne,24);
i=0;
for I=1:ne
   i=i+1;
   Forces(:,:,i) = (k_element(:,:,i)*transpose(Displacements(i,:)))-(thermal_load(:,:,i));
   FORCES(:,i) = (k_element(:,:,i)*transpose(Displacements(i,:)))-(thermal_load(:,:,i));
end
```

APPENDIX G

DATA FROM TRADE STUDY FOR STRESSES IN LAMINATES FOR STACKING SEQUENCES AS A FUNCTION OF RADIUS OF CURVATURE: RESULTS FROM MATLAB FINITE ELEMENT ANALYSIS PROGRAM

Table 19. Stresses for aluminum as the angle spanned by the simply curved beam (arc) goes from 0^o to 90^o. Stacking sequence: $[0]_6 \rightarrow$ isotropic

	Layer	σ_x	σ_y	σ_z	τ_{yz}	τ_{xz}	τ_{xy}
0°	**6**	-13958.083	-1652.3447	-1204.5417	2.633E-13	-4.916E-13	31.464018
	5	-13319.443	-1460.0172	-1247.6639	2.914E-13	-4.205E-13	32.339104
	4	-13214.951	-1439.7632	-1285.4729	-1.764E-13	-6.086E-13	32.883874
	3	-13214.951	-1439.7632	-1285.4729	-1.324E-13	-6.342E-13	32.883874
	2	-13319.443	-1460.0172	-1247.6639	2.238E-13	-5.327E-13	32.339104
	1	-13958.083	-1652.3447	-1204.5417	2.593E-14	-2.123E-13	31.464018
30°	**6**	-13172.645	-1603.7143	-1174.6813	-149.94498	-752.96814	-45.265053
	5	-12613.524	-1418.4405	-1149.2205	-168.97851	-680.59352	-42.322931
	4	-12532.501	-1404.9128	-1178.5999	-172.45959	-659.66046	-41.694372
	3	-12532.501	-1404.9128	-1178.5999	-172.45959	-659.66046	-41.694372
	2	-12613.524	-1418.4405	-1149.2205	-168.97851	-680.59352	-42.322931
	1	-13172.645	-1603.7143	-1174.6813	-149.94498	-752.96814	-45.265053
45°	**6**	-12258.062	-1632.4567	-1271.7396	-252.40312	-1412.602	-110.20491
	5	-11760.178	-1450.4966	-1167.4102	-277.9631	-1290.3015	-105.13753
	4	-11690.04	-1439.3323	-1179.0927	-282.9801	-1259.1339	-104.93797
	3	-11690.04	-1439.3323	-1179.0927	-282.9801	-1259.1339	-104.93797
	2	-11760.178	-1450.4966	-1167.4102	-277.9631	-1290.3015	-105.13753
	1	-12258.062	-1632.4567	-1271.7396	-252.40312	-1412.602	-110.20491
60°	**6**	-10841.064	-1749.9388	-1560.0784	-260.3841	-1960.5129	-130.175
	5	-10355.361	-1545.8944	-1338.3694	-274.30446	-1792.3157	-124.508
	4	-10266.887	-1522.0839	-1312.8707	-278.38235	-1753.1228	-125.22873
	3	-10266.887	-1522.0839	-1312.8707	-278.38235	-1753.1228	-125.22873
	2	-10355.361	-1545.8944	-1338.3694	-274.30446	-1792.3157	-124.508
	1	-10841.064	-1749.9388	-1560.0784	-260.3841	-1960.5129	-130.175
90°	**6**	-4867.2931	-2233.1093	-2545.211	283.52985	-1927.3424	283.36139
	5	-4194.8264	-1876.9407	-1911.718	283.40184	-1578.522	283.082
	4	-3990.4901	-1777.0394	-1727.7978	289.7864	-1472.348	289.30256
	3	-3990.4901	-1777.0394	-1727.7978	289.7864	-1472.348	289.30256
	2	-4194.8264	-1876.9407	-1911.718	283.40184	-1578.522	283.082
	1	-4867.2931	-2233.1093	-2545.211	283.52985	-1927.3424	283.36139

Table 20. Stresses for glass/epoxy as the angle spanned by the simply curved beam (arc) goes from 0^o to 90^o.Stacking sequence: $[(+/-)\ 45/\ 0\ ]_s \rightarrow$ balanced and symmetric

	Layer	σ_x	σ_y	σ_z	τ_{yz}	τ_{xz}	τ_{xy}
0°	**6**	-691.67611	-691.67611	-242.42157	-11.518623	-11.518623	-390.12438
	5	-775.29718	-775.29718	-305.97416	-15.998009	-15.998009	-429.64078
	4	-2243.3284	171.804	-211.05131	-7.0459904	64.92118	271.02863
	3	-2243.3284	171.804	-211.05131	-7.0459904	64.92118	271.02863
	2	-775.29718	-775.29718	-305.97416	-15.998009	-15.998009	-429.64078
	1	-691.67611	-691.67611	-242.42157	-11.518623	-11.518623	-390.12438
30°	**6**	-2457.5675	-2637.5852	-2666.954	2488.0731	2246.57	-1211.7289
	5	-2202.2529	-2300.2921	-1196.3034	759.20934	649.58382	-1165.9538
	4	-2571.4877	-23.899459	-182.13182	-78.296844	-32.595931	-277.03994
	3	-2571.4877	-23.899459	-182.13182	-78.296844	-32.595931	-277.03994
	2	-2202.2529	-2300.2921	-1196.3034	759.20934	649.58382	-1165.9538
	1	-2457.5675	-2637.5852	-2666.954	2488.0731	2246.57	-1211.7289
45°	**6**	-630.07878	-668.0594	-236.21887	-288.68818	-351.91711	-336.62549
	5	-514.87035	-491.98516	34.320997	-339.20492	-286.83254	-323.10525
	4	-1884.4865	234.03648	36.757536	26.16304	-171.79703	168.827
	3	-1884.4865	234.03648	36.757536	26.16304	-171.79703	168.827
	2	-514.87035	-491.98516	34.320997	-339.20492	-286.83254	-323.10525
	1	-630.07878	-668.0594	-236.21887	-288.68818	-351.91711	-336.62549
60°	**6**	7240.4641	7524.3909	9165.5011	-6471.7293	-5024.0851	2962.1211
	5	6449.2701	7729.0181	8275.6306	918.19358	4869.8874	1498.115
	4	7789.5167	590.81224	3009.4851	2403.0062	-743.98838	350.47354
	3	7789.5167	590.81224	3009.4851	2403.0062	-743.98838	350.47354
	2	6449.2701	7729.0181	8275.6306	918.19358	4869.8874	1498.115
	1	7240.4641	7524.3909	9165.5011	-6471.7293	-5024.0851	2962.1211
90°	**6**	-3394.166	-3978.526	-5163.7426	2468.6518	1597.5002	-927.45014
	5	7749.6896	7363.4314	10794.311	-4489.374	-1572.7552	1263.9562
	4	5558.2868	3121.6203	3549.4004	-139.6498	1195.1231	-556.5531
	3	5558.2868	3121.6203	3549.4004	-139.6498	1195.1231	-556.5531
	2	7749.6896	7363.4314	10794.311	-4489.374	-1572.7552	1263.9562
	1	-3394.166	-3978.526	-5163.7426	2468.6518	1597.5002	-927.45014

Table 21. Stresses for glass/epoxy as the angle spanned by the simply curved beam (arc) goes from 0^o to 90^o. Stacking sequence: $[+45/-45/0/0/45/-45]_T$ → antisymmetrical (balanced and unsymmetrical)

	Layer	σ_x	σ_y	σ_z	τ_{yz}	τ_{xz}	τ_{xy}
0°	**6**	-691.67611	-691.67611	-242.42157	-11.518623	-11.518623	-390.12438
	5	-775.29718	-775.29718	-305.97416	-15.998009	-15.998009	-429.64078
	4	-2243.3284	171.804	-211.05131	-7.0459904	64.92118	271.02863
	3	-2243.3284	171.804	-211.05131	-7.0459904	64.92118	271.02863
	2	-775.29718	-775.29718	-305.97416	-15.998009	-15.998009	-429.64078
	1	-691.67611	-691.67611	-242.42157	-11.518623	-11.518623	-390.12438
30°	**6**	151.45475	208.73958	947.34392	-1149.0274	-1050.6163	-0.5726182
	5	-1191.684	-1249.5272	-692.35665	174.32817	95.081058	-583.09834
	4	-2449.4143	174.94638	-244.77387	-110.99457	-19.542882	148.96651
	3	-858.66717	-898.79031	-724.34255	396.35655	329.58225	-466.76016
	2	-1003.2193	-1048.11	-808.7118	589.82368	521.94461	-549.19736
	1	-2175.4964	-36.777583	-172.80545	17.715975	-30.437531	169.64183
45°	**6**	-630.07878	-668.0594	-236.21887	-288.68818	-351.91711	-336.62549
	5	-514.87035	-491.98516	34.320997	-339.20492	-286.83254	-323.10525
	4	-1884.4865	234.03648	36.757536	26.16304	-171.79703	168.827
	3	-1884.4865	234.03648	36.757536	26.16304	-171.79703	168.827
	2	-514.87035	-491.98516	34.320997	-339.20492	-286.83254	-323.10525
	1	-630.07878	-668.0594	-236.21887	-288.68818	-351.91711	-336.62549
60°	**6**	-8632.5501	-9446.488	-8201.4345	-851.18314	-3435.1782	-3087.3492
	5	-11438.649	-13555.976	-7587.655	-122.67401	-2960.7598	-4520.0151
	4	4427.9233	1898.5137	5445.0068	78.886784	1724.179	831.99584
	3	-2419.2064	-3813.0724	-1028.1147	160.62699	-987.86592	-838.96042
	2	-4476.6377	-6186.2585	1171.2516	-2694.9945	-2876.2905	-2817.6262
	1	-4105.3991	-462.71374	-264.9589	1447.0122	40.763775	1143.8821
90°	**6**	-3394.166	-3978.526	-5163.7426	2468.6518	1597.5002	-927.45014
	5	7749.6896	7363.4314	10794.311	-4489.374	-1572.7552	1263.9562
	4	5558.2868	3121.6203	3549.4004	-139.6498	1195.1231	-556.5531
	3	5558.2868	3121.6203	3549.4004	-139.6498	1195.1231	-556.5531
	2	7749.6896	7363.4314	10794.311	-4489.374	-1572.7552	1263.9562
	1	-3394.166	-3978.526	-5163.7426	2468.6518	1597.5002	-927.45014

Table 22. Stresses for glass/epoxy as the angle spanned by the simply curved beam (arc) goes from 0^o to 90^o. Stacking sequence: $[45_2/\ 0\ /45_2/\ 0]_T \rightarrow$ unbalanced and unsymmetrical

	Layer	σ_x	σ_y	σ_z	τ_{yz}	τ_{xz}	τ_{xy}
0°	**6**	-712.05789	-712.05789	-330.59493	55.273241	55.273241	-392.37155
	5	-755.29988	-755.29988	-344.66323	30.563276	30.563276	-415.2338
	4	-2240.0588	208.12769	-203.25389	-10.368876	85.918021	284.79149
	3	-765.66091	-765.66091	-291.14793	-27.085423	-27.085423	-428.15147
	2	-788.37049	-788.37049	-246.76194	-67.273907	-67.273907	-443.70542
	1	-2304.149	126.25512	-166.7532	-3.9775689	65.78702	177.36876
30°	**6**	151.45475	208.73958	947.34392	-1149.0274	-1050.6163	-0.5726182
	5	-1191.684	-1249.5272	-692.35665	174.32817	95.081058	-583.09834
	4	-2449.4143	174.94638	-244.77387	-110.99457	-19.542882	148.96651
	3	-858.66717	-898.79031	-724.34255	396.35655	329.58225	-466.76016
	2	-1003.2193	-1048.11	-808.7118	589.82368	521.94461	-549.19736
	1	-2175.4964	-36.777583	-172.80545	17.715975	-30.437531	169.64183
45°	**6**	678.09253	950.51009	2116.5742	-3626.7938	-4054.1608	371.64196
	5	-4219.4699	-4262.7125	-7184.2157	8706.5559	8907.7468	-2324.466
	4	2539.6664	2024.4283	2124.7674	-169.86677	770.88732	662.55553
	3	204.20071	-402.7287	-1430.7924	2889.1633	1939.6776	496.9256
	2	-7368.7393	-8955.5112	-7837.0643	3660.3994	1260.5393	-2989.4387
	1	-291.70295	-497.77936	159.26187	526.73684	794.69012	-1678.9675
60°	**6**	-8632.5501	-9446.488	-8201.4345	-851.18314	-3435.1782	-3087.3492
	5	-11438.649	-13555.976	-7587.655	-122.67401	-2960.7598	-4520.0151
	4	4427.9233	1898.5137	5445.0068	78.886784	1724.179	831.99584
	3	-2419.2064	-3813.0724	-1028.1147	160.62699	-987.86592	-838.96042
	2	-4476.6377	-6186.2585	1171.2516	-2694.9945	-2876.2905	-2817.6262
	1	-4105.3991	-462.71374	-264.9589	1447.0122	40.763775	1143.8821
90°	**6**	-35531.819	-44807.876	-28066.827	-4606.3254	-11763.363	-14705.457
	5	10533.987	8545.7319	14265.015	-3723.6145	1797.6155	1373.7384
	4	8321.2718	758.41266	4976.4748	1974.1839	2270.0436	2410.2876
	3	-2961.8092	-2822.2259	-760.53817	-983.22661	-1495.5788	-1366.6648
	2	2699.6212	3164.9007	3921.6467	1490.1767	2626.4458	551.26144
	1	1321.8315	-783.49371	542.72809	466.30815	576.94013	268.56045

REFERENCES

1) GOD. *Holy Bible*. Multiple, Circa 2nd century

2) Daniel, Isaac M. and Ishai, Ori. *Engineering Mechanics Of Composite Material*. New York and Oxford: Oxford University Press, 2003.

3) Li, Y.H. and Zhao, X.F. *Exact Solution For In-Plane Displacement For Curved Beams Under Thermo Load*. Investigative Modeling, Dalian: Institute of Road and Bridge Engineering, Dalian Maritime University

4) Manoach, Ribeiro, & Emil. "The Effect of Temperature On Large Amplitude Vibrations of Curved Beams." *Journal Sound Vibration*, 2005. 1093-1107.

5) Cristina Padavani, Giuseppe Pasquinelli, and Nicola Zani. "A Numerical Method For Solving Equilibrium Problems of No-Tension Solids Subjected To Thermal Loads." *Computational Method Applied Mathematics*. 200: 55-73

6) Nguyen, Thien. "Effect of Curvature On A Curved Laminated Beams Subjected To Bending." *Master Thesis*. Arlington: University of Texas at Arlington, May 2010.

7) Wen Chan, F. Alamgir, X. Tan, Kent L. Lawrence. "Modeling For Composite Structures By Finite Element Method." *27th Annual Technical Conference For The American Society of Composites*. 2012

8) Logan, Daryl L. *A First Course In The Finite Element Method*. Thomson Learning, 2007.

9) Naotake Noda, Richard B. Hetna

BIOGRAPHICAL INFORMATION

Jared Cornelius Polk received his Bachelor's in Aerospace Engineering from Georgia Institute of Technology in Atlanta, Georgia. His academic interest are in design, modeling, structural analysis, and mechanics of composites. He plans to work in a field commensurate with his education, be happy, and have peace. After working in the industry for at least five years, he plans to pursue a Doctorate in Aerospace Engineering in his field of work on a part-time basis while working.